

ADVERTIMENT. La consulta d'aquesta tesi queda condicionada a l'acceptació de les següents condicions d'ús: La difusió d'aquesta tesi per mitjà del servei TDX (www.tesisenxarxa.net) ha estat autoritzada pels titulars dels drets de propietat intel·lectual únicament per a usos privats emmarcats en activitats d'investigació i docència. No s'autoritza la seva reproducció amb finalitats de lucre ni la seva difusió i posada a disposició des d'un lloc aliè al servei TDX. No s'autoritza la presentació del seu contingut en una finestra o marc aliè a TDX (framing). Aquesta reserva de drets afecta tant al resum de presentació de la tesi com als seus continguts. En la utilització o cita de parts de la tesi és obligat indicar el nom de la persona autora.

ADVERTENCIA. La consulta de esta tesis queda condicionada a la aceptación de las siguientes condiciones de uso: La difusión de esta tesis por medio del servicio TDR (www.tesisenred.net) ha sido autorizada por los titulares de los derechos de propiedad intelectual únicamente para usos privados enmarcados en actividades de investigación y docencia. No se autoriza su reproducción con finalidades de lucro ni su difusión y puesta a disposición desde un sitio ajeno al servicio TDR. No se autoriza la presentación de su contenido en una ventana o marco ajeno a TDR (framing). Esta reserva de derechos afecta tanto al resumen de presentación de la tesis como a sus contenidos. En la utilización o cita de partes de la tesis es obligado indicar el nombre de la persona autora.

WARNING. On having consulted this thesis you're accepting the following use conditions: Spreading this thesis by the TDX (www.tesisenxarxa.net) service has been authorized by the titular of the intellectual property rights only for private uses placed in investigation and teaching activities. Reproduction with lucrative aims is not authorized neither its spreading and availability from a site foreign to the TDX service. Introducing its content in a window or frame foreign to the TDX service is not authorized (framing). This rights affect to the presentation summary of the thesis as well as to its contents. In the using or citation of parts of the thesis it's obliged to indicate the name of the author



CONTRIBUTION TO THE ADVANCED ANALYSIS AND PREVENTION OF THE MECHANISMS OF NATURAL FIRE INDUCED STRUCTURAL COLLAPSE IN HIGH-RISE BUILDINGS

APORTACIÓN AL ANÁLISIS AVANZADO Y PREVENCIÓN DE LOS MECANISMOS DE COLAPSO ESTRUCTURAL DE EDIFICIOS DE GRAN ALTURA ANTE UNA SOLICITACIÓN DE INCENDIO REAL

Doctoral Thesis presented by / Tesis Doctoral presentada por

Angel Guerrero Castells *Ingeniero Industrial con Suficiencia Investigadora*

in February 2009 to obtain the degree of Doctor in Industrial Engineering

en Febrero de 2009 para obtener el grado de Doctor Ingeniero Industrial.

Thesis Directors / Directores de la Tesis:

Dr Frederic Marimon Carvajal from the / *de la Universidad Politécnica de Cataluña*

Dr Francesco Pesavento from the / *de la Università degli Studi di Padova*

PROGRAMA DE DOCTORADO DE ANÁLISIS ESTRUCTURAL

Departamento de Resistencia de Materiales y Estructuras en la Ingeniería

Escuela Técnica Superior de Ingenieros Industriales de Barcelona



Appendix 6A

Appendix 6A.1 ATLAS OF INFORMATION FOR THE ANALYSIS OF THE INFLUENCE ON COOLING OF PARAMETERS NOT RELATED TO COOLING PROCESS.

In this Appendix it is supplied an atlas of information needed for the analysis of the influence on the hygro-thermo-chemo-mechanical behaviour of the structural element during the cooling processes of several parameters non-related to the own cooling processes – such as the initial moisture content of concrete, its intrinsic permeability, the rate of temperature increase (fire intensity), the porosity, compressive strength, type of aggregate and, in general, the whole set of hygro-thermo-chemical properties of concrete –. This atlas of information will enable the generation of an extension to cooling processes of the Spalling Nomograms initially obtained just for heating processes and previously described on Chapter 4.

As it was explained in paragraph 6.1 of Chapter 6, although the generation of the stated Spalling Nomograms for the cooling stage is not an aim of this Thesis and it is proposed as an extended task for future research works, in this Appendix it is analyzed if the variation of any of these parameters leads to an increase of the maximum value of the adopted Spalling Index I_{s4} (i.e. the risk of Thermal Spalling) during the cooling stage of the cases dealt in this Chapter.

As introduced in paragraph 6.3 of Chapter 6, the values adopted for each of the ranging parameters considered in this atlas, must be combined with all of the others. The whole set of the forty five resulting combinations of the parameters' values initially considered is described in Table 6A-1. For a better and faster understanding and identification of the values characterizing each combination, the type of notation used to describe each of these forty five combinations is the following one:

TH**K***RH**PAR*C**, where,

TH** indicates the value of the thickness of the model (in cm) used in the computation
– Parameter 3 –

K*** indicates the value of the intrinsic permeability (in m^2) – Parameter 2 –,

RH** indicates the value of the initial saturation degree (in %) – Parameter 1 –,

PAR* indicates the parametric heating curve taken into account in the computation,
– Parameter 4 – explained in next paragraphs in detail.

C** indicates the material considered in the computation – Parameter 5 –.

Hence, for example, the combination TH12K018RH50PAR1C60 stands for a case characterised by a *thickness*=12 cm, $k=10^{-18} m^2$, $S_{init}=50\%$, *Parametric curve*=ISO Curve (Par1) and C60 material.

In some of the reference cases, several cooling start instants have been chosen in order to develop, in paragraph 6.5.3 of Chapter 6, an analysis of the influence of the cooling start instant on the phenomena occurred during cooling. The explanation of the selection of the cooling start instants and rates of cooling is included on paragraph 6.4.3.2 of Chapter 6.

The set of represented results for each case is constituted by four Cartesian continuum representations of the following parameters, chosen as those more representative of the thermal spalling risk (what represents a total amount of 180 graphics introduced in paragraph 6.5.4 and included in this Appendix):

Spalling Index I_{s4}

Mechanical Damage d

General Velocity of Spalled-Off pieces v

Velocity affected by Mechanical Damage ‘ $v \cdot d$ criterion’

It is remarkable that in all of these 180 graphics only the time interval corresponding to the First Surface Cooling simulated is represented, in order to achieve a higher level of detail in the representation.

COOLING START TIME [s]	COOLING TYPE	COOLING SUBTYPE	CODE	Combination	PC1 (RH) [%]			PC2 (K) [m ²]			PC3 (TH) [cm]	PC4 (Heating curve)			PC5 (Mat)	
					40	50	60	10 ⁻¹⁹	10 ⁻¹⁸	10 ⁻¹⁷	12	PAR1	PAR2	PAR4	C60	C90
600	SURF	FIRST COOL	1SFC	TH12K017RH40PAR1C60	X					X	X	X			X	
600	SURF	FIRST COOL	2SFC	TH12K018RH40PAR1C60	X				X		X	X			X	
600	SURF	FIRST COOL*	3SFC	TH12K019RH40PAR1C60	X			X			X	X			X	
600	SURF	FIRST COOL	4SFC	TH12K017RH50PAR1C60		X				X	X	X			X	
600	SURF	FIRST COOL	5SFC	TH12K018RH50PAR1C60		X			X		X	X			X	
600	SURF	FIRST COOL	6SFC	TH12K019RH50PAR1C60		X		X			X	X			X	
600	SURF	FIRST COOL	7SFC	TH12K017RH60PAR1C60			X			X	X	X			X	
600	SURF	FIRST COOL	8SFC	TH12K018RH60PAR1C60			X		X		X	X			X	
600	SURF	FIRST COOL*	9SFC	TH12K019RH60PAR1C60			X	X			X	X			X	
3360	SURF	FIRST COOL	10SFC	TH12K017RH40PAR2C60	X					X	X		X		X	
3360	SURF	FIRST COOL	11SFC	TH12K018RH40PAR2C60	X				X		X		X		X	
3360	SURF	FIRST COOL	12SFC	TH12K019RH40PAR2C60	X			X			X		X		X	
3360	SURF	FIRST COOL	13SFC	TH12K017RH50PAR2C60		X			X		X		X		X	
1800	SURF	FIRST COOL	14SFC	TH12K018RH50PAR2C60		X			X		X		X		X	
2400	SURF	FIRST COOL (10K/s)	14SFC	TH12K018RH50PAR2C60		X			X		X		X		X	
2400	SURF	FIRST COOL (15K/s)	14SFC	TH12K018RH50PAR2C60		X			X		X		X		X	
3000	SURF	FIRST COOL	14SFC	TH12K018RH50PAR2C60		X			X		X		X		X	
3360	SURF	FIRST COOL	14SFC	TH12K018RH50PAR2C60		X			X		X		X		X	
1260	SURF	FIRST COOL	15SFC	TH12K019RH50PAR2C60		X		X			X		X		X	
3360	SURF	FIRST COOL	15SFC	TH12K019RH50PAR2C60		X		X			X		X		X	
3360	SURF	FIRST COOL	16SFC	TH12K017RH60PAR2C60			X			X	X		X		X	
3360	SURF	FIRST COOL	17SFC	TH12K018RH60PAR2C60			X		X		X		X		X	
3360	SURF	FIRST COOL	18SFC	TH12K019RH60PAR2C60			X	X			X		X		X	
600	SURF	FIRST COOL	37SFC	TH12K017RH40PAR1C90	X					X	X	X			X	
600	SURF	FIRST COOL	38SFC	TH12K018RH40PAR1C90	X				X		X	X			X	
600	SURF	FIRST COOL	39SFC	TH12K019RH40PAR1C90	X			X			X	X			X	
600	SURF	FIRST COOL	40SFC	TH12K017RH50PAR1C90		X				X	X	X			X	
600	SURF	FIRST COOL	41SFC	TH12K018RH50PAR1C90		X			X		X	X			X	
600	SURF	FIRST COOL*	42SFC	TH12K019RH50PAR1C90		X		X			X	X			X	
600	SURF	FIRST COOL	43SFC	TH12K017RH60PAR1C90			X			X	X	X			X	

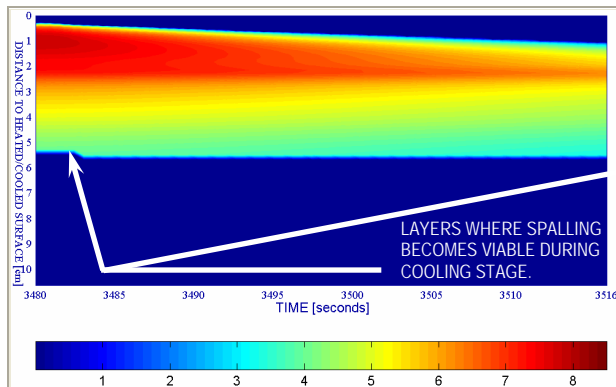
Table 6A-1. Forty five resulting combinations of the parameters' values initially considered.

(continued)

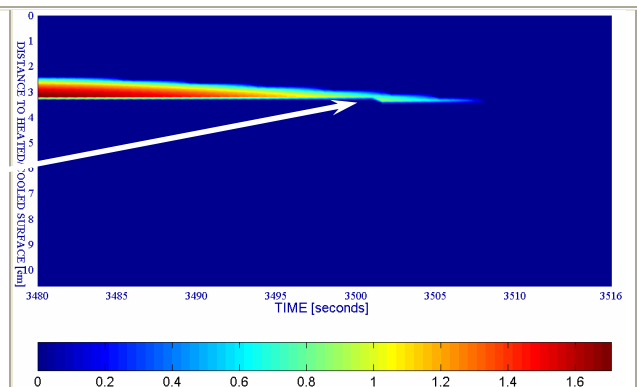
COOLING START TIME [s]	COOLING TYPE	COOLING SUBTYPE	CODE	Combination	PC1 (RH) [%]			PC2 (K) [m ²]			PC3 (TH) [cm]			PC4 (Heating curve)			PC5 (Mat)		
600	SURF	FIRST COOL	44SFC	TH12K018RH60PAR1C90			X		X		X	X						X	
600	SURF	FIRST COOL	45SFC	TH12K019RH60PAR1C90			X	X			X	X						X	
3360	SURF	FIRST COOL	46SFC	TH12K017RH40PAR2C90	X					X	X		X					X	
3360	SURF	FIRST COOL	47SFC	TH12K018RH40PAR2C90	X				X		X		X					X	
3360	SURF	FIRST COOL	48SFC	TH12K019RH40PAR2C90	X				X		X		X					X	
3360	SURF	FIRST COOL	49SFC	TH12K017RH50PAR2C90		X				X	X		X					X	
1800	SURF	FIRST COOL	50SFC	TH12K018RH50PAR2C90		X			X		X		X					X	
3360	SURF	FIRST COOL	50SFC	TH12K018RH50PAR2C90		X			X		X		X					X	
1260	SURF	FIRST COOL	51SFC	TH12K019RH50PAR2C90		X		X			X		X					X	
1560	SURF	FIRST COOL	51SFC	TH12K019RH50PAR2C90		X		X			X		X					X	
3360	SURF	FIRST COOL	51SFC	TH12K019RH50PAR2C90		X		X			X		X					X	
3360	SURF	FIRST COOL	52SFC	TH12K017RH60PAR2C90			X			X	X		X		X			X	
3360	SURF	FIRST COOL	53SFC	TH12K018RH60PAR2C90			X		X		X		X		X			X	
3360	SURF	FIRST COOL	54SFC	TH12K019RH60PAR2C90			X	X			X		X		X			X	
4800	SURF	FIRST COOL	100SFC	TH12K019RH50PAR3C90		X		X			X		X		X			X	

Table 6A-1. Forty five resulting combinations of the parameters' values initially considered (continued)

From the analysis of figures 6A-1 to 6A-45 (and more precisely from the evolution of the Spalling Index I_{s4} shown at the upper left corner of each group of four Cartesian continuum representations) it is clearly observed that, as it was already described on the analyses of the reference cases developed in Chapter 6, the values of the Spalling Index I_{s4} always decrease at all the depths as soon as the surface cooling process starts being reduced, hence, the risk of Thermal Spalling during this process (what does not mean that Thermal Spalling is no longer viable during the surface cooling process if, for instance, layers where Thermal Spalling would be energetically viable but mechanical damage showed too low values during heating increase their level of cracking during the cooling stage enabling mechanically the development of Thermal Spalling). This situation is detectable by means of the analysis of the lower right corner of each group of four Cartesian continuum representations (which shows the evolution of the velocity of spalled-off pieces at those layers with mechanical damage values higher than the 10 per cent): for instance, it can be clearly observed in cases corresponding to figures 6A-3 (code 3SFC), 6A-5 (code 5SFC), 6A-6 (code 6SFC), 6a-8 (code 8SFC), 6a-12 (code 12SFC), 6a-24 (code 37SFC), 6a-25 (code 38SFC), 6a-26 (code 39SFC), 6a-27 (code 40SFC), 6a-31 (code 44SFC), 6a-32 (code 45SFC), 6a-33 (code 46SFC) and 6a-41 (code 51SFC), as it is explained on the next examples:



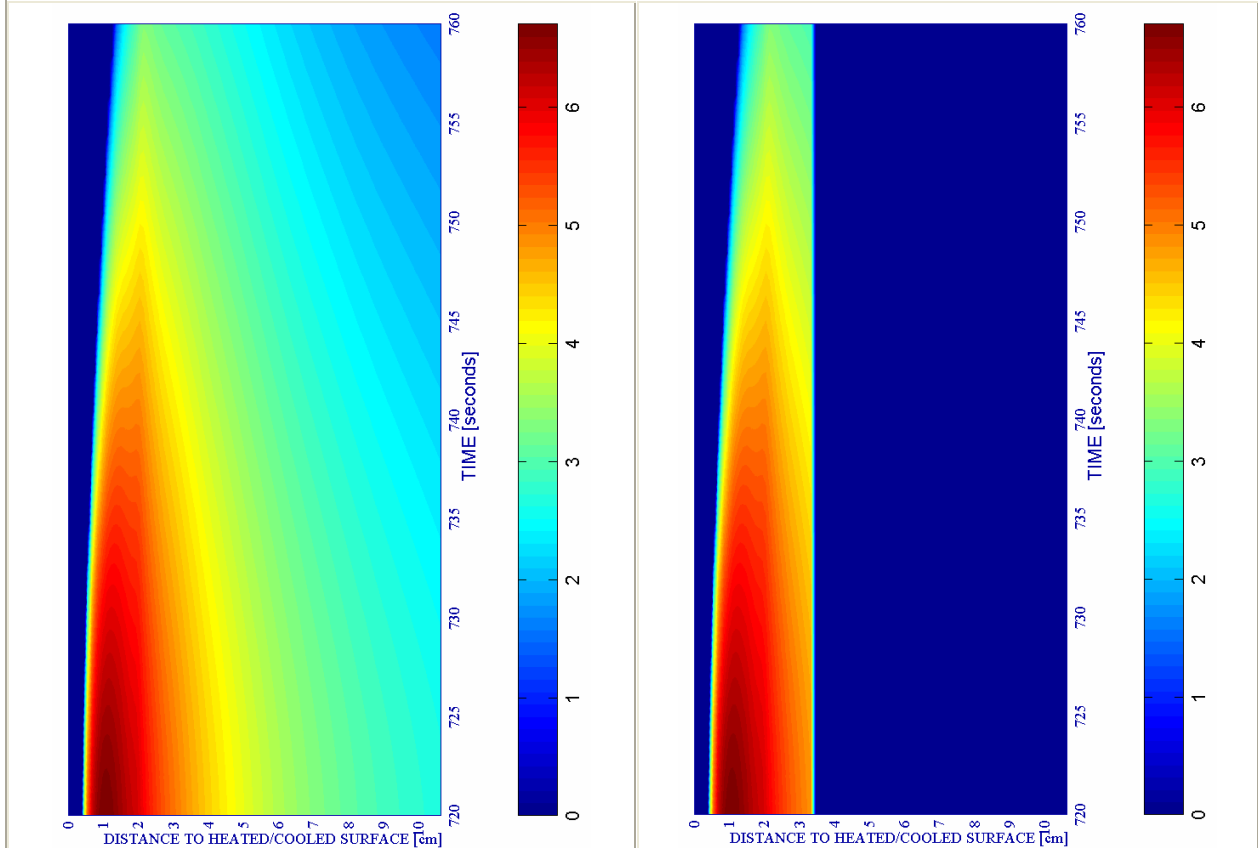
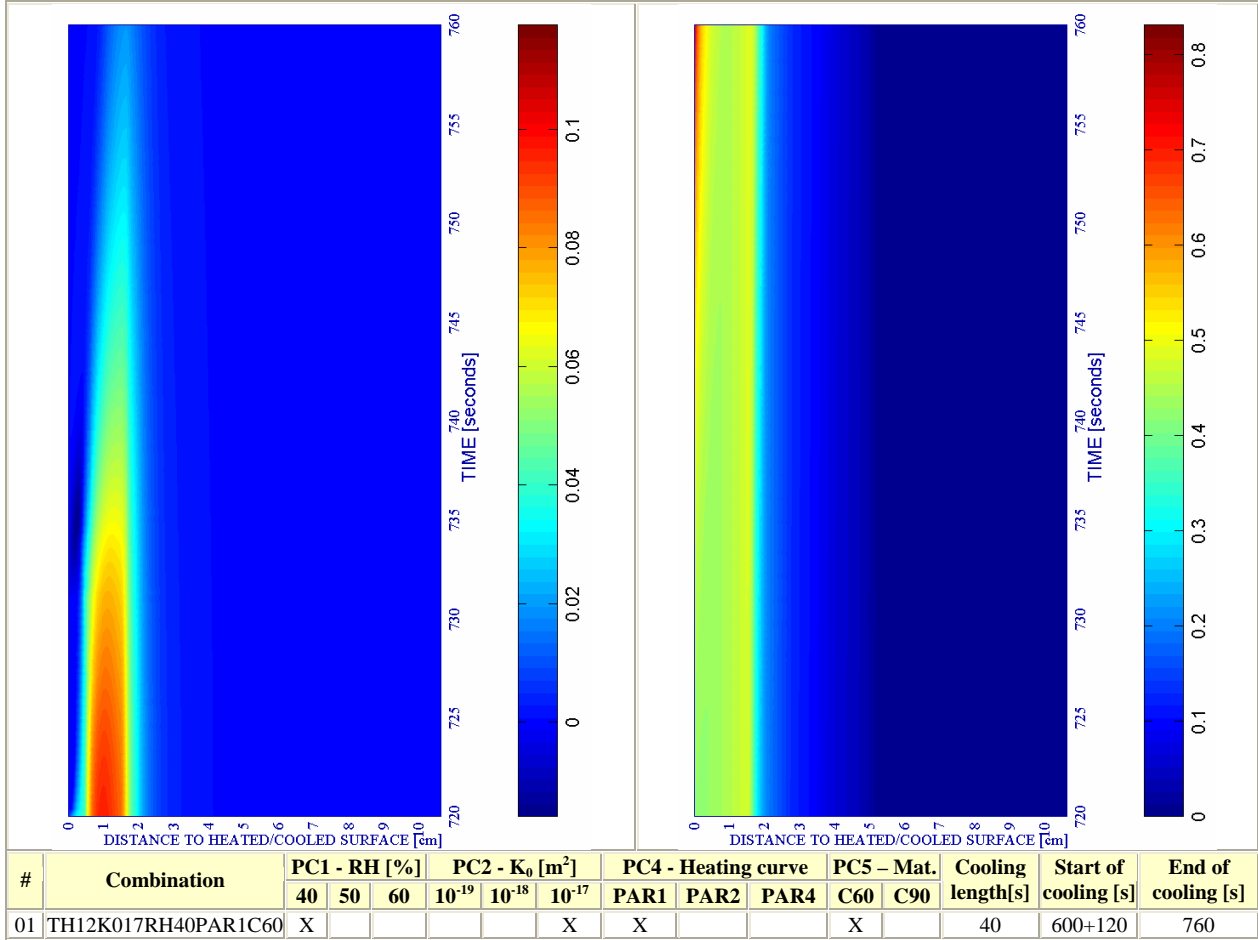
Example 1: Case 12SFC (figure (6A-12 d))



Example 2: Case 46SFC (figure 6A-33 d))

a) Up left: Spalling Index IS_4 [-]

b) Up right: Mechanical damage d [-]



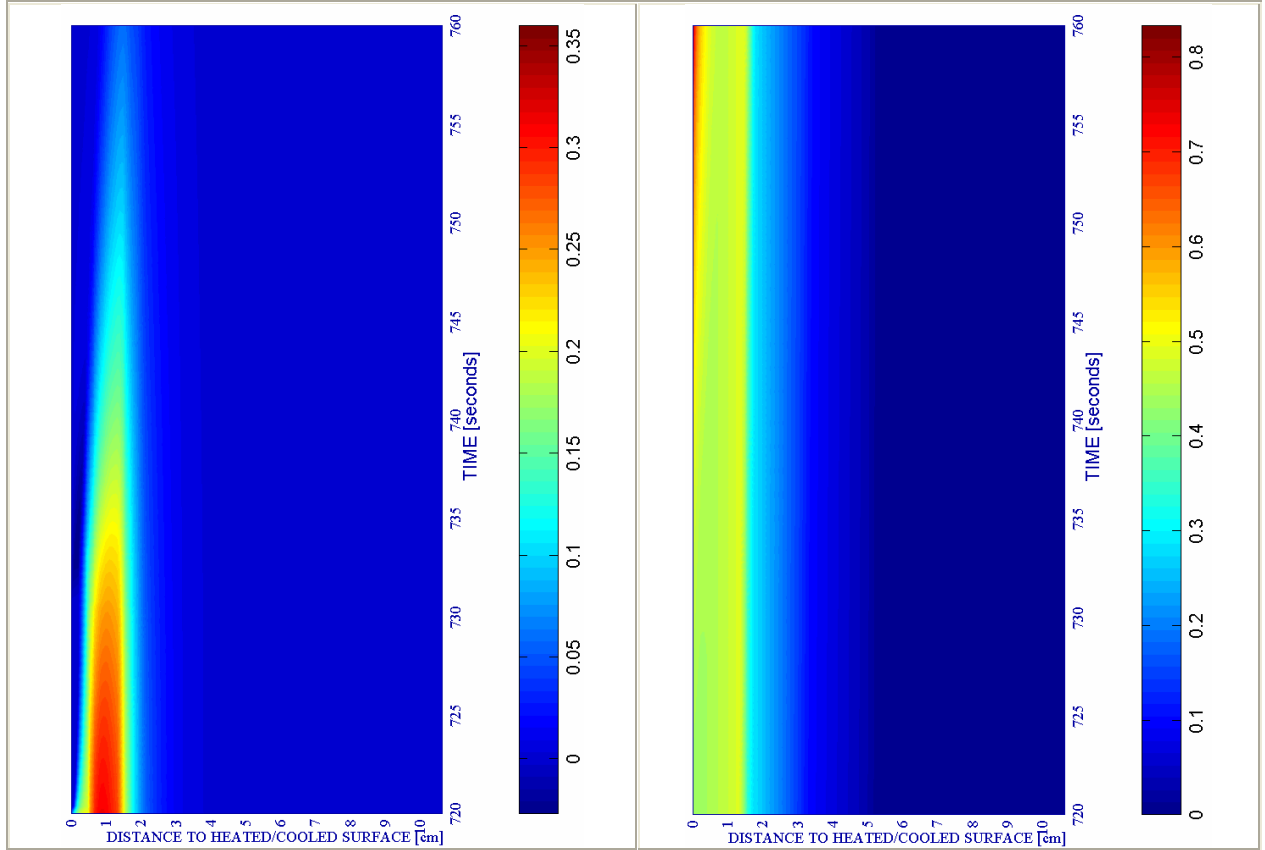
c) Down left: Velocity of spalled pieces [m/s]

Figure 6A-1.

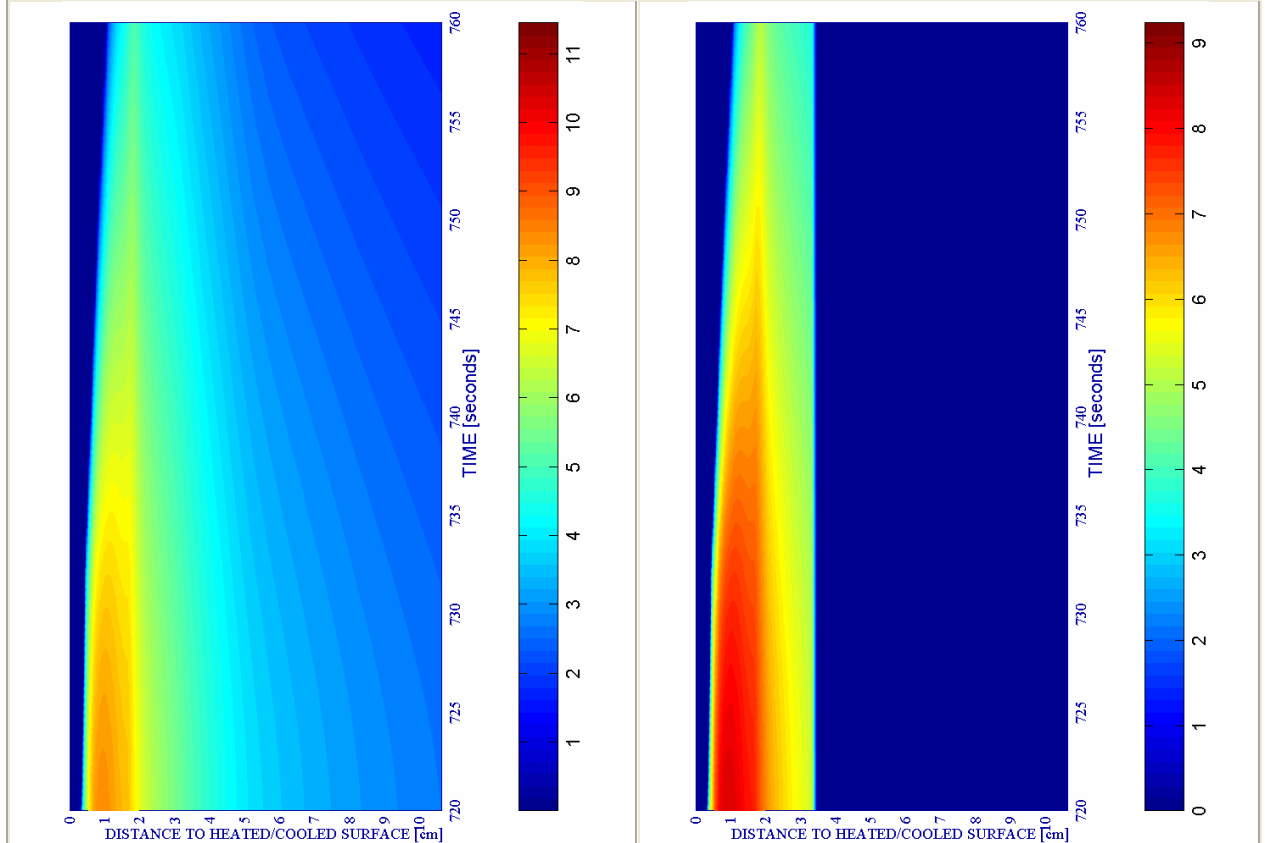
d) Down right: Velocity [m/s] where $d \geq 0,10$

a) Up left: Spalling Index IS_4 [-]

b) Up right: Mechanical damage d [-]



#	Combination	PC1 - RH [%]			PC2 - K_0 [m ²]			PC4 - Heating curve			PC5 - Mat.		Cooling length[s]	Start of cooling [s]	End of cooling [s]
		40	50	60	10 ⁻¹⁹	10 ⁻¹⁸	10 ⁻¹⁷	PAR1	PAR2	PAR4	C60	C90			
02	TH12K018RH40PAR1C60	X				X		X			X		40	600+120	760



c) Down left: Velocity of spalled pieces [m/s]

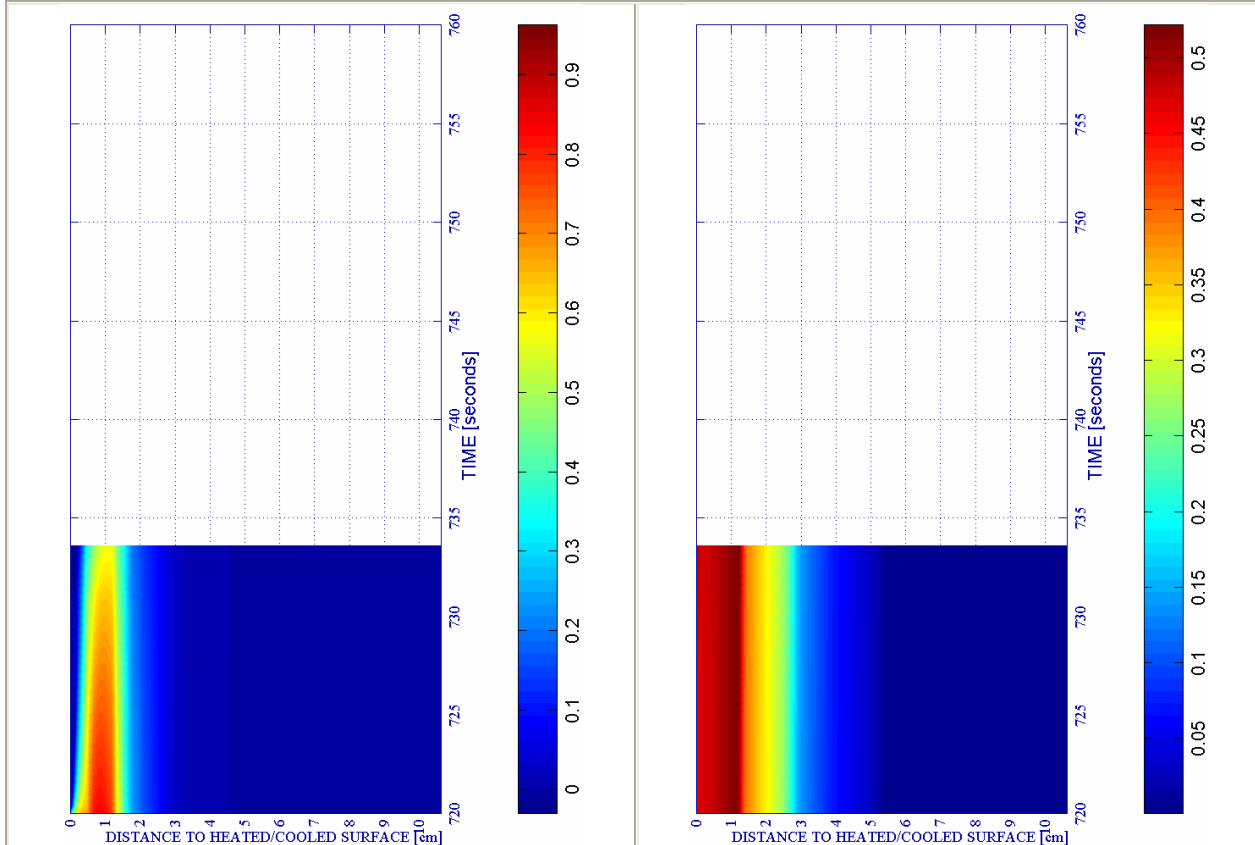
Figure 6A-2.

d) Down right: Velocity [m/s] where $d \geq 0,10$

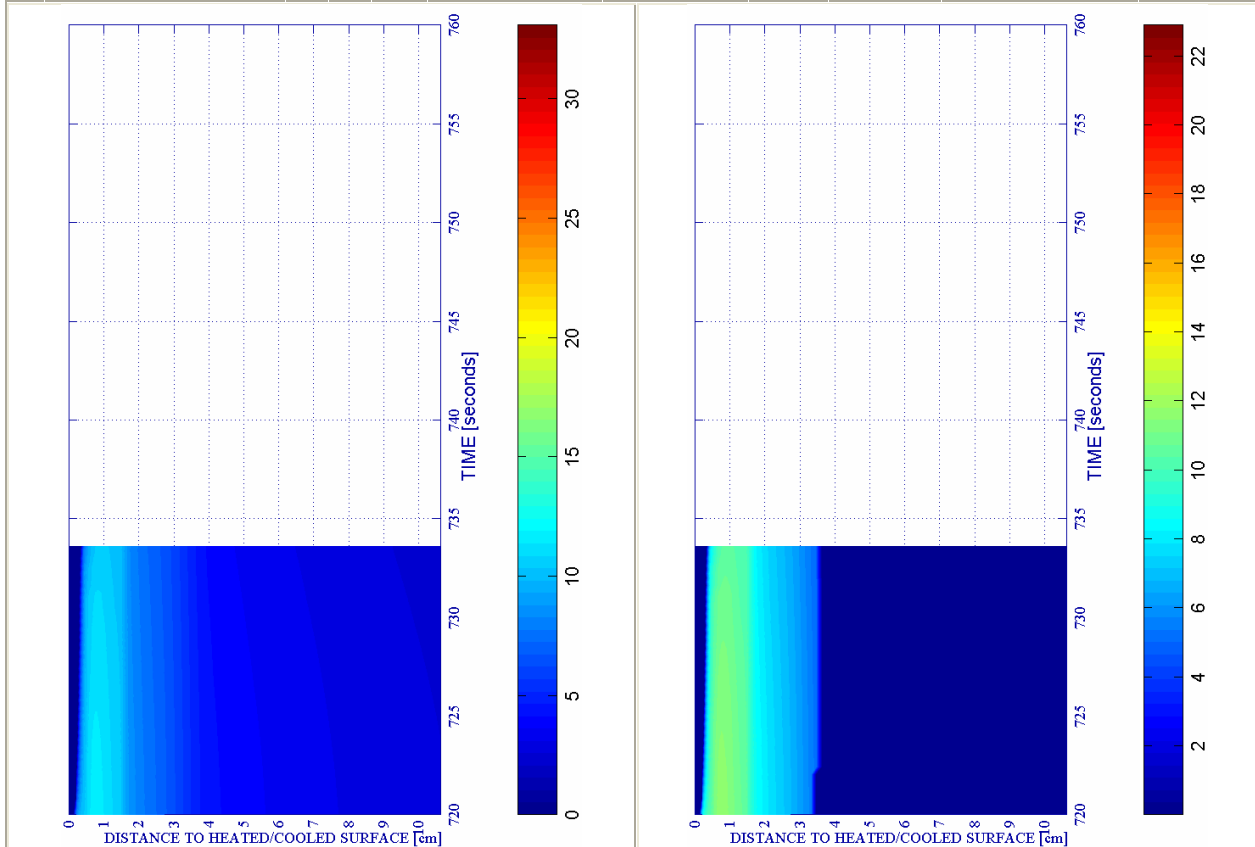
a) Up left: Spalling Index IS4 [-]

*Remark: Calculation failed at 733,7s

b) Up right: Mechanical damage d [-]



#	Combination	PC1 - RH [%]			PC2 - K ₀ [m ²]			PC4 - Heating curve			PC5 - Mat.		Cooling length[s]	Start of cooling [s]	End of cooling [s]
		40	50	60	10 ⁻¹⁹	10 ⁻¹⁸	10 ⁻¹⁷	PAR1	PAR2	PAR4	C60	C90			
03	TH12K019RH40PAR1C60	X			X			X			X		40	600+120	760*



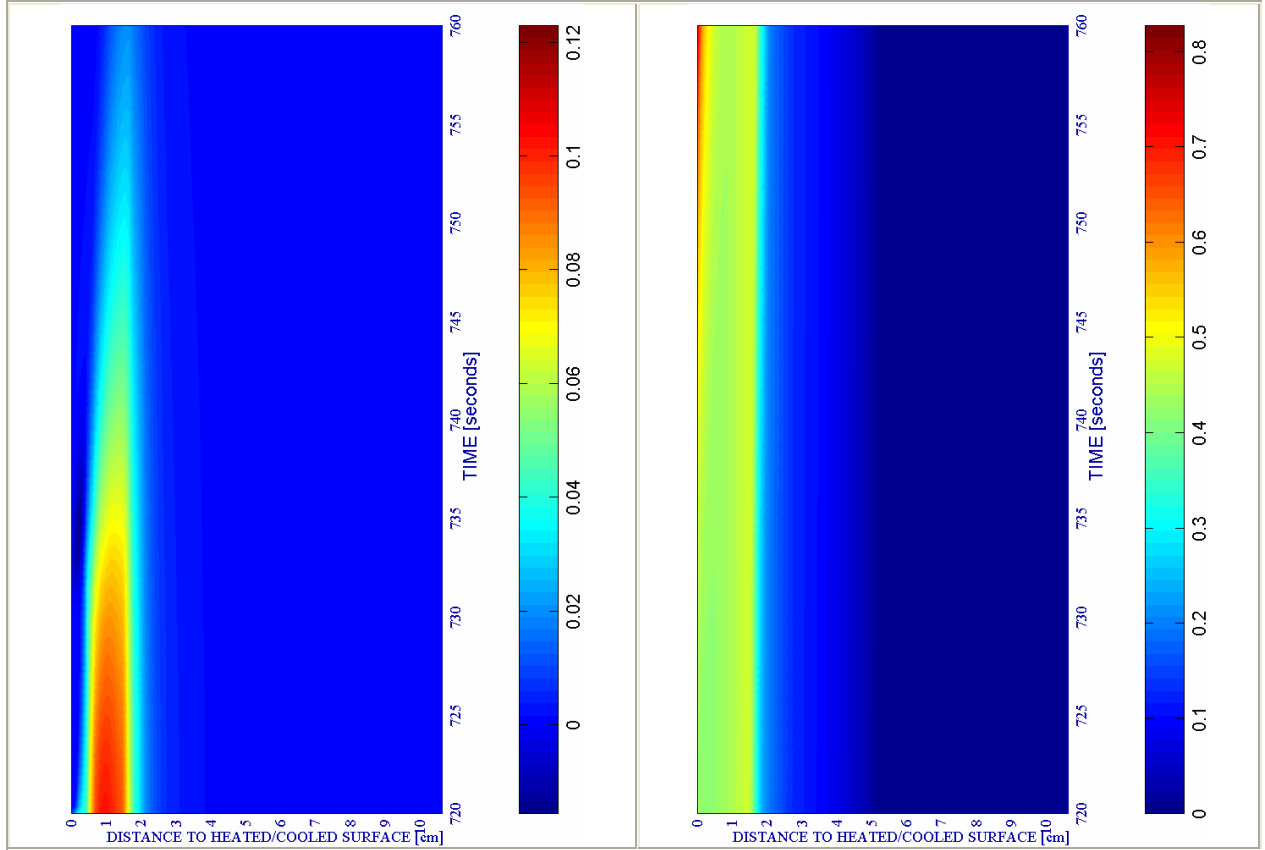
c) Down left: Velocity of spalled pieces [m/s]

Figure 6A-3.

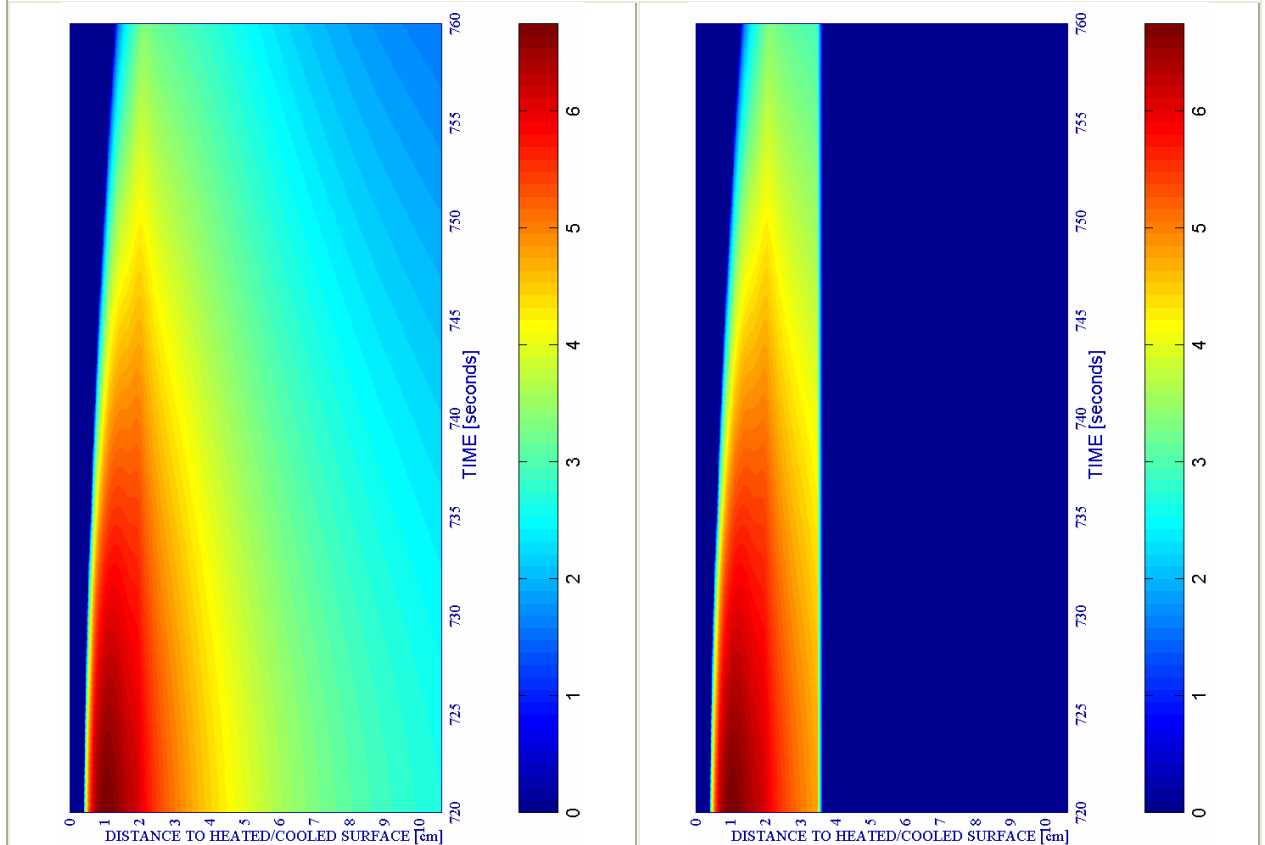
d) Down right: Velocity [m/s] where $d \geq 0,10$

a) Up left: Spalling Index IS_4 [-]

b) Up right: Mechanical damage d [-]



#	Combination	PC1 - RH [%]			PC2 - K_0 [m ²]			PC4 - Heating curve			PC5 - Mat.		Cooling length[s]	Start of cooling [s]	End of cooling [s]
		40	50	60	10 ⁻¹⁹	10 ⁻¹⁸	10 ⁻¹⁷	PAR1	PAR2	PAR4	C60	C90			
04	TH12K017RH50PAR1C60		X				X	X			X		40	600+120	760



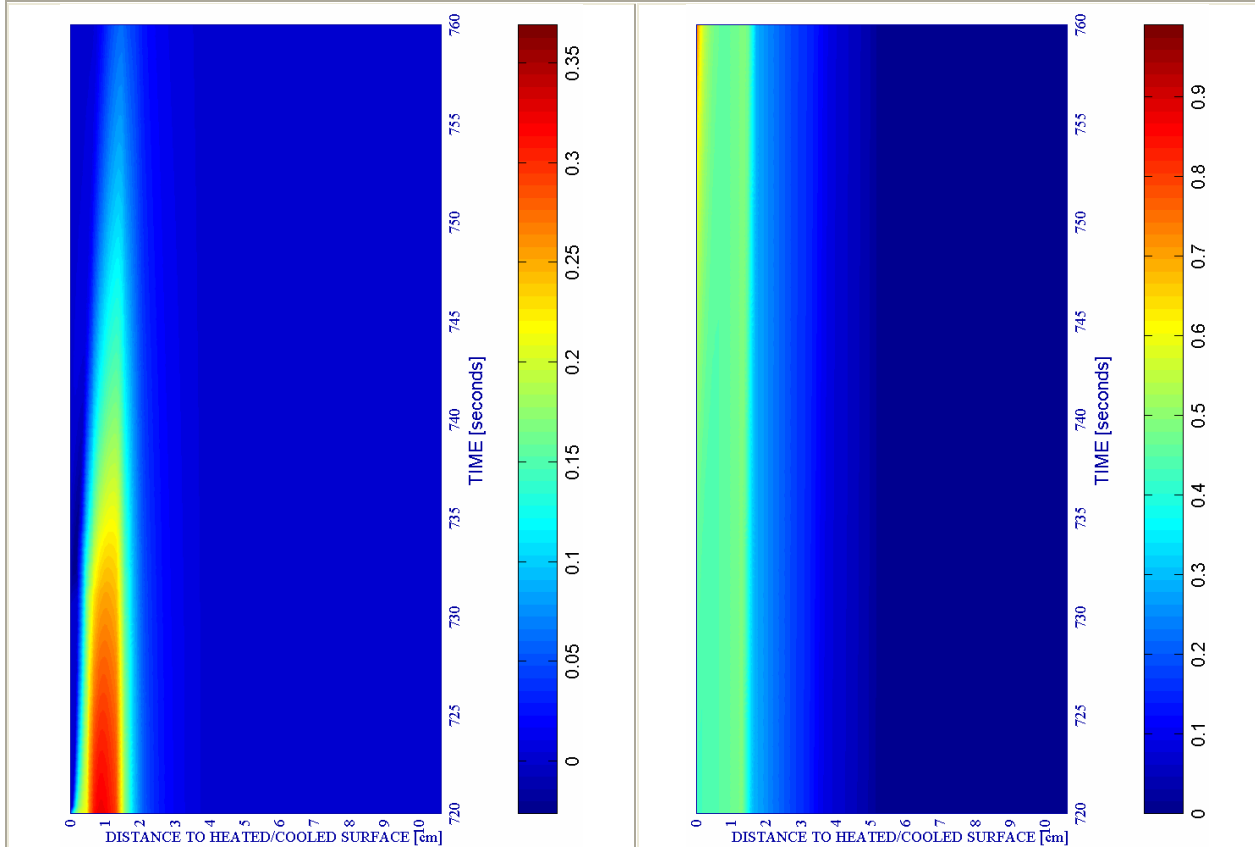
c) Down left: Velocity of spalled pieces [m/s]

Figure 6A-4.

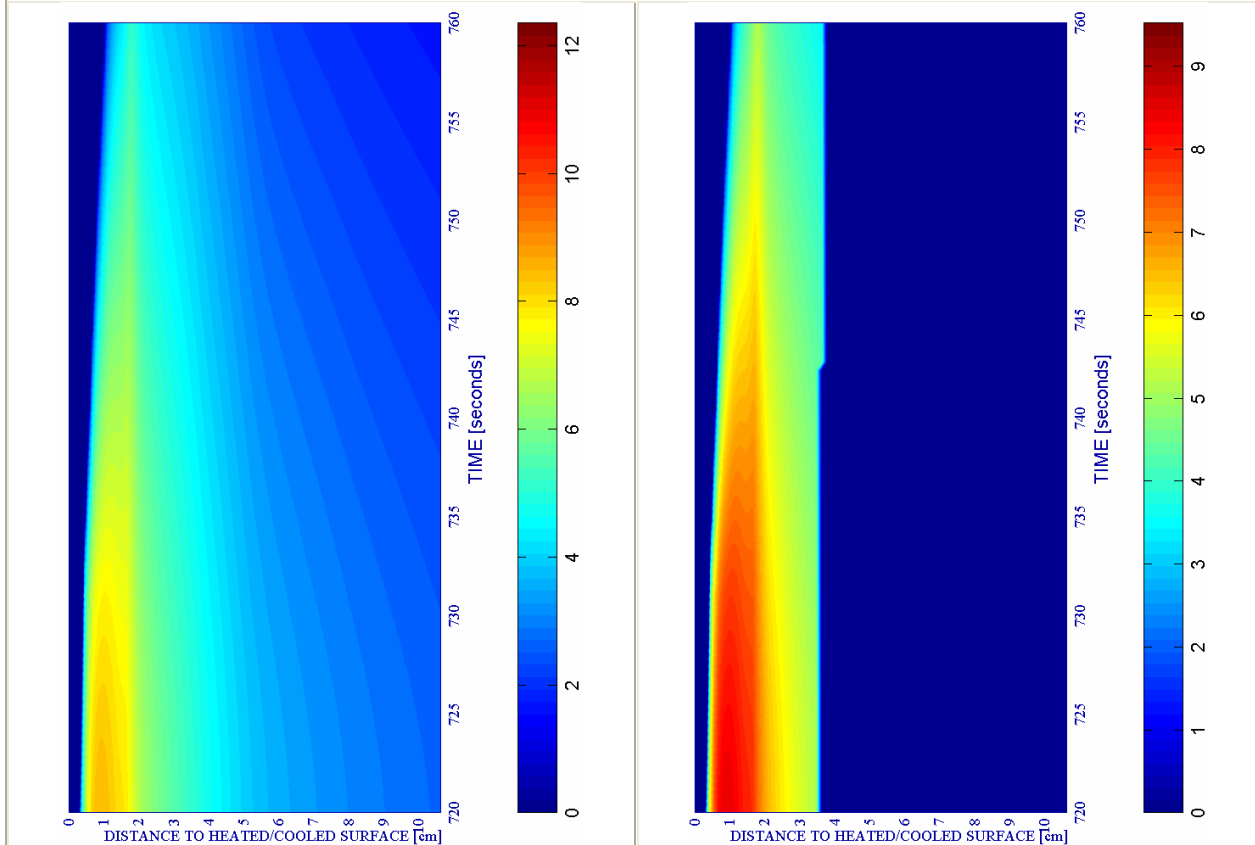
d) Down right: Velocity [m/s] where $d \geq 0,10$

a) Up left: Spalling Index IS_4 [-]

b) Up right: Mechanical damage d [-]



#	Combination	PC1 - RH [%]			PC2 - K_0 [m^2]			PC4 - Heating curve			PC5 - Mat.		Cooling length[s]	Start of cooling [s]	End of cooling [s]
		40	50	60	10^{-19}	10^{-18}	10^{-17}	PAR1	PAR2	PAR4	C60	C90			
05	TH12K018RH50PAR1C60		X			X		X			X		40	600+120	760



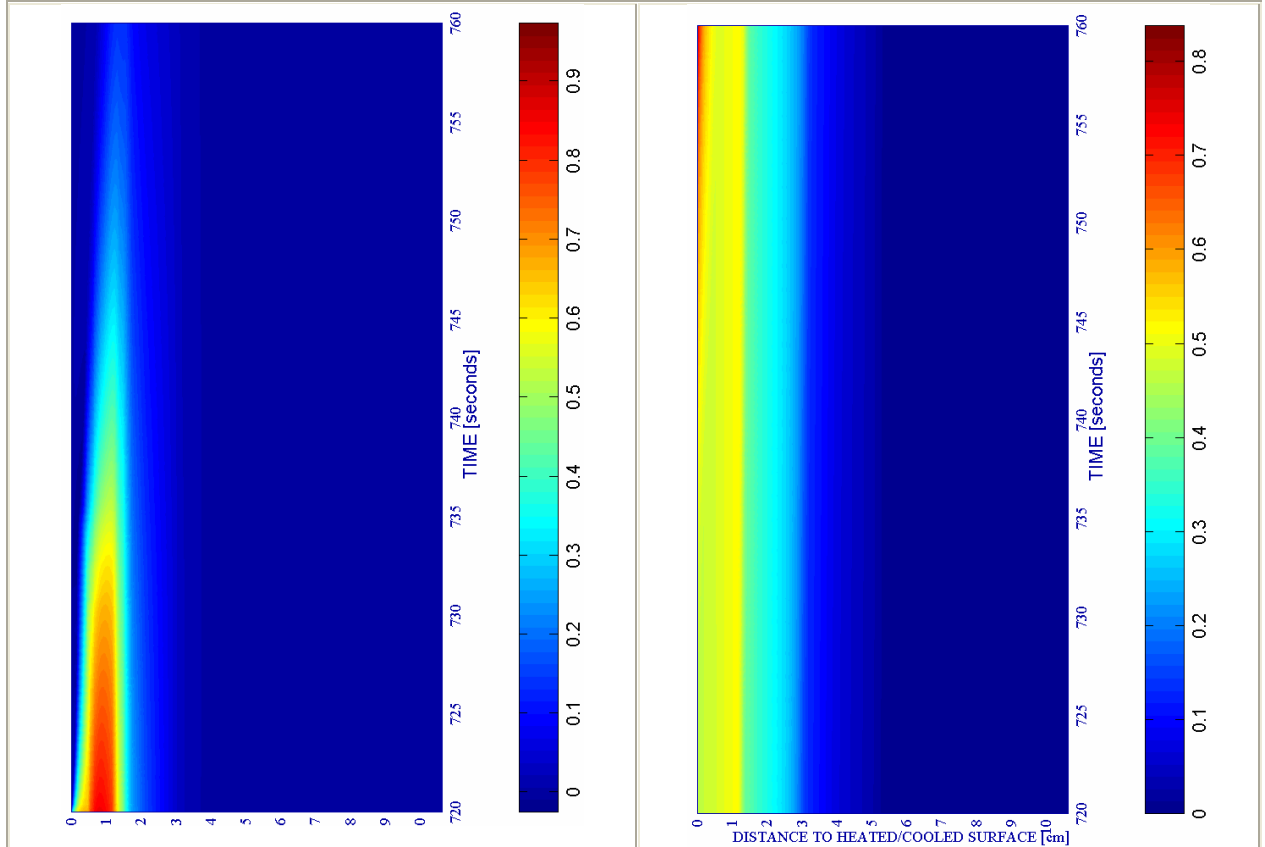
c) Down left: Velocity of spalled pieces [m/s]

Figure 6A-5.

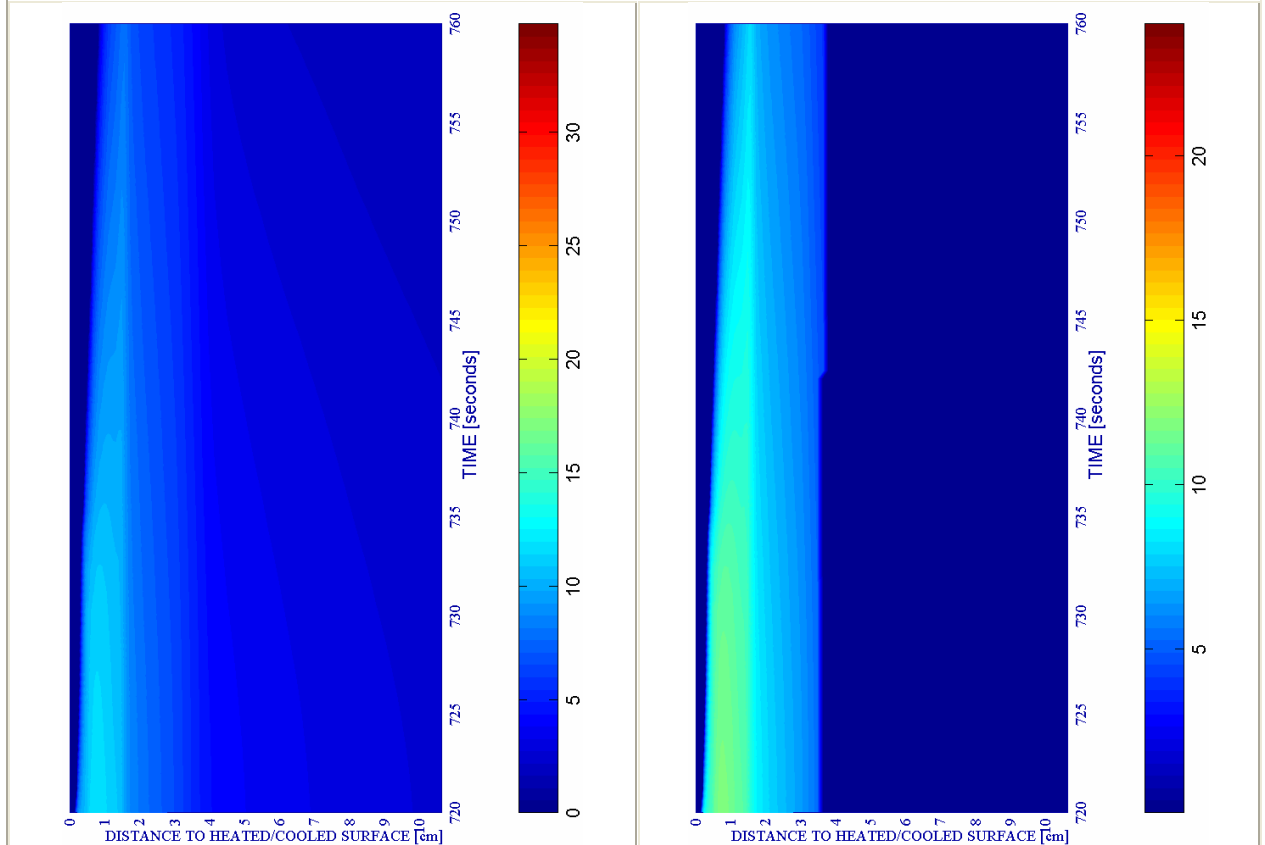
d) Down right: Velocity [m/s] where $d \geq 0,10$

a) Up left: Spalling Index IS_4 [-]

b) Up right: Mechanical damage d [-]



#	Combination	PC1 - RH [%]			PC2 - K_0 [m ²]			PC4 - Heating curve			PC5 - Mat.		Cooling length[s]	Start of cooling [s]	End of cooling [s]
		40	50	60	10 ⁻¹⁹	10 ⁻¹⁸	10 ⁻¹⁷	PAR1	PAR2	PAR4	C60	C90			
06	TH12K019RH50PAR1C60		X		X			X			X		40	600+120	760



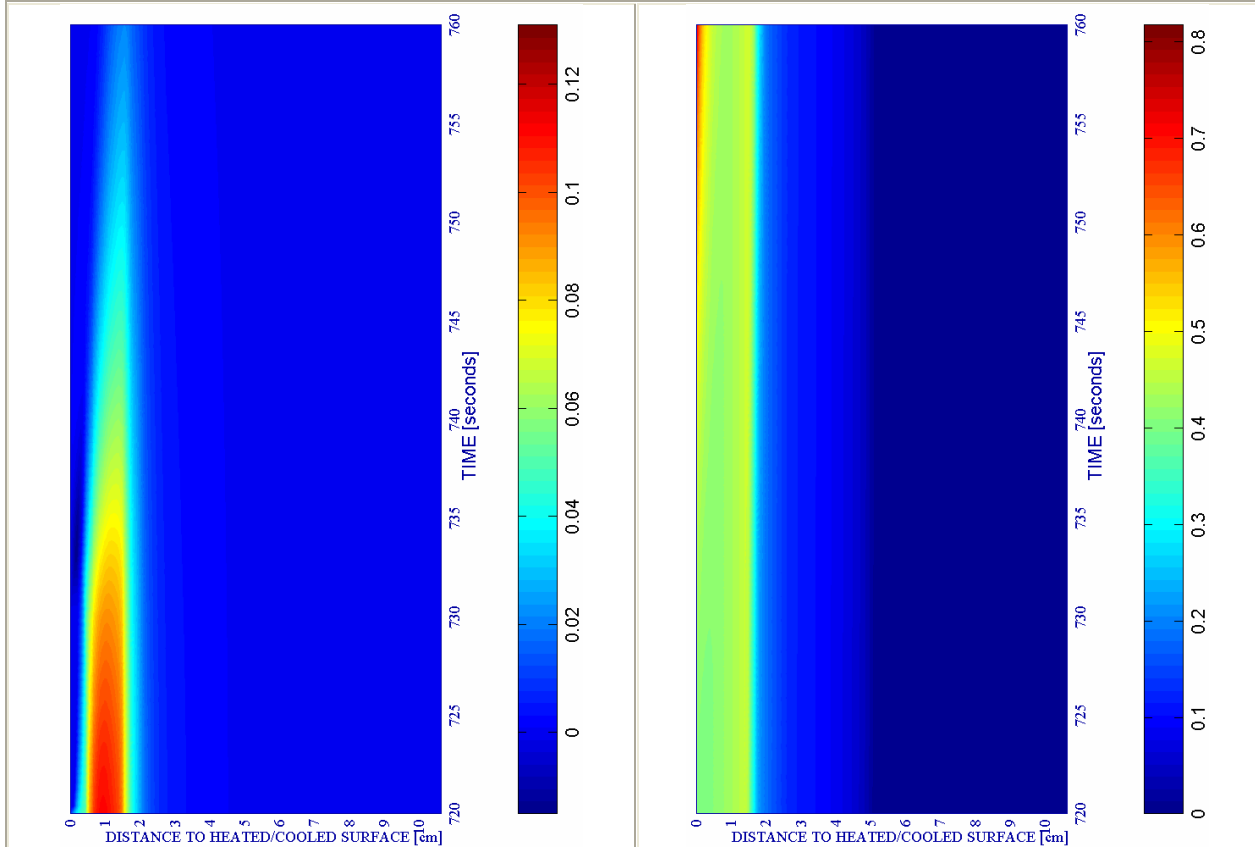
c) Down left: Velocity of spalled pieces [m/s]

Figure 6A-6.

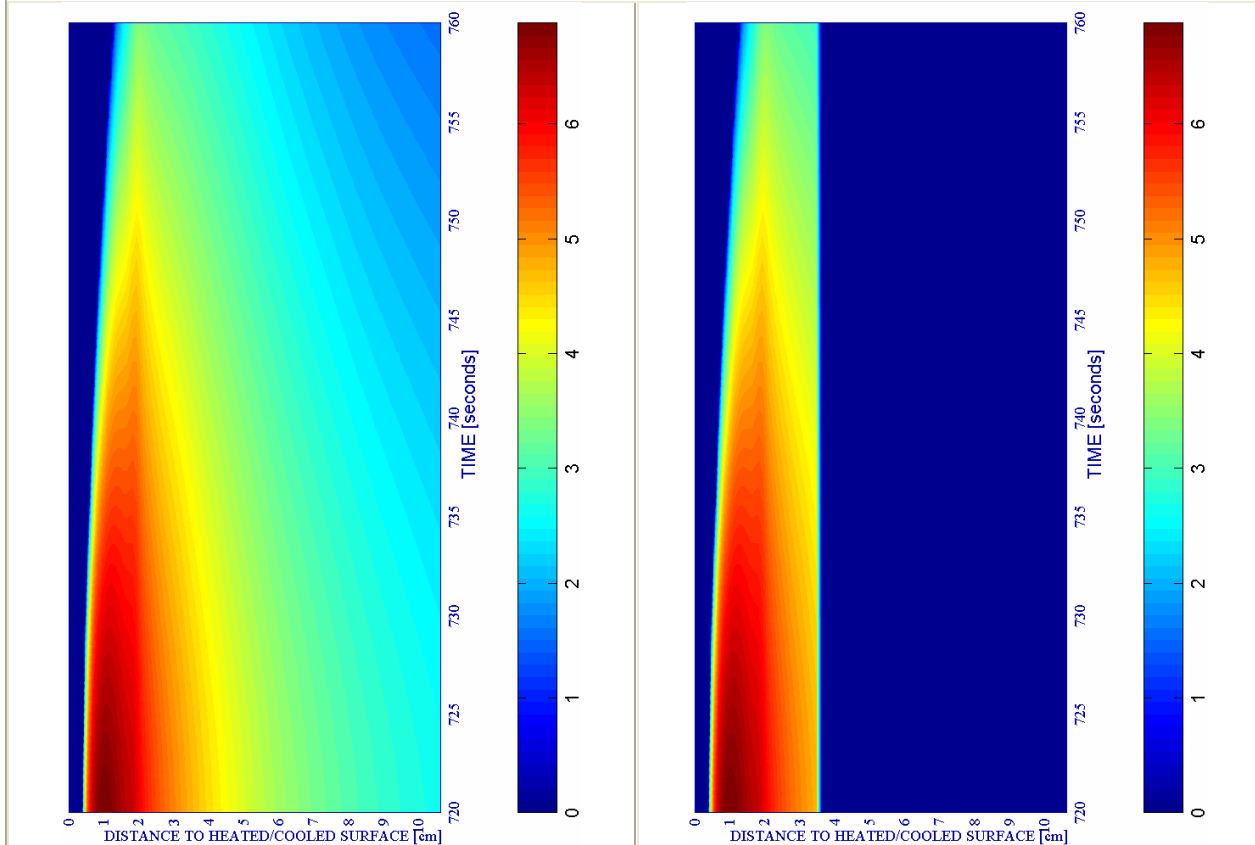
d) Down right: Velocity [m/s] where $d \geq 0,10$

a) Up left: Spalling Index IS_4 [-]

b) Up right: Mechanical damage d [-]



#	Combination	PC1 - RH [%]			PC2 - K_0 [m ²]			PC4 - Heating curve			PC5 - Mat.		Cooling length[s]	Start of cooling [s]	End of cooling [s]
		40	50	60	10 ⁻¹⁹	10 ⁻¹⁸	10 ⁻¹⁷	PAR1	PAR2	PAR4	C60	C90			
07	TH12K019RH50PAR1C60		X		X			X			X		40	600+120	760



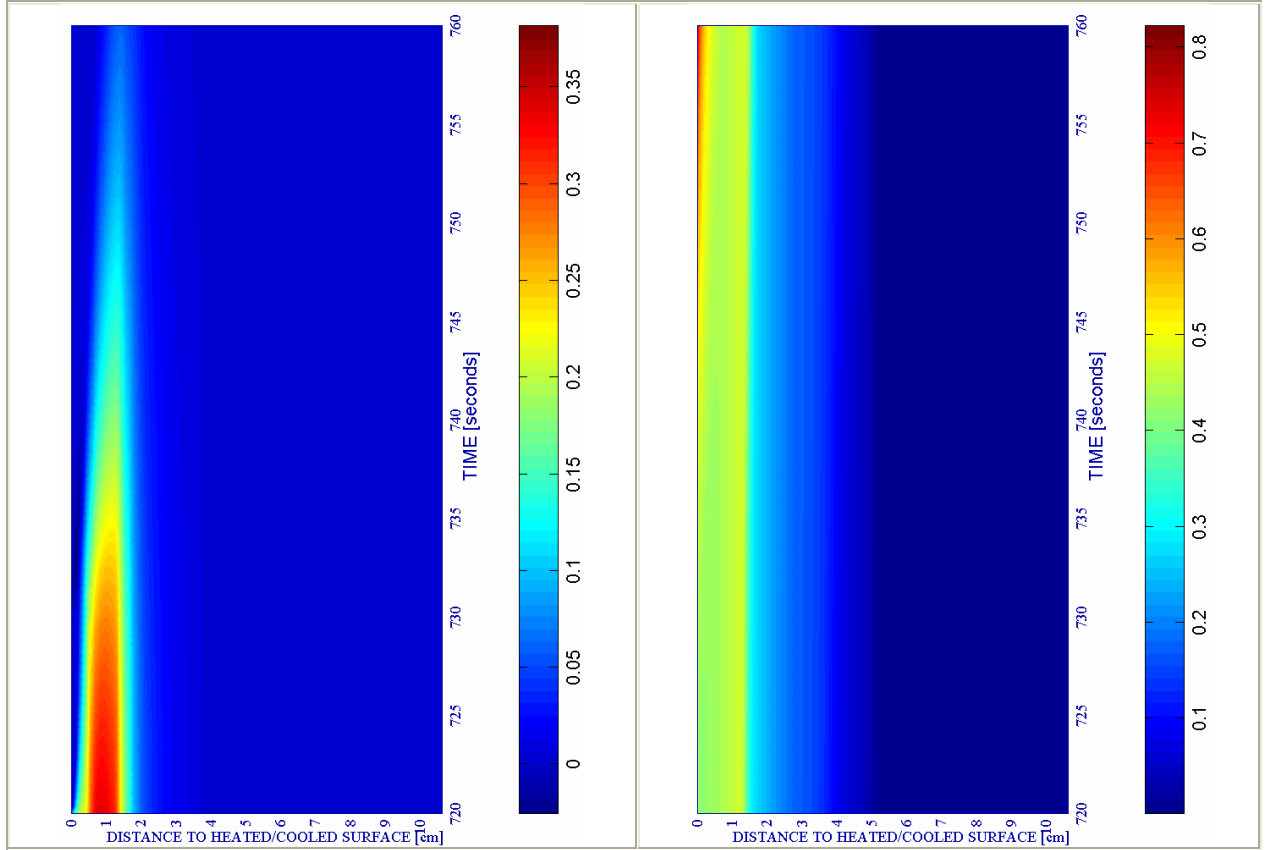
c) Down left: Velocity of spalled pieces [m/s]

Figure 6A-7.

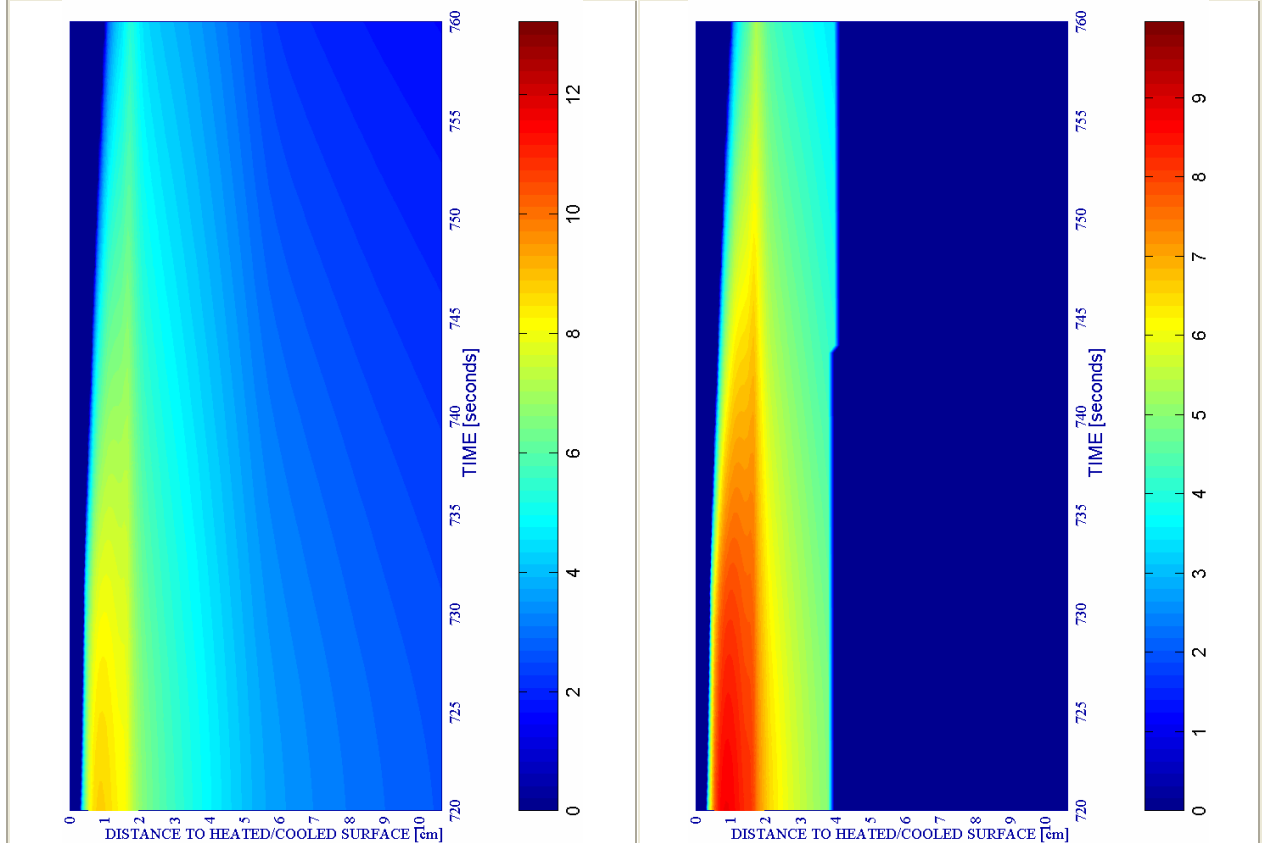
d) Down right: Velocity [m/s] where $d \geq 0,10$

a) Up left: Spalling Index IS_4 [-]

b) Up right: Mechanical damage d [-]



#	Combination	PC1 - RH [%]			PC2 - K_0 [m ²]			PC4 - Heating curve			PC5 - Mat.		Cooling length[s]	Start of cooling [s]	End of cooling [s]
		40	50	60	10 ⁻¹⁹	10 ⁻¹⁸	10 ⁻¹⁷	PAR1	PAR2	PAR4	C60	C90			
08	TH12K018RH60PAR1C60			X		X		X			X		40	600+120	760



c) Down left: Velocity of spalled pieces [m/s]

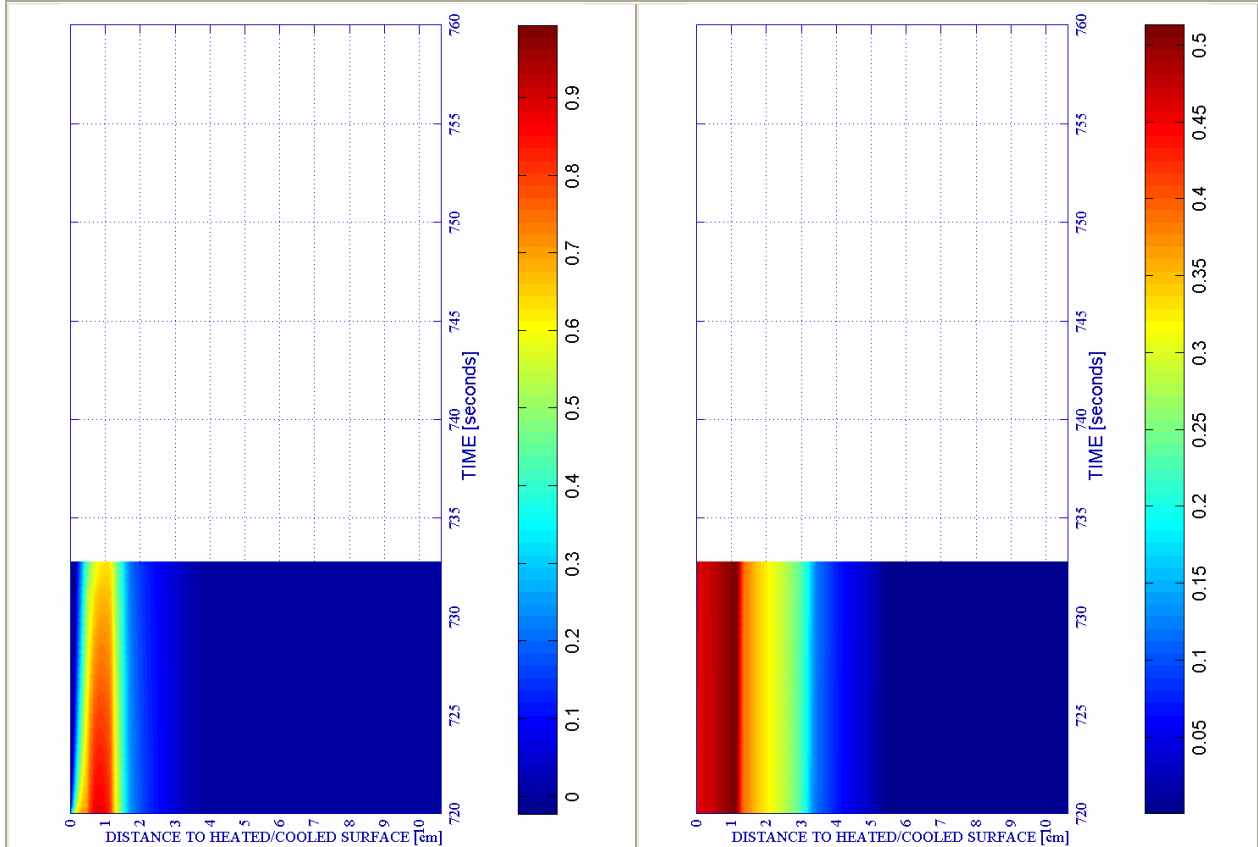
Figure 6A-8.

d) Down right: Velocity [m/s] where $d \geq 0,10$

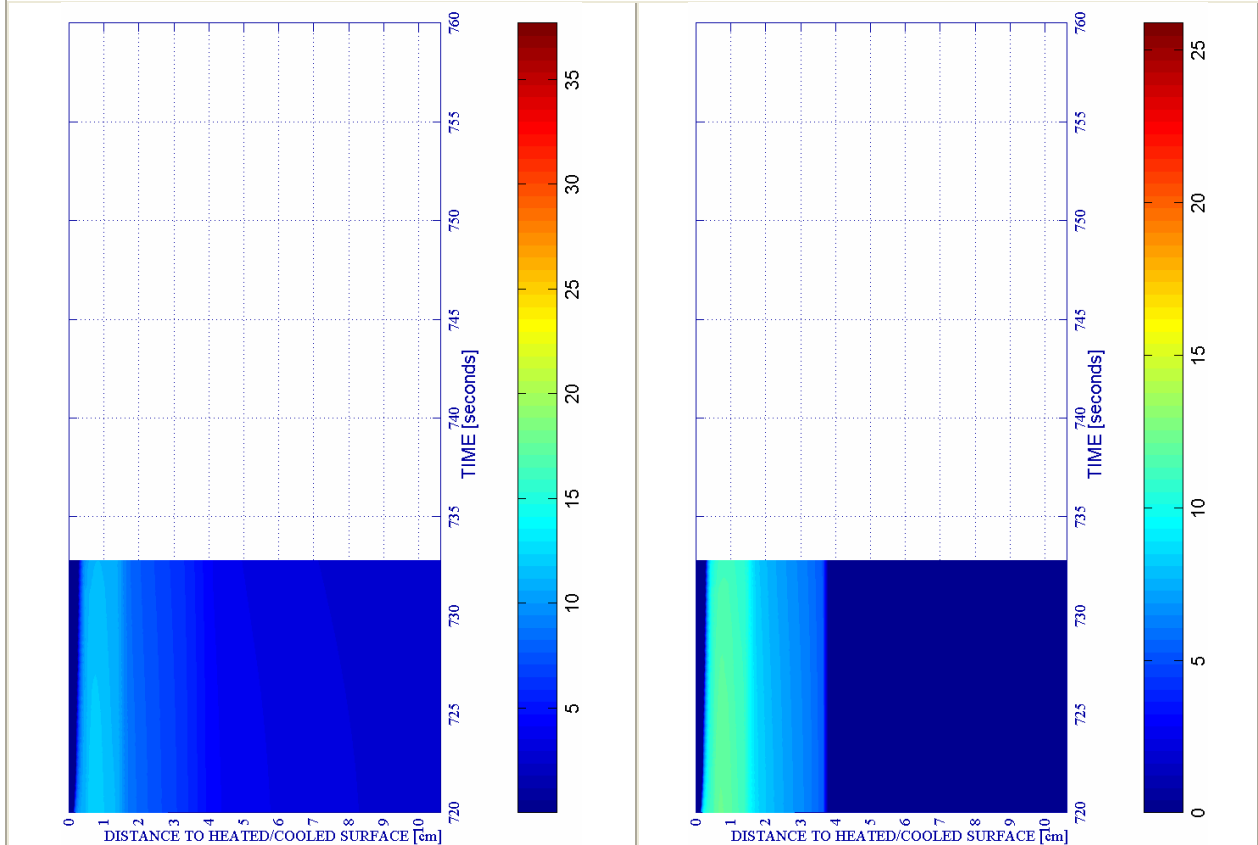
a) Up left: Spalling Index IS_4 [-]

*Remark: Calculation failed at 733,1s

b) Up right: Mechanical damage d [-]



#	Combination	PC1 - RH [%]			PC2 - K_0 [m^2]			PC4 - Heating curve			PC5 - Mat.		Cooling length[s]	Start of cooling [s]	End of cooling [s]
		40	50	60	10^{-19}	10^{-18}	10^{-17}	PAR1	PAR2	PAR4	C60	C90			
09	TH12K019RH60PAR1C60			X	X			X			X		40	600+120	760*



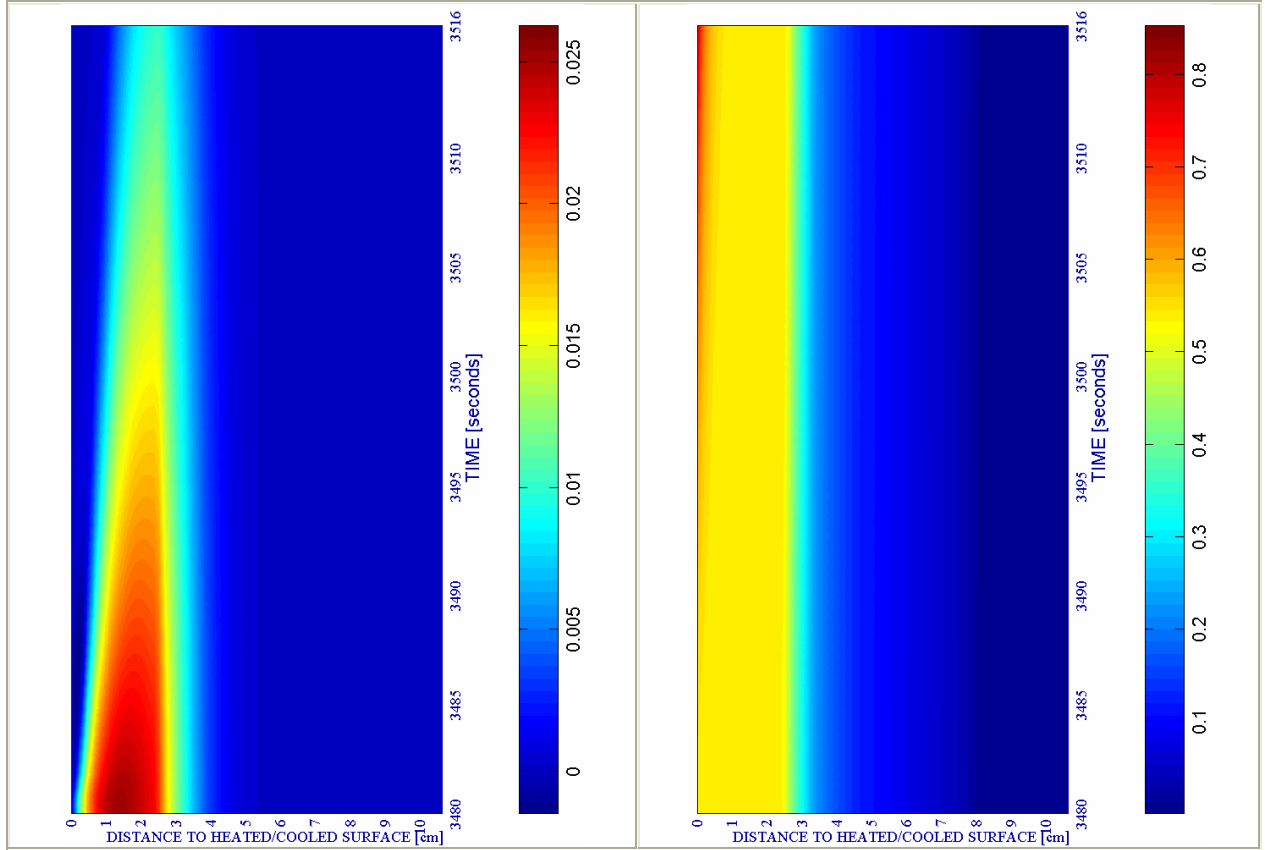
c) Down left: Velocity of spalled pieces [m/s]

Figure 6A-9.

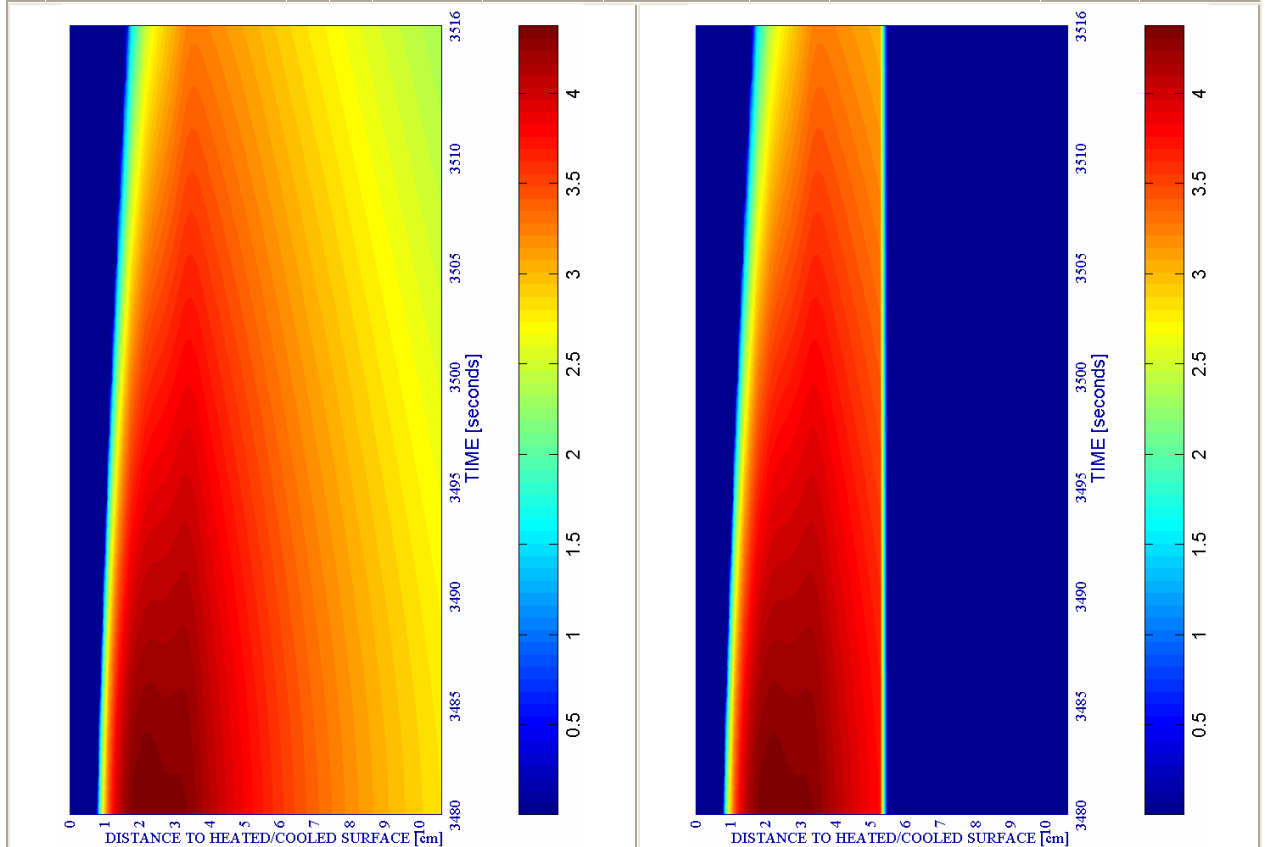
d) Down right: Velocity [m/s] where $d \geq 0,10$

a) Up left: Spalling Index IS_4 [-]

b) Up right: Mechanical damage d [-]



#	Combination	PC1 - RH [%]			PC2 - K_0 [m ²]			PC4 - Heating curve			PC5 - Mat.		Cooling length[s]	Start of cooling [s]	End of cooling [s]
		40	50	60	10 ⁻¹⁹	10 ⁻¹⁸	10 ⁻¹⁷	PAR1	PAR2	PAR4	C60	C90			
10	TH12K017RH40PAR2C60	X					X		X		X		36	3360+120	3516



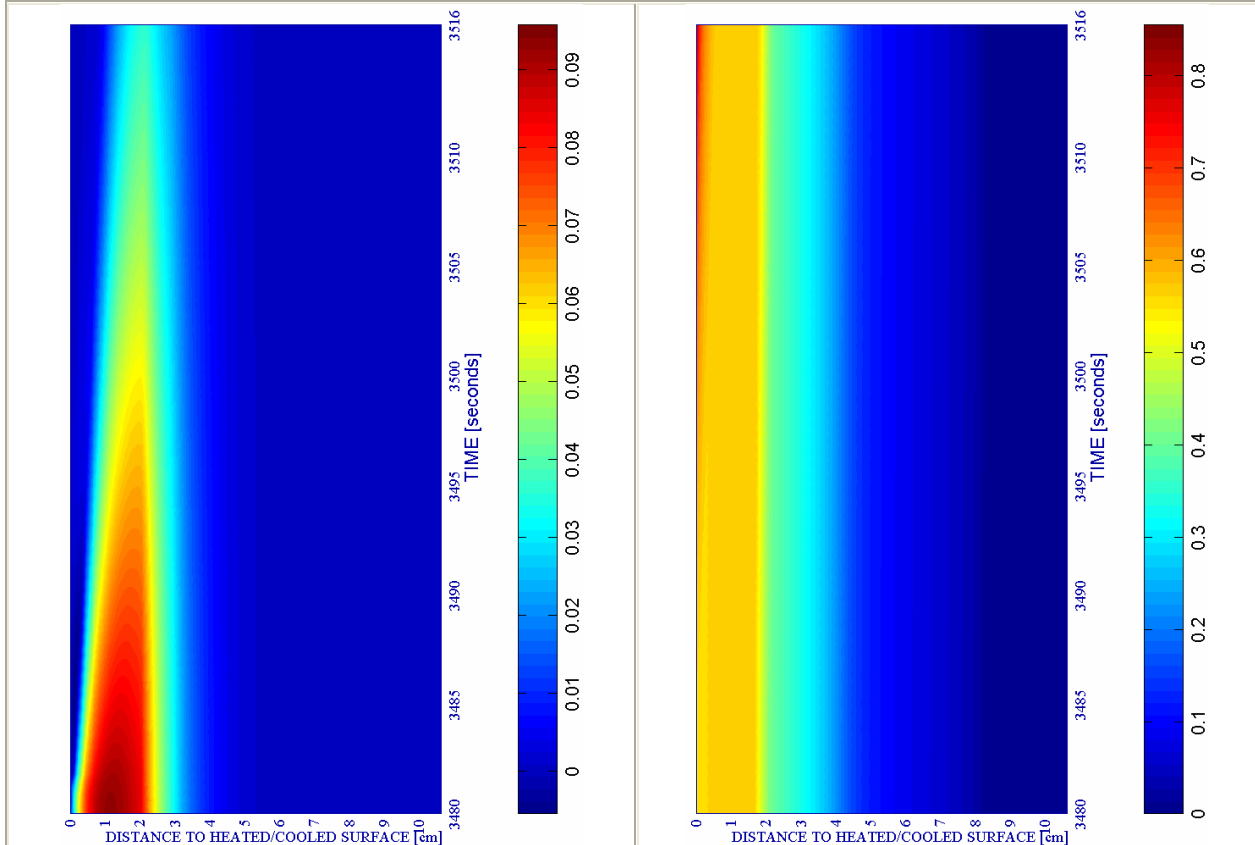
c) Down left: Velocity of spalled pieces [m/s]

Figure 6A-10.

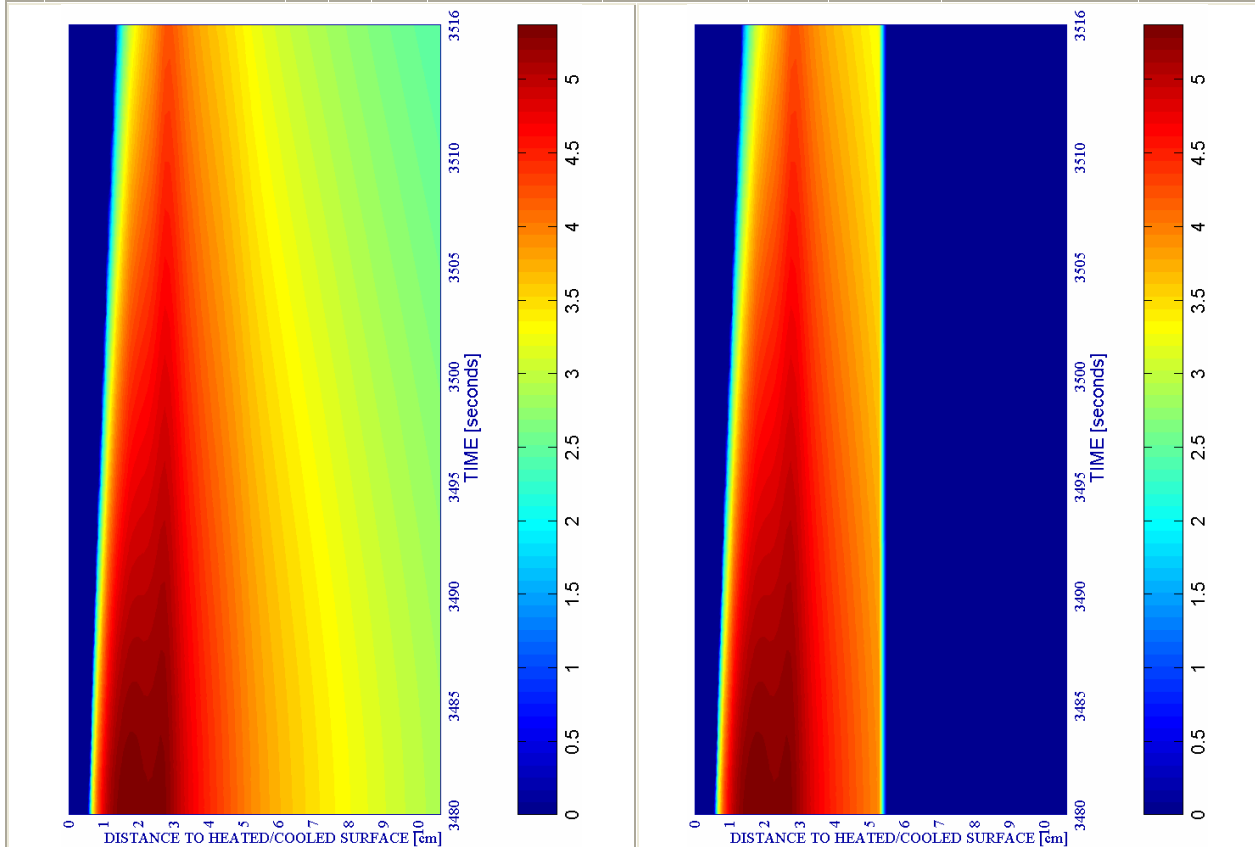
d) Down right: Velocity [m/s] where $d \geq 0,10$

a) Up left: Spalling Index IS_4 [-]

b) Up right: Mechanical damage d [-]



#	Combination	PC1 - RH [%]			PC2 - K_0 [m^2]			PC4 - Heating curve			PC5 - Mat.		Cooling length[s]	Start of cooling [s]	End of cooling [s]
		40	50	60	10^{-19}	10^{-18}	10^{-17}	PAR1	PAR2	PAR4	C60	C90			
11	TH12K018RH40PAR2C60	X					X				X		36	3360+120	3516



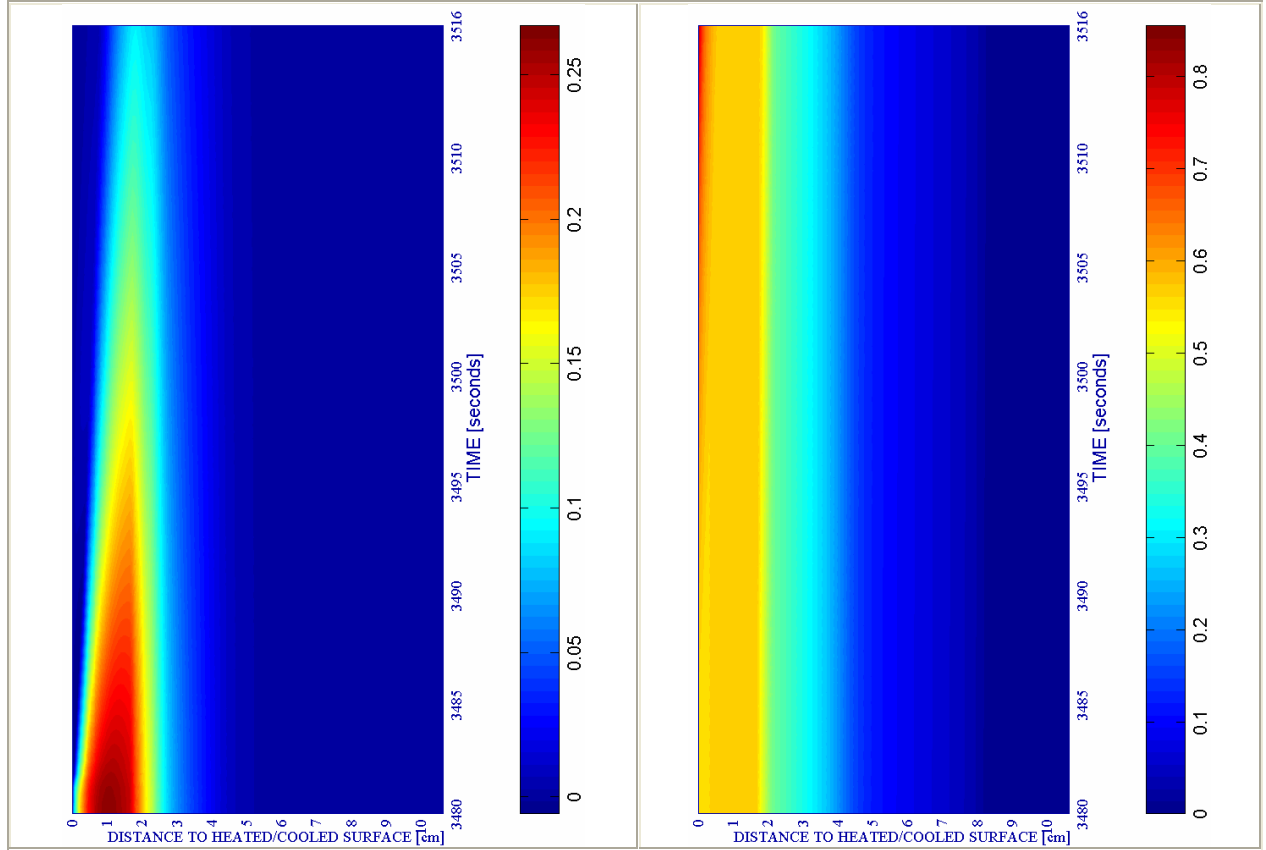
c) Down left: Velocity of spalled pieces [m/s]

Figure 6A-11.

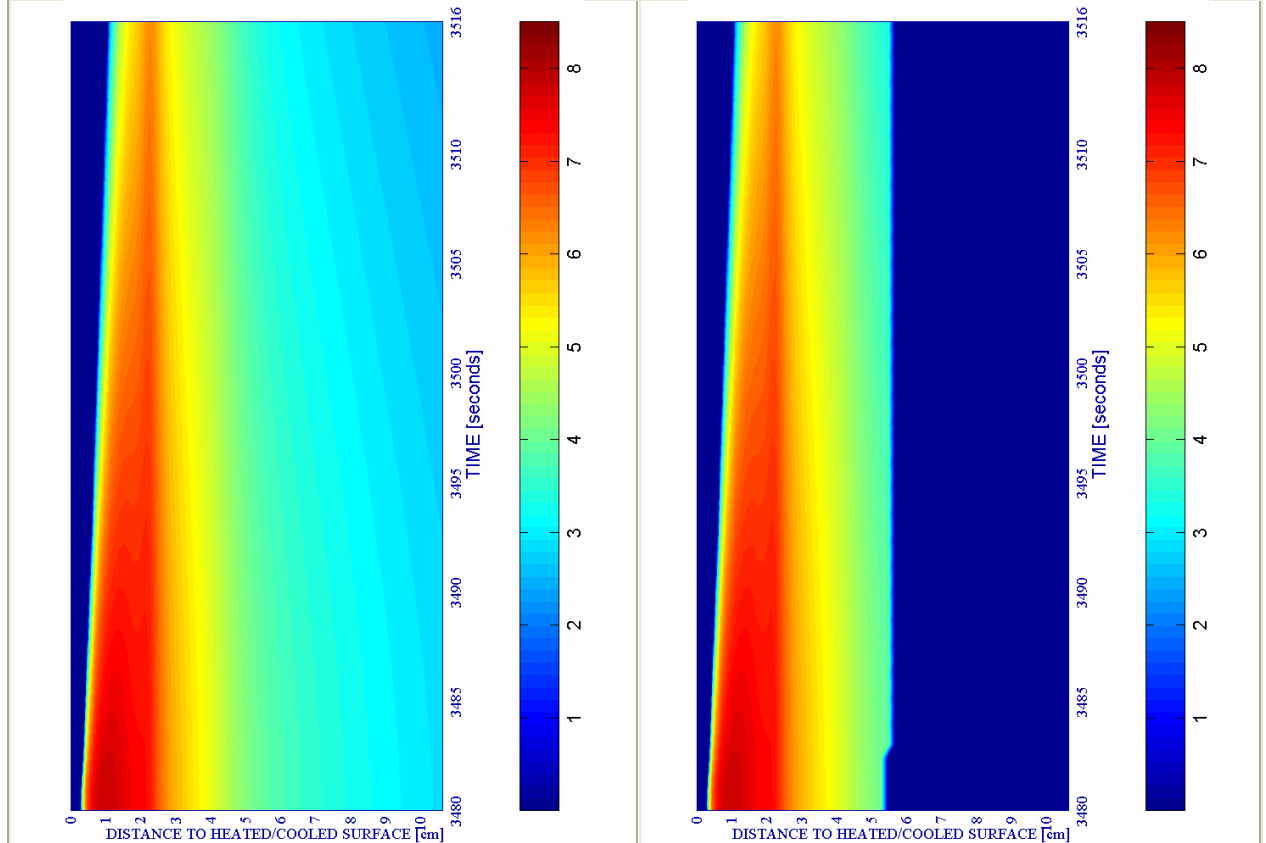
d) Down right: Velocity [m/s] where $d \geq 0,10$

a) Up left: Spalling Index IS_4 [-]

b) Up right: Mechanical damage d [-]



#	Combination	PC1 - RH [%]			PC2 - K_0 [m^2]			PC4 - Heating curve			PC5 - Mat.		Cooling length[s]	Start of cooling [s]	End of cooling [s]	
		40	50	60	10^{-19}	10^{-18}	10^{-17}	PAR1	PAR2	PAR4	C60	C90				
12	TH12K019RH40PAR2C60	X			X				X			X		36	3360+120	3516



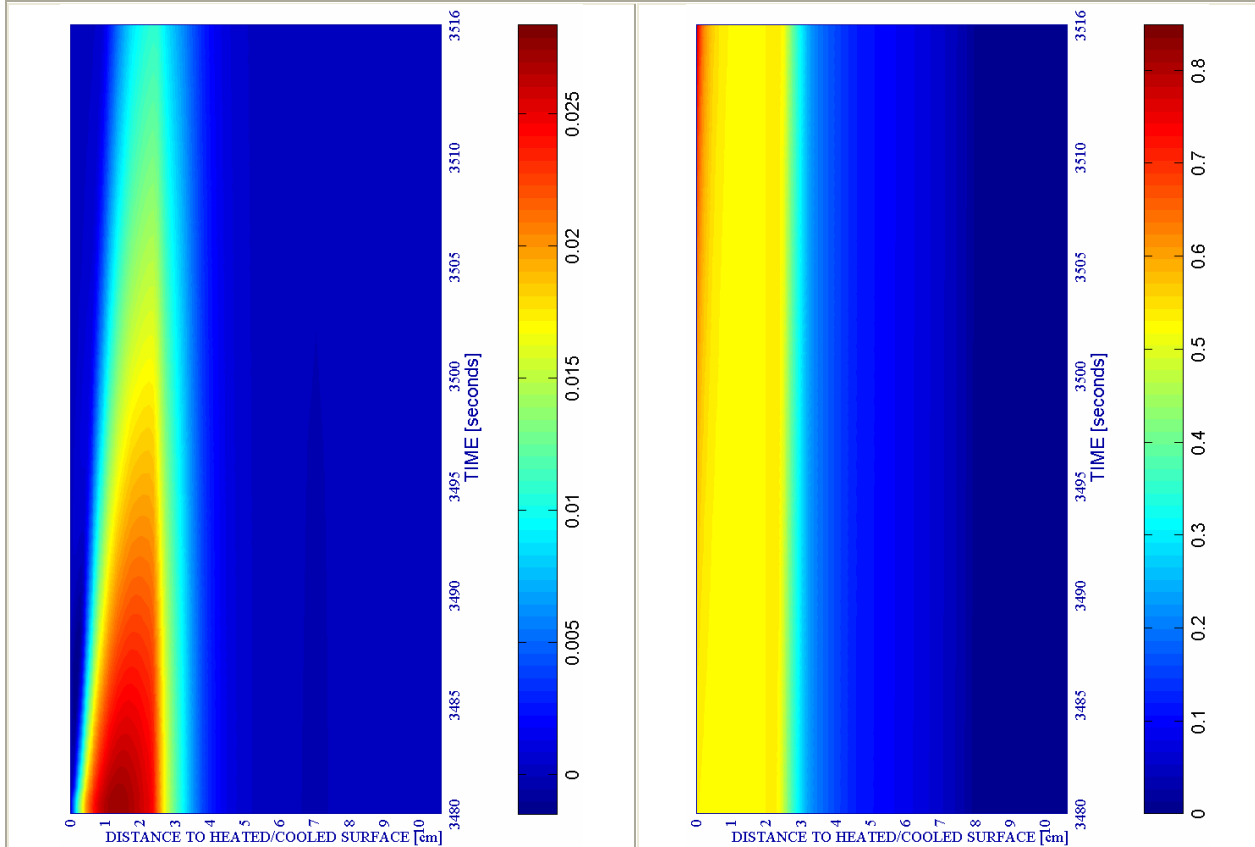
c) Down left: Velocity of spalled pieces [m/s]

Figure 6A-12.

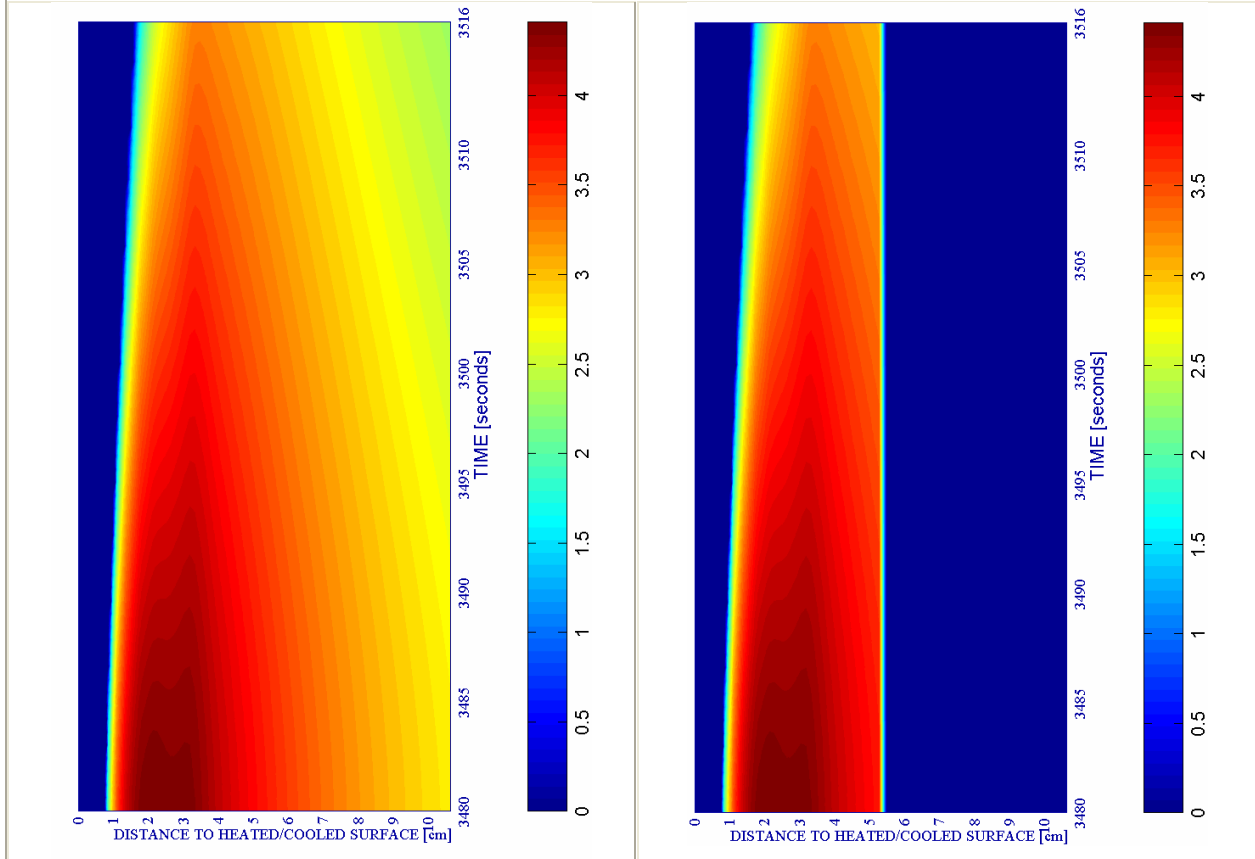
d) Down right: Velocity [m/s] where $d \geq 0,10$

a) Up left: Spalling Index IS_4 [-]

b) Up right: Mechanical damage d [-]



#	Combination	PC1 - RH [%]			PC2 - K_0 [m^2]			PC4 - Heating curve			PC5 - Mat.		Cooling length[s]	Start of cooling [s]	End of cooling [s]
		40	50	60	10^{-19}	10^{-18}	10^{-17}	PAR1	PAR2	PAR4	C60	C90			
13	TH12K017RH50PAR2C60		X				X		X		X		36	3360+120	3516



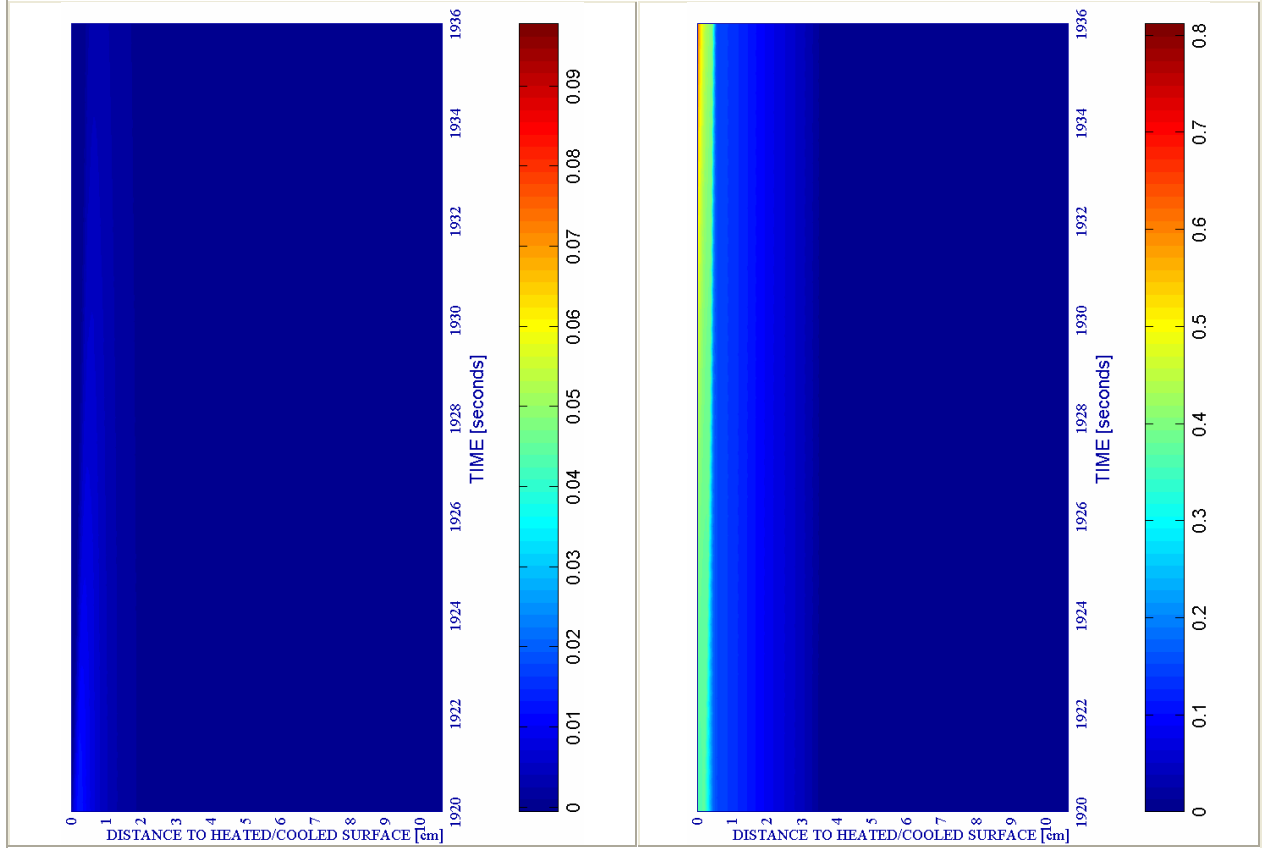
c) Down left: Velocity of spalled pieces [m/s]

Figure 6A-13.

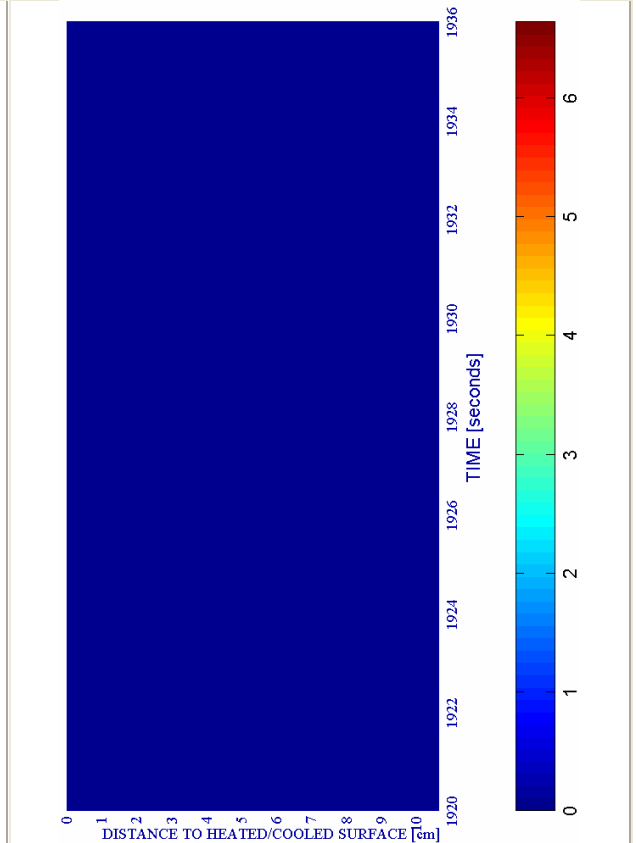
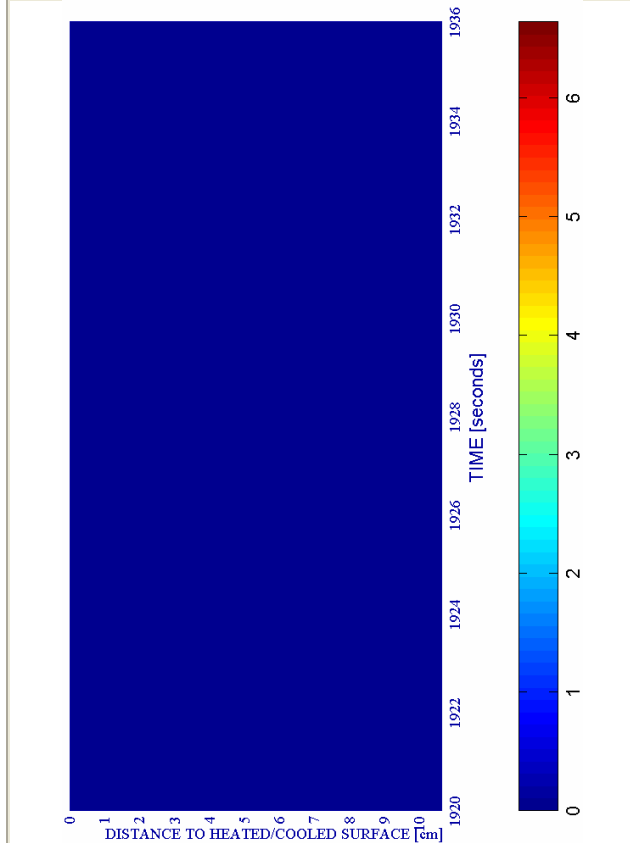
d) Down right: Velocity [m/s] where $d \geq 0,10$

a) Up left: Spalling Index IS_4 [-]

b) Up right: Mechanical damage d [-]



#	Combination	PC1 - RH [%]			PC2 - K_0 [m ²]			PC4 - Heating curve			PC5 - Mat.		Cooling length[s]	Start of cooling [s]	End of cooling [s]	
		40	50	60	10 ⁻¹⁹	10 ⁻¹⁸	10 ⁻¹⁷	PAR1	PAR2	PAR4	C60	C90				
14	TH12K018RH50PAR2C60		X			X			X			X		16	1800+120	1936



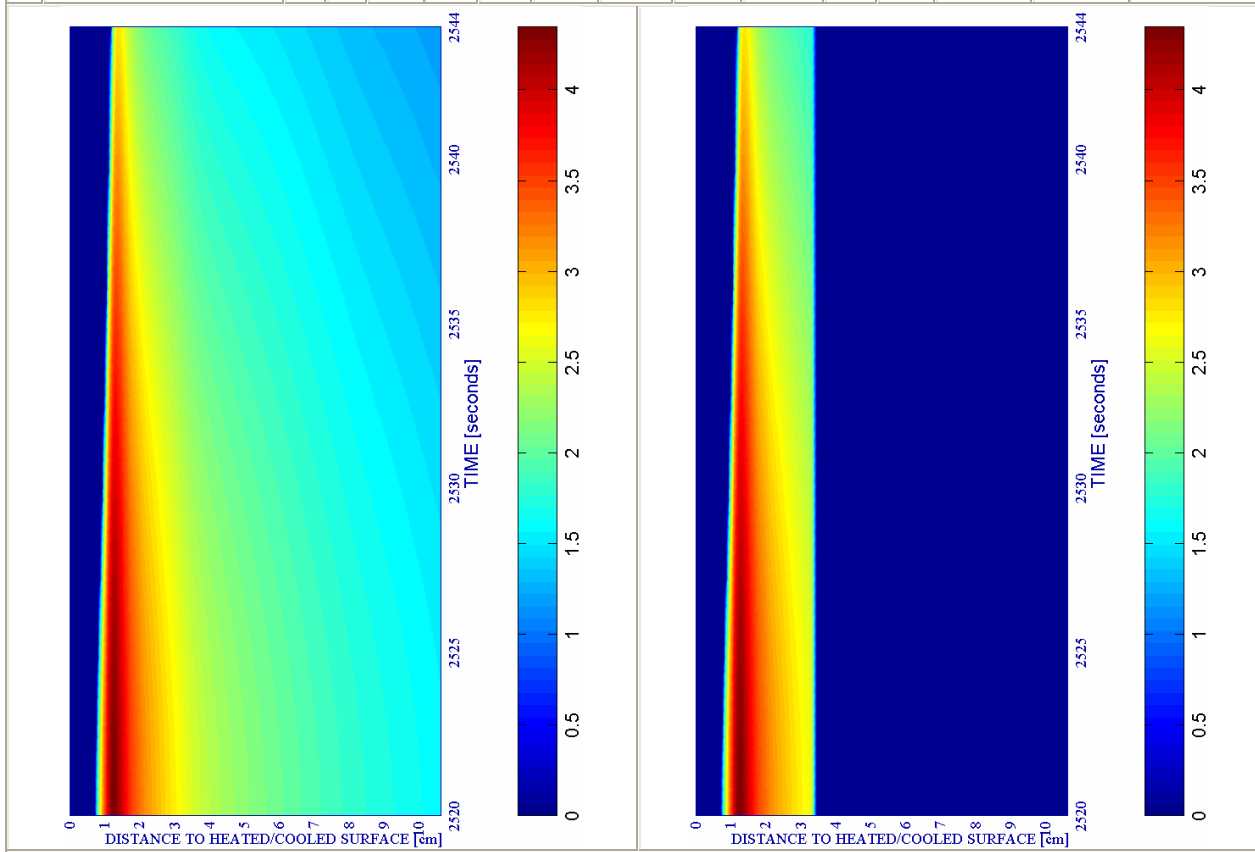
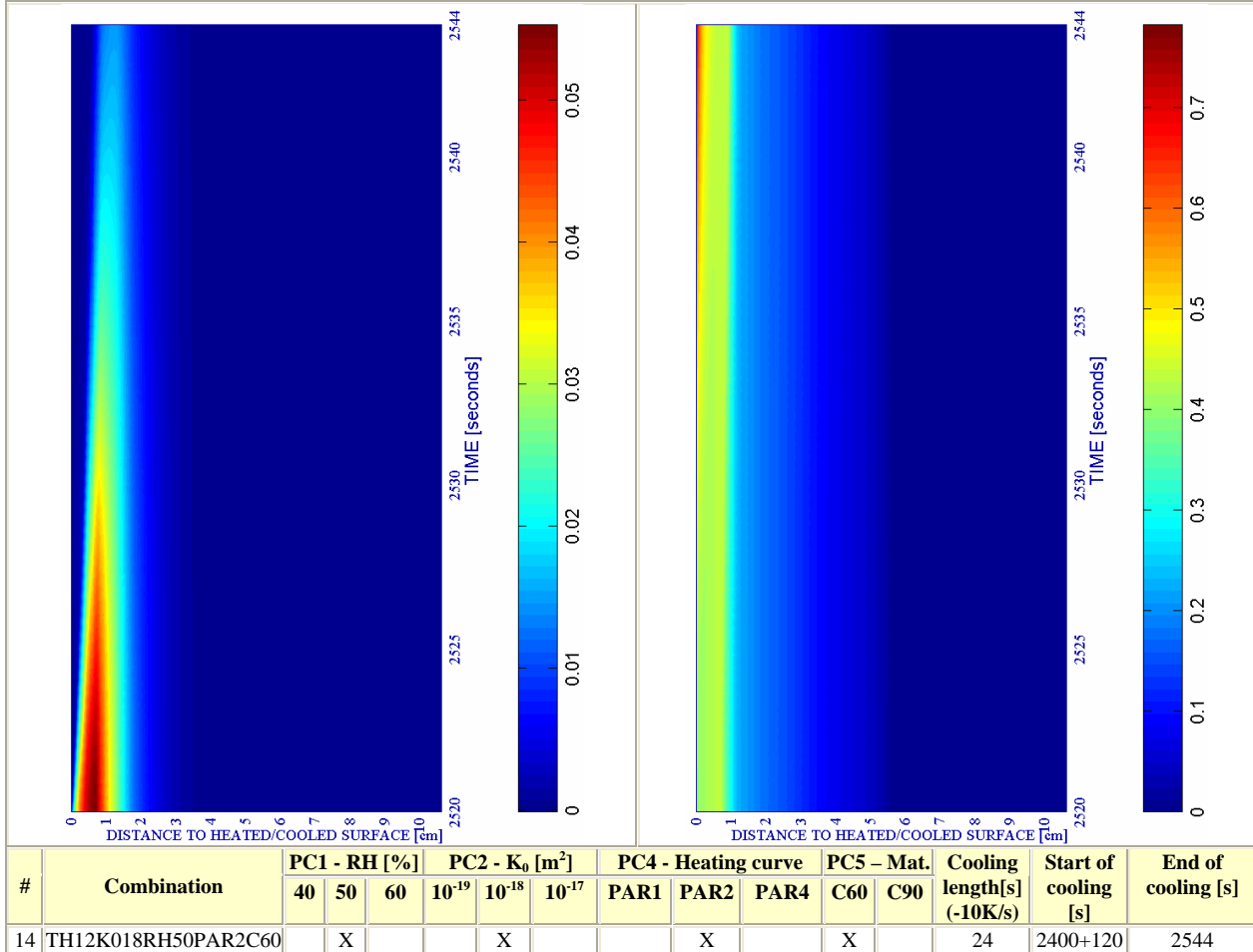
c) Down left: Velocity of spalled pieces [m/s]

Figure 6A-14.

d) Down right: Velocity [m/s] where $d \geq 0,10$

a) Up left: Spalling Index IS_4 [-]

b) Up right: Mechanical damage d [-]



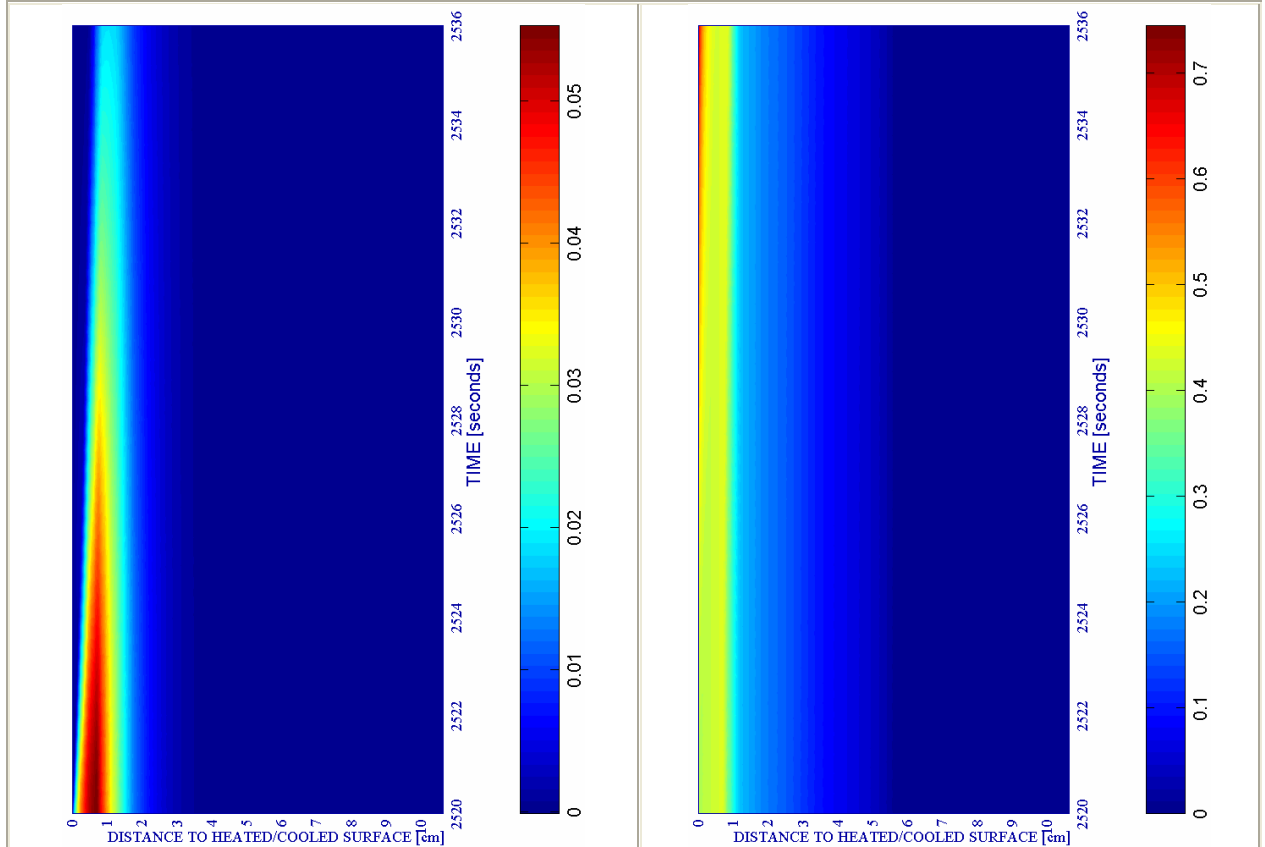
c) Down left: Velocity of spalled pieces [m/s]

Figure 6A-15.

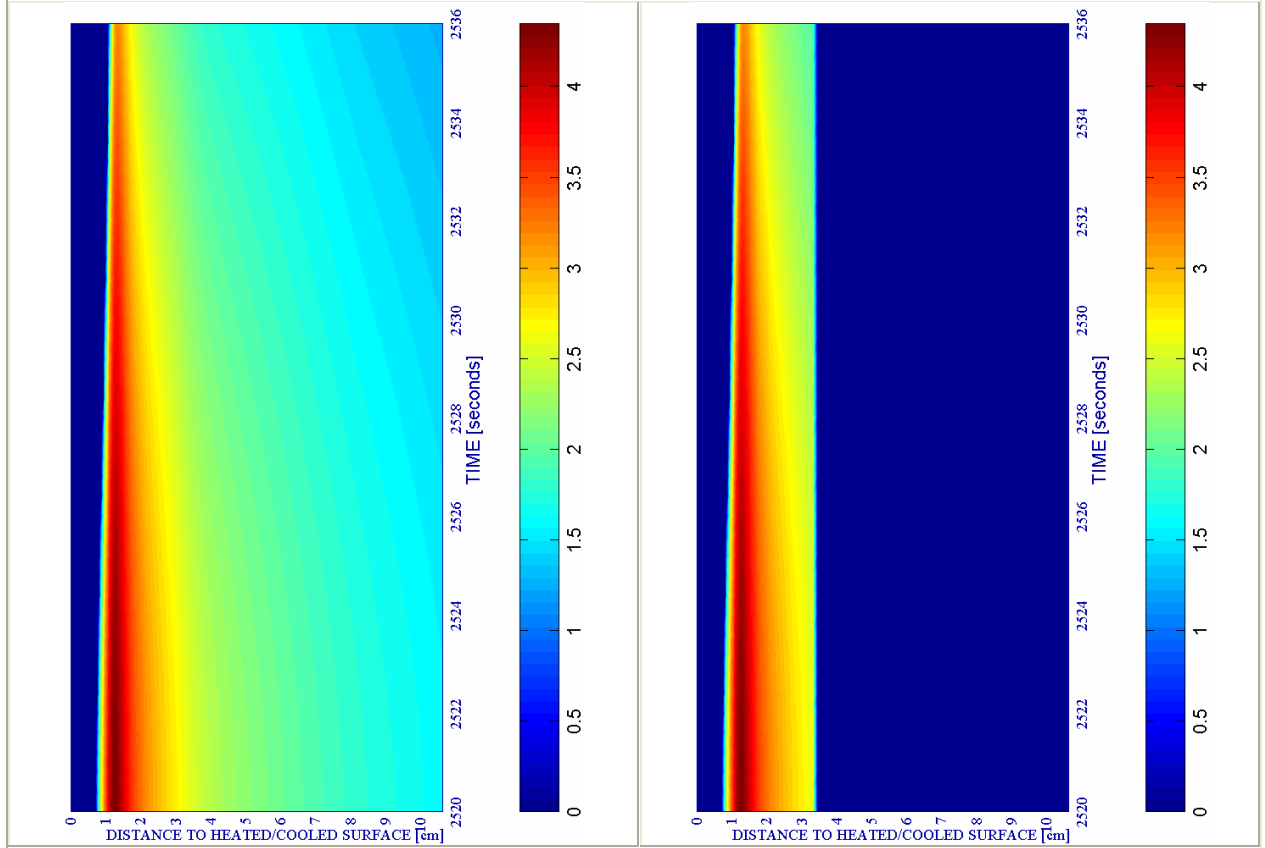
d) Down right: Velocity [m/s] where $d \geq 0,10$

a) Up left: Spalling Index IS_4 [-]

b) Up right: Mechanical damage d [-]



#	Combination	PC1 - RH [%]			PC2 - K_0 [m^2]			PC4 - Heating curve			PC5 - Mat.		Cooling length[s] (-15K/s)	Start of cooling [s]	End of cooling [s]
		40	50	60	10^{-19}	10^{-18}	10^{-17}	PAR1	PAR2	PAR4	C60	C90			
14	TH12K018RH50PAR2C60		X			X			X		X		16	2400+120	2536



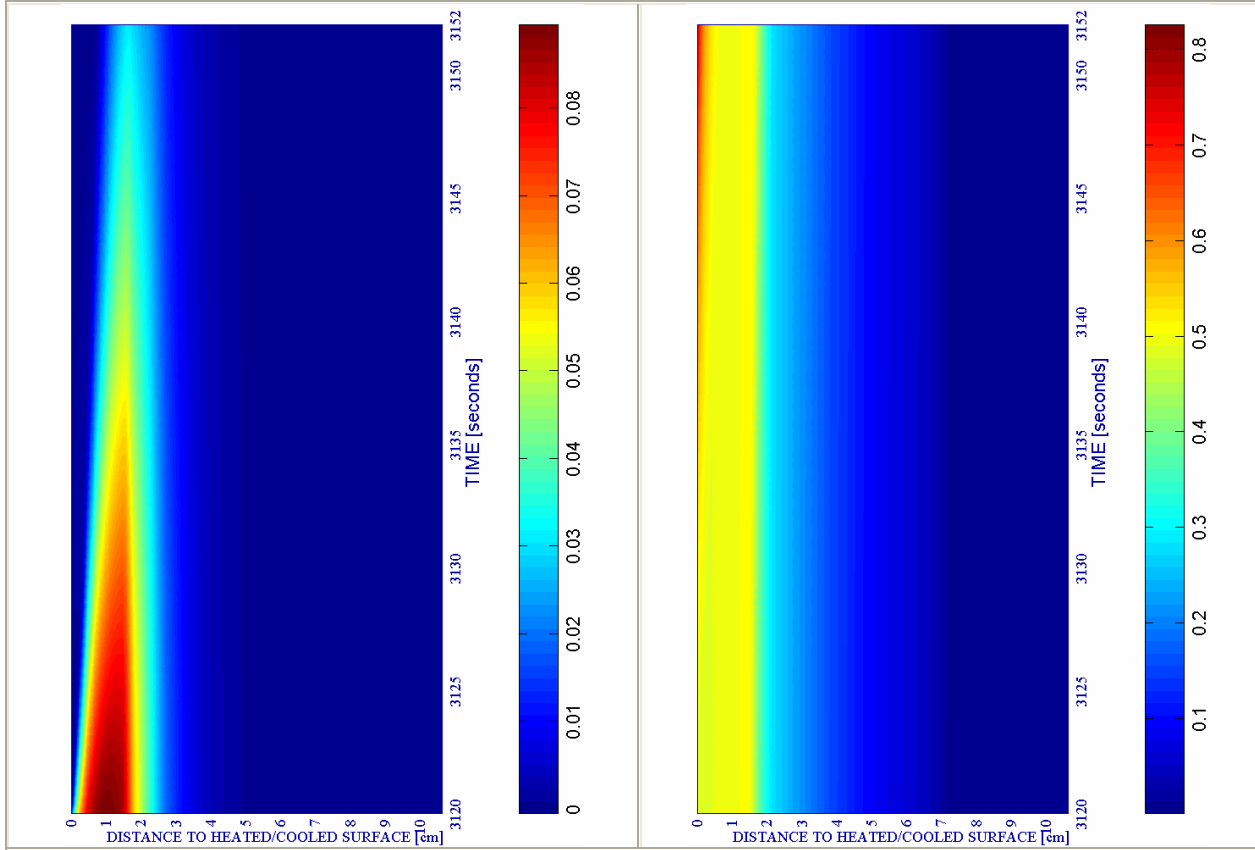
c) Down left: Velocity of spalled pieces [m/s]

Figure 6A-16.

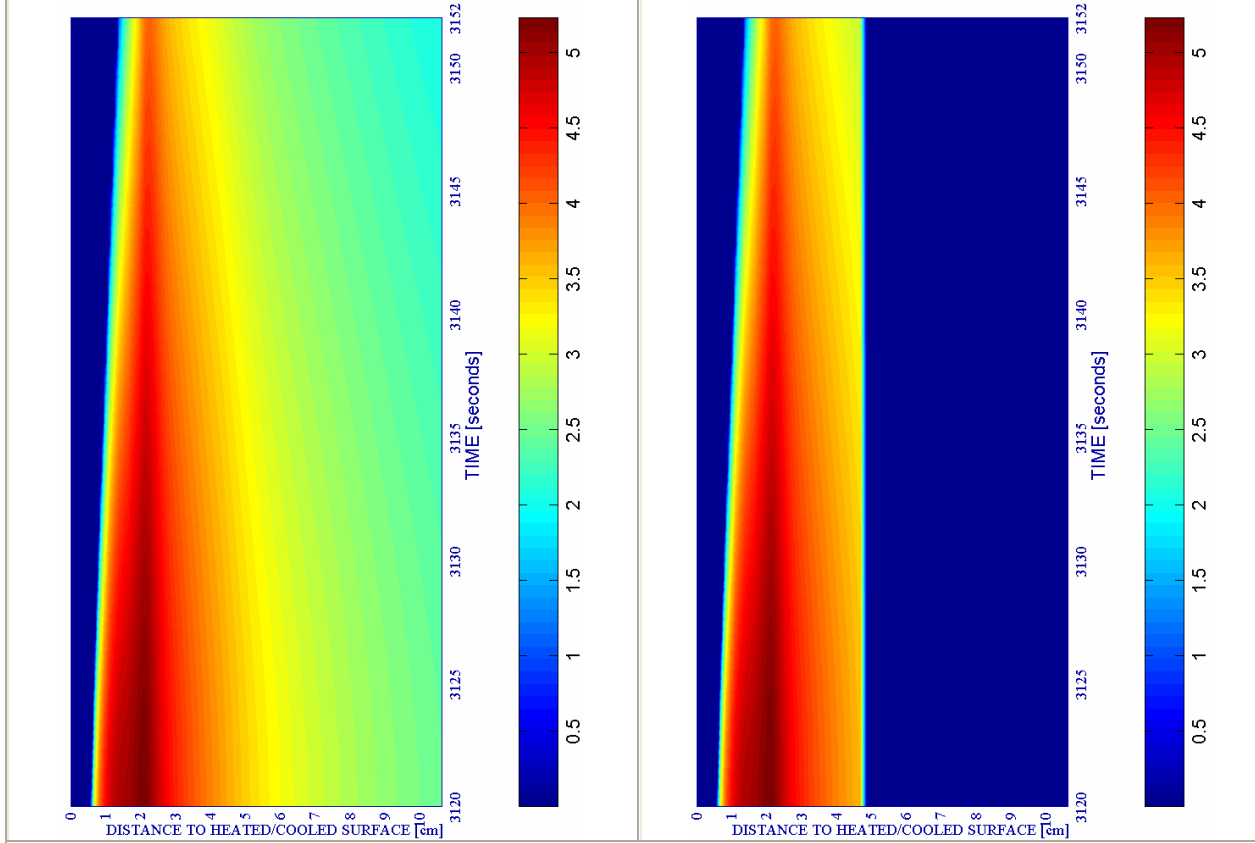
d) Down right: Velocity [m/s] where $d \geq 0,10$

a) Up left: Spalling Index IS_4 [-]

b) Up right: Mechanical damage d [-]



#	Combination	PC1 - RH [%]			PC2 - K_0 [m^2]			PC4 - Heating curve			PC5 - Mat.		Cooling length[s]	Start of cooling [s]	End of cooling [s]	
		40	50	60	10^{-19}	10^{-18}	10^{-17}	PAR1	PAR2	PAR4	C60	C90				
14	TH12K018RH50PAR2C60		X			X			X			X		32	3000+120	3152



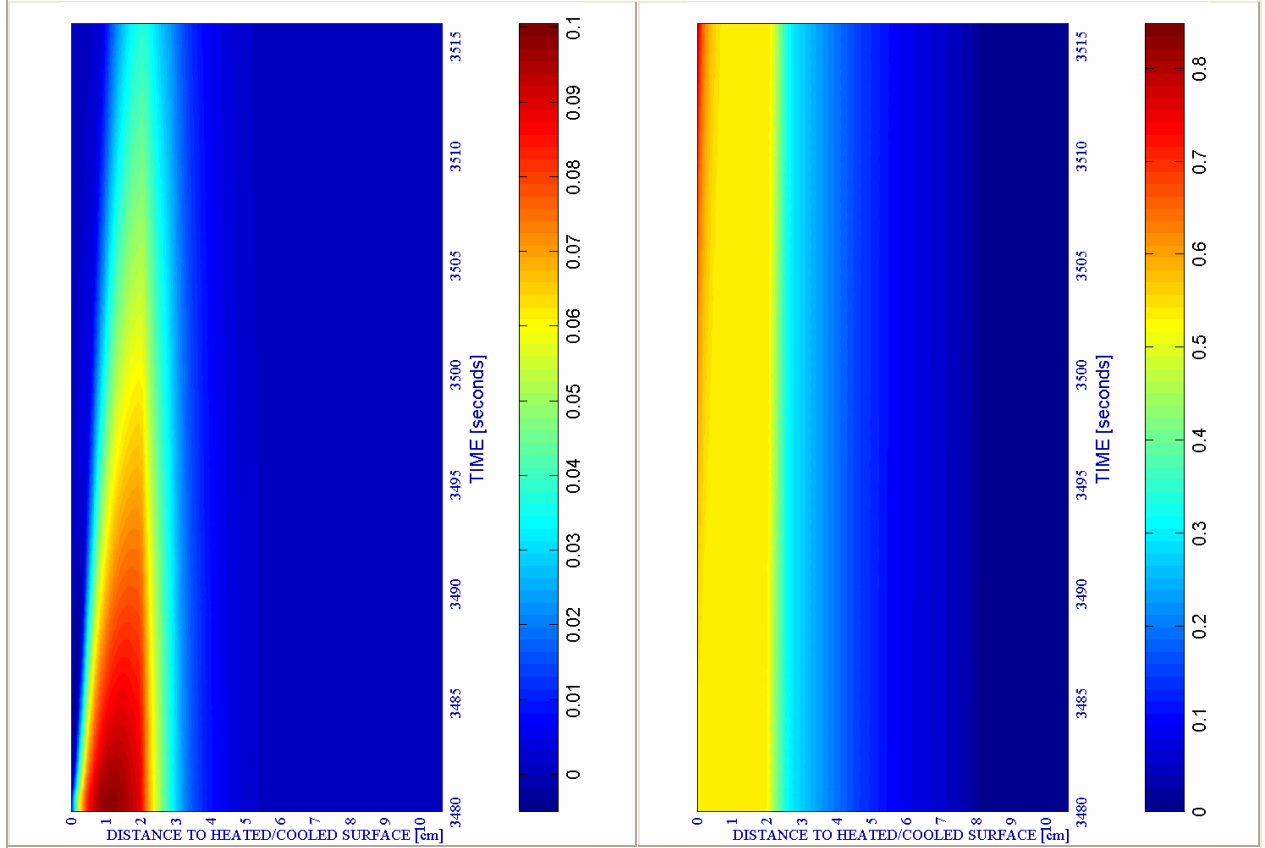
c) Down left: Velocity of spalled pieces [m/s]

Figure 6A-17

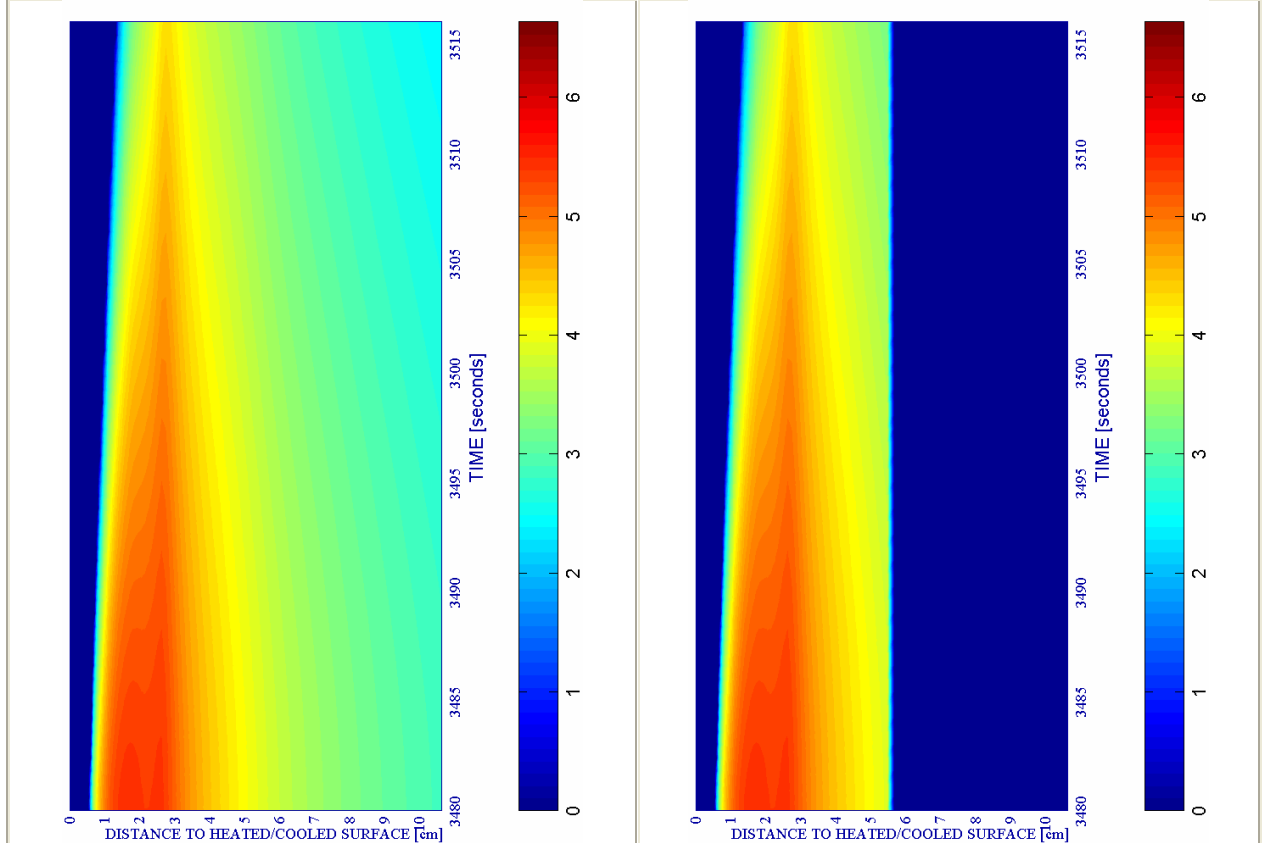
d) Down right: Velocity [m/s] where $d \geq 0,10$

a) Up left: Spalling Index IS_4 [-]

b) Up right: Mechanical damage d [-]



#	Combination	PC1 - RH [%]			PC2 - K_0 [m ²]			PC4 - Heating curve			PC5 - Mat.		Cooling length[s]	Start of cooling [s]	End of cooling [s]
		40	50	60	10 ⁻¹⁹	10 ⁻¹⁸	10 ⁻¹⁷	PAR1	PAR2	PAR4	C60	C90			
14	TH12K018RH50PAR2C60		X			X			X		X		36	3360+120	3516



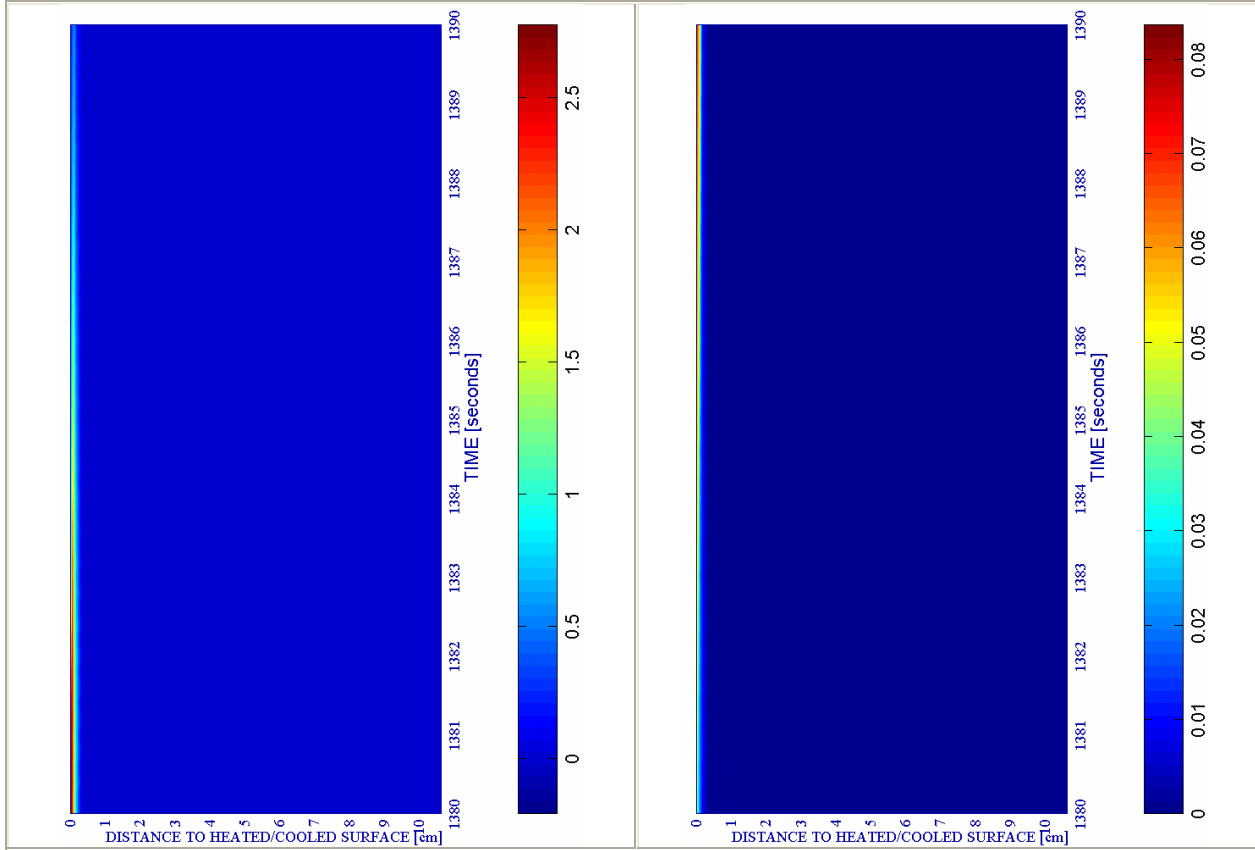
c) Down left: Velocity of spalled pieces [m/s]

Figure 6A-18.

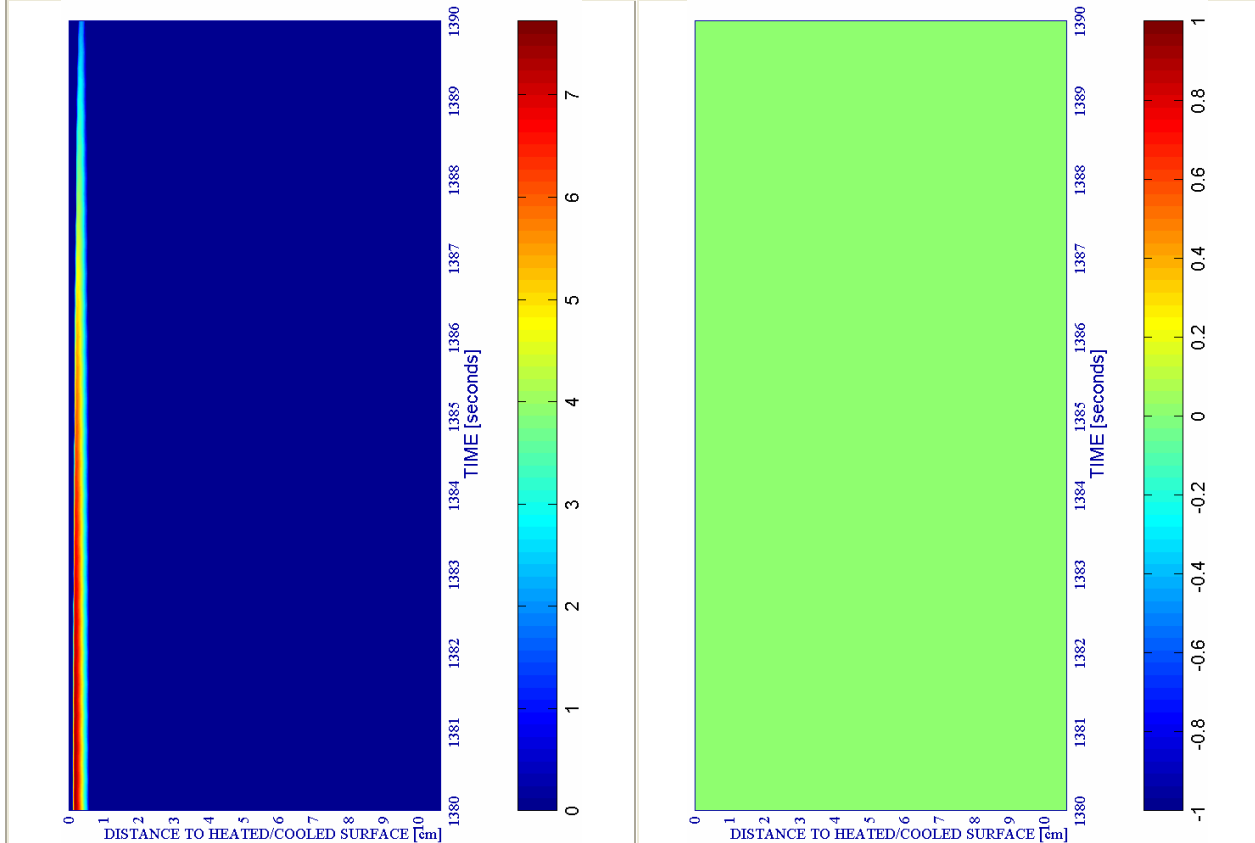
d) Down right: Velocity [m/s] where $d \geq 0,10$

a) Up left: Spalling Index $IS_4 * 10^3 [-]$

b) Up right: Mechanical damage $d [-]$



#	Combination	PC1 - RH [%]			PC2 - K_0 [m ²]			PC4 - Heating curve			PC5 - Mat.		Cooling length[s]	Start of cooling [s]	End of cooling [s]	
		40	50	60	10 ⁻¹⁹	10 ⁻¹⁸	10 ⁻¹⁷	PAR1	PAR2	PAR4	C60	C90				
15	TH12K019RH50PAR2C60		X		X				X			X		10	1260+120	1390



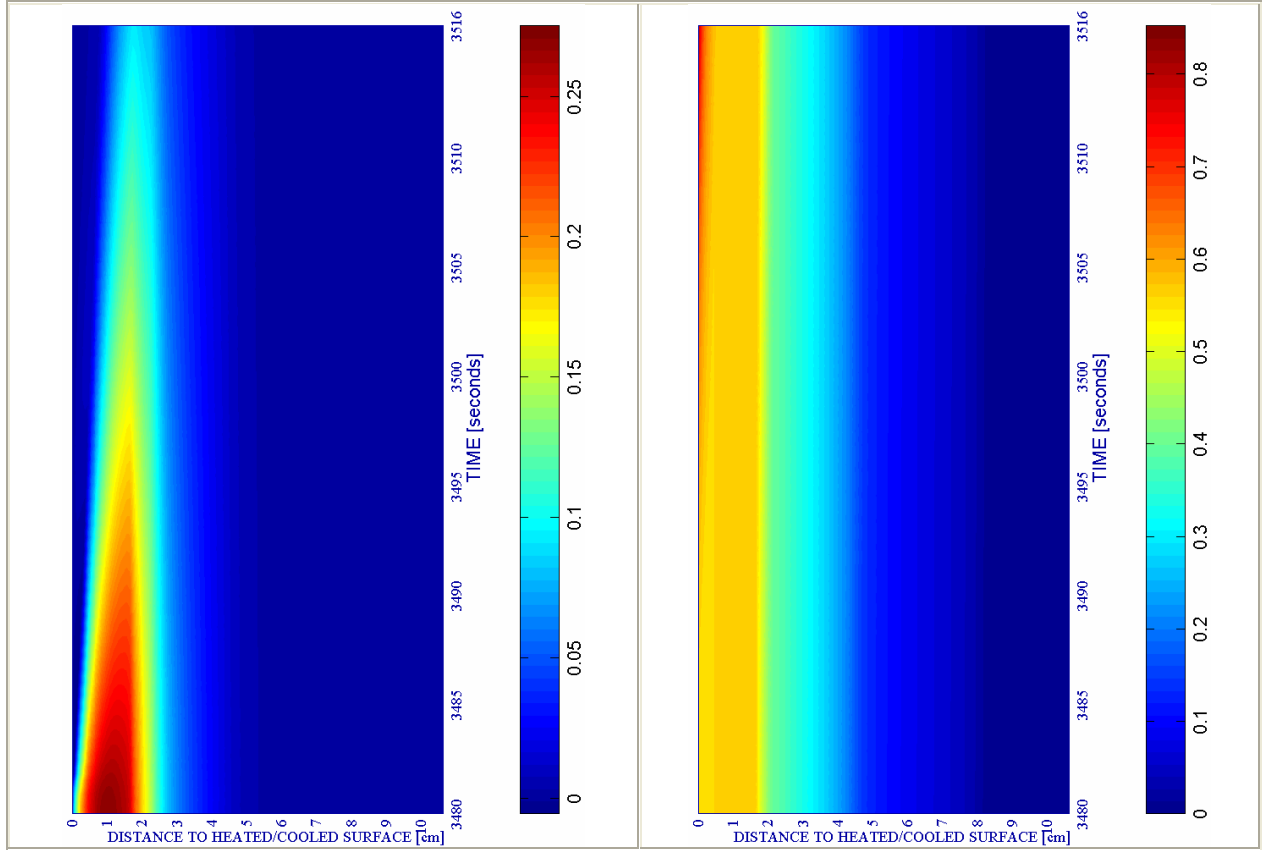
c) Down left: Velocity of spalled pieces [m/s]

Figure 6A-19.

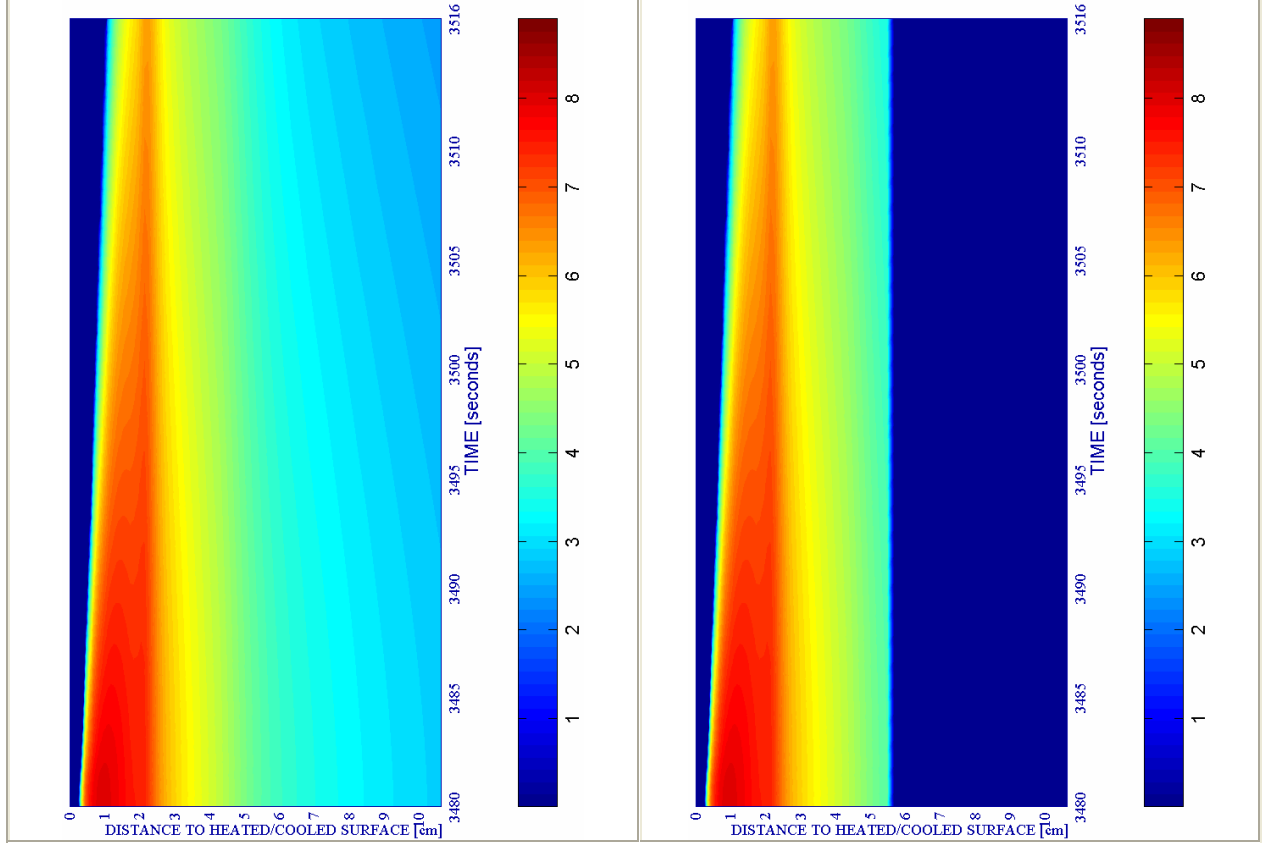
d) Down right: Velocity [m/s] where $d \geq 0,10$

a) Up left: Spalling Index IS_4 [-]

b) Up right: Mechanical damage d [-]



#	Combination	PC1 - RH [%]			PC2 - K_0 [m^2]			PC4 - Heating curve			PC5 - Mat.		Cooling length[s]	Start of cooling [s]	End of cooling [s]
		40	50	60	10^{-19}	10^{-18}	10^{-17}	PAR1	PAR2	PAR4	C60	C90			
15	TH12K019RH50PAR2C60		X		X				X		X		36	3360+120	3516



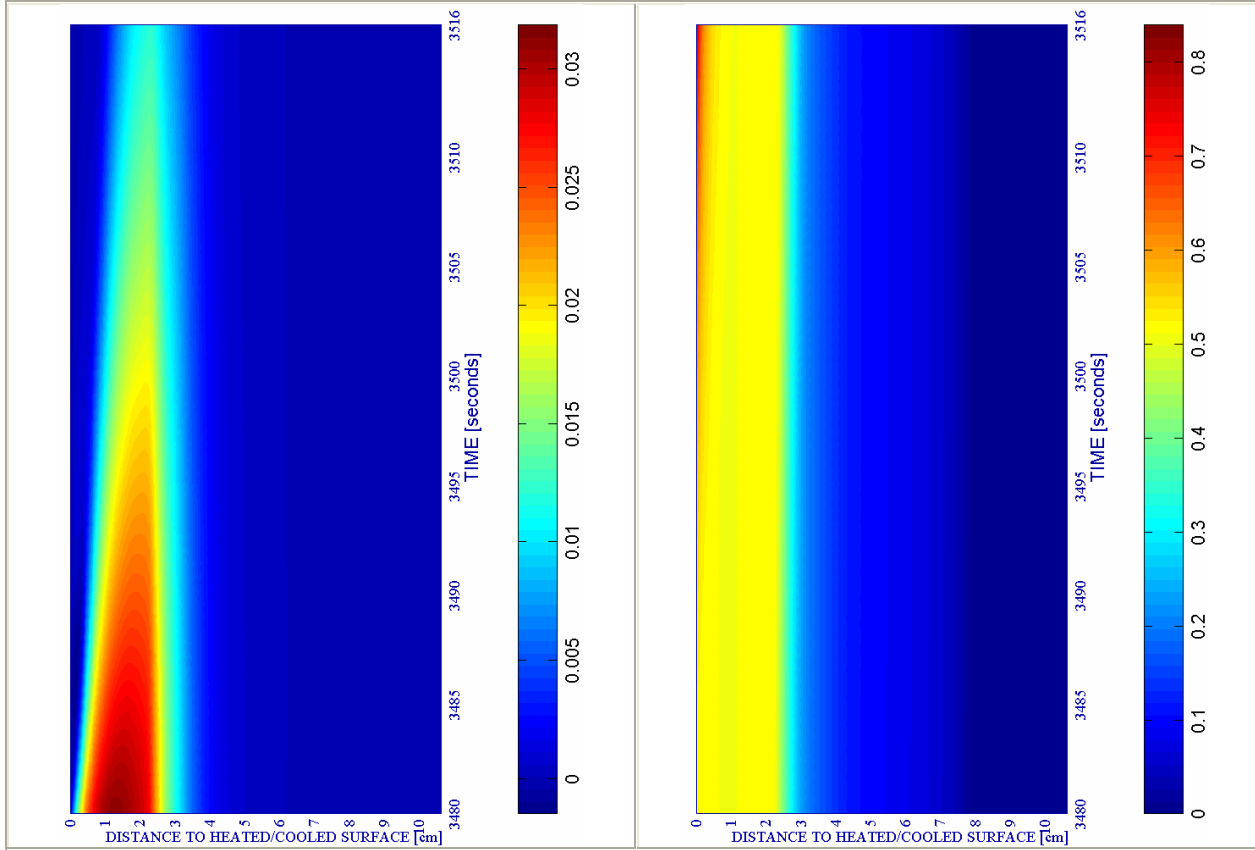
c) Down left: Velocity of spalled pieces [m/s]

Figure 6A-20.

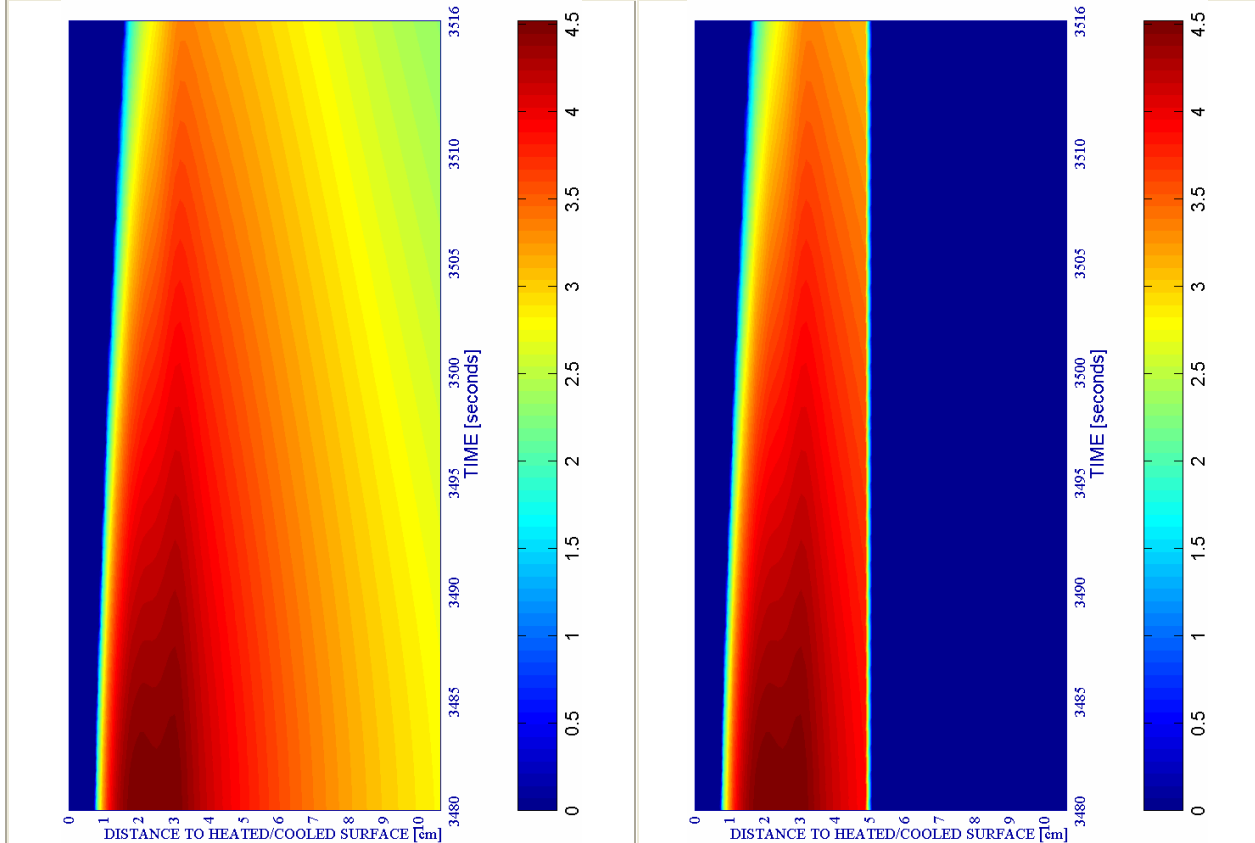
d) Down right: Velocity [m/s] where $d \geq 0,10$

a) Up left: Spalling Index IS_4 [-]

b) Up right: Mechanical damage d [-]



#	Combination	PC1 - RH [%]			PC2 - K_0 [m ²]			PC4 - Heating curve			PC5 - Mat.		Cooling length[s]	Start of cooling [s]	End of cooling [s]
		40	50	60	10 ⁻¹⁹	10 ⁻¹⁸	10 ⁻¹⁷	PAR1	PAR2	PAR4	C60	C90			
16	TH12K017RH60PAR2C60			X			X			X		X	36	3360+120	3516



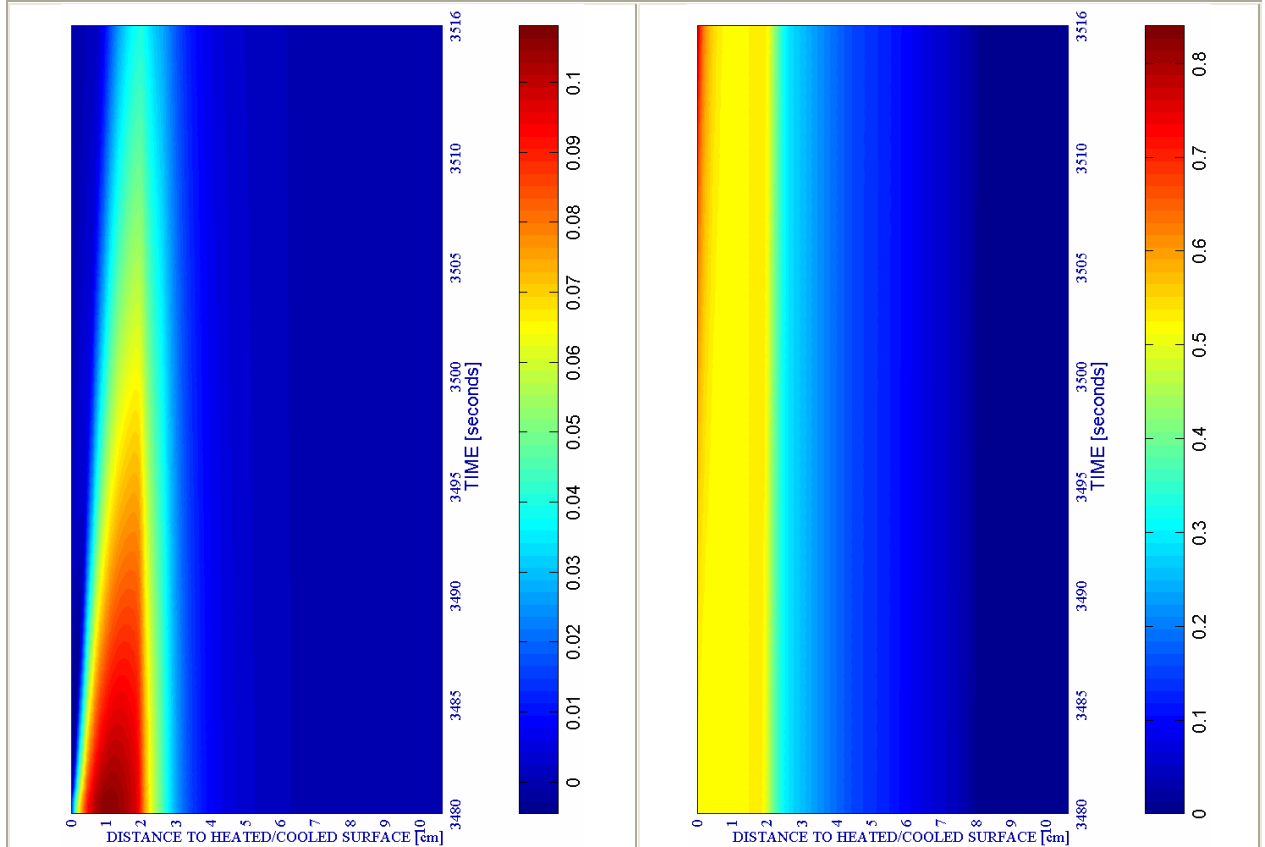
c) Down left: Velocity of spalled pieces [m/s]

Figure 6A-21.

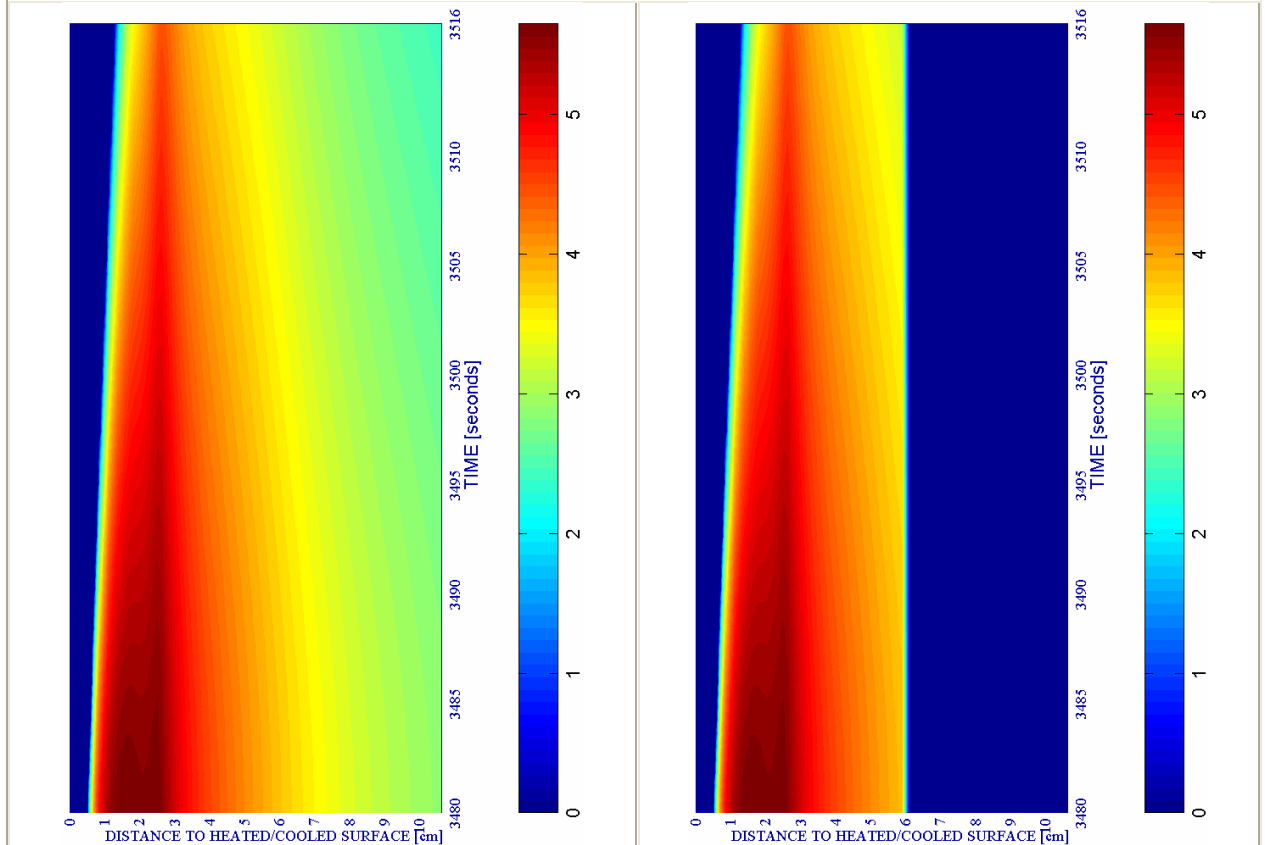
d) Down right: Velocity [m/s] where $d \geq 0,10$

a) Up left: Spalling Index IS_4 [-]

b) Up right: Mechanical damage d [-]



#	Combination	PC1 - RH [%]			PC2 - K_0 [m ²]			PC4 - Heating curve			PC5 - Mat.		Cooling length[s]	Start of cooling [s]	End of cooling [s]
		40	50	60	10 ⁻¹⁹	10 ⁻¹⁸	10 ⁻¹⁷	PAR1	PAR2	PAR4	C60	C90			
17	TH12K018RH60PAR2C60			X		X			X		X		36	3360+120	3516



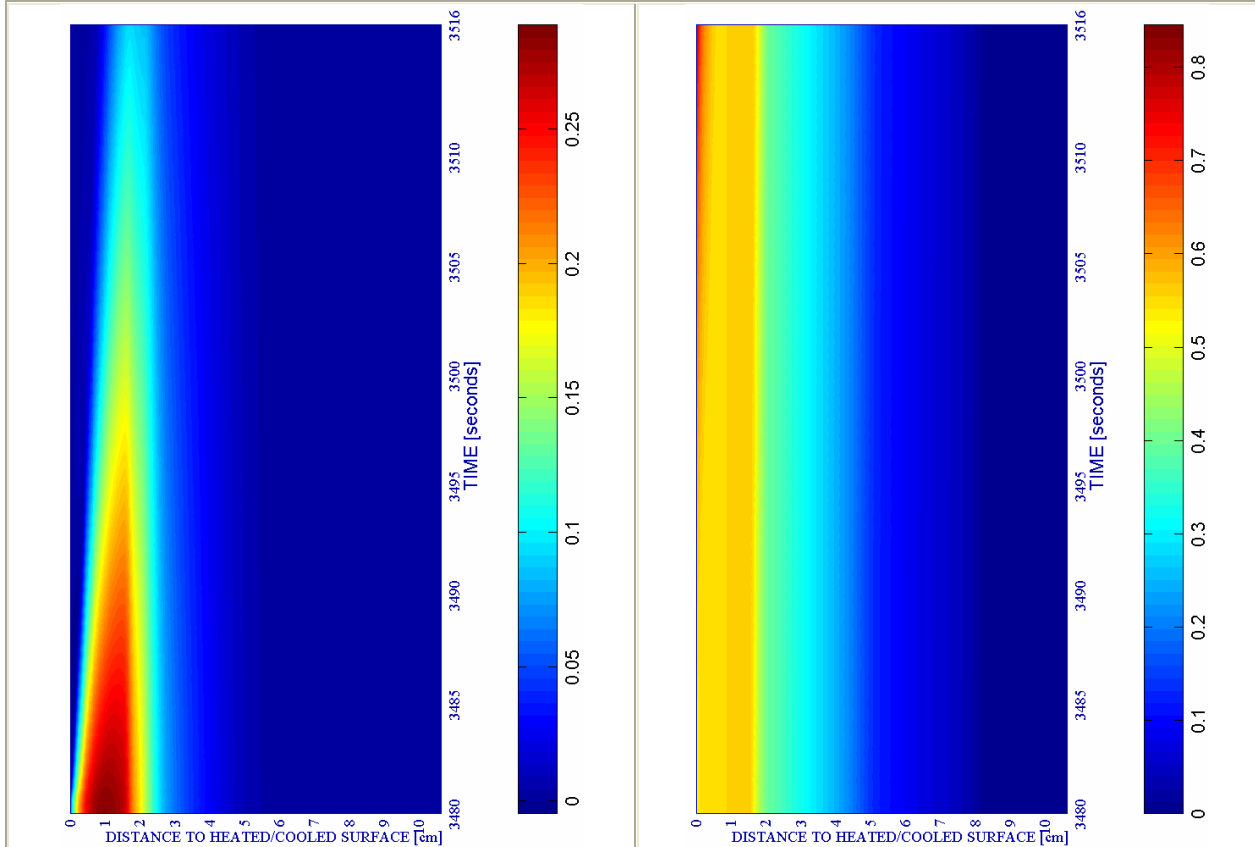
c) Down left: Velocity of spalled pieces [m/s]

Figure 6A-22.

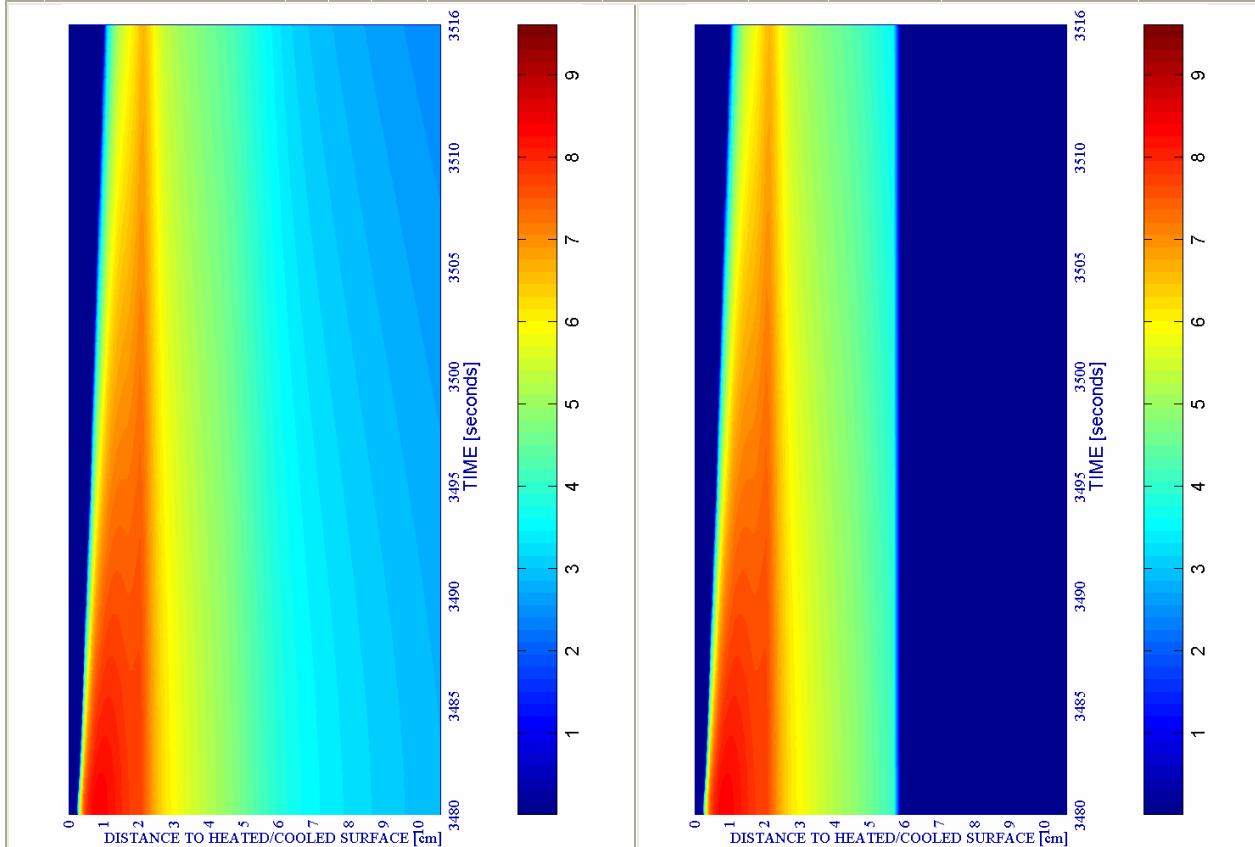
d) Down right: Velocity [m/s] where $d \geq 0,10$

a) Up left: Spalling Index IS_4 [-]

b) Up right: Mechanical damage d [-]



#	Combination	PC1 - RH [%]			PC2 - K_0 [m^2]			PC4 - Heating curve			PC5 - Mat.		Cooling length[s]	Start of cooling [s]	End of cooling [s]
		40	50	60	10^{-19}	10^{-18}	10^{-17}	PAR1	PAR2	PAR4	C60	C90			
18	TH12K019RH60PAR2C60			X	X				X		X		36	3360+120	3516

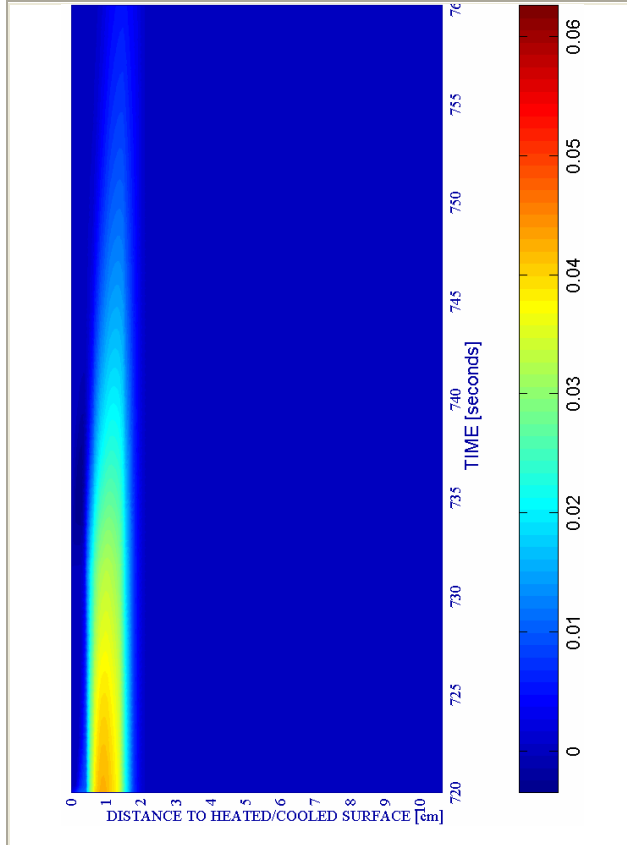


c) Down left: Velocity of spalled pieces [m/s]

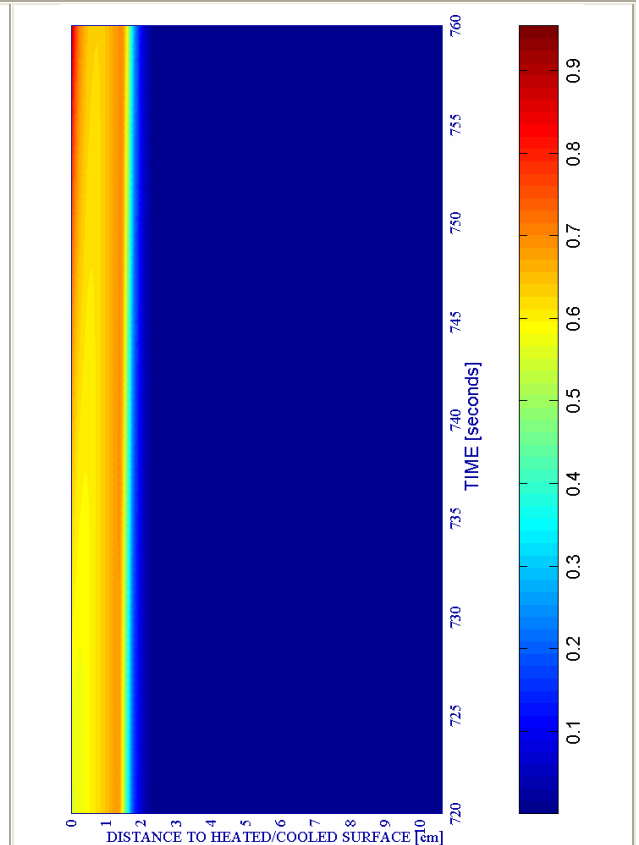
Figure 6A-23.

d) Down right: Velocity [m/s] where $d \geq 0,10$

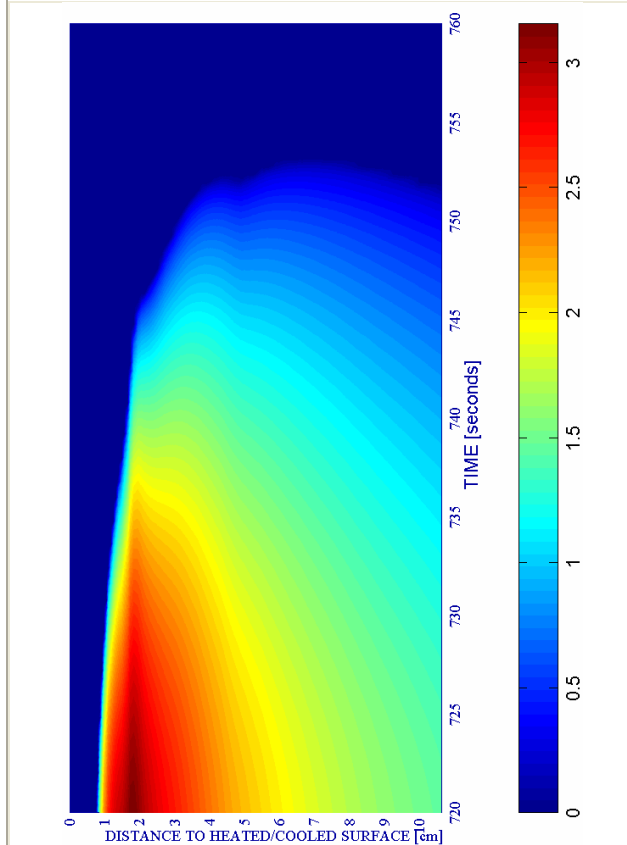
a) Up left: Spalling Index IS_4 [-]



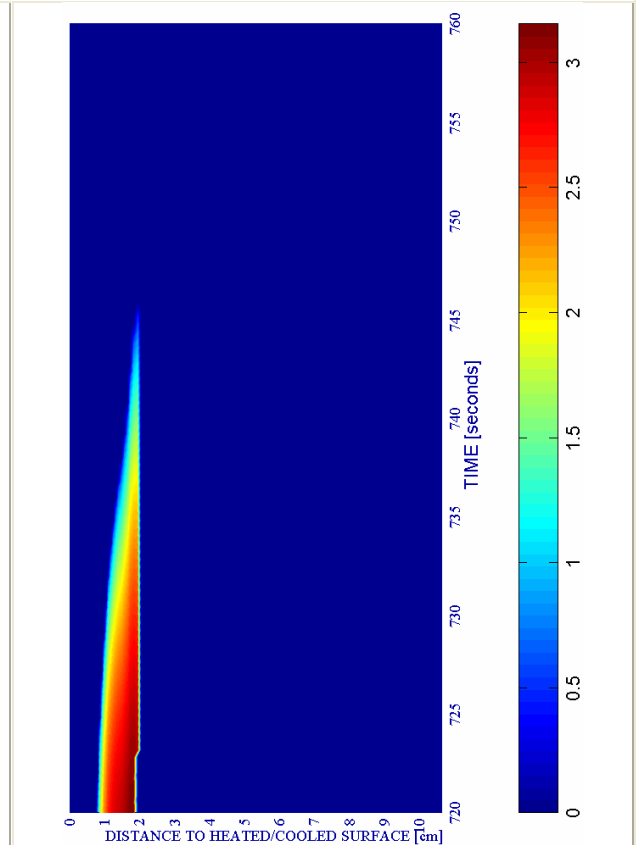
b) Up right: Mechanical damage d [-]



#	Combination	PC1 - RH [%]			PC2 - K_0 [m ²]			PC4 - Heating curve			PC5 - Mat.		Cooling length[s]	Start of cooling [s]	End of cooling [s]
		40	50	60	10 ⁻¹⁹	10 ⁻¹⁸	10 ⁻¹⁷	PAR1	PAR2	PAR4	C60	C90			
37	TH12K017RH40PAR1C90	X					X	X				X	40	600+120	760



c) Down left: Velocity of spalled pieces [m/s]

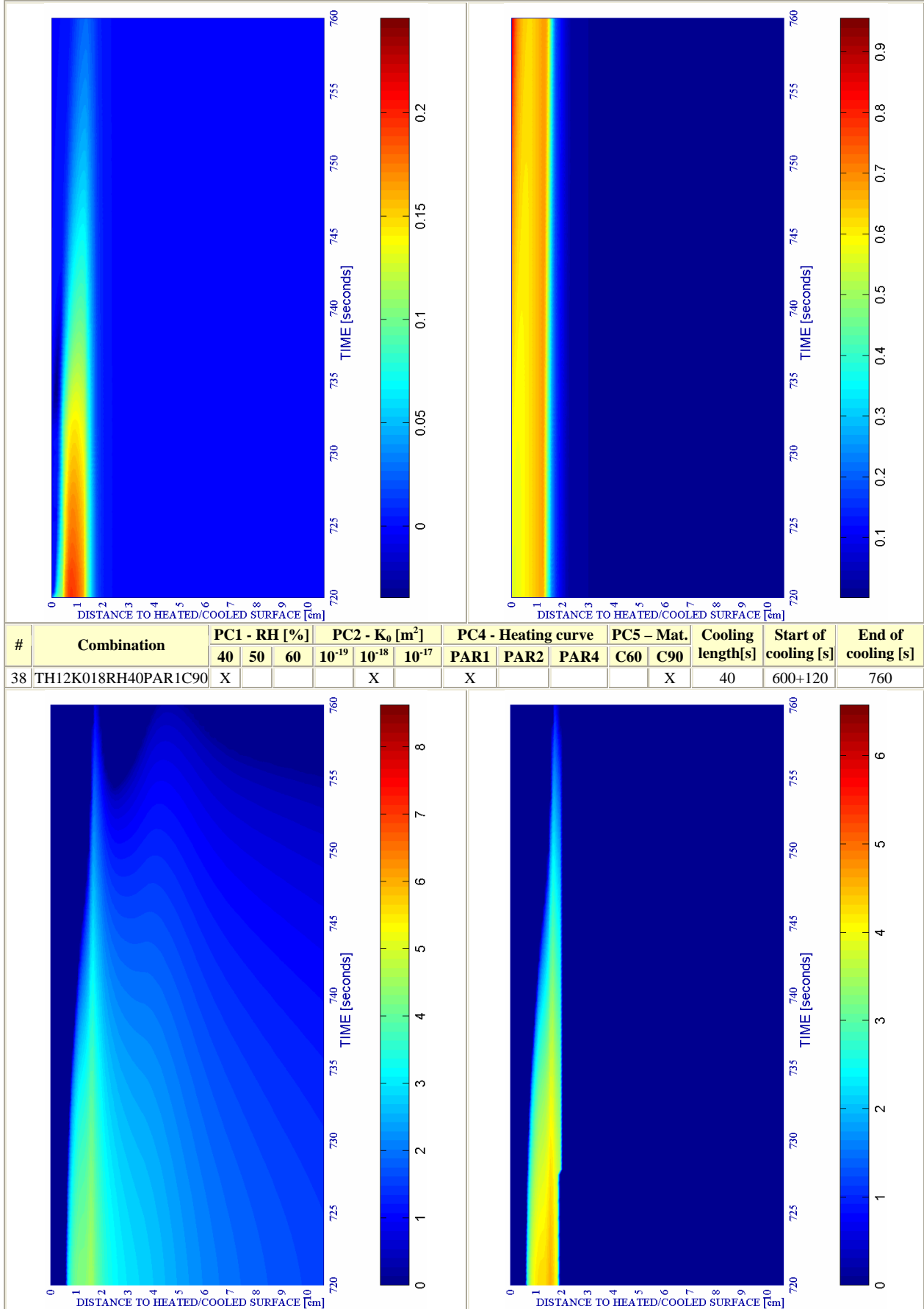


d) Down right: Velocity [m/s] where $d \geq 0,10$

Figure 6A-24.

a) Up left: Spalling Index IS_4 [-]

b) Up right: Mechanical damage d [-]



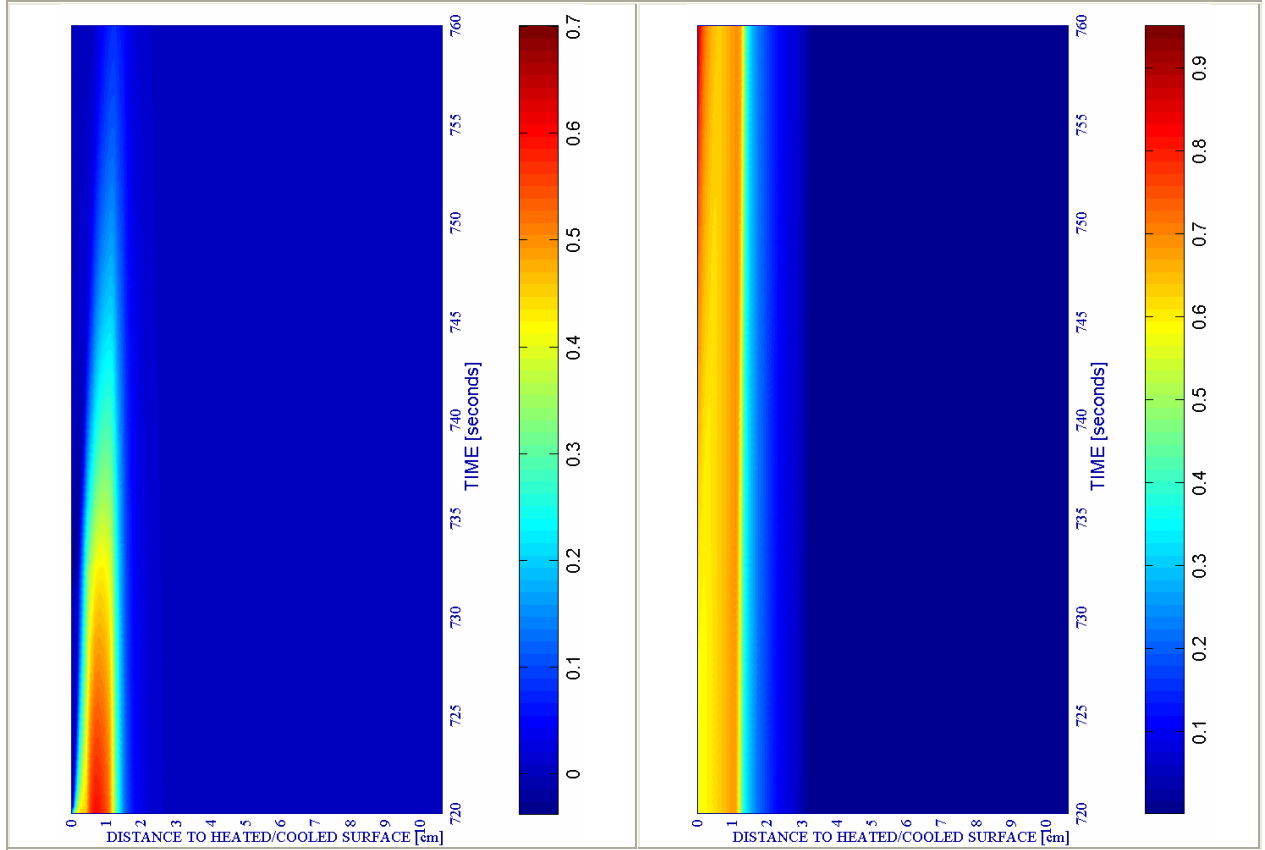
c) Down left: Velocity of spalled pieces [m/s]

Figure 6A-25.

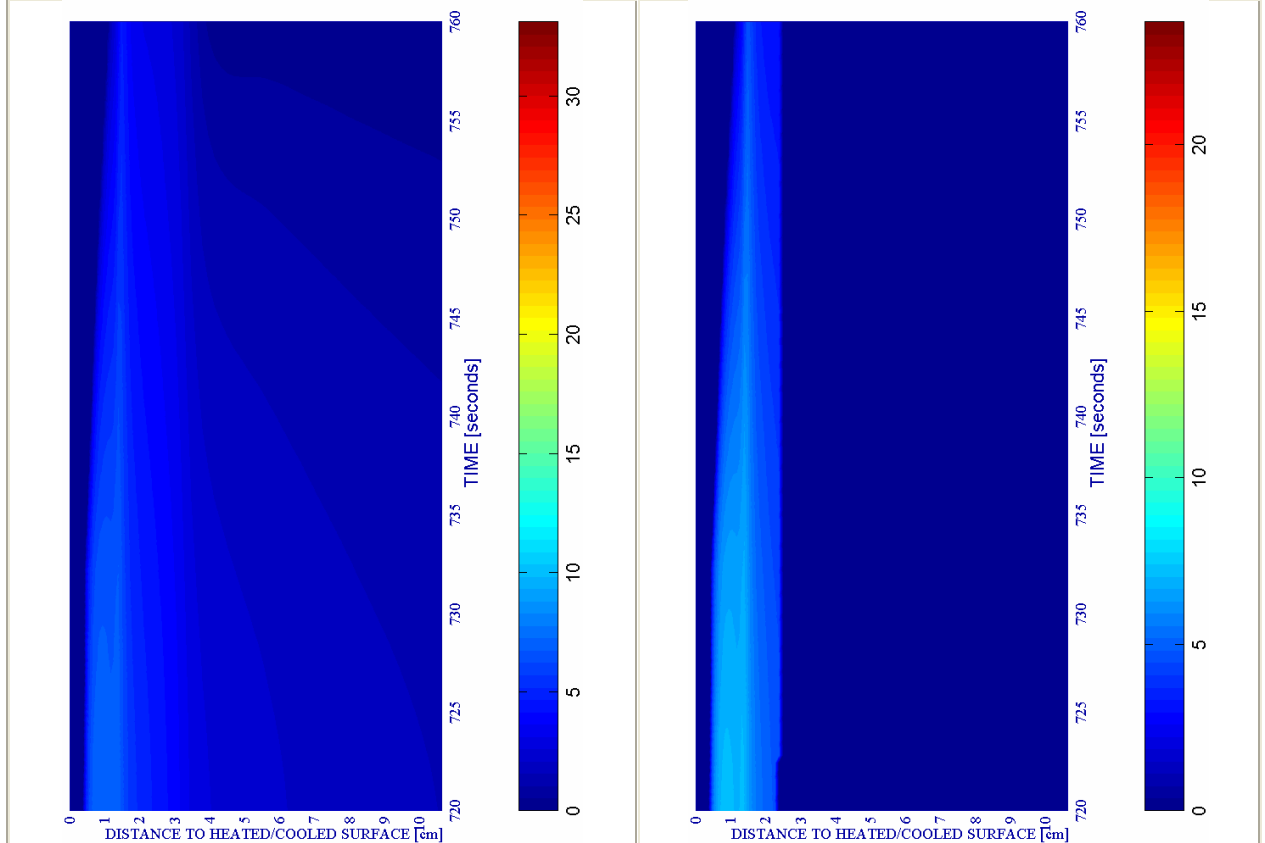
d) Down right: Velocity [m/s] where $d \geq 0,10$

a) Up left: Spalling Index IS_4 [-]

b) Up right: Mechanical damage d [-]



#	Combination	PC1 - RH [%]			PC2 - K_0 [m ²]			PC4 - Heating curve			PC5 - Mat.		Cooling length[s]	Start of cooling [s]	End of cooling [s]
		40	50	60	10 ⁻¹⁹	10 ⁻¹⁸	10 ⁻¹⁷	PAR1	PAR2	PAR4	C60	C90			
39	TH12K019RH40PAR1C90	X			X			X				X	40	600+120	760



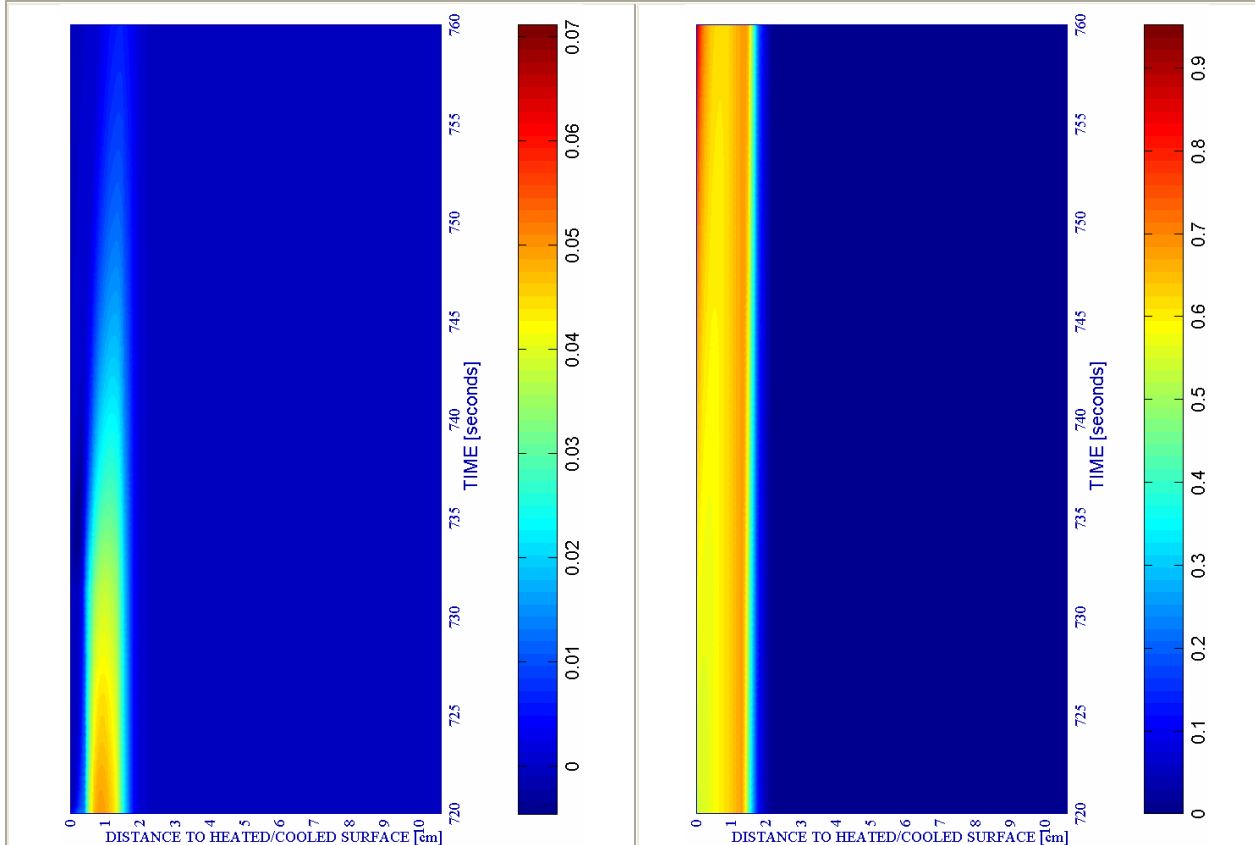
c) Down left: Velocity of spalled pieces [m/s]

Figure 6A-26.

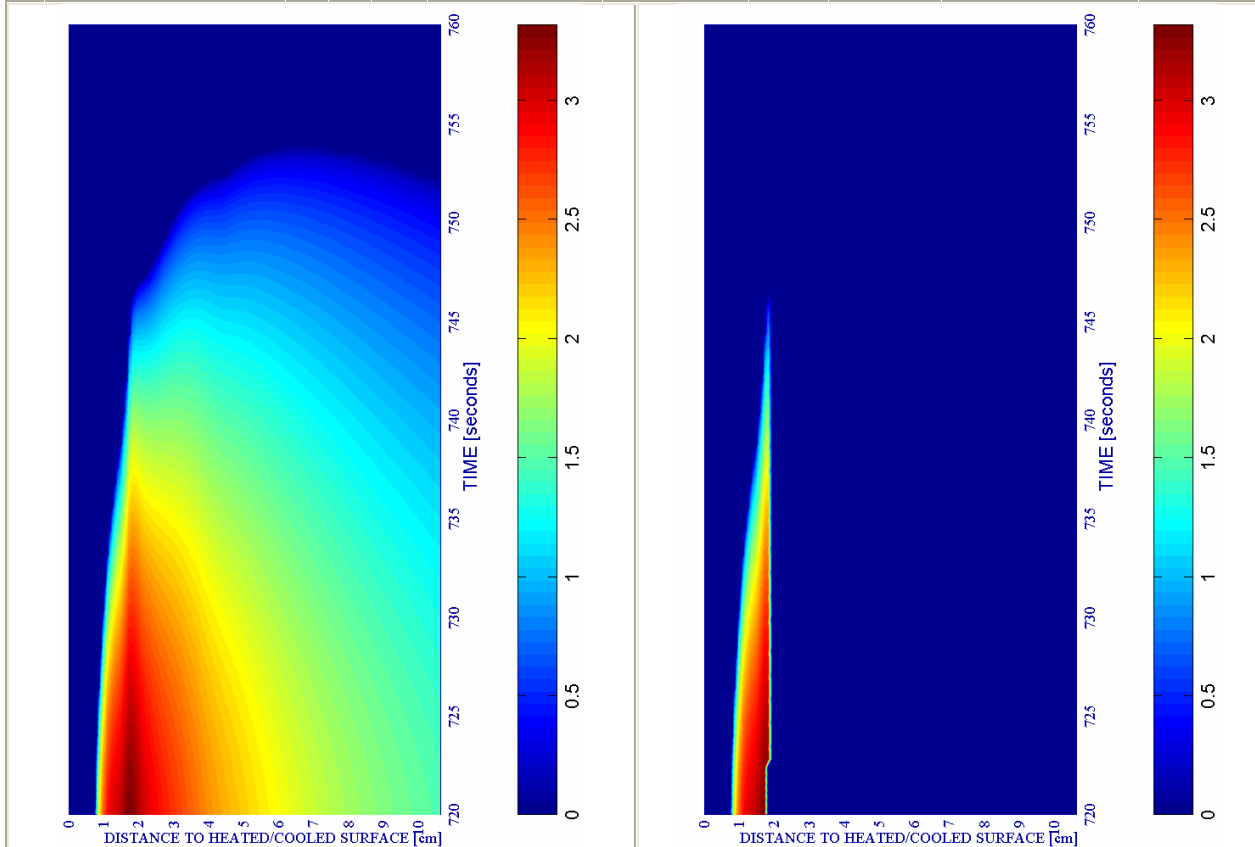
d) Down right: Velocity [m/s] where $d \geq 0,10$

a) Up left: Spalling Index IS_4 [-]

b) Up right: Mechanical damage d [-]



#	Combination	PC1 - RH [%]			PC2 - K_0 [m^2]			PC4 - Heating curve			PC5 - Mat.		Cooling length[s]	Start of cooling [s]	End of cooling [s]
		40	50	60	10^{-19}	10^{-18}	10^{-17}	PAR1	PAR2	PAR4	C60	C90			
40	TH12K017RH50PAR1C90		X				X	X				X	40	600+120	760



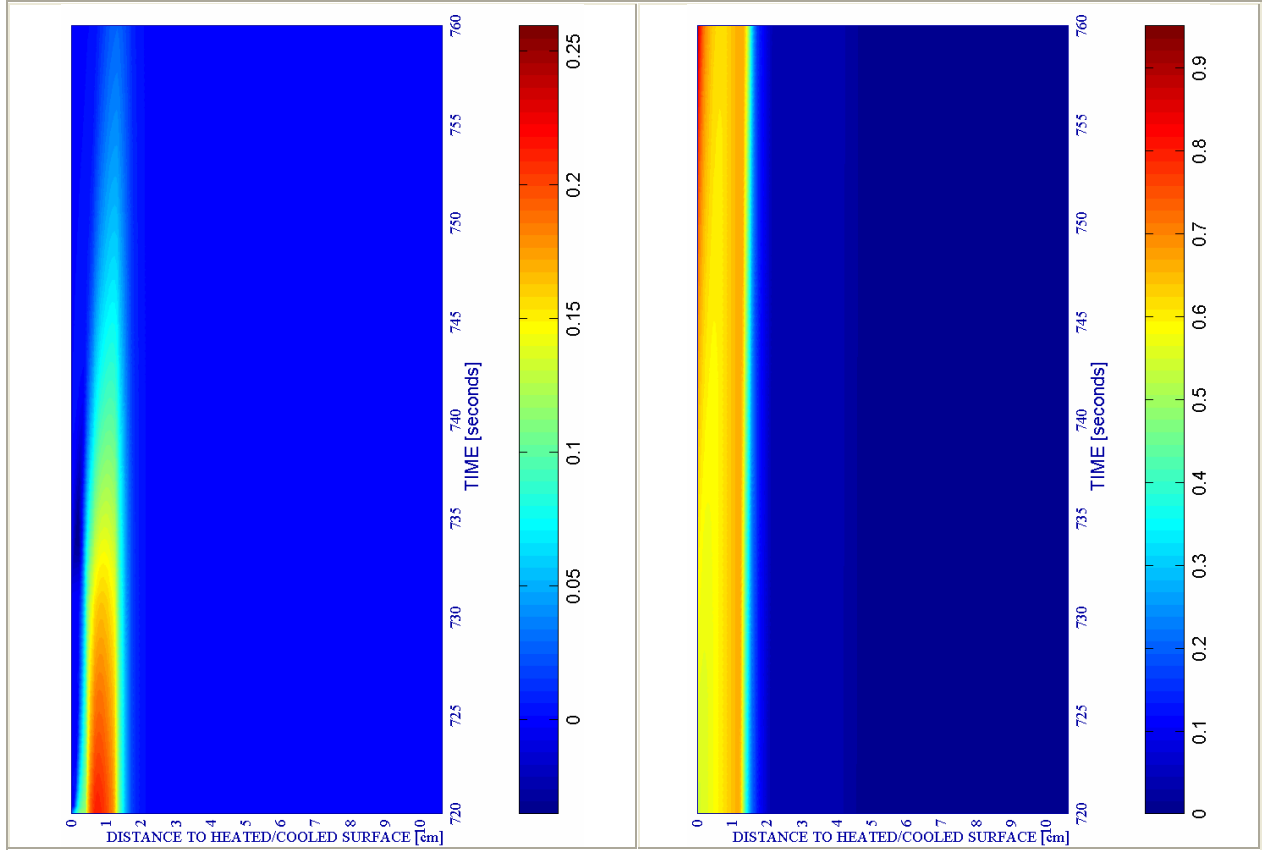
c) Down left: Velocity of spalled pieces [m/s]

Figure 6A-27.

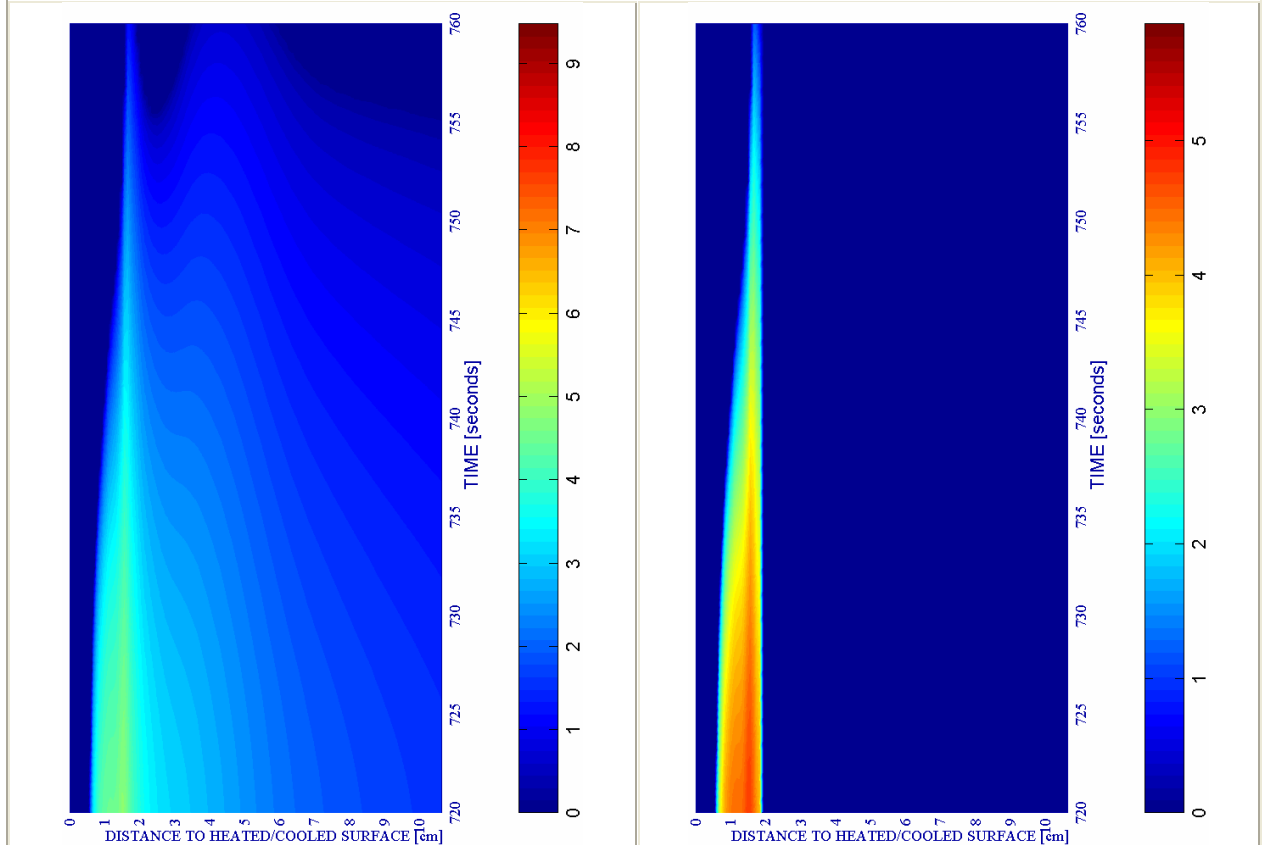
d) Down right: Velocity [m/s] where $d \geq 0,10$

a) Up left: Spalling Index IS_4 [-]

b) Up right: Mechanical damage d [-]



#	Combination	PC1 - RH [%]			PC2 - K_0 [m ²]			PC4 - Heating curve			PC5 - Mat.		Cooling length[s]	Start of cooling [s]	End of cooling [s]
		40	50	60	10 ⁻¹⁹	10 ⁻¹⁸	10 ⁻¹⁷	PAR1	PAR2	PAR4	C60	C90			
41	TH12K018RH50PAR1C90		X			X		X				X	40	600+120	760



c) Down left: Velocity of spalled pieces [m/s]

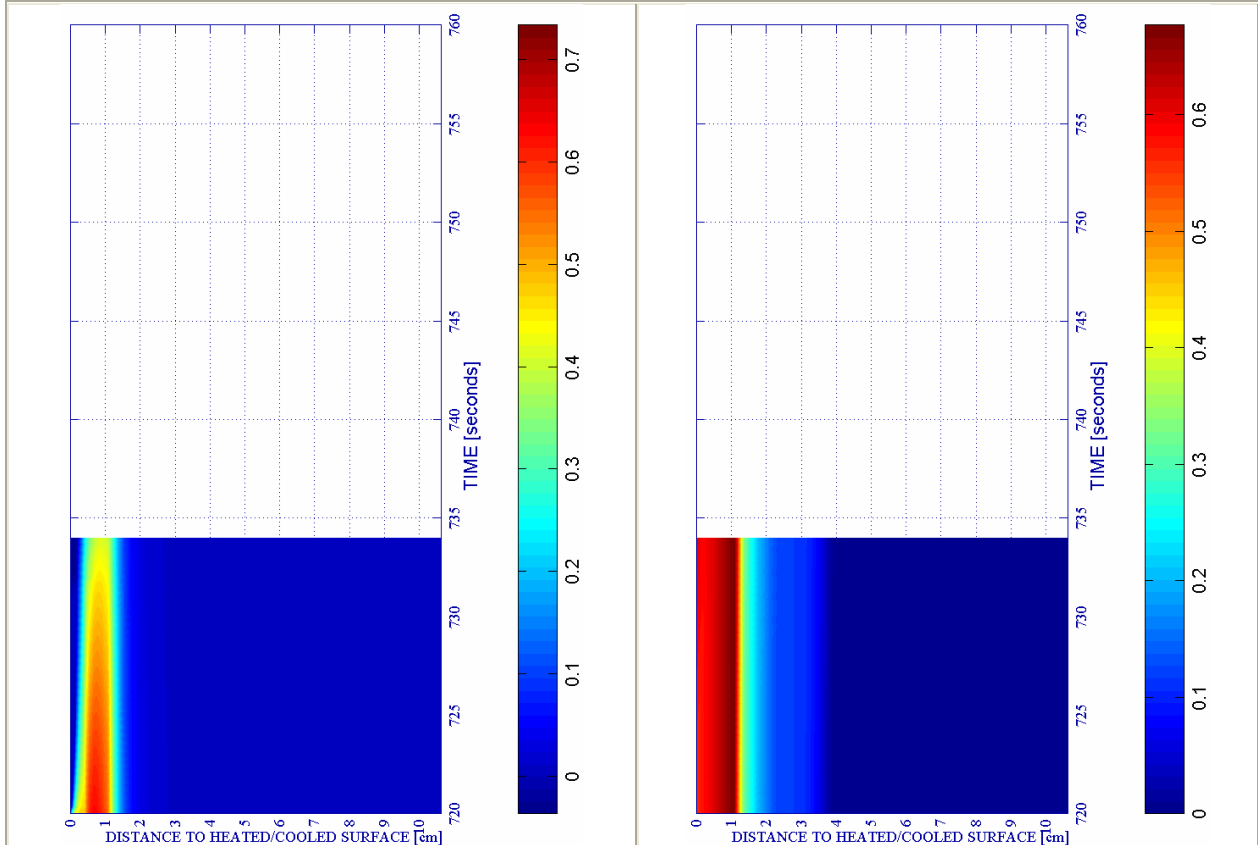
Figure 6A-28.

d) Down right: Velocity [m/s] where $d \geq 0,10$

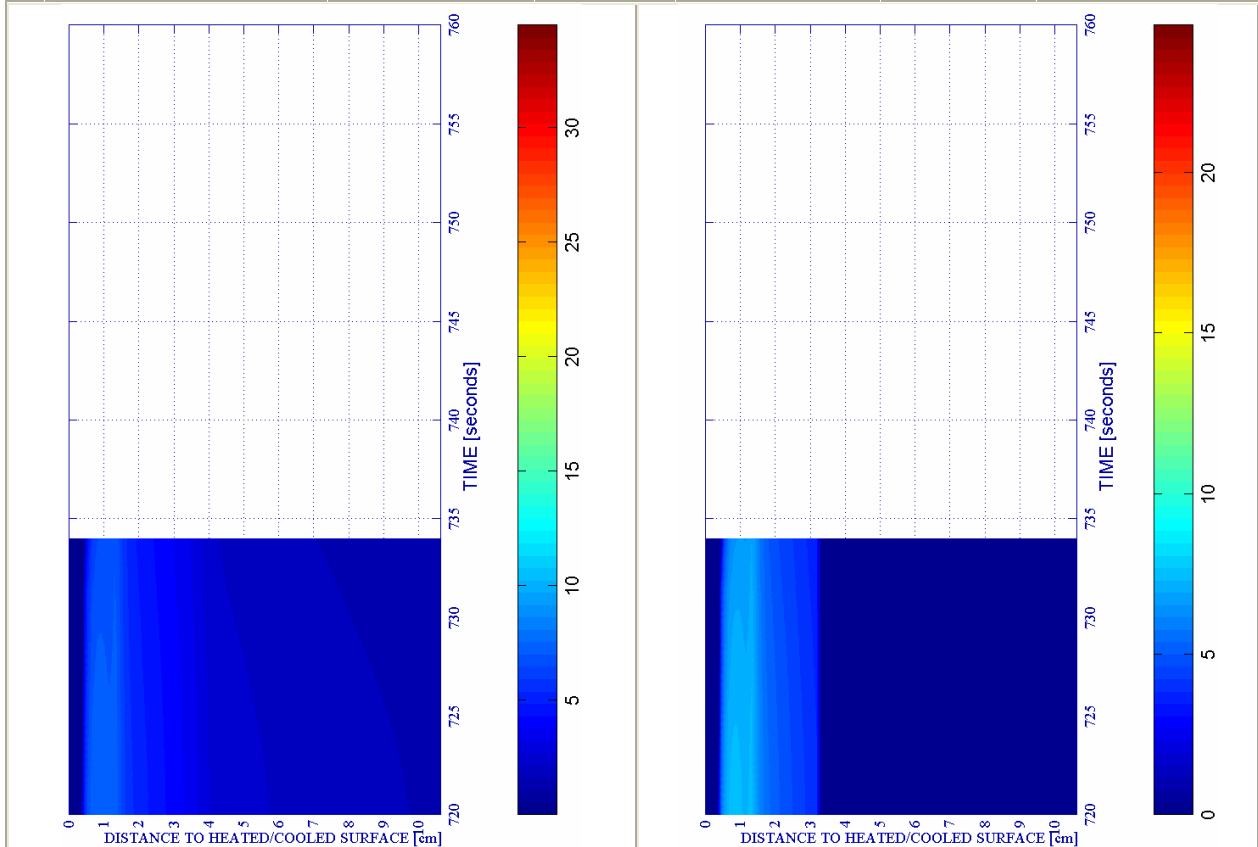
a) Up left: Spalling Index IS_4 [-]

***Remark:** Calculation failed at 734,3s

b) Up right: Mechanical damage d [-]



#	Combination	PC1 - RH [%]			PC2 - K_0 [m^2]			PC4 - Heating curve			PC5 - Mat.		Cooling length[s]	Start of cooling [s]	End of cooling [s]
		40	50	60	10^{-19}	10^{-18}	10^{-17}	PAR1	PAR2	PAR4	C60	C90			
42	TH12K019RH50PAR1C90		X		X			X				X	40	600+120	760*



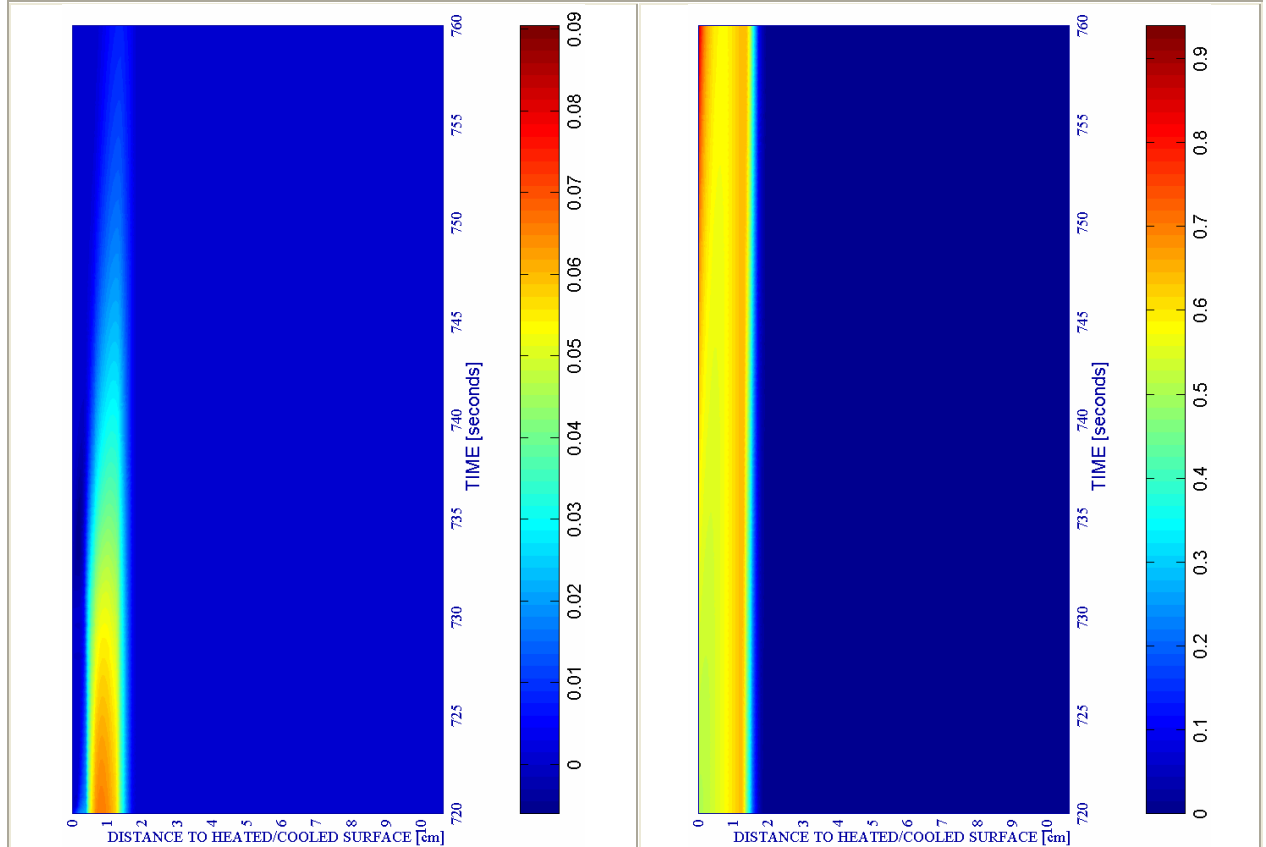
c) Down left: Velocity of spalled pieces [m/s]

Figure 6A-29.

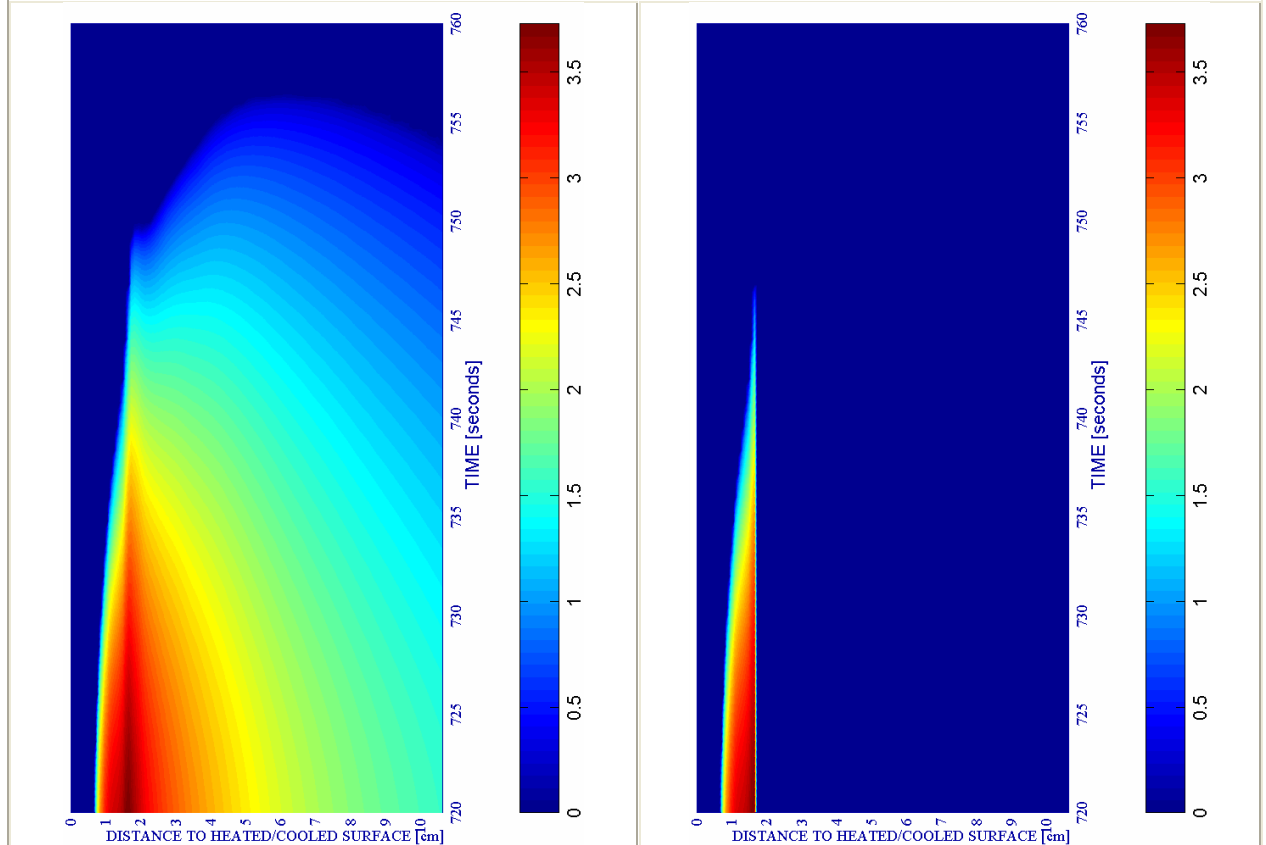
d) Down right: Velocity [m/s] where $d \geq 0,10$

a) Up left: Spalling Index IS_4 [-]

b) Up right: Mechanical damage d [-]



#	Combination	PC1 - RH [%]			PC2 - K_0 [m ²]			PC4 - Heating curve			PC5 - Mat.		Cooling length[s]	Start of cooling [s]	End of cooling [s]
		40	50	60	10 ⁻¹⁹	10 ⁻¹⁸	10 ⁻¹⁷	PAR1	PAR2	PAR4	C60	C90			
43	TH12K017RH60PAR1C90			X			X	X				X	40	600+120	760



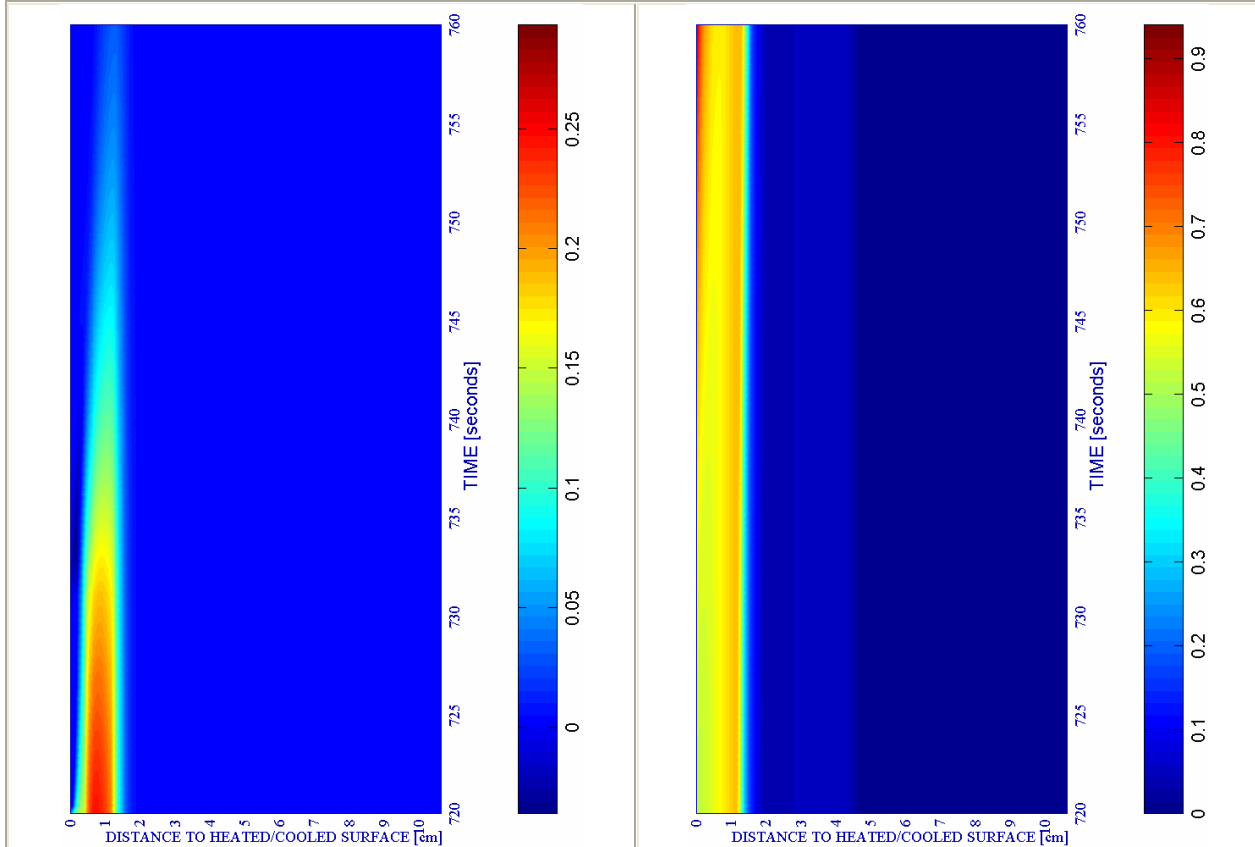
c) Down left: Velocity of spalled pieces [m/s]

Figure 6A-30.

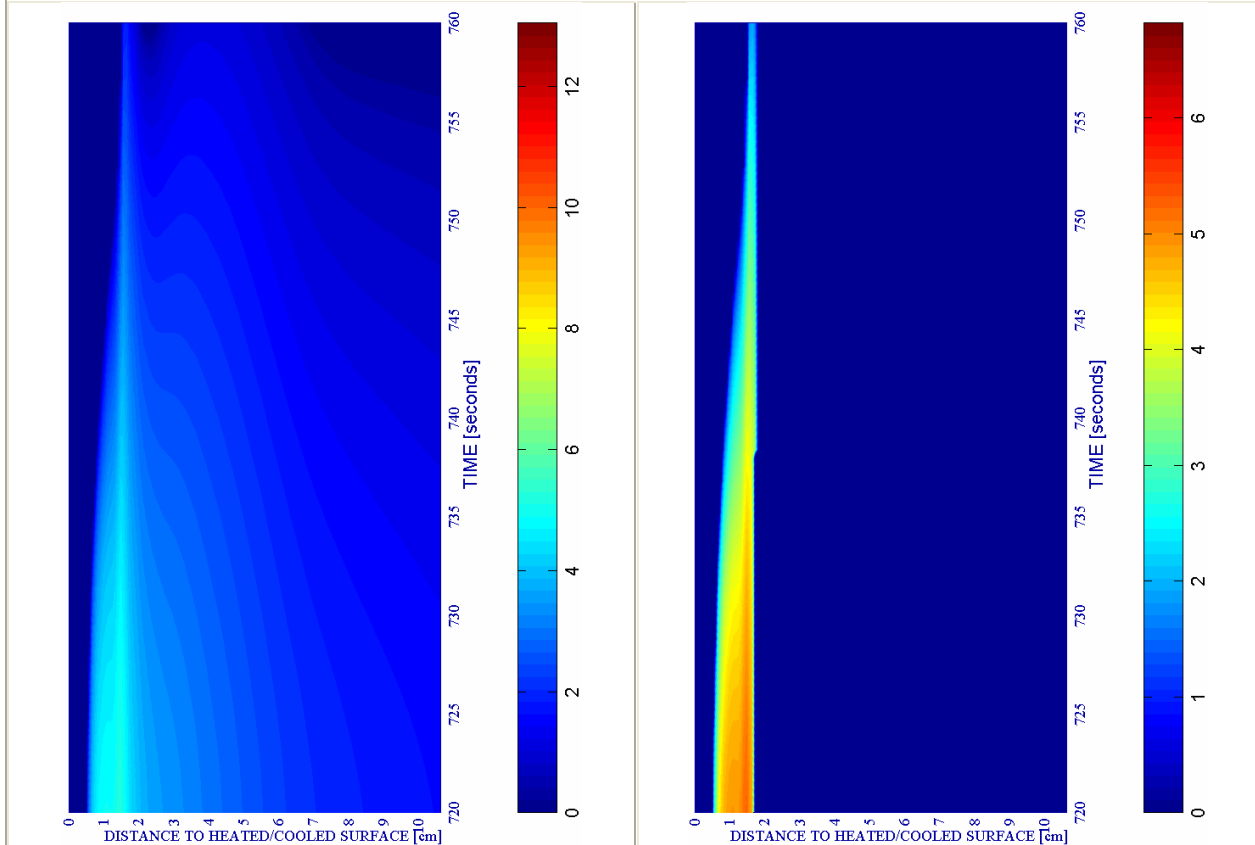
d) Down right: Velocity [m/s] where $d \geq 0,10$

a) Up left: Spalling Index IS_4 [-]

b) Up right: Mechanical damage d [-]



#	Combination	PC1 - RH [%]			PC2 - K_0 [m^2]			PC4 - Heating curve			PC5 - Mat.		Cooling length[s]	Start of cooling [s]	End of cooling [s]
		40	50	60	10^{-19}	10^{-18}	10^{-17}	PAR1	PAR2	PAR4	C60	C90			
44	TH12K018RH60PAR1C90			X		X		X				X	40	600+120	760



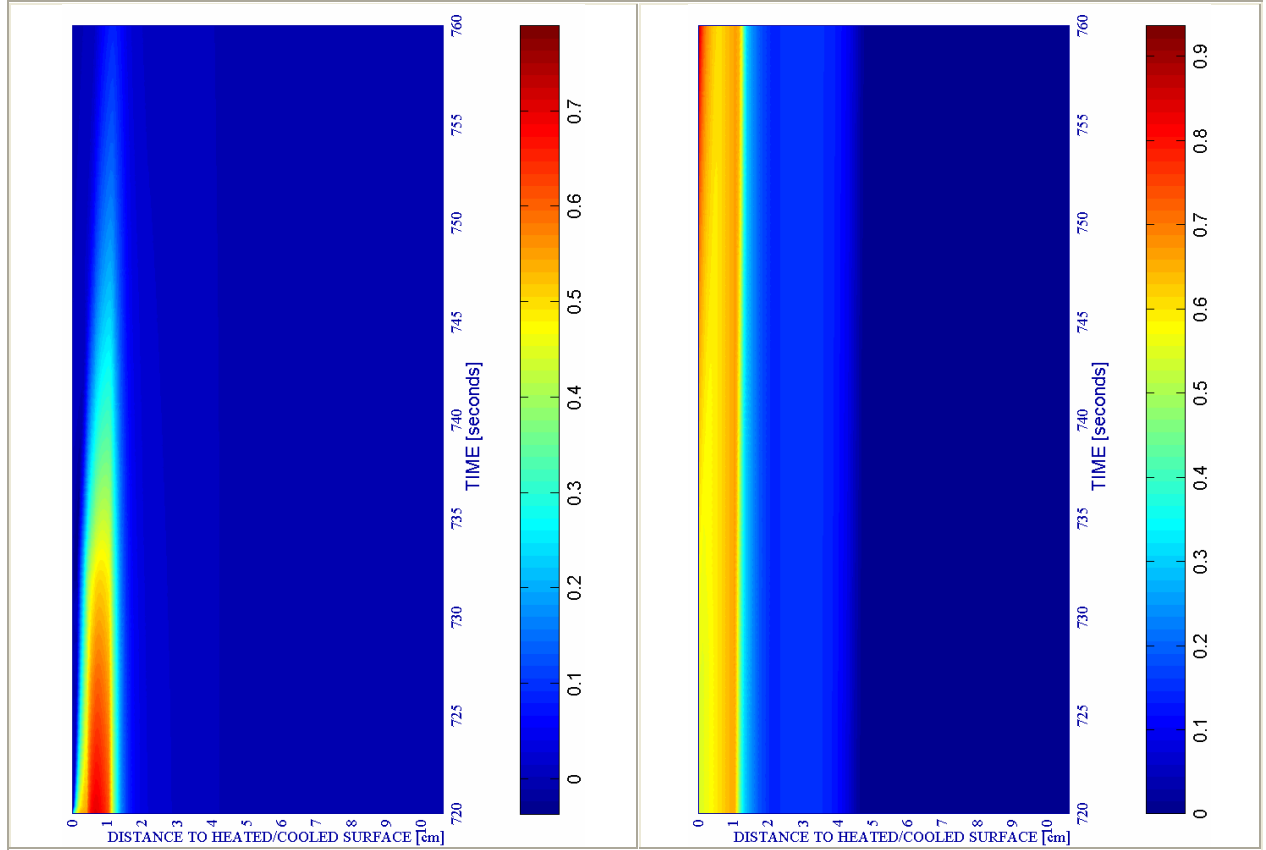
c) Down left: Velocity of spalled pieces [m/s]

Figure 6A-31.

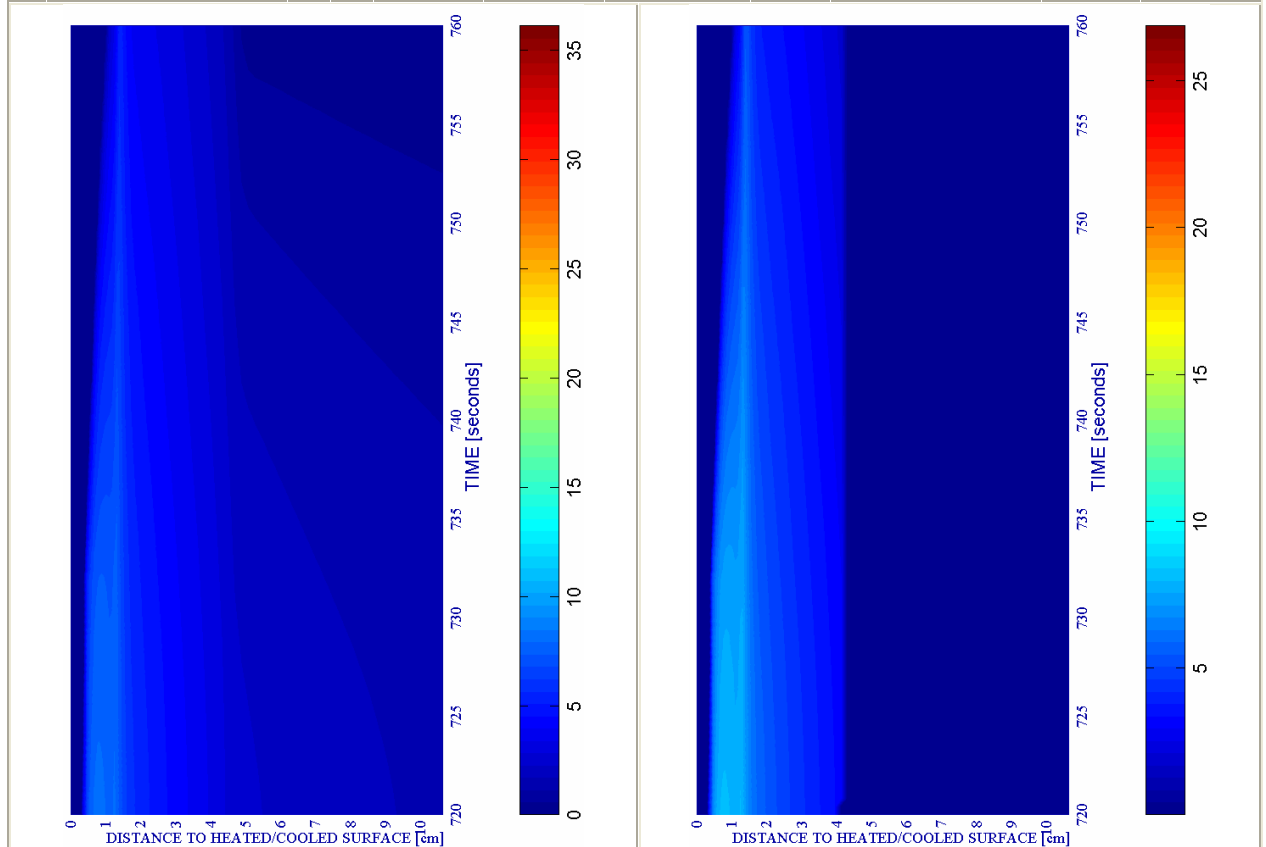
d) Down right: Velocity [m/s] where $d \geq 0,10$

a) Up left: Spalling Index IS_4 [-]

b) Up right: Mechanical damage d [-]



#	Combination	PC1 - RH [%]			PC2 - K_0 [m ²]			PC4 - Heating curve			PC5 - Mat.		Cooling length[s]	Start of cooling [s]	End of cooling [s]
		40	50	60	10 ⁻¹⁹	10 ⁻¹⁸	10 ⁻¹⁷	PAR1	PAR2	PAR4	C60	C90			
45	TH12K019RH60PAR1C90			X	X			X				X	40	600+120	760



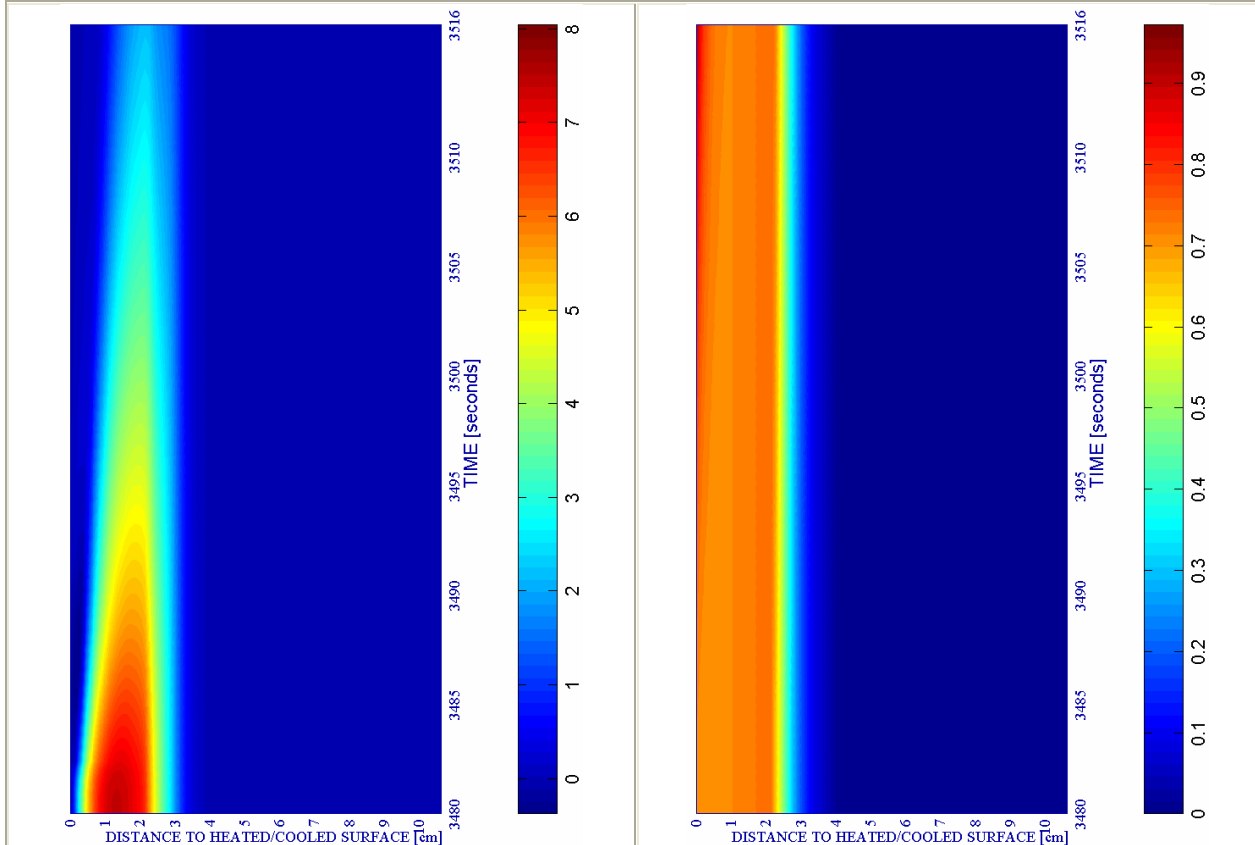
c) Down left: Velocity of spalled pieces [m/s]

Figure 6A-32.

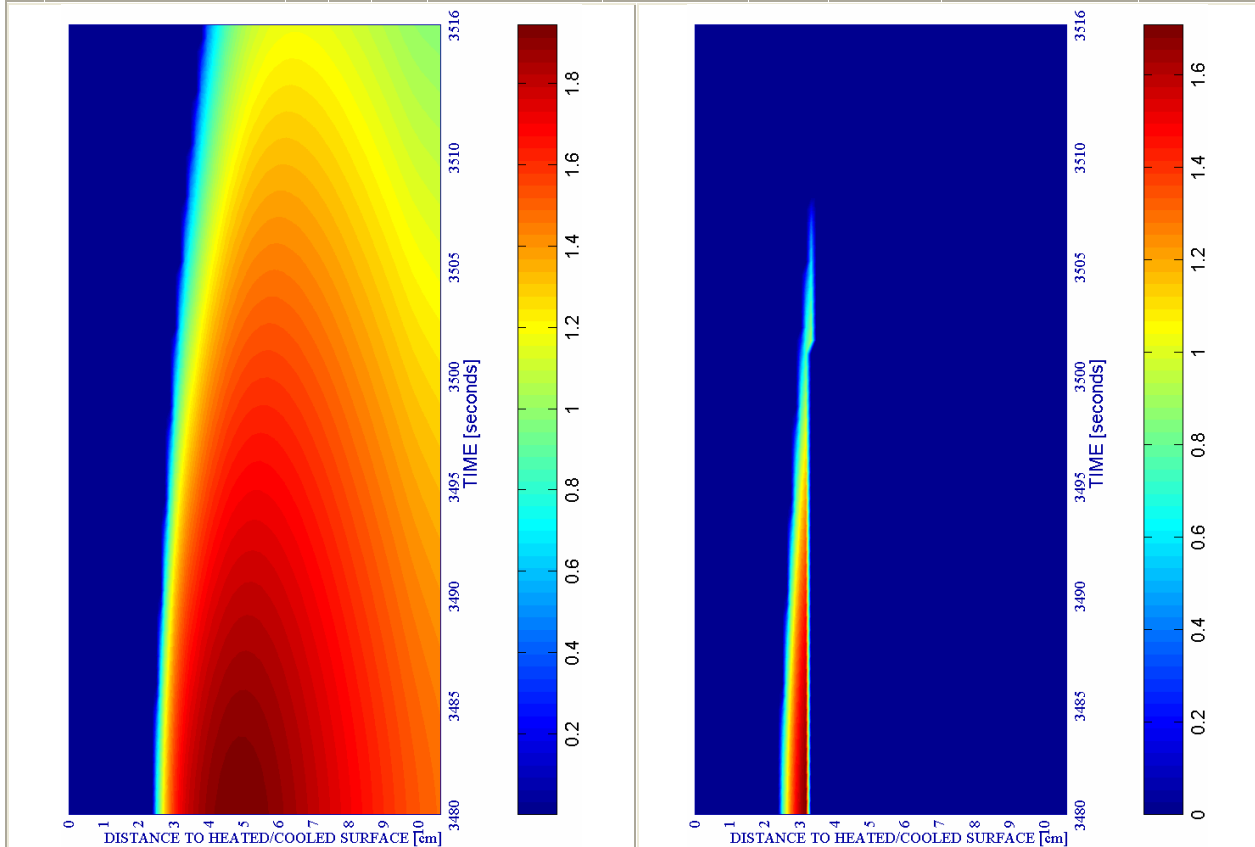
d) Down right: Velocity [m/s] where $d \geq 0,10$

a) Up left: Spalling Index $IS_4 * 10^3 [-]$

b) Up right: Mechanical damage $d [-]$



#	Combination	PC1 - RH [%]			PC2 - K_0 [m^2]			PC4 - Heating curve			PC5 - Mat.		Cooling length[s]	Start of cooling [s]	End of cooling [s]
		40	50	60	10^{-19}	10^{-18}	10^{-17}	PAR1	PAR2	PAR4	C60	C90			
46	TH12K017RH40PAR2C90	X					X		X			X	36	3360+120	3516



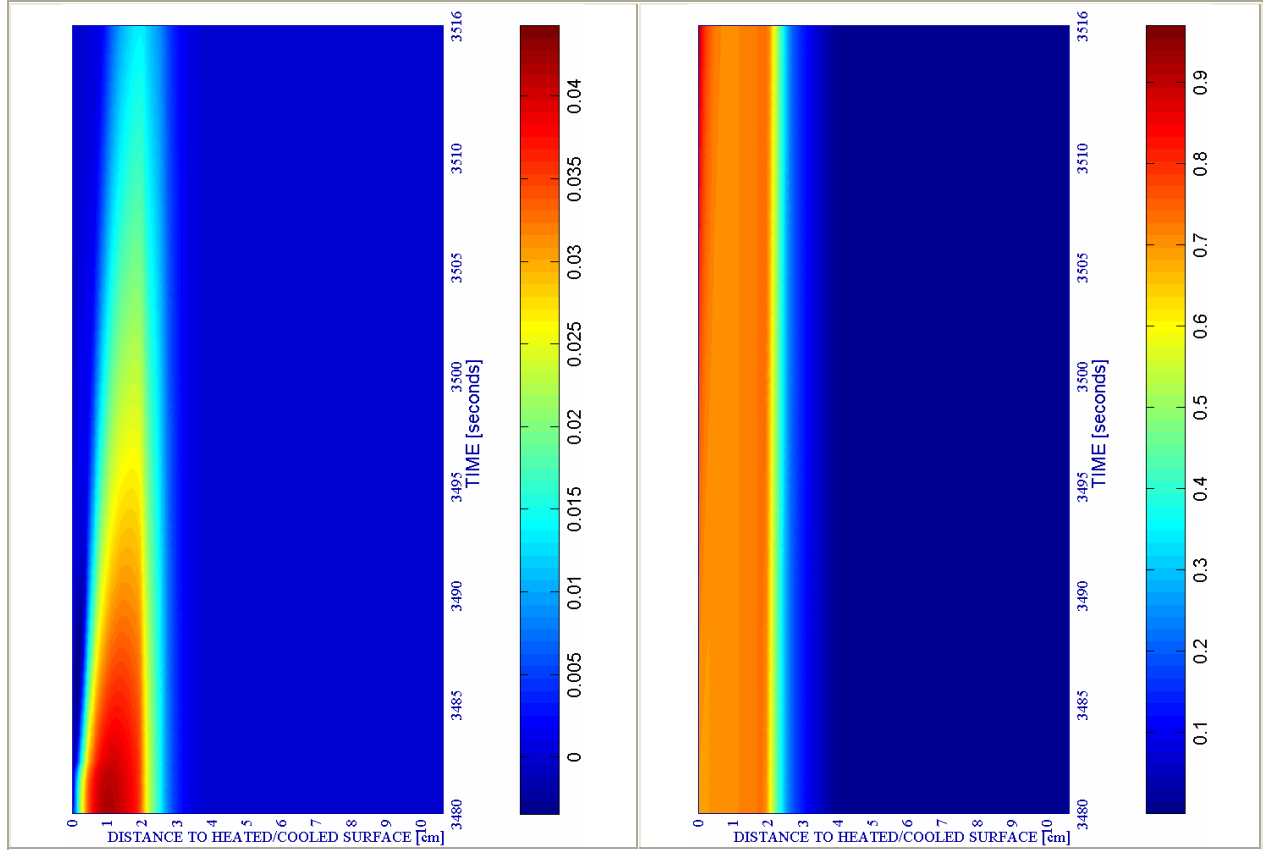
c) Down left: Velocity of spalled pieces [m/s]

Figure 6A-33.

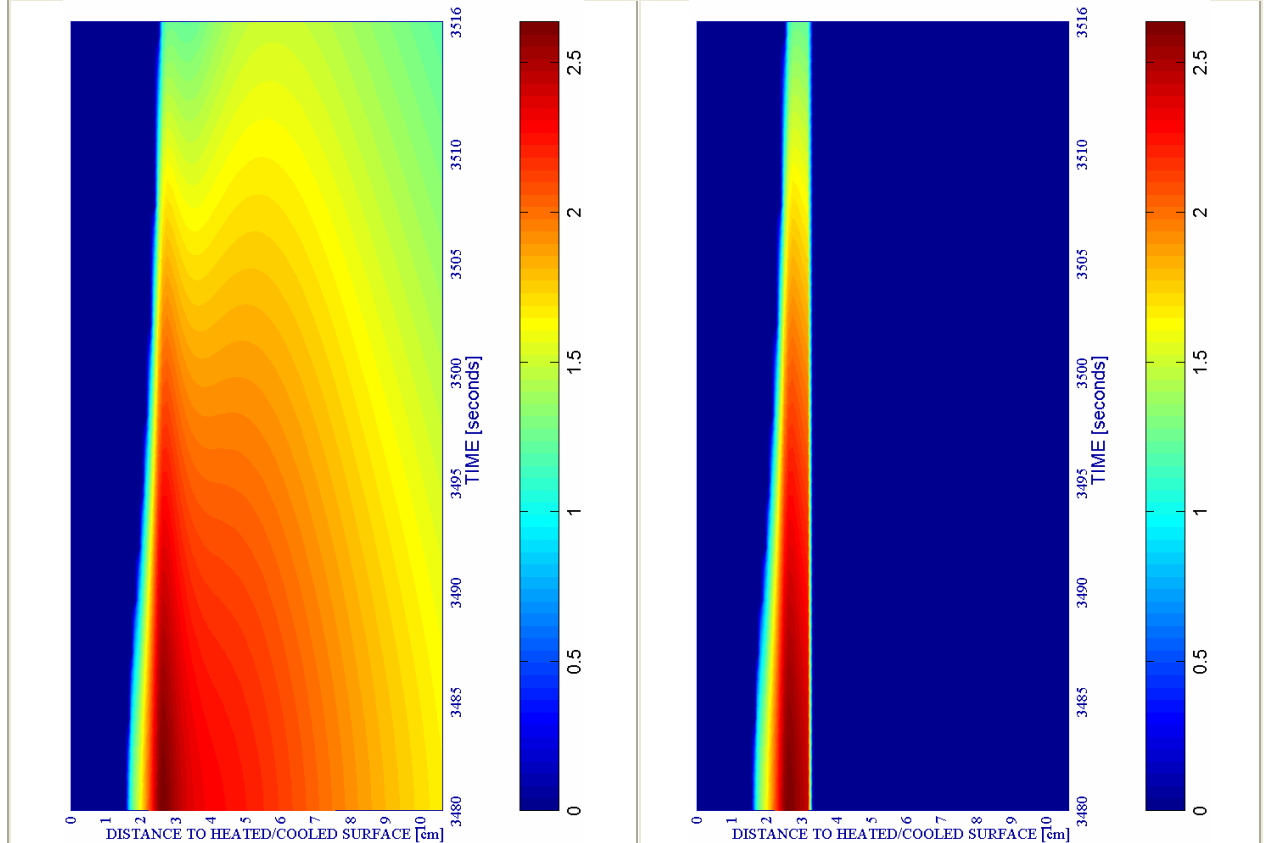
d) Down right: Velocity [m/s] where $d \geq 0,10$

a) Up left: Spalling Index IS_4 [-]

b) Up right: Mechanical damage d [-]



#	Combination	PC1 - RH [%]			PC2 - K_0 [m ²]			PC4 - Heating curve			PC5 - Mat.		Cooling length[s]	Start of cooling [s]	End of cooling [s]	
		40	50	60	10^{-19}	10^{-18}	10^{-17}	PAR1	PAR2	PAR4	C60	C90				
47	TH12K018RH40PAR2C90	X					X			X			X	36	3360+120	3516



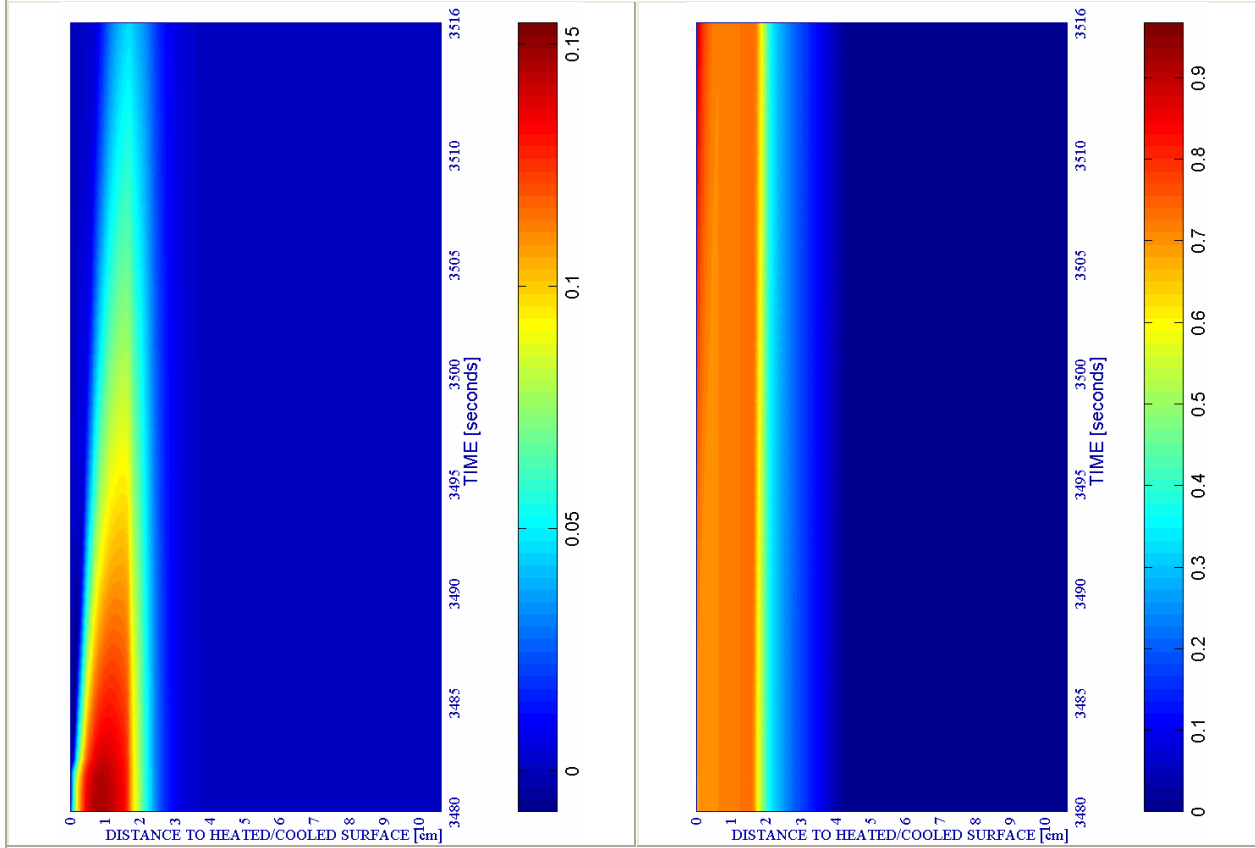
c) Down left: Velocity of spalled pieces [m/s]

Figure 6A-34.

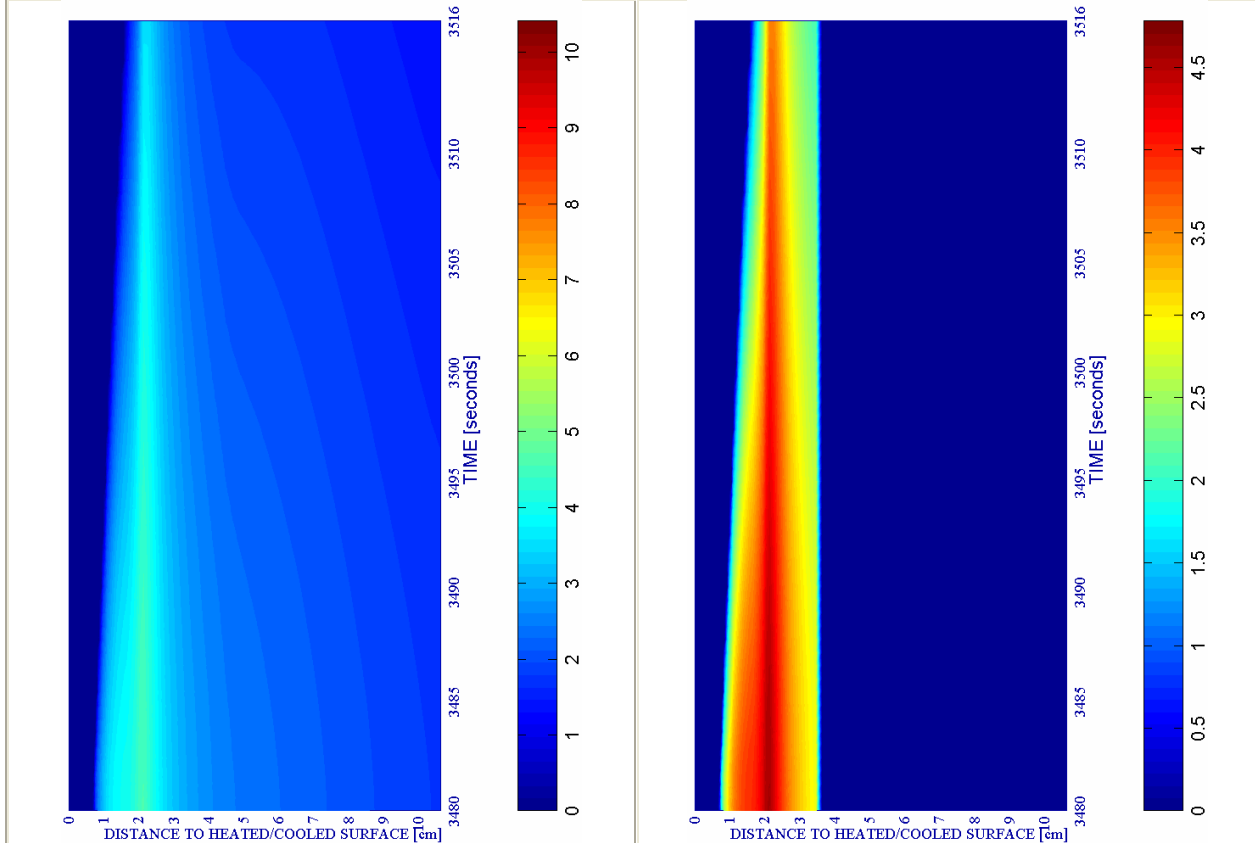
d) Down right: Velocity [m/s] where $d \geq 0,10$

a) Up left: Spalling Index IS_4 [-]

b) Up right: Mechanical damage d [-]



#	Combination	PC1 - RH [%]			PC2 - K_0 [m^2]			PC4 - Heating curve			PC5 - Mat.		Cooling length[s]	Start of cooling [s]	End of cooling [s]
		40	50	60	10^{-19}	10^{-18}	10^{-17}	PAR1	PAR2	PAR4	C60	C90			
48	TH12K019RH40PAR2C90	X			X				X			X	36	3360+120	3516



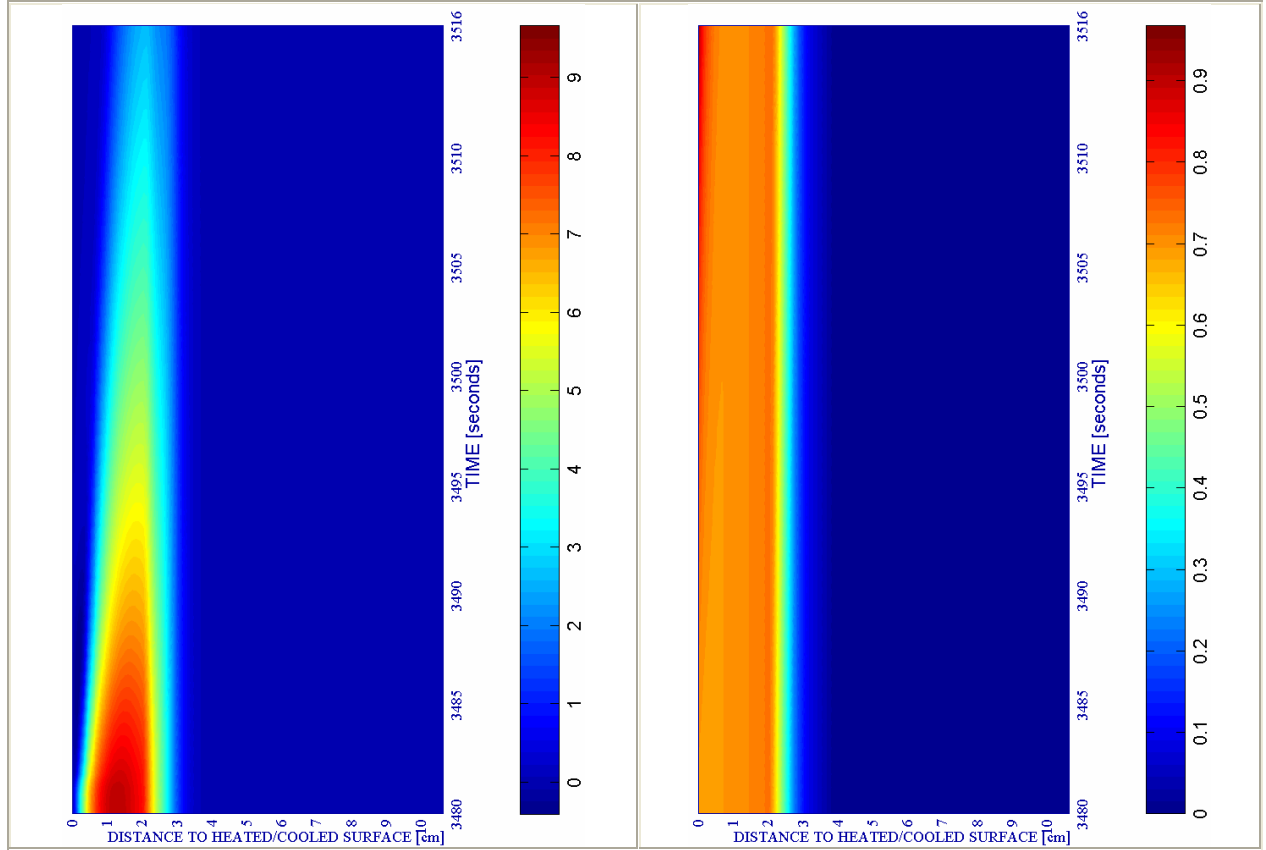
c) Down left: Velocity of spalled pieces [m/s]

Figure 6A-35.

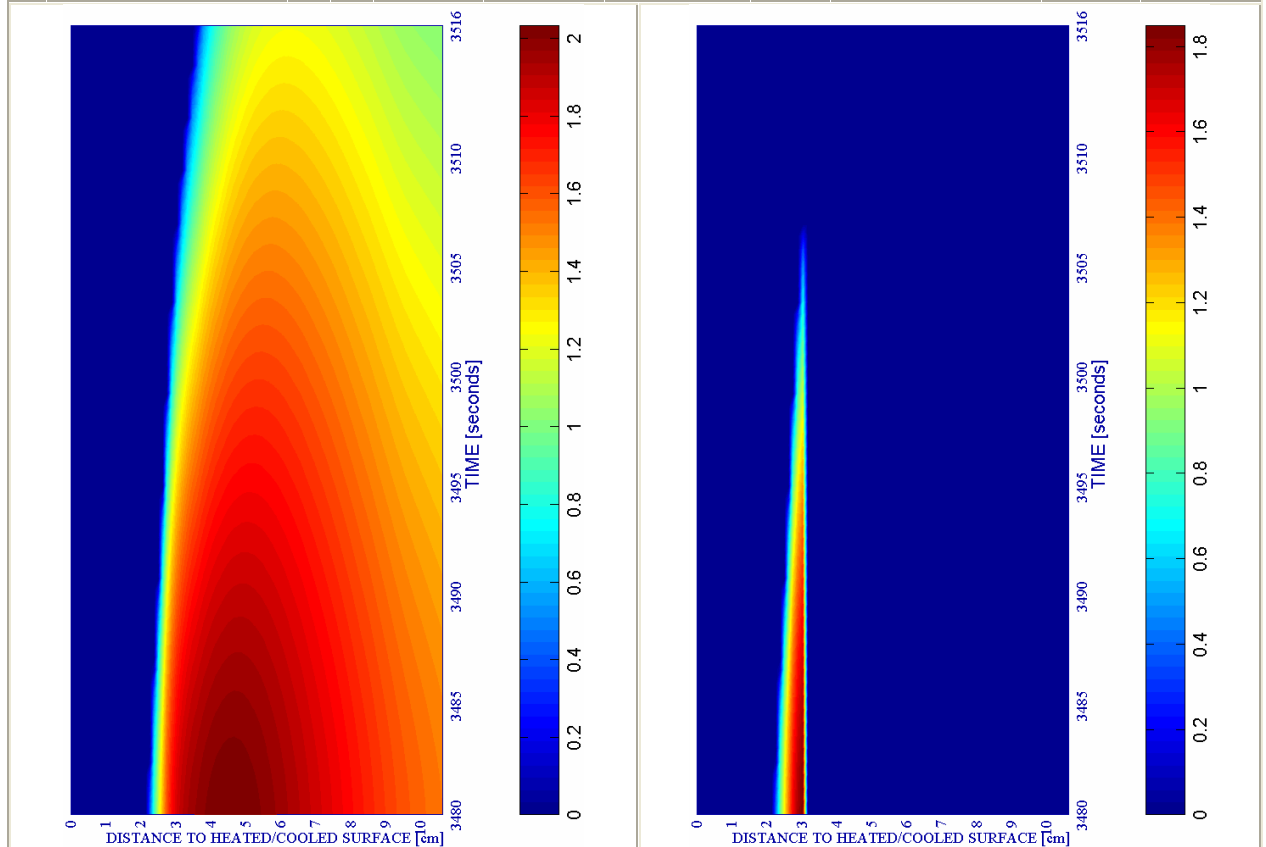
d) Down right: Velocity [m/s] where $d \geq 0,10$

a) Up left: Spalling Index $IS_4 * 10^3 [-]$

b) Up right: Mechanical damage $d [-]$



#	Combination	PC1 - RH [%]			PC2 - $K_0 [m^2]$			PC4 - Heating curve			PC5 - Mat.		Cooling length[s]	Start of cooling [s]	End of cooling [s]
		40	50	60	10^{-19}	10^{-18}	10^{-17}	PAR1	PAR2	PAR4	C60	C90			
49	TH12K017RH50PAR2C90		X				X		X			X	36	3360+120	3516



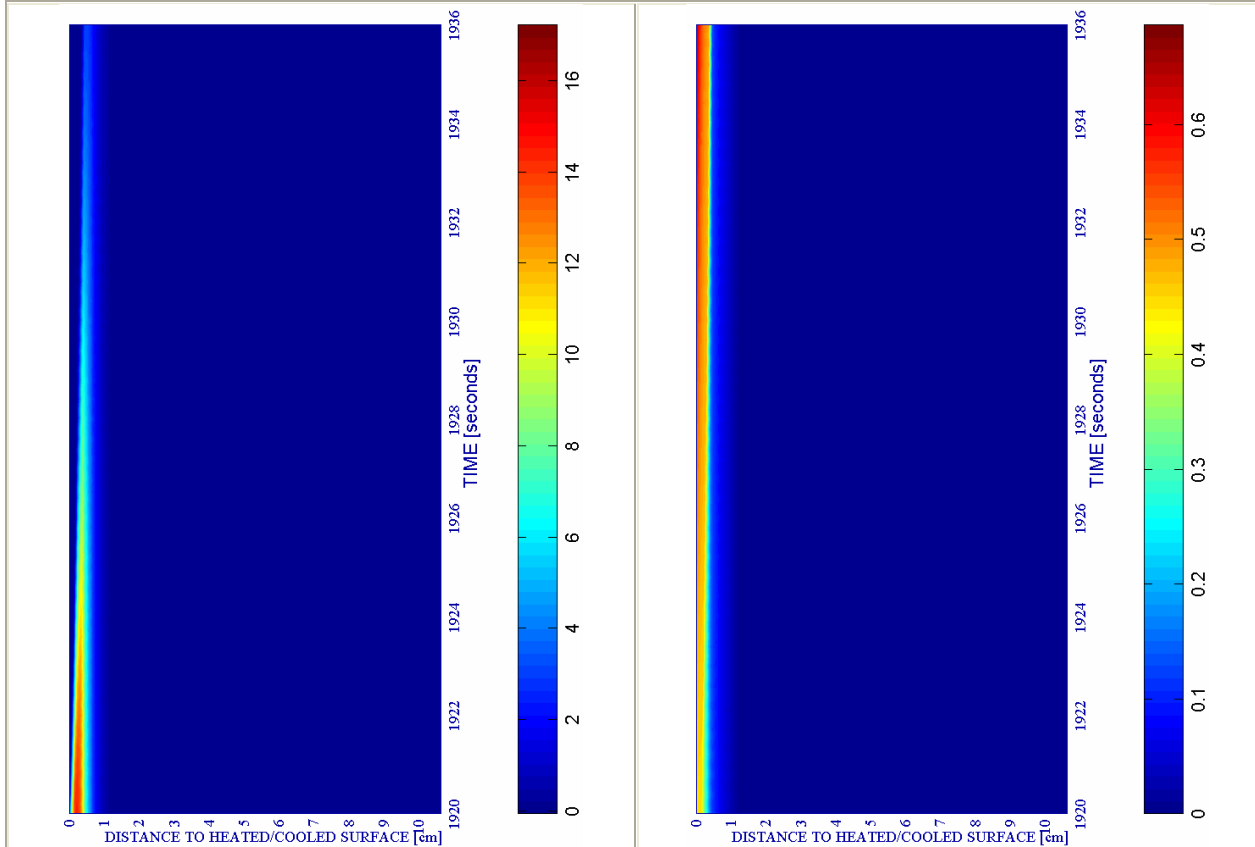
c) Down left: Velocity of spalled pieces [m/s]

Figure 6A-36.

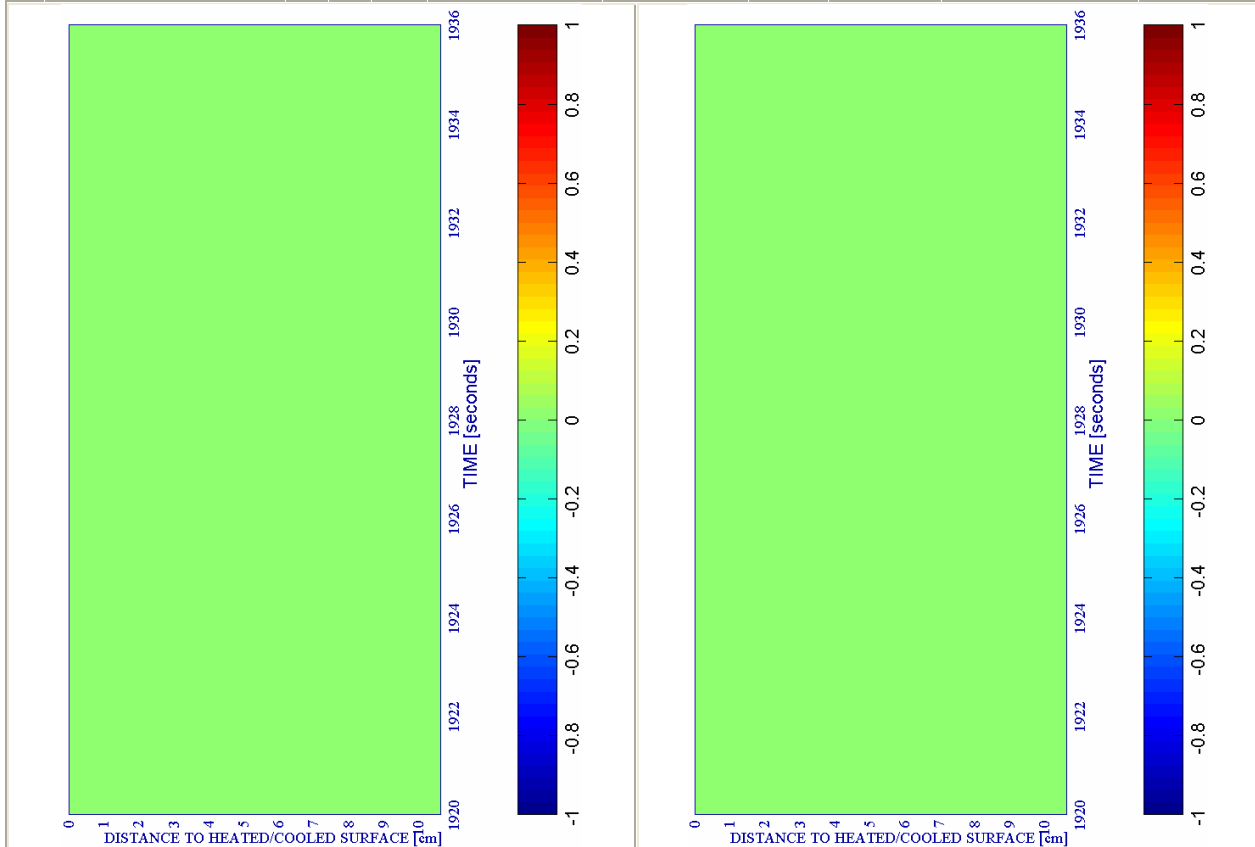
d) Down right: Velocity [m/s] where $d \geq 0,10$

a) Up left: Spalling Index $IS_4 * 10^3 [-]$

b) Up right: Mechanical damage $d [-]$



#	Combination	PC1 - RH [%]			PC2 - K_0 [m ²]			PC4 - Heating curve			PC5 - Mat.		Cooling length[s]	Start of cooling [s]	End of cooling [s]
		40	50	60	10 ⁻¹⁹	10 ⁻¹⁸	10 ⁻¹⁷	PAR1	PAR2	PAR4	C60	C90			
50	TH12K018RH50PAR2C90		X			X			X			X	16	1800+120	1936



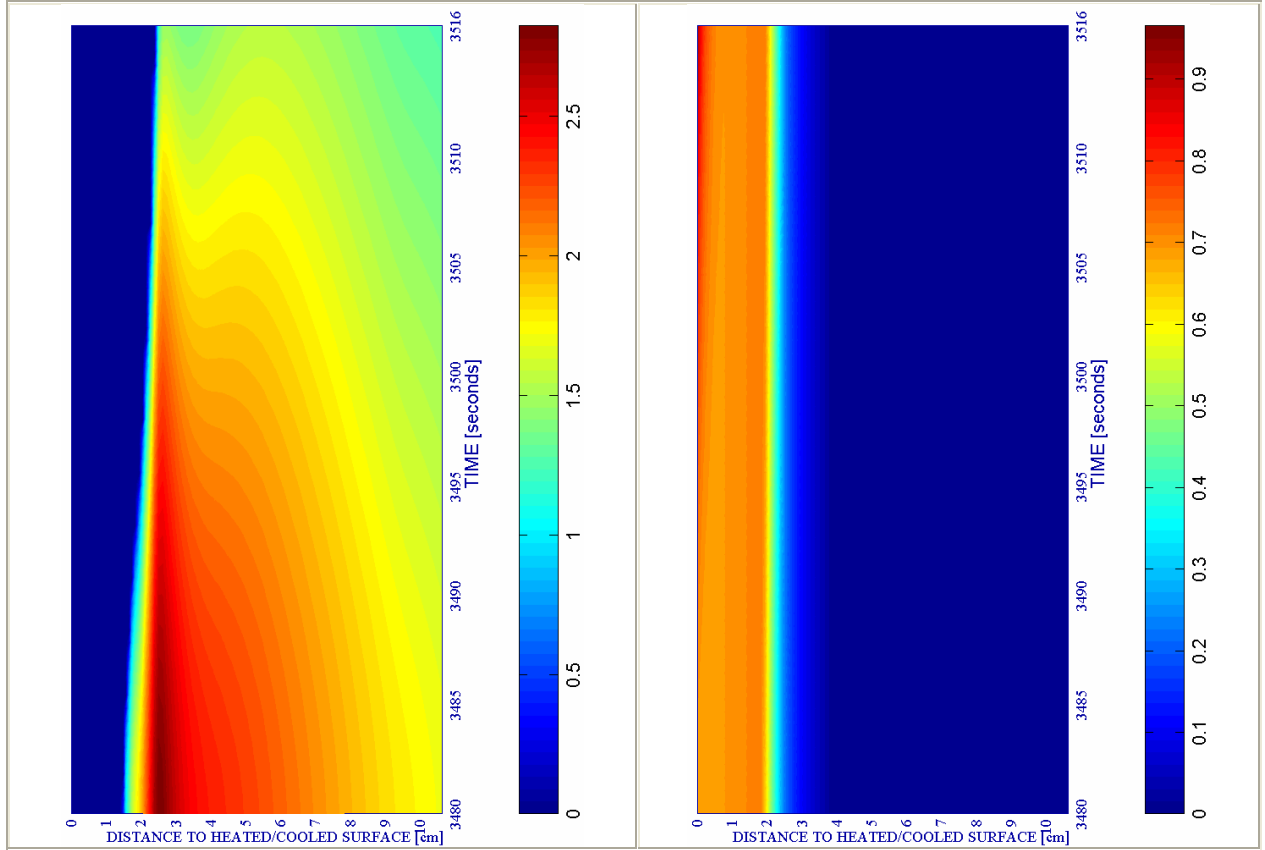
c) Down left: Velocity of spalled pieces [m/s]

Figure 6A-37.

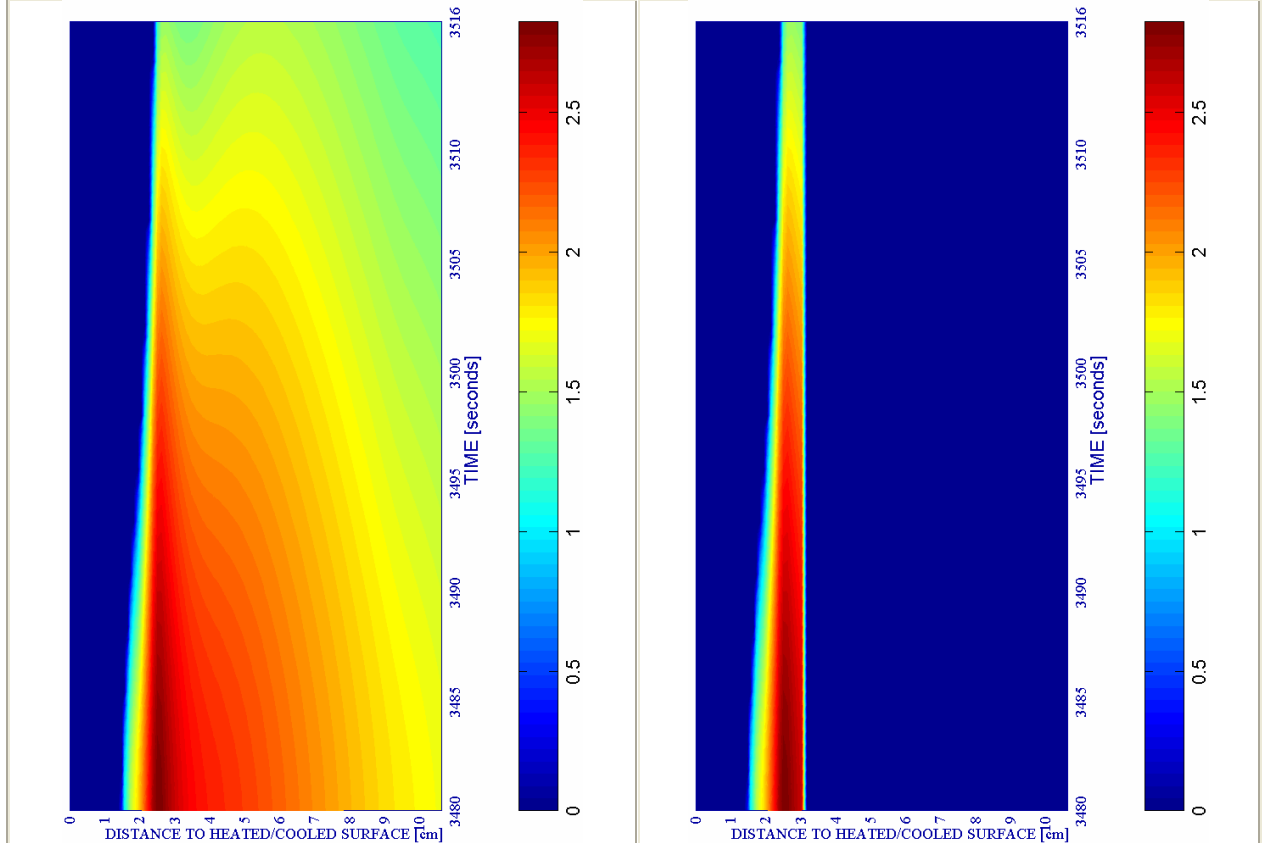
d) Down right: Velocity [m/s] where $d \geq 0,10$

a) Up left: Spalling Index IS_4 [-]

b) Up right: Mechanical damage d [-]



#	Combination	PC1 - RH [%]			PC2 - K_0 [m ²]			PC4 - Heating curve			PC5 - Mat.		Cooling length[s]	Start of cooling [s]	End of cooling [s]
		40	50	60	10 ⁻¹⁹	10 ⁻¹⁸	10 ⁻¹⁷	PAR1	PAR2	PAR4	C60	C90			
50	TH12K018RH50PAR2C90		X			X			X			X	36	3360+120	3516



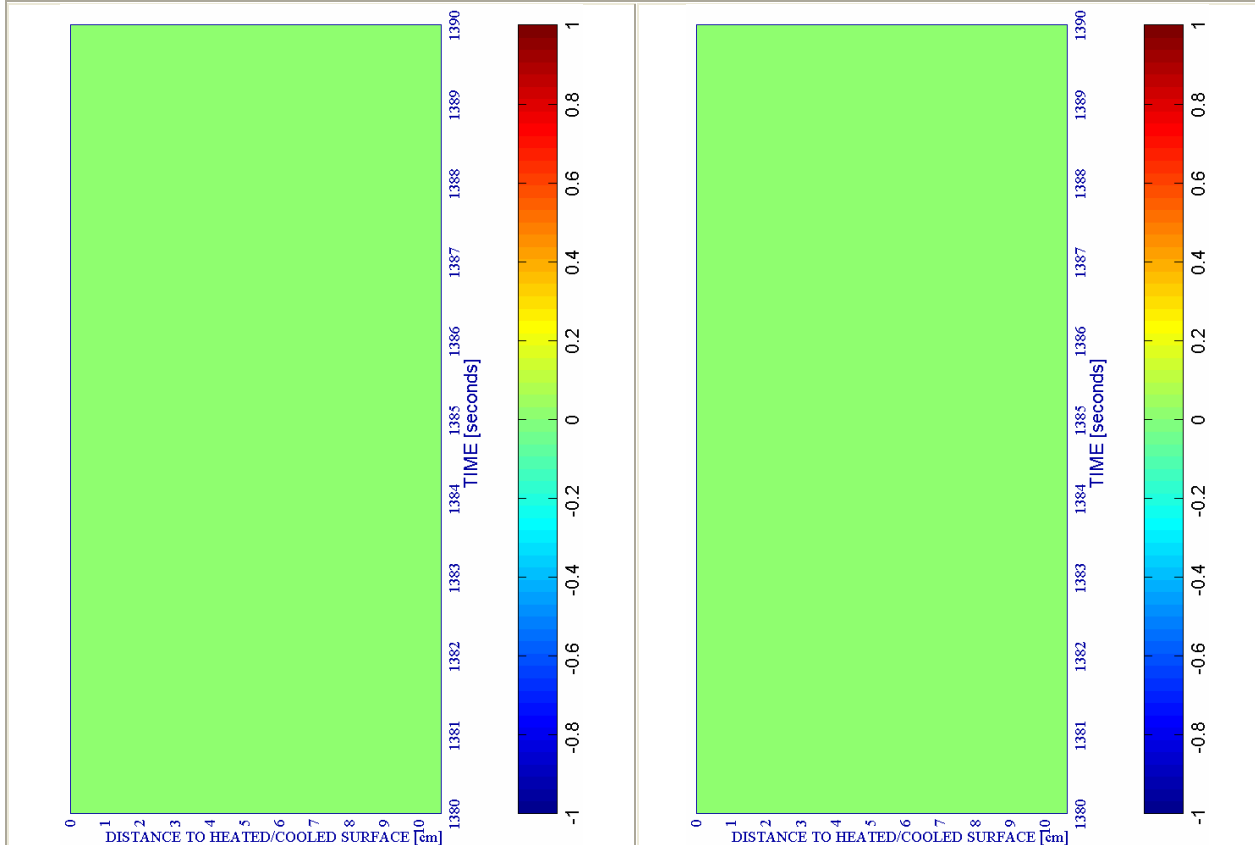
c) Down left: Velocity of spalled pieces [m/s]

Figure 6A-38.

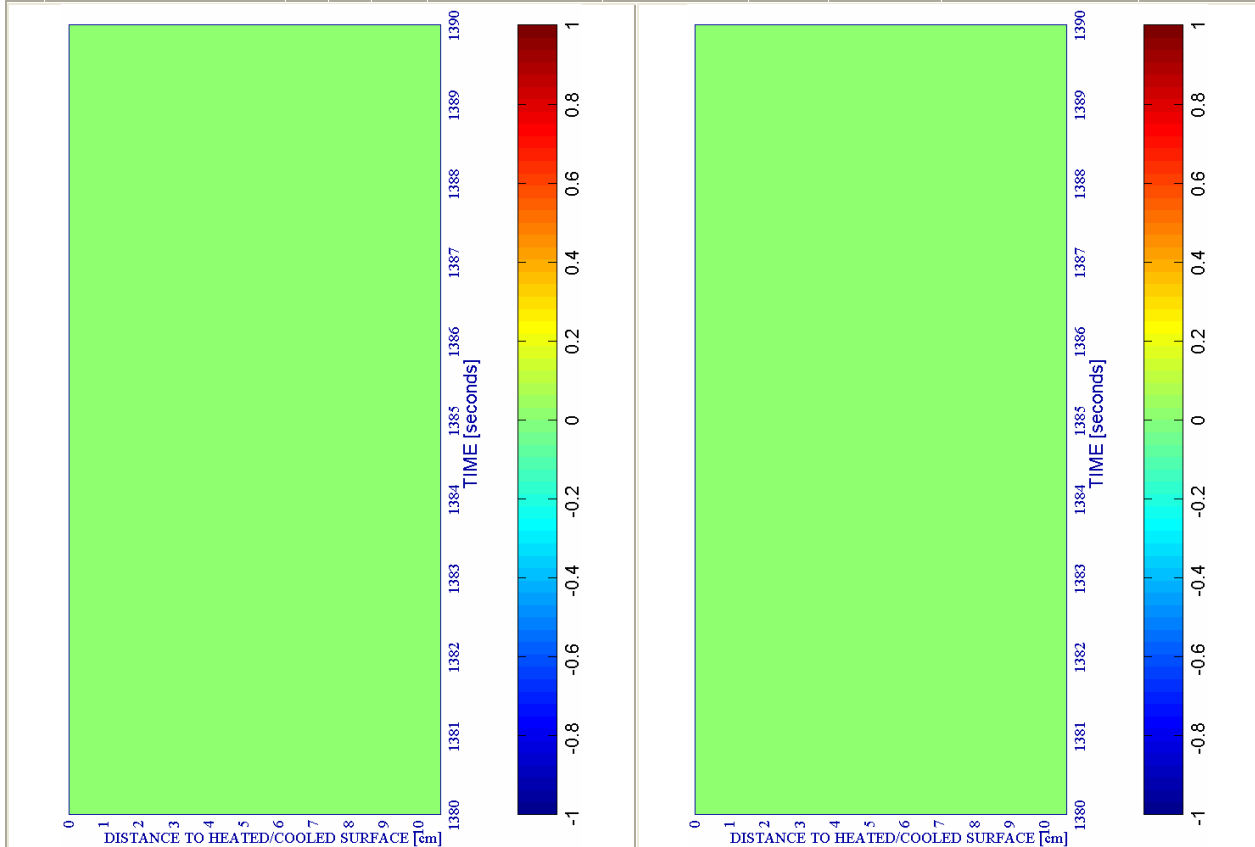
d) Down right: Velocity [m/s] where $d \geq 0,10$

a) Up left: Spalling Index IS_4 [-]

b) Up right: Mechanical damage d [-]



#	Combination	PC1 - RH [%]			PC2 - K_0 [m ²]			PC4 - Heating curve			PC5 - Mat.		Cooling length[s]	Start of cooling [s]	End of cooling [s]
		40	50	60	10 ⁻¹⁹	10 ⁻¹⁸	10 ⁻¹⁷	PAR1	PAR2	PAR4	C60	C90			
51	TH12K019RH50PAR2C90		X		X				X			X	10	1260+120	1390



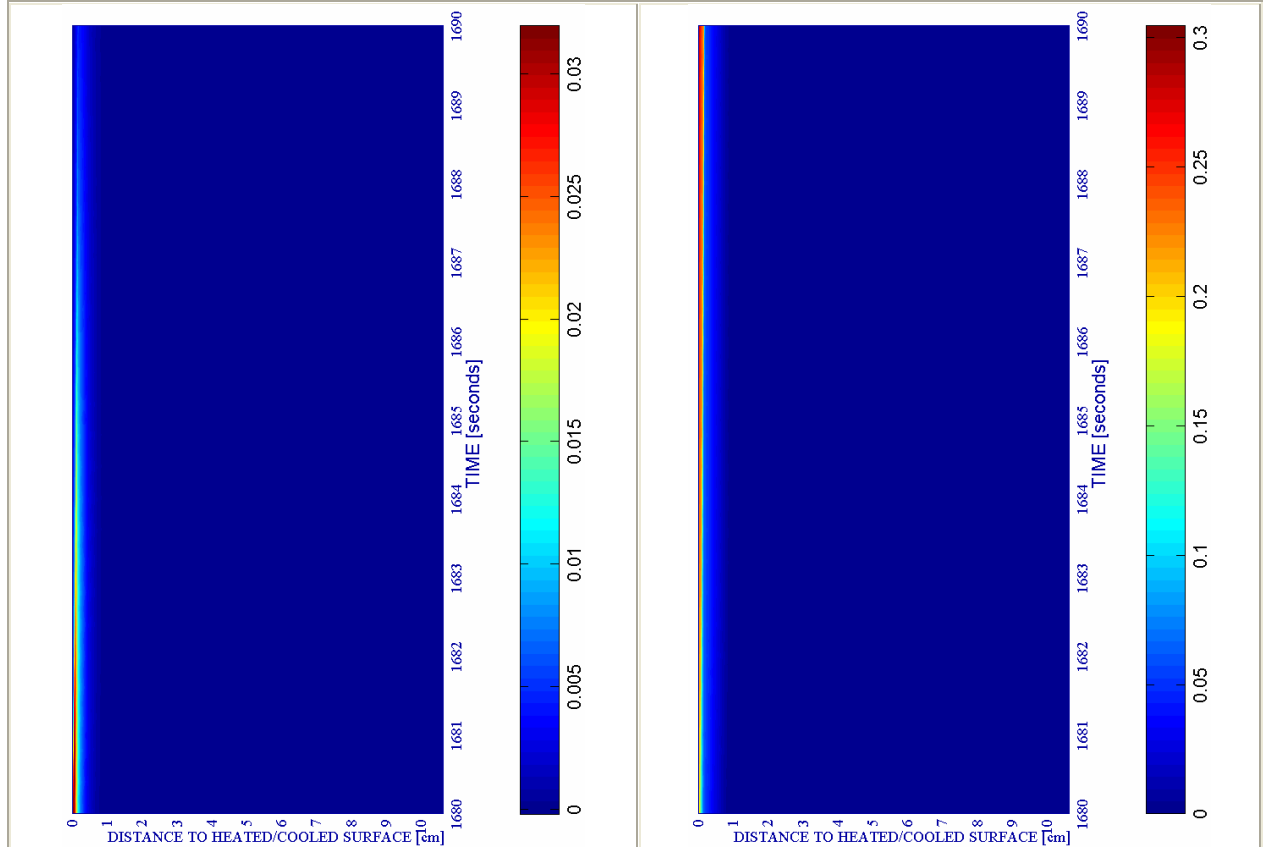
c) Down left: Velocity of spalled pieces [m/s]

Figure 6A-39.

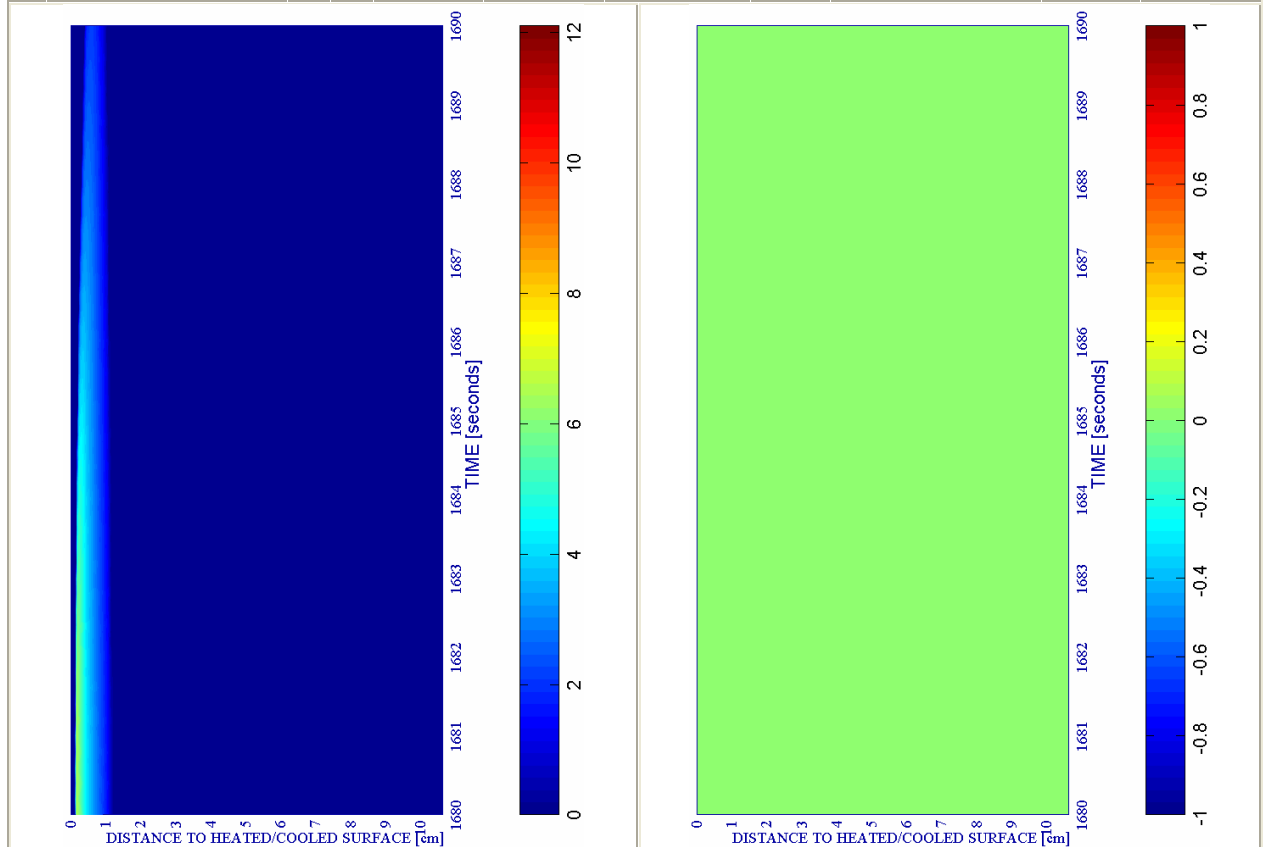
d) Down right: Velocity [m/s] where $d \geq 0,10$

a) Up left: Spalling Index IS_4 [-]

b) Up right: Mechanical damage d [-]



#	Combination	PC1 - RH [%]			PC2 - K_0 [m ²]			PC4 - Heating curve			PC5 - Mat.		Cooling length[s]	Start of cooling [s]	End of cooling [s]
		40	50	60	10 ⁻¹⁹	10 ⁻¹⁸	10 ⁻¹⁷	PAR1	PAR2	PAR4	C60	C90			
51	TH12K019RH50PAR2C90		X		X				X			X	10	1560+120	1690



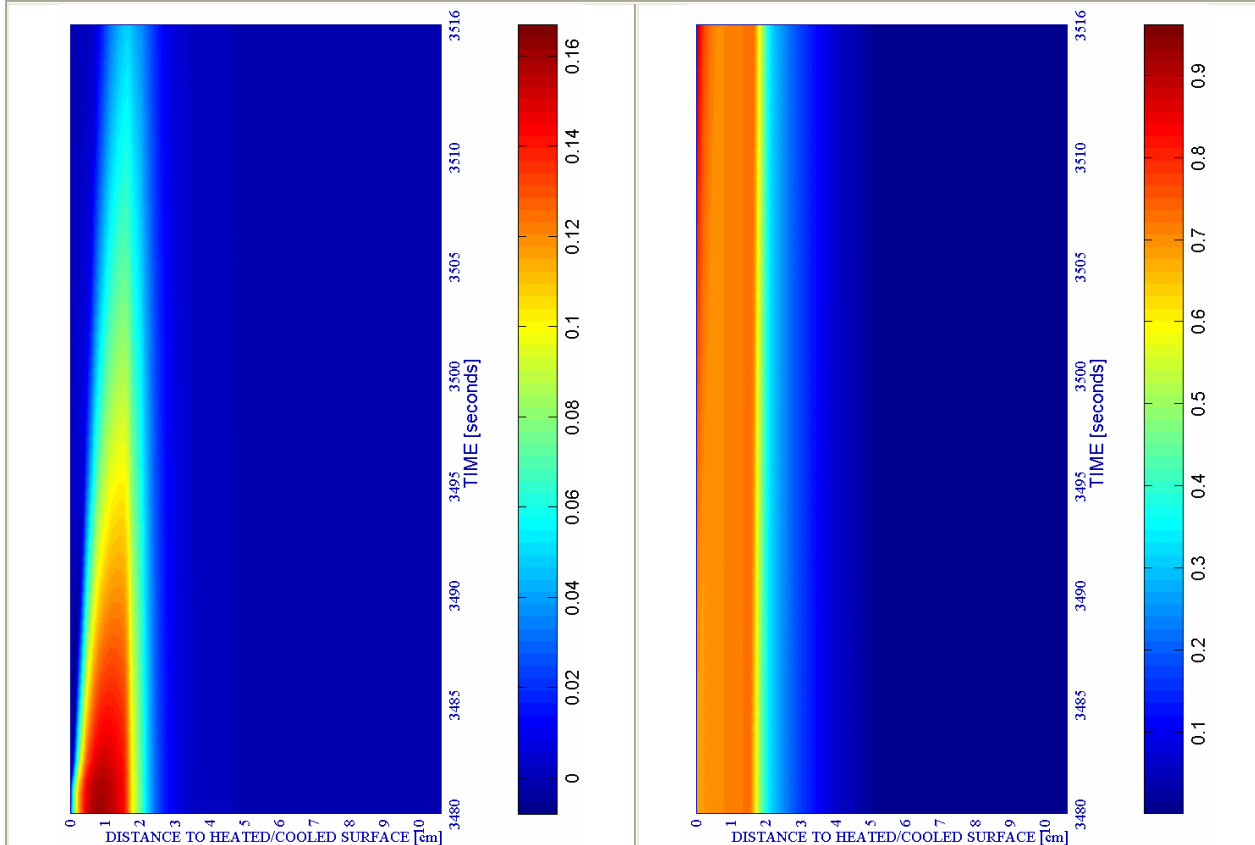
c) Down left: Velocity of spalled pieces [m/s]

Figure 6A-40.

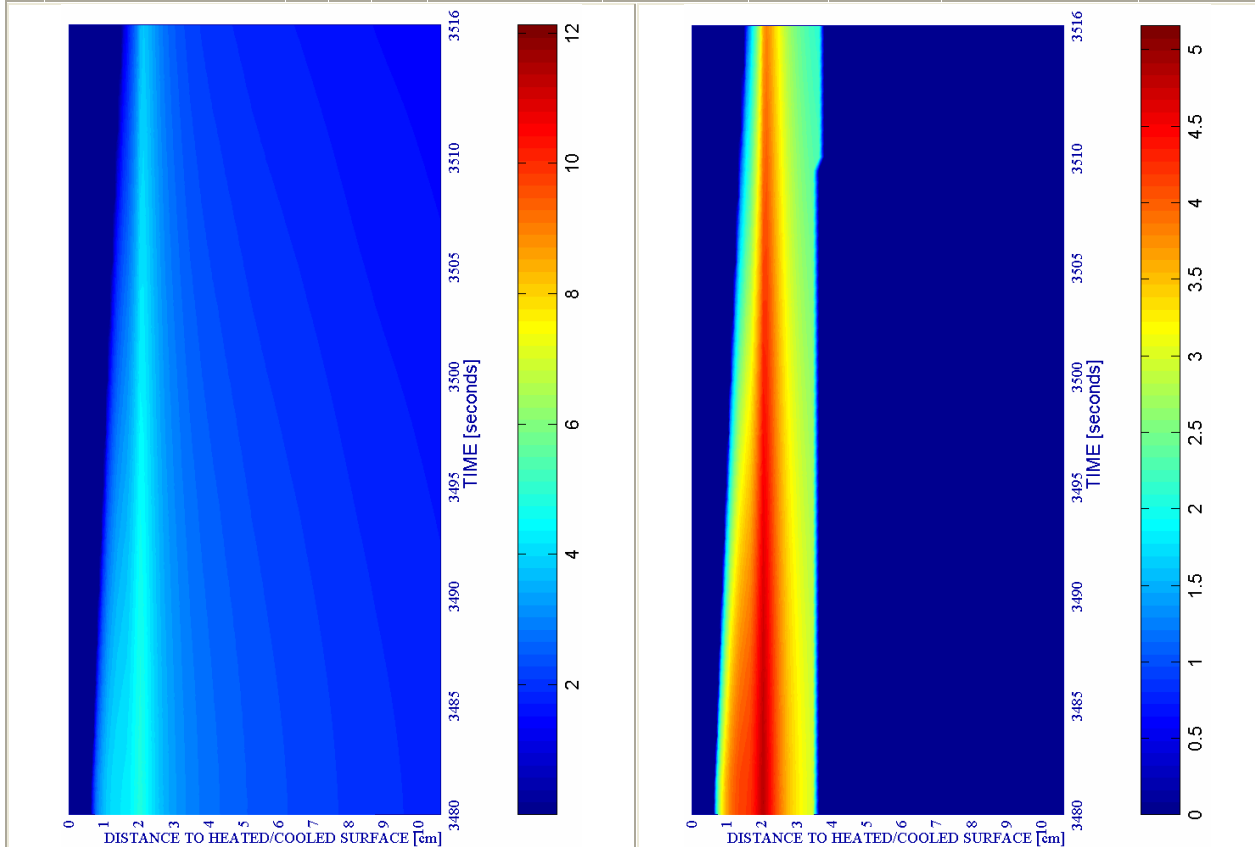
d) Down right: Velocity [m/s] where $d \geq 0,10$

a) Up left: Spalling Index IS_4 [-]

b) Up right: Mechanical damage d [-]



#	Combination	PC1 - RH [%]			PC2 - K_0 [m^2]			PC4 - Heating curve			PC5 - Mat.		Cooling length[s]	Start of cooling [s]	End of cooling [s]
		40	50	60	10^{-19}	10^{-18}	10^{-17}	PAR1	PAR2	PAR4	C60	C90			
51	TH12K019RH50PAR2C90		X		X				X			X	36	3360+120	3516



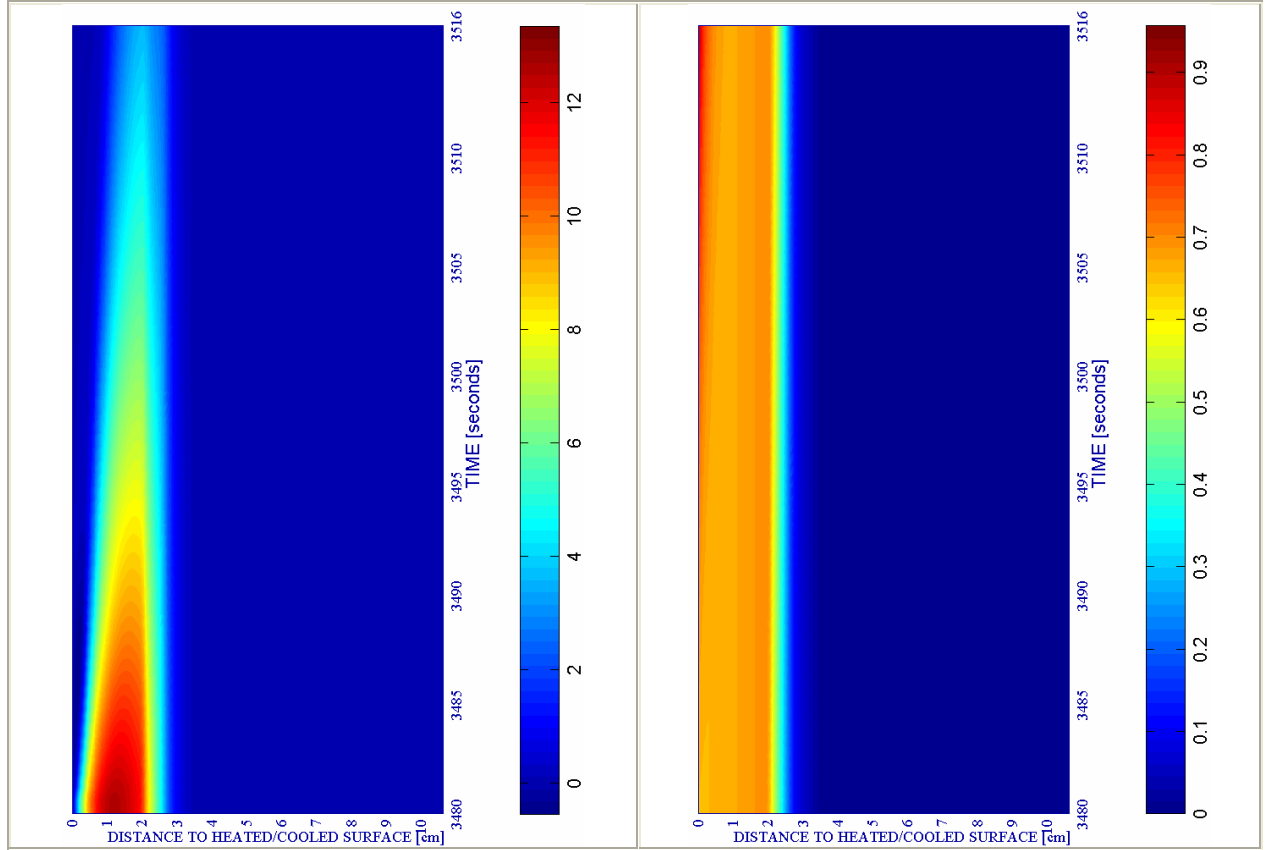
c) Down left: Velocity of spalled pieces [m/s]

Figure 6A-41.

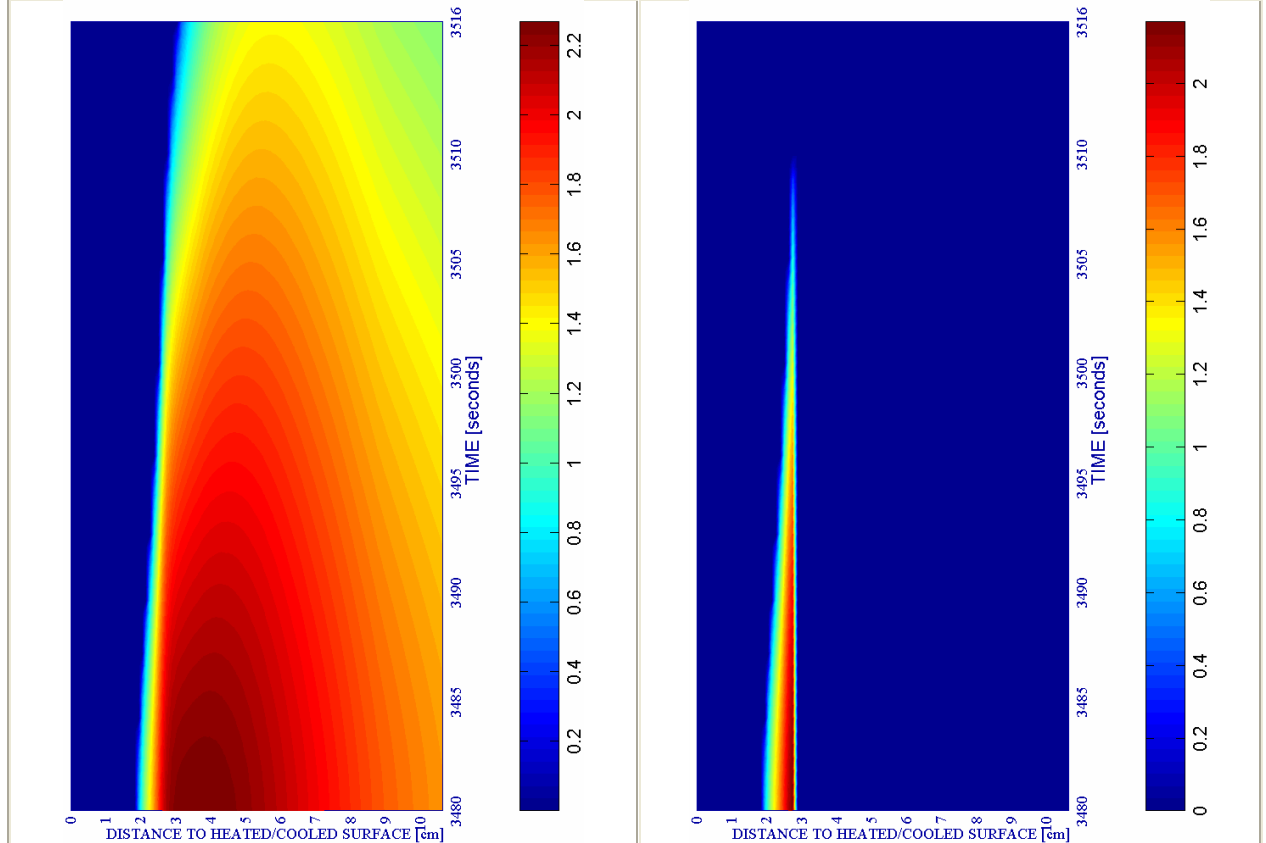
d) Down right: Velocity [m/s] where $d \geq 0,10$

a) Up left: Spalling Index $IS_4 * 10^3 [-]$

b) Up right: Mechanical damage $d [-]$



#	Combination	PC1 - RH [%]			PC2 - $K_0 [m^2]$			PC4 - Heating curve			PC5 - Mat.		Cooling length[s]	Start of cooling [s]	End of cooling [s]
		40	50	60	10^{-19}	10^{-18}	10^{-17}	PAR1	PAR2	PAR4	C60	C90			
52	TH12K017RH60PAR2C90			X			X		X			X	36	3360+120	3516



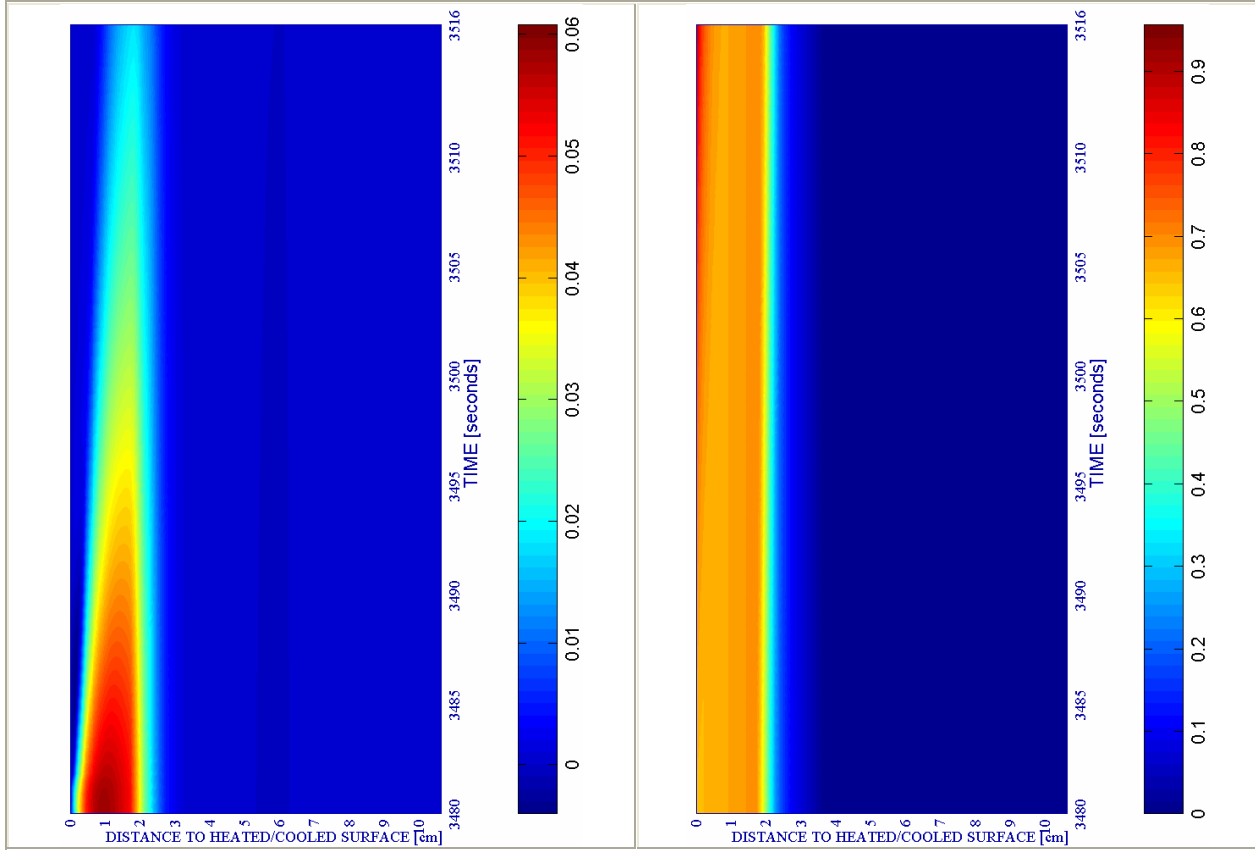
c) Down left: Velocity of spalled pieces [m/s]

Figure 6A-42.

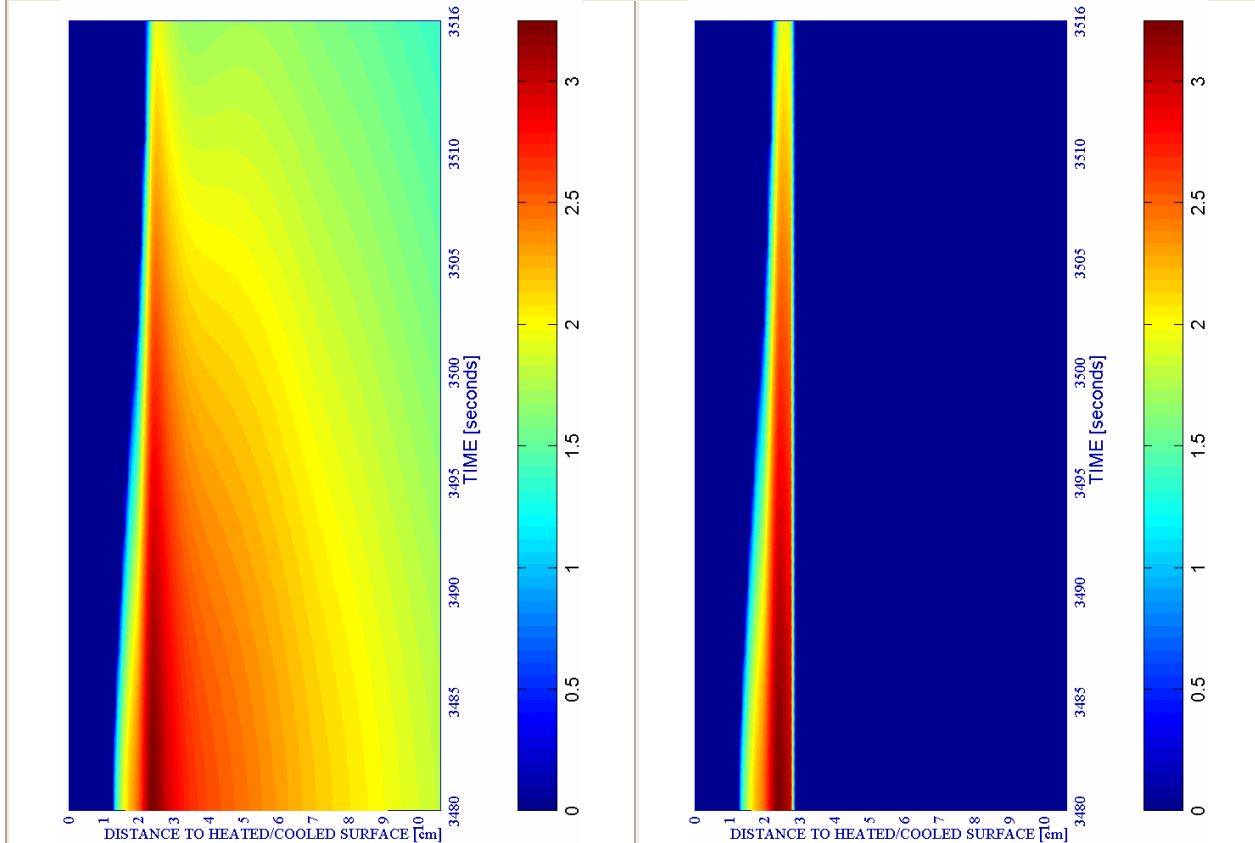
d) Down right: Velocity [m/s] where $d \geq 0,10$

a) Up left: Spalling Index IS_4 [-]

b) Up right: Mechanical damage d [-]



#	Combination	PC1 - RH [%]			PC2 - K_0 [m ²]			PC4 - Heating curve			PC5 - Mat.		Cooling length[s]	Start of cooling [s]	End of cooling [s]	
		40	50	60	10 ⁻¹⁹	10 ⁻¹⁸	10 ⁻¹⁷	PAR1	PAR2	PAR4	C60	C90				
53	TH12K018RH60PAR2C90			X			X			X			X	36	3360+120	3516



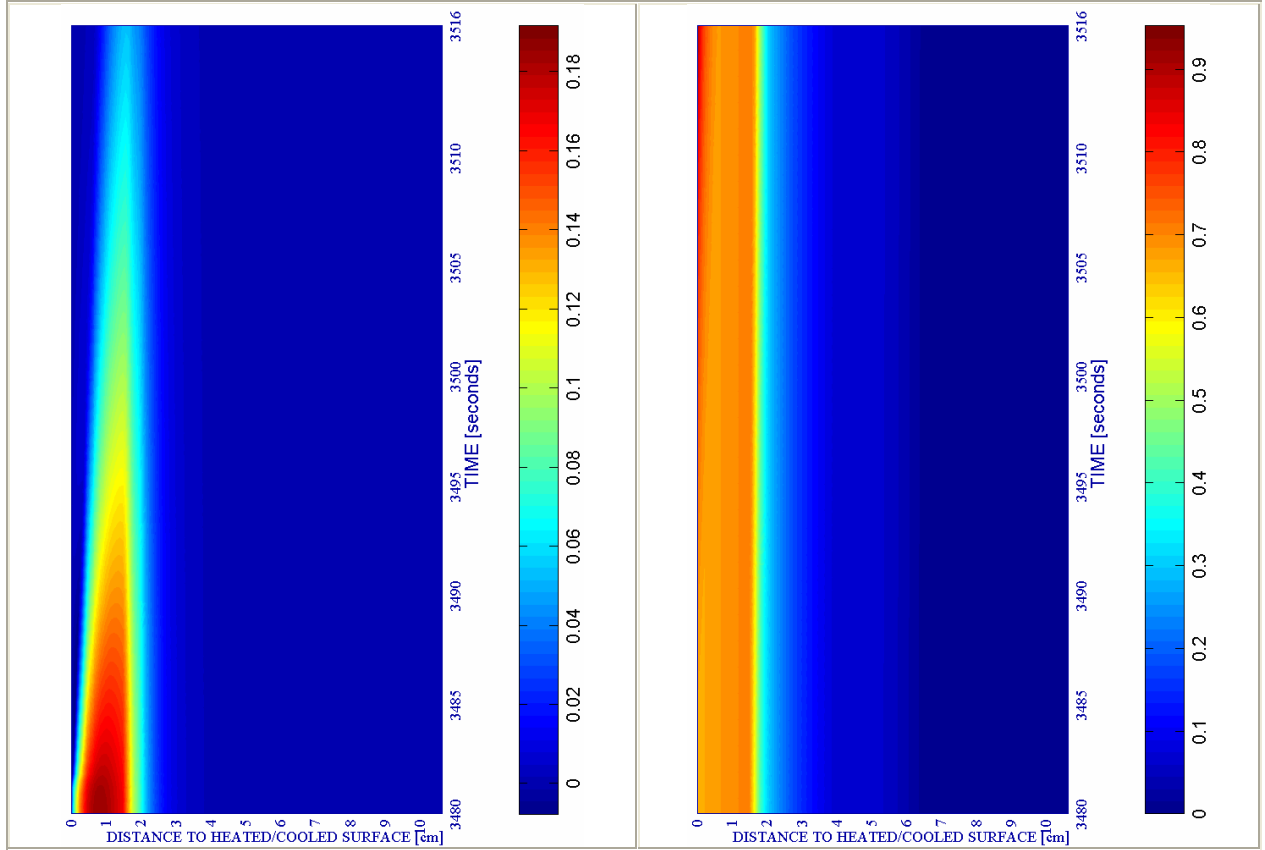
c) Down left: Velocity of spalled pieces [m/s]

Figure 6A-43.

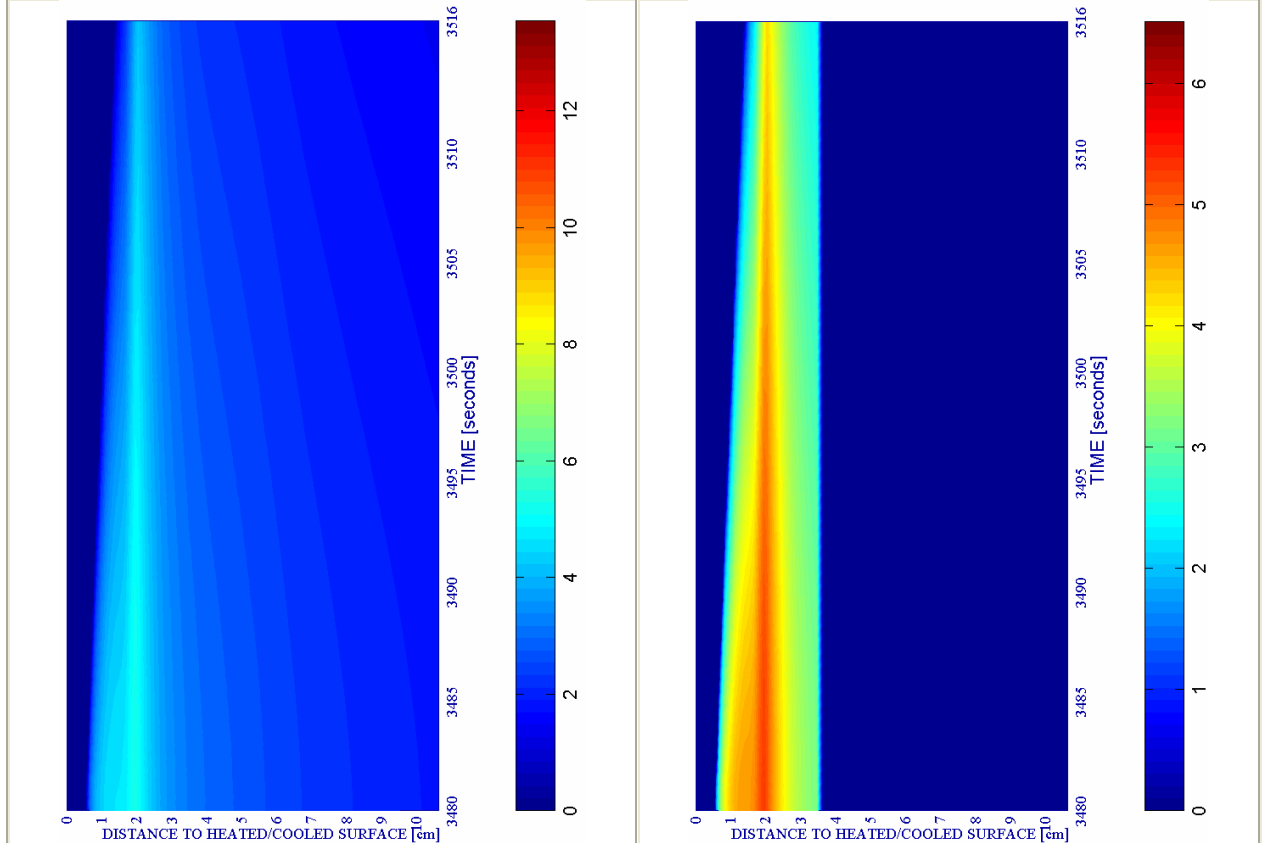
d) Down right: Velocity [m/s] where $d \geq 0,10$

a) Up left: Spalling Index IS_4 [-]

b) Up right: Mechanical damage d [-]



#	Combination	PC1 - RH [%]			PC2 - K_0 [m ²]			PC4 - Heating curve			PC5 - Mat.		Cooling length[s]	Start of cooling [s]	End of cooling [s]
		40	50	60	10^{-19}	10^{-18}	10^{-17}	PAR1	PAR2	PAR4	C60	C90			
54	TH12K019RH60PAR2C90			X	X				X			X	36	3360+120	3516



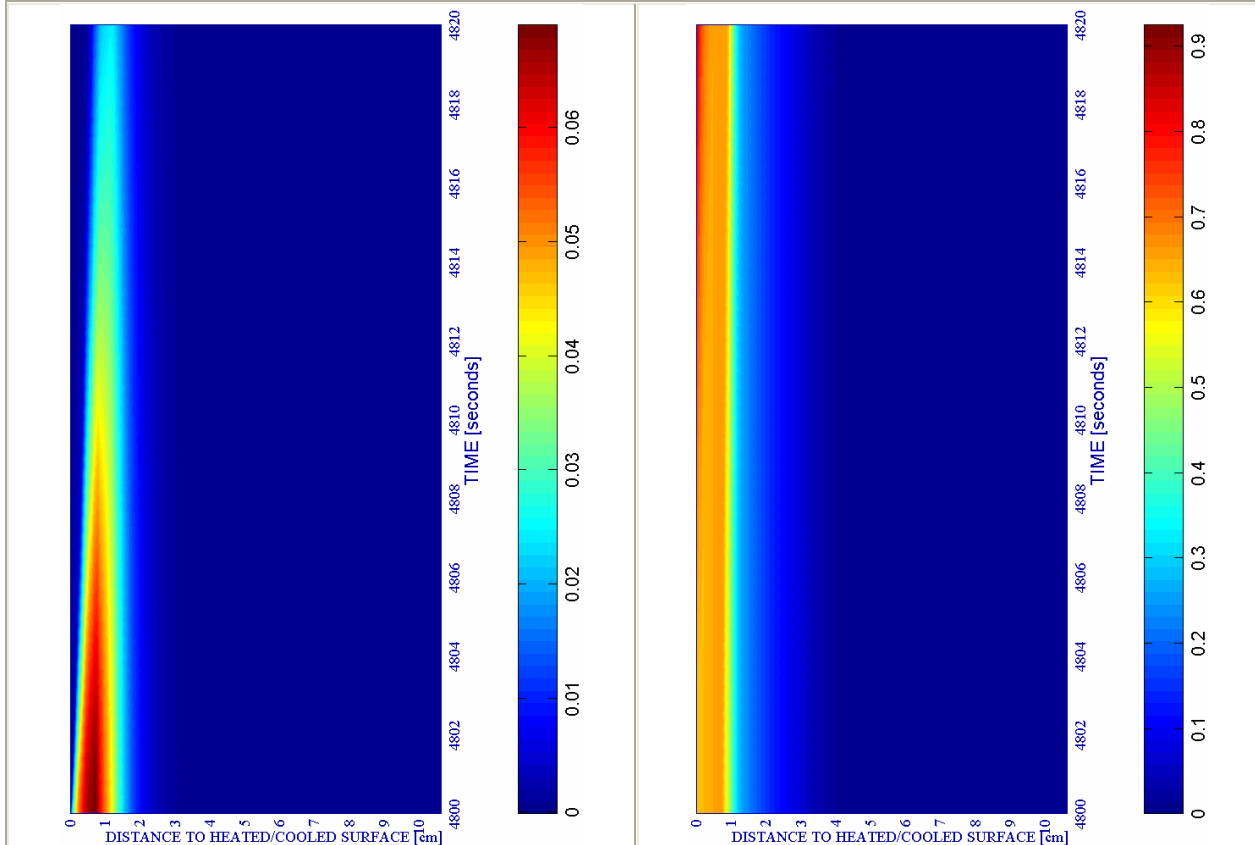
c) Down left: Velocity of spalled pieces [m/s]

Figure 6A-44.

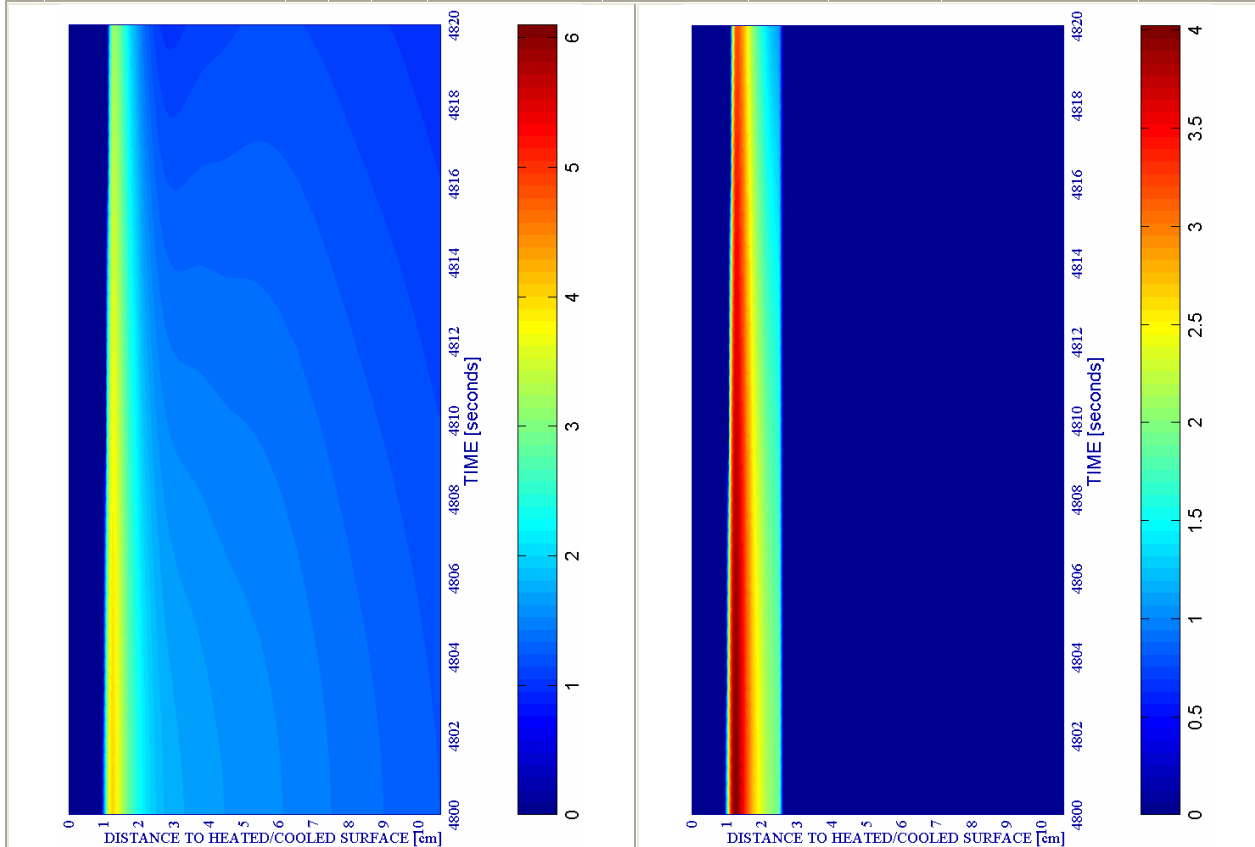
d) Down right: Velocity [m/s] where $d \geq 0,10$

a) Up left: Spalling Index IS_4 [-]

b) Up right: Mechanical damage d [-]



#	Combination	PC1 - RH [%]			PC2 - K_0 [m^2]			PC4 - Heating curve			PC5 - Mat.		Cooling length[s]	Start of cooling [s]	End of cooling [s]
		40	50	60	10^{-19}	10^{-18}	10^{-17}	PAR1	PAR2	PAR4	C60	C90			
100	TH12K019RH50PAR4C90		X		X					X		X	20	4800	4820



c) Down left: Velocity of spalled pieces [m/s]

Figure 6A-45.

d) Down right: Velocity [m/s] where $d \geq 0,10$

Appendix 6B

Appendix 6B.1 INPUT FILES FOR THE FIRE DYNAMICS SIMULATOR (FDS) CALCULATIONS.

In this Appendix are shown the Input files developed for the calculations done by means of the software Fire Dynamics Simulator (FDS) [B.1, B.2]. Some comments have been added to the input files (in blue colour) in order to provide a better understanding of each statement:

OFFICE_FIRE.FDS

**Office fire test case, based on the actual configuration of Guerrero's Office.
All material properties are completely fabricated.**

General Data

&HEAD CHID='office_fire', TITLE='Guerreros Office Fire Simulation, SVN \$Revision\$' /

&MESH IJK=90,60,25, XB=-0.5,8.5,-0.2,5.7,0.0,2.5 /

&TIME T_END=1390.0 /

&MISC SURF_DEFAULT = 'WALL',
RESTART = .FALSE.,
POROUS_FLOOR = .TRUE.,
HUMIDITY = 50. /

Definition of water nozzle features

&PART ID = 'water',
WATER = .TRUE.,
QUANTITIES = 'DROPLET_DIAMETER',
AGE = 30.,
DIAMETER = 1000.,
GAMMA_D = 2.4,
DROPLETS_PER_SECOND = 3000,
DT_INSERT = 0.01, /

&PROP ID='nozzle_1', PART_ID='water', FLOW_RATE=220, SPRAY_ANGLE=3.,20., DROPLET_VELOCITY=8. /
&PROP ID='nozzle_2', PART_ID='water', FLOW_RATE=220, SPRAY_ANGLE=3.,6., DROPLET_VELOCITY=10. /

Definition of material properties

&REAC ID = 'POLYURETHANE'
FYI = 'C_6.3 H_7.1 N O_2.1, NFPA Handbook, Babrauskas'
SOOT_YIELD = 0.10
N = 1.0
C = 6.3
H = 7.1
O = 2.1 /

&SURF ID='BURNER', HRRPUA=1000., COLOR='RASPBERRY' /

&MATL ID = 'FABRIC'
FYI = 'Properties completely fabricated'
SPECIFIC_HEAT = 1.0
CONDUCTIVITY = 0.1
DENSITY = 100.0
N_REACTIONS = 1
NU_FUEL = 1.
REFERENCE_TEMPERATURE = 350.
HEAT_OF_REACTION = 3000.
HEAT_OF_COMBUSTION = 15000. /

&MATL ID = 'FOAM'
FYI = 'Properties completely fabricated'
SPECIFIC_HEAT = 1.0
CONDUCTIVITY = 0.05
DENSITY = 40.0
N_REACTIONS = 1
NU_FUEL = 1.

REFERENCE_TEMPERATURE = 350.
 HEAT_OF_REACTION = 1500.
 HEAT_OF_COMBUSTION = 30000. /

&MATL ID = 'GYPSUM PLASTER'
 FYI = 'Quintiere, Fire Behavior'
 CONDUCTIVITY = 0.48
 SPECIFIC_HEAT = 0.84
 DENSITY = 1440. /

&MATL ID = 'CARPET PILE'
 FYI = 'Completely made up'
 CONDUCTIVITY = 0.16
 SPECIFIC_HEAT = 2.0
 DENSITY = 750.
 N_REACTIONS = 1
 NU_FUEL = 1.
 REFERENCE_TEMPERATURE = 290.
 HEAT_OF_COMBUSTION = 22300.
 HEAT_OF_REACTION = 2000. /

&MATL ID = 'CONCRETE'
 FYI = 'Quintiere, Fire Behavior'
 CONDUCTIVITY = 1.8079
 SPECIFIC_HEAT = 0.855
 DENSITY = 2627.4 /

&MATL ID = 'PAPER'
 FYI = 'NIST NCSTAR 1-5C, Project 5,Annex 3,App.A'
 SPECIFIC_HEAT = 1.0
 DENSITY = 60.0
 N_REACTIONS = 1
 NU_FUEL = 1.
 REFERENCE_TEMPERATURE = 369.
 HEAT_OF_REACTION = 4500.
 HEAT_OF_COMBUSTION = 14200. /

&MATL ID = 'HARDWARE'
 FYI = 'NIST NCSTAR 1-5C, Project 5,Annex 3,App.A'
 SPECIFIC_HEAT = 1.0
 DENSITY = 150.0
 N_REACTIONS = 1
 NU_FUEL = 0.5
 REFERENCE_TEMPERATURE = 402.
 HEAT_OF_REACTION = 1700.
 HEAT_OF_COMBUSTION = 15800. /

&MATL ID = 'SPRUCE'
 FYI = 'Charring material'
 DENSITY = 450.
 CONDUCTIVITY_RAMP = 'KS'
 SPECIFIC_HEAT_RAMP = 'CPV' /
 &RAMP ID = 'KS', T = 20., F = 0.13 /
 &RAMP ID = 'KS', T = 500., F = 0.29 /
 &RAMP ID = 'CPV', T = 20., F = 1.2 /
 &RAMP ID = 'CPV', T = 500., F = 3.0 /

&SURF ID = 'UPHOLSTERY'
 COLOR = 'BLUE'
 BURN_AWAY = .TRUE.
 MATL_ID(1:2,1) = 'FABRIC','FOAM'
 THICKNESS(1:2) = 0.002,0.1 /

&SURF ID = 'WALL'
 RGB = 200,200,200
 MATL_ID(1:2,1) = 'GYPSUM PLASTER','CONCRETE'
 THICKNESS(1:2) = 0.012,0.188 /

&SURF ID = 'FLOOR'
 MATL_ID = 'CONCRETE'
 COLOR = 'GRAY'
 THICKNESS = 0.20 /

&SURF ID = 'BOOKS'
 MATL_ID = 'PAPER'
 COLOR = 'WHITE'

```

BURN_AWAY = .TRUE.
THICKNESS = 0.10 /

&SURF ID = 'COMPUTER'
MATL_ID = 'HARDWARE'
COLOR = 'GRAY'
THICKNESS = 0.20 /

&SURF ID = 'FURNITURE'
MATL_ID = 'SPRUCE'
COLOR = 'PURPLE'
BURN_AWAY = .TRUE.
THICKNESS = 0.10
IGNITION_TEMPERATURE = 360.0
HEAT_OF_VAPORIZATION = 500.
TRANSPARENCY = 0.40
BACKING = 'EXPOSED' /

&SURF ID = 'CARPET'
MATL_ID = 'CARPET PILE'
COLOR = 'KHAKI'
BACKING = 'INSULATED'
THICKNESS = 0.006 /
    
```

Definition of geometry

```

&OBST XB= -0.20, 0.00, -0.20, 5.70, 0.00, 2.50 / Front wall
&HOLE XB= -0.30, 0.10, 0.20, 1.10, 0.00, 2.10 / Door
&VENT MB='XMIN',SURF_ID='OPEN' /
&VENT MB='XMAX',SURF_ID='OPEN' /

&OBST XB= 0.00, 7.90, -0.20, 0.00, 0.00, 2.50 / East wall
&OBST XB= 0.00, 7.90, 5.50, 5.70, 0.00, 2.50 / West wall

&OBST XB= 7.70, 7.90, 0.00, 5.50, 0.00, 2.50 / Street wall
&HOLE XB= 7.60, 8.00, 1.00, 2.20, 1.00, 2.10, COLOR='BLUE',TRANSPARENCY=0.2, DEVC_ID='window1' / Windows
&HOLE XB= 7.60, 8.00, 2.20, 3.30, 1.00, 2.10, COLOR='BLUE',TRANSPARENCY=0.2, DEVC_ID='window2' / Windows
&HOLE XB= 7.60, 8.00, 3.30, 4.50, 1.00, 2.10, COLOR='BLUE',TRANSPARENCY=0.2, DEVC_ID='window3' / Windows
&DEVC XYZ=7.7,1.6,1.6, ID='window1', SETPOINT= 20.0, QUANTITY='TEMPERATURE', INITIAL_STATE=.FALSE./
&DEVC XYZ=7.7,2.8,1.6, ID='window2', SETPOINT= 300.0, QUANTITY='TEMPERATURE', INITIAL_STATE=.FALSE./
&DEVC XYZ=7.7,3.9,1.6, ID='window3', SETPOINT= 300.0, QUANTITY='TEMPERATURE', INITIAL_STATE=.FALSE./

&OBST XB= 3.00, 3.40, 0.00, 0.40, 0.00, 2.50 / East column
&OBST XB= 2.00, 3.40, 5.40, 5.50, 0.00, 2.50 / West overwall
&OBST XB= 0.00, 2.00, 4.30, 4.50, 0.00, 2.50 / Bath East wall
&OBST XB= 1.80, 2.00, 4.50, 5.50, 0.00, 2.50 / Bath Front wall
&HOLE XB= 1.70, 2.10, 4.50, 5.40, 0.00, 2.10 / Door
&OBST XB= 7.20, 7.70, 0.00, 0.50, 0.00, 2.50 / East corner column
&OBST XB= 7.20, 7.70, 5.00, 5.50, 0.00, 2.50 / West corner column

&OBST XB= 1.50, 2.50, 0.10, 0.50, 0.00, 0.40, SURF_ID='BOOKS' / East front books shelf, level 1
&OBST XB= 1.50, 2.50, 0.10, 0.50, 0.50, 0.90, SURF_ID='BOOKS' / East front books shelf, level 2
&OBST XB= 1.50, 2.50, 0.10, 0.50, 1.00, 1.40, SURF_ID='BOOKS' / East front books shelf, level 3
&OBST XB= 1.50, 2.50, 0.10, 0.50, 1.50, 1.80, SURF_ID='BOOKS' / East front books shelf, level 4

&OBST XB= 6.00, 7.00, 0.10, 0.50, 0.00, 0.40, SURF_ID='BOOKS' / East back books shelf, level 1
&OBST XB= 6.00, 7.00, 0.10, 0.50, 0.50, 0.90, SURF_ID='BOOKS' / East back books shelf, level 2
&OBST XB= 6.00, 7.00, 0.10, 0.50, 1.00, 1.40, SURF_ID='BOOKS' / East back books shelf, level 3
&OBST XB= 6.00, 7.00, 0.10, 0.50, 1.50, 1.80, SURF_ID='BOOKS' / East back books shelf, level 4

&OBST XB= 0.10, 0.50, 1.50, 2.50, 0.00, 0.40, SURF_ID='BOOKS' / Front books shelf, level 1
&OBST XB= 0.10, 0.50, 1.50, 2.50, 0.50, 0.90, SURF_ID='BOOKS' / Front books shelf, level 2
&OBST XB= 0.10, 0.50, 1.50, 2.50, 1.00, 1.40, SURF_ID='BOOKS' / Front books shelf, level 3
&OBST XB= 0.10, 0.50, 1.50, 2.50, 1.50, 1.80, SURF_ID='BOOKS' / Front books shelf, level 4

&OBST XB= 3.00, 3.40, 0.50, 1.50, 0.00, 0.40, SURF_ID='BOOKS' / Middle books shelf 1, level 1
&OBST XB= 3.00, 3.40, 0.50, 1.50, 0.50, 0.90, SURF_ID='BOOKS' / Middle books shelf 1, level 2
&OBST XB= 3.00, 3.40, 0.50, 1.50, 1.00, 1.40, SURF_ID='BOOKS' / Middle books shelf 1, level 3
&OBST XB= 3.00, 3.40, 0.50, 1.50, 1.50, 1.80, SURF_ID='BOOKS' / Middle books shelf 1, level 4

&OBST XB= 3.00, 3.40, 1.60, 2.60, 0.00, 0.40, SURF_ID='BOOKS' / Middle books shelf 2, level 1
&OBST XB= 3.00, 3.40, 1.60, 2.60, 0.50, 0.90, SURF_ID='BOOKS' / Middle books shelf 2, level 2
&OBST XB= 3.00, 3.40, 1.60, 2.60, 1.00, 1.40, SURF_ID='BOOKS' / Middle books shelf 2, level 3
&OBST XB= 3.00, 3.40, 1.60, 2.60, 1.50, 1.80, SURF_ID='BOOKS' / Middle books shelf 2, level 4

&OBST XB= 7.10, 7.60, 0.60, 4.90, 0.00, 0.40, SURF_ID='BOOKS' / Files under windows
    
```

&OBST XB= 5.20, 6.50, 4.40, 5.40, 0.80, 0.90, SURF_ID='FURNITURE' / Main computers table
 &OBST XB= 5.20, 5.30, 4.40, 4.50, 0.00, 0.80, SURF_ID='FURNITURE' / Leg 1
 &OBST XB= 6.50, 6.60, 4.40, 4.70, 0.00, 0.80, SURF_ID='FURNITURE' / Leg 2
 &OBST XB= 5.20, 5.30, 5.30, 5.40, 0.00, 0.80, SURF_ID='FURNITURE' / Leg 3
 &OBST XB= 6.50, 6.60, 5.30, 5.40, 0.00, 0.80, SURF_ID='FURNITURE' / Leg 4
 &OBST XB= 4.70, 5.20, 4.40, 5.40, 0.30, 0.40, SURF_ID='FURNITURE' / Secondary computers table, left
 &OBST XB= 6.50, 7.10, 4.40, 5.40, 0.30, 0.40, SURF_ID='FURNITURE' / Secondary computers table, right
 &OBST XB= 4.70, 4.90, 4.40, 5.40, 0.30, 1.00, SURF_ID='COMPUTER' / First computer on the left, in computers table
 &OBST XB= 5.00, 5.20, 4.40, 5.40, 0.30, 1.00, SURF_ID='COMPUTER' / Second computer on the left, in computers table
 &OBST XB= 6.60, 6.80, 4.40, 5.40, 0.30, 1.00, SURF_ID='COMPUTER' / Third computer on the left, in computers table
 &OBST XB= 6.90, 7.10, 4.40, 5.40, 0.30, 1.00, SURF_ID='COMPUTER' / Fourth computer on the left, in computers table
 &OBST XB= 5.70, 6.10, 4.70, 5.10, 0.90, 1.40, SURF_ID='COMPUTER' / Monitor, in computers table
 &OBST XB= 6.10, 6.60, 4.90, 5.30, 0.90, 1.20, SURF_ID='COMPUTER' / Printer, in computers table
 &OBST XB= 5.30, 5.60, 4.80, 5.10, 0.90, 1.30, SURF_ID='BOOKS' / Papers and books, in computers table

 &OBST XB= 5.60, 6.20, 4.20, 4.80, 0.40, 0.60, SURF_ID='UPHOLSTERY' / Chair in computers table, seat cushion
 &OBST XB= 5.60, 6.20, 4.00, 4.20, 0.40, 1.30, SURF_ID='UPHOLSTERY' / Chair in computers table, back cushion
 &OBST XB= 5.40, 5.60, 4.00, 4.80, 0.40, 0.80, SURF_ID='UPHOLSTERY' / Chair in computers table, left arm
 &OBST XB= 6.20, 6.40, 4.00, 4.80, 0.40, 0.80, SURF_ID='UPHOLSTERY' / Chair in computers table, right arm

 &OBST XB= 5.20, 6.70, 1.50, 2.50, 0.80, 0.90, SURF_ID='FURNITURE' / Main boss table
 &OBST XB= 4.20, 5.20, 1.00, 2.50, 0.40, 0.50, SURF_ID='FURNITURE' / Secondary boss table
 &OBST XB= 4.20, 4.30, 1.00, 1.10, 0.00, 0.40, SURF_ID='FURNITURE' / Leg 1
 &OBST XB= 4.20, 4.30, 2.40, 2.50, 0.00, 0.40, SURF_ID='FURNITURE' / Leg 2
 &OBST XB= 5.10, 5.20, 1.00, 1.10, 0.00, 0.40, SURF_ID='FURNITURE' / Leg 3
 &OBST XB= 6.60, 6.70, 1.50, 1.60, 0.00, 0.80, SURF_ID='FURNITURE' / Leg 4
 &OBST XB= 6.60, 6.70, 2.40, 2.50, 0.00, 0.80, SURF_ID='FURNITURE' / Leg 5
 &OBST XB= 5.20, 5.30, 2.40, 2.50, 0.40, 0.80, SURF_ID='FURNITURE' / Leg 6
 &OBST XB= 5.20, 5.30, 1.50, 1.60, 0.40, 0.80, SURF_ID='FURNITURE' / Leg 7
 &OBST XB= 4.20, 5.20, 0.70, 0.90, 0.00, 0.70, SURF_ID='COMPUTER' / Computer on boss secondary table
 &OBST XB= 4.40, 4.80, 1.10, 1.50, 0.50, 1.00, SURF_ID='COMPUTER' / Monitor on boss secondary table
 &OBST XB= 4.40, 4.80, 1.60, 2.10, 0.50, 0.80, SURF_ID='COMPUTER' / Printer on boss secondary table
 &OBST XB= 4.30, 4.60, 2.20, 2.50, 0.50, 0.90, SURF_ID='BOOKS' / Papers and books, in boss secondary table
 &OBST XB= 4.70, 5.00, 2.20, 2.50, 0.50, 0.90, SURF_ID='BOOKS' / Papers and books, in boss secondary table
 &OBST XB= 5.30, 5.60, 2.20, 2.50, 0.90, 1.20, SURF_ID='BOOKS' / Papers and books, in boss secondary table
 &OBST XB= 5.30, 5.60, 1.80, 2.10, 0.90, 1.20, SURF_ID='BOOKS' / Papers and books, in boss secondary table
 &OBST XB= 5.70, 6.00, 2.20, 2.50, 0.90, 1.20, SURF_ID='BOOKS' / Papers and books, in boss secondary table
 &OBST XB= 5.70, 6.00, 1.80, 2.10, 0.90, 1.20, SURF_ID='BOOKS' / Papers and books, in boss secondary table
 &OBST XB= 5.40, 6.20, 0.80, 1.60, 0.40, 0.60, SURF_ID='UPHOLSTERY' / Armchair in boss table, seat cushion
 &OBST XB= 5.40, 6.20, 0.60, 0.80, 0.60, 1.50, SURF_ID='UPHOLSTERY' / Armchair in boss table, back cushion

 &OBST XB= 4.90, 5.90, 0.10, 0.50, 0.80, 1.40, SURF_ID='COMPUTER' / Plotter

 &OBST XB= 3.00, 4.80, 3.20, 4.40, 0.80, 0.90, SURF_ID='FURNITURE' / Meetings table
 &OBST XB= 3.00, 3.10, 3.20, 3.30, 0.00, 0.80, SURF_ID='FURNITURE' / Leg 1
 &OBST XB= 3.00, 3.10, 4.30, 4.40, 0.00, 0.80, SURF_ID='FURNITURE' / Leg 2
 &OBST XB= 4.70, 4.80, 3.20, 3.30, 0.00, 0.80, SURF_ID='FURNITURE' / Leg 3
 &OBST XB= 4.70, 4.80, 4.30, 4.30, 0.00, 0.80, SURF_ID='FURNITURE' / Leg 4
 &OBST XB= 3.60, 4.20, 3.00, 3.60, 0.40, 0.60, SURF_ID='UPHOLSTERY' / East Chair in computers table, seat cushion
 &OBST XB= 3.60, 4.20, 2.80, 3.00, 0.60, 1.20, SURF_ID='UPHOLSTERY' / East Chair in computers table, back cushion
 &OBST XB= 3.60, 4.20, 4.00, 4.60, 0.40, 0.60, SURF_ID='UPHOLSTERY' / West Chair in computers table, seat cushion
 &OBST XB= 3.60, 4.20, 4.60, 4.80, 0.60, 1.20, SURF_ID='UPHOLSTERY' / West Chair in computers table, back cushion
 &OBST XB= 2.80, 3.40, 3.50, 4.10, 0.40, 0.60, SURF_ID='UPHOLSTERY' / South Chair in computers table, seat cushion
 &OBST XB= 2.60, 2.80, 3.50, 4.10, 0.60, 1.20, SURF_ID='UPHOLSTERY' / South Chair in computers table, back cushion
 &OBST XB= 4.30, 4.90, 3.50, 4.10, 0.40, 0.60, SURF_ID='UPHOLSTERY' / North Chair in computers table, seat cushion
 &OBST XB= 4.90, 5.10, 3.50, 4.10, 0.60, 1.20, SURF_ID='UPHOLSTERY' / North Chair in computers table, back cushion
 &OBST XB= 3.20, 3.50, 3.40, 3.80, 0.90, 1.20, SURF_ID='BOOKS' / Papers and books, in meetings table, pile 1
 &OBST XB= 3.20, 3.50, 3.90, 4.30, 0.90, 1.20, SURF_ID='BOOKS' / Papers and books, in meetings table, pile 2
 &OBST XB= 3.60, 3.90, 3.40, 3.80, 0.90, 1.20, SURF_ID='BOOKS' / Papers and books, in meetings table, pile 3
 &OBST XB= 3.60, 3.90, 3.90, 4.30, 0.90, 1.20, SURF_ID='BOOKS' / Papers and books, in meetings table, pile 4
 &OBST XB= 4.00, 4.30, 3.40, 3.80, 0.90, 1.20, SURF_ID='BOOKS' / Papers and books, in meetings table, pile 5
 &OBST XB= 4.00, 4.30, 3.90, 4.30, 0.90, 1.20, SURF_ID='BOOKS' / Papers and books, in meetings table, pile 6
 &OBST XB= 4.40, 4.70, 3.40, 3.80, 0.90, 1.20, SURF_ID='BOOKS' / Papers and books, in meetings table, pile 7
 &OBST XB= 4.40, 4.70, 3.90, 4.30, 0.90, 1.20, SURF_ID='BOOKS' / Papers and books, in meetings table, pile 8

 &OBST XB= 0.10, 1.90, 3.70, 4.20, 0.00, 1.50, SURF_ID='BOOKS' / Piano, main
 &OBST XB= 0.10, 1.90, 3.40, 3.70, 0.70, 1.00, SURF_ID='BOOKS' / Piano, keyboard
 &OBST XB= 0.70, 1.30, 2.90, 3.30, 0.40, 0.60, SURF_ID='UPHOLSTERY' / Piano chair, seat cushion

 &VENT XB= 5.80, 5.90, 4.20, 4.30, 0.60, 0.60, SURF_ID='BURNER' / Ignition source on computers table

 &VENT XB=0.00,7.70,0.00,5.50,0.0,0.0, SURF_ID='CARPET' / Specify that inside's floor is carpet
 &VENT XB=-0.50,0.00,-0.20,5.70,0.00,0.00,SURF_ID='FLOOR' / Specify that the corridor floor has the attributes of Floor.
 &VENT XB=-0.50,-0.20,-0.20,5.70,2.50,2.50,SURF_ID='OPEN' / Specify that the corridor ceiling is open.
 &VENT XB=-0.50,-0.20,-0.20,-0.20,0.00,2.50,SURF_ID='OPEN' / Specify that corridor surfaces are open.

&VENT XB=-0.50,-0.20,5.70,5.70,0.00,2.50,SURF_ID='OPEN' / Specify that corridor surfaces are open.

&VENT XB=7.90,8.50,-0.20,5.70,0.00,0.00,SURF_ID='OPEN' / Specify that outside surfaces are open.

&VENT XB=7.90,8.50,-0.20,5.70,2.50,2.50,SURF_ID='OPEN' / Specify that outside surfaces are open.

&VENT XB=7.90,8.50,-0.20,-0.20,0.00,2.50,SURF_ID='OPEN' / Specify that outside surfaces are open.

&VENT XB=7.90,8.50,5.70,5.70,0.00,2.50,SURF_ID='OPEN' / Specify that outside surfaces are open.

*** creates device that appears as yellow sphere in lower left front corner of domain at (0.1, 0.1, 0.1), identified as 'clock 1', quantity is time**

&DEVIC XYZ=-0.2,0.0,0.1, ID='clock 1', QUANTITY='TIME' /

&DEVIC XYZ=0.00,0.60,0.40, PROP_ID='nozzle_1', ORIENTATION=1.0,0.95,3.00, QUANTITY='CONTROL', CTRL_ID='controller 1', LATCH=.FALSE.,ID='noz_1' /

&DEVIC XYZ=2.80,2.60,1.20, PROP_ID='nozzle_2', ORIENTATION=1.0,0.95,0.80, QUANTITY='CONTROL', CTRL_ID='controller 2', LATCH=.FALSE.,ID='noz_2' /

Nozzles turn on and off at prescribed times

&CTRL ID='controller 1', FUNCTION_TYPE='CUSTOM', INPUT_ID='clock 1', RAMP_ID='ramp 1', LATCH=.FALSE. /

&RAMP ID='ramp 1', T= 0.00, F=-1. /

&RAMP ID='ramp 1', T= 1259.99, F=-1. /

&RAMP ID='ramp 1', T= 1260.01, F= 1. /

&RAMP ID='ramp 1', T= 1269.99, F= 1. /

&RAMP ID='ramp 1', T= 1270.01, F=-1. /

&RAMP ID='ramp 1', T= 1299.99, F=-1. /

&RAMP ID='ramp 1', T= 1300.01, F= 1. /

&RAMP ID='ramp 1', T= 1309.99, F= 1. /

&RAMP ID='ramp 1', T= 1310.01, F=-1. /

&RAMP ID='ramp 1', T= 1339.99, F=-1. /

&RAMP ID='ramp 1', T= 1340.01, F= 1. /

&RAMP ID='ramp 1', T= 1349.99, F= 1. /

&RAMP ID='ramp 1', T= 1350.01, F=-1. /

&CTRL ID='controller 2', FUNCTION_TYPE='CUSTOM', INPUT_ID='clock 1', RAMP_ID='ramp 2', LATCH=.FALSE. /

&RAMP ID='ramp 2', T= 0.00, F=-1. /

&RAMP ID='ramp 2', T= 1379.99, F=-1. /

&RAMP ID='ramp 2', T= 1380.01, F= 1. /

&RAMP ID='ramp 2', T= 1389.98, F= 1. /

&RAMP ID='ramp 2', T= 1390.00, F=-1. /

Output definition

&BNDF QUANTITY='WALL TEMPERATURE' /

&BNDF QUANTITY='BURNING RATE' /

&ISOF QUANTITY='water vapor' /

&SLCF PBX=5.80, QUANTITY='TEMPERATURE' /

&SLCF PBX=5.80, QUANTITY='HRRPUV' / Heat Release Rate per Unit Volume

&SLCF PBX=5.80, QUANTITY='MIXTURE FRACTION' /

&SLCF PBY=2.80, QUANTITY='TEMPERATURE' /

&SLCF PBY=2.80, QUANTITY='HRRPUV' / Heat Release Rate per Unit Volume

&SLCF PBY=2.80, QUANTITY='MIXTURE FRACTION' /

The following thermocouple (THCP) lines instruct FDS to record various values at the single point specified by XYZ=.... QUANTITY='TEMPERATURE' tells FDS that the gas temperature should be recorded at this point.

&DEVIC XYZ=5.90,5.40,2.40, QUANTITY='TEMPERATURE', ID='ENV11' /

&DEVIC XYZ=5.90,5.40,2.10, QUANTITY='TEMPERATURE', ID='ENV21' /

&DEVIC XYZ=5.90,5.40,1.80, QUANTITY='TEMPERATURE', ID='ENV31' /

&DEVIC XYZ=5.90,5.40,1.50, QUANTITY='TEMPERATURE', ID='ENV41' /

&DEVIC XYZ=5.90,5.20,2.40, QUANTITY='TEMPERATURE', ID='ENV12' /

&DEVIC XYZ=5.90,5.20,2.10, QUANTITY='TEMPERATURE', ID='ENV22' /

&DEVIC XYZ=5.90,5.20,1.80, QUANTITY='TEMPERATURE', ID='ENV32' /

&DEVIC XYZ=5.90,5.20,1.50, QUANTITY='TEMPERATURE', ID='ENV42' /

&DEVIC XYZ=5.90,5.00,2.40, QUANTITY='TEMPERATURE', ID='ENV13' /

&DEVIC XYZ=5.90,5.00,2.10, QUANTITY='TEMPERATURE', ID='ENV23' /

&DEVIC XYZ=5.90,5.00,1.80, QUANTITY='TEMPERATURE', ID='ENV33' /

&DEVIC XYZ=5.90,5.00,1.50, QUANTITY='TEMPERATURE', ID='ENV43' /

&DEVIC XYZ=5.90,4.80,2.40, QUANTITY='TEMPERATURE', ID='ENV14' /

&DEVIC XYZ=5.90,4.80,2.10, QUANTITY='TEMPERATURE', ID='ENV24' /

&DEVIC XYZ=5.90,4.80,1.80, QUANTITY='TEMPERATURE', ID='ENV34' /

&DEVIC XYZ=5.90,4.80,1.50, QUANTITY='TEMPERATURE', ID='ENV44' /

&DEVIC XYZ=5.90,4.60,2.40, QUANTITY='TEMPERATURE', ID='ENV15' /

&DEVIC XYZ=5.90,4.60,2.10, QUANTITY='TEMPERATURE', ID='ENV25' /

&DEVIC XYZ=5.90,4.60,1.80, QUANTITY='TEMPERATURE', ID='ENV35' /

&DEVIC XYZ=5.90,4.60,1.50, QUANTITY='TEMPERATURE', ID='ENV45' /

&DEVIC XYZ=5.90,4.40,2.40, QUANTITY='TEMPERATURE', ID='ENV16' /

&DEVIC XYZ=5.90,4.40,2.10, QUANTITY='TEMPERATURE', ID='ENV26' /

&DEVC XYZ=5.90,4.40,1.80, QUANTITY='TEMPERATURE', ID='ENV36' /
&DEVC XYZ=5.90,4.40,1.50, QUANTITY='TEMPERATURE', ID='ENV46' /

&DEVC XYZ=5.30,5.50,2.40, QUANTITY='WALL TEMPERATURE', IOR=-2, ID='WALL11' /
&DEVC XYZ=5.30,5.50,2.10, QUANTITY='WALL TEMPERATURE', IOR=-2, ID='WALL21' /
&DEVC XYZ=5.30,5.50,1.80, QUANTITY='WALL TEMPERATURE', IOR=-2, ID='WALL31' /
&DEVC XYZ=5.30,5.50,1.50, QUANTITY='WALL TEMPERATURE', IOR=-2, ID='WALL41' /
&DEVC XYZ=5.30,5.50,1.20, QUANTITY='WALL TEMPERATURE', IOR=-2, ID='WALL51' /
&DEVC XYZ=5.30,5.50,0.90, QUANTITY='WALL TEMPERATURE', IOR=-2, ID='WALL61' /
&DEVC XYZ=5.50,5.50,2.40, QUANTITY='WALL TEMPERATURE', IOR=-2, ID='WALL12' /
&DEVC XYZ=5.50,5.50,2.10, QUANTITY='WALL TEMPERATURE', IOR=-2, ID='WALL22' /
&DEVC XYZ=5.50,5.50,1.80, QUANTITY='WALL TEMPERATURE', IOR=-2, ID='WALL32' /
&DEVC XYZ=5.50,5.50,1.50, QUANTITY='WALL TEMPERATURE', IOR=-2, ID='WALL42' /
&DEVC XYZ=5.50,5.50,1.20, QUANTITY='WALL TEMPERATURE', IOR=-2, ID='WALL52' /
&DEVC XYZ=5.50,5.50,0.90, QUANTITY='WALL TEMPERATURE', IOR=-2, ID='WALL62' /
&DEVC XYZ=5.70,5.50,2.40, QUANTITY='WALL TEMPERATURE', IOR=-2, ID='WALL13' /
&DEVC XYZ=5.70,5.50,2.10, QUANTITY='WALL TEMPERATURE', IOR=-2, ID='WALL23' /
&DEVC XYZ=5.70,5.50,1.80, QUANTITY='WALL TEMPERATURE', IOR=-2, ID='WALL33' /
&DEVC XYZ=5.70,5.50,1.50, QUANTITY='WALL TEMPERATURE', IOR=-2, ID='WALL43' /
&DEVC XYZ=5.70,5.50,1.20, QUANTITY='WALL TEMPERATURE', IOR=-2, ID='WALL53' /
&DEVC XYZ=5.70,5.50,0.90, QUANTITY='WALL TEMPERATURE', IOR=-2, ID='WALL63' /
&DEVC XYZ=5.90,5.50,2.40, QUANTITY='WALL TEMPERATURE', IOR=-2, ID='WALL14' /
&DEVC XYZ=5.90,5.50,2.10, QUANTITY='WALL TEMPERATURE', IOR=-2, ID='WALL24' /
&DEVC XYZ=5.90,5.50,1.80, QUANTITY='WALL TEMPERATURE', IOR=-2, ID='WALL34' /
&DEVC XYZ=5.90,5.50,1.50, QUANTITY='WALL TEMPERATURE', IOR=-2, ID='WALL44' /
&DEVC XYZ=5.90,5.50,1.20, QUANTITY='WALL TEMPERATURE', IOR=-2, ID='WALL54' /
&DEVC XYZ=5.90,5.50,0.90, QUANTITY='WALL TEMPERATURE', IOR=-2, ID='WALL64' /
&DEVC XYZ=6.10,5.50,2.40, QUANTITY='WALL TEMPERATURE', IOR=-2, ID='WALL15' /
&DEVC XYZ=6.10,5.50,2.10, QUANTITY='WALL TEMPERATURE', IOR=-2, ID='WALL25' /
&DEVC XYZ=6.10,5.50,1.80, QUANTITY='WALL TEMPERATURE', IOR=-2, ID='WALL35' /
&DEVC XYZ=6.10,5.50,1.50, QUANTITY='WALL TEMPERATURE', IOR=-2, ID='WALL45' /
&DEVC XYZ=6.10,5.50,1.20, QUANTITY='WALL TEMPERATURE', IOR=-2, ID='WALL55' /
&DEVC XYZ=6.10,5.50,0.90, QUANTITY='WALL TEMPERATURE', IOR=-2, ID='WALL65' /
&DEVC XYZ=6.30,5.50,2.40, QUANTITY='WALL TEMPERATURE', IOR=-2, ID='WALL16' /
&DEVC XYZ=6.30,5.50,2.10, QUANTITY='WALL TEMPERATURE', IOR=-2, ID='WALL26' /
&DEVC XYZ=6.30,5.50,1.80, QUANTITY='WALL TEMPERATURE', IOR=-2, ID='WALL36' /
&DEVC XYZ=6.30,5.50,1.50, QUANTITY='WALL TEMPERATURE', IOR=-2, ID='WALL46' /
&DEVC XYZ=6.30,5.50,1.20, QUANTITY='WALL TEMPERATURE', IOR=-2, ID='WALL56' /
&DEVC XYZ=6.30,5.50,0.90, QUANTITY='WALL TEMPERATURE', IOR=-2, ID='WALL66' /

&TAIL /

Chapter 7

HEURISTIC ANALYSIS OF COOLING PROCESSES IN HIGH STRENGTH CONCRETE SQUARE COLUMNS

7.1	IDENTIFICATION OF THE ORIGINAL CONTRIBUTION.....	762
7.2	METHODOLOGY TO DEVELOP THE HEURISTIC ANALYSIS	762
7.3	DEFINITION OF THE ANALYSIS CASE	762
7.3.1	Description of the general features of the analysis case and causes for its selection.....	762
7.4	RESULTS.....	764
7.4.1	Heuristic Analysis of the Heating Stage.....	764
7.4.2	Heuristic Analysis of the Cooling Stage.....	768
7.4.2.1	Slow Environmental Cooling.....	768
7.4.2.2	Fast Environmental Cooling	782
7.5	RESUME OF THE CONCLUSIONS OF THE CHAPTER.....	796
7.5.1	About the Heuristic Analysis of Cooling Processes in HSC Square Columns.....	796
7.5.2	About extended tasks to go more deeply into Thermal Spalling Research in Square Columns.....	797
7.6	BIBLIOGRAPHY OF THE CHAPTER	798
Appendix 7A.	INPUT FILES FOR THE HYGRO-THERMO-CHEMO-MECHANICAL CALCULATIONS OF A SQUARE COLUMN.....	798

*THIS PAGE IS INTENTIONALLY
LEFT BLANK*

Chapter 7

HEURISTIC ANALYSIS OF COOLING PROCESSES IN HIGH STRENGTH CONCRETE SQUARE COLUMNS

The aim of this chapter is to develop an heuristic analysis of the effect of cooling processes on the hygro-thermo-chemo-mechanical state of a square column, manufactured with High-Strength concrete, during the development of a natural fire in a High-Rise Building. The work presented in this Chapter must be understood as an introductory extension of the analyses already presented in *Chapter 6: Analysis of cooling processes in High Strength Concretes* to cases with bidimensional fluxes – of both heat and mass – such as square columns, where Corner Thermal Spalling is often the most dangerous type.



NSC [1]

HSC: Conventional Tie Configuration [2]

HSC: Modified Tie Configuration [2]

Figure 7-1. Comparison of Thermal Spalling in NSC and HSC columns fire resistance tests.



Figure 7-2. Corner Thermal Spalling examples during Fire Resistance Tests [3].

The heuristic typology of the analyses presented herein is due, as it was explained on *Chapter 6*, to the current lack of development of Spalling Indexes suitable for bidimensional cases and correlated against experimental data.

7.1 IDENTIFICATION OF THE ORIGINAL CONTRIBUTION

As stated, the main original contribution of the works presented in this Chapter is the heuristic analysis of the effect of cooling processes on the hygro-thermo-chemo-mechanical state of a square column manufactured with High-Strength concrete.

7.2 METHODOLOGY TO DEVELOP THE HEURISTIC ANALYSIS

A set of state variables and other related parameters mainly concerning the level of damage in the square column are needed to accomplish the heuristic analysis of the effect of cooling processes on the hygro-thermo-chemo-mechanical state of a square column manufactured with High-Strength concrete. This set of variables and parameters has already been defined and explained in depth in paragraph 6.2.2 of *Chapter 6*.

Hence, comparing the evolution of the values of the variables favouring Thermal Spalling – such as high local values of gas overpressure, $p^g - p_{atm}$, and mechanical damage parameter, d , high values of averaged transversal traction stresses, $\bar{\sigma}_{th}$, and constrained elastic energy \bar{U} – against those corresponding to the factors impeding Thermal Spalling – such as high average values of traction strength, \bar{f}_t , and specific fracture energy, $\bar{G}f$, for the material layer between a current position and the heated surface – the risk of Thermal Spalling may be analyzed through an heuristic methodology.

7.3 DEFINITION OF THE ANALYSIS CASE

7.3.1 Description of the general features of the analysis case and causes for its selection

The structural element selected for the analyses to develop in this Chapter is widely found in most of the High Strength Concrete structures usually found in High-Rise Buildings: the square column (see Table 4-7 in *Chapter 4: Spalling Nomograms*, where it can be observed some common sizes of the square columns in High-Rise Buildings ranging from quite small 30x30 cm columns up to several metres in size).

The general features and the mesh needed for the numerical simulation of the analysis case described herein must be defined with enough refinement to show the sharp gradients of parameters such as gas pressure mostly in the zone close to the heated and cooled surfaces. On figure 7-3, a brief description of the plane strain model used in the simulations is observed.

This case deals with a square column (30 x 30 centimetres) made of the C60 High Strength Concrete whose material properties have been completely defined in paragraph 4.3.2.5.2 of *Chapter 4*. The column is assumed to present an initial relative humidity of 50%.

The Cauchy's type boundary conditions (mixed radiative-convective) described on Table 7-1 represent, in the case of the heated faces, a constant in time value of the relative humidity in the environment and a fixed value of mass (of water vapour) exchange coefficient. The four faces of the square column are supposed to be identically exposed to the fire in the enclosure, both in the heating stage and during the environmental cooling stage. In this way, only one fourth of the column has to be modelled leading to computational efforts significantly lower (although still huge).

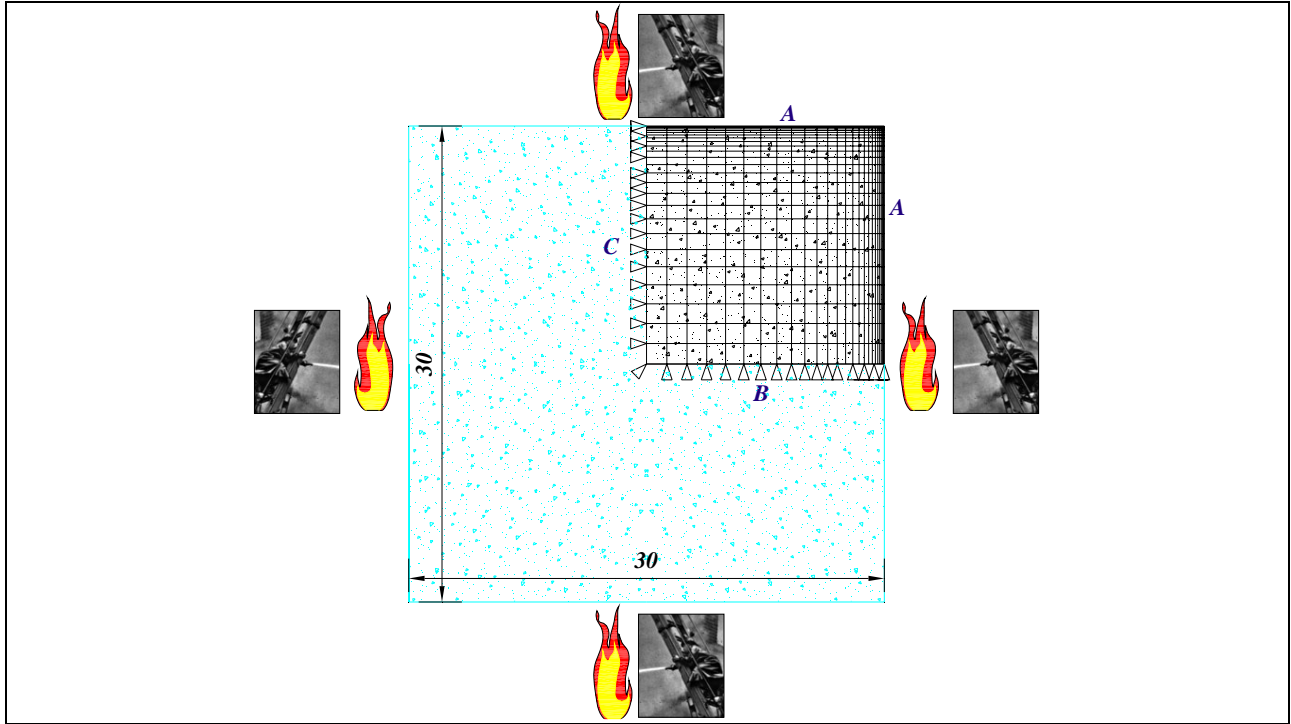


Figure 7-3. Plane strain finite element model of the Structural Concrete element slice.

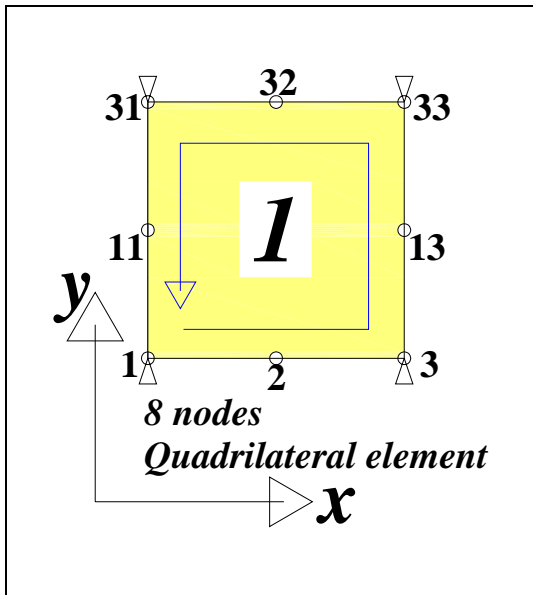


Figure 7-4. Finite Element detail.

Side	Variables	Values and coefficients
A	p^g	$p^g = 101.325 \text{ Pa}$
	p^c	$R.H_{\text{Environment}} = 0, \beta_c = 0,025 \text{ m/s}$
	T: convective	T = See next explanation
	T: radiative	$\epsilon\sigma_0 = 5,1 \times 10^{-8} \text{ W m}^{-2} \text{ K}^{-1}$
B	u_y	$u_y = 0$
	p^g	$q^g = 0$
	p^c	$q^{gw} = q^w = 0$
	T	$q^T = 0$
C	u_x	$u_x = 0$
	p^g	$q^g = 0$
	p^c	$q^{gw} = q^w = 0$
	T	$q^T = 0$

Table 7-1. Boundary conditions used in the numerical simulation.

The definition of the heating profile applied to face A up to eighty minutes (4.800 seconds) after the start of the fire is extensively described on paragraph 4.3.2.4 of Chapter 4, being always related to the evolution of the environment temperature (and not to the evolution of the heated surface temperature), and particularized in paragraph 6.4.3.1.3 of Chapter 6 to account for a fire with a extremely low development. Hence, to achieve quite a slow heating profile, an opening coefficient below the minimum permitted in Eurocode 1, Part 1-2 [4] is used ($O = 0,013 \text{ m}^{1/2}$), matching also this heating profile with the one used in Chapter 5 – Preliminary and Simplified Analysis of Cooling Effect on HSCs Spalling Behaviour (paragraph 5.2.1 for more details)

Heating profile	$\Theta_g [^\circ\text{C}], t [\text{h}]$
	$\Theta_g = 20 + 1.325 \cdot (1 - 0,324 \cdot e^{-0,0077t} - 0,204 \cdot e^{-0,06545t} - 0,472 \cdot e^{-0,7315t})$

Table 7-2. Heating profile.

while the heat exchange coefficient is selected at a value of 20, within the reasonable range of values for natural convection on air [5-20] W/m²K.

After the heating stage end (4.800 seconds), as previously explained in *Chapter 6* the environmental cooling processes are preceded by a 120 seconds interval (up to 4.920 seconds from the start of the fire) where environment temperature is kept constant in order to ease the achievement of numerical convergence. Then, the environmental temperature is progressively decreased according to the cooling rates detailed next and until it reaches ambient temperature, which is considered 25 °C, following the calculations – in the fast cooling case (see below) – with a constant ambient temperature (not until the whole structural element shows a temperature within the range *Ambient Temperature* ± 10°C because this would lead to extremely long calculations in the case of the square column model). Among them, several subtypes of cooling profiles are defined depending on the cooling rates:

- ❖ ‘*Slow cooling*’: It is characterized by a cooling rate of the air of – 0,20 °C/s.
- ❖ ‘*Fast cooling*’: It is characterized by a cooling rate of the air of – 20,0 °C/s.

According to the different stages of the heating and cooling processes above described, simulations have been divided into the following five stages described by different time steps and frequency of results recording:

SUBTYPE OF COOLING	Input file name	Initial time (s)	Time step (s)	Number of time steps	Frequency of results record (in time steps)	Final time (s)
<i>HEATING STAGES COMMON TO ALL OF THE CALCULATIONS</i>	COLUMN_01	0	1E-6	10	10	1E-5
	COLUMN_02	1E-5	3,0	1.600	40	4.800
	COLUMN_03	4.800	1,0	120	20	4.920
<i>SLOW ENVIRONMENTAL COOLING</i>	COLUMN_04	4.920	1,0	2.400	60	7.320
<i>FAST ENVIRONMENTAL COOLING</i>	COLUMN_04	4.920	0,5	40	2	4.940
	COLUMN_05	4.940	1,0	900	60	5.840

Table 7-3. Time history of the simulation stages.

Consequently, a plane strain model with a total number of 625 eight-nodes quadrilateral elements, with 40 degrees of freedom and a 3x3 order of integration, and 1.976 nodes, and the boundary conditions exposed on the table 7-1 has been implemented and calculated by means of the advanced Hitecosp Software [5].

7.4 RESULTS

7.4.1 Heuristic Analysis of the Heating Stage

During the heating stage, the resulting distributions of temperature, gas pressure, vapour pressure, capillary pressure, mechanical damage, total damage, first effective principal stress, third effective principal stress, relative humidity, saturation and elastic energy at 20 minutes and 40 minutes from the start of the fire are shown in figures 7-5 to 7-7. In sight of these evolutions, during the heating of the column it is observed a gradual increase of temperature in the surface zone – beyond the critical point of water, see figure 7-5 a) – where moisture content and relative humidity decrease fast – figures 7-7 a) and b) – reaching very low values. Sharp fronts with very high gradients of temperature and relative humidity, moving towards the central part of the sample, are observed. In this zone, as explained in *Chapters 4, 5 and 6* for the one-dimensional case, rapid evaporation causes an increase of vapour pressure up to values exceeding 0,25 MPa (although these values might be much higher under a faster heating process) – see figure 7.5 c) –.

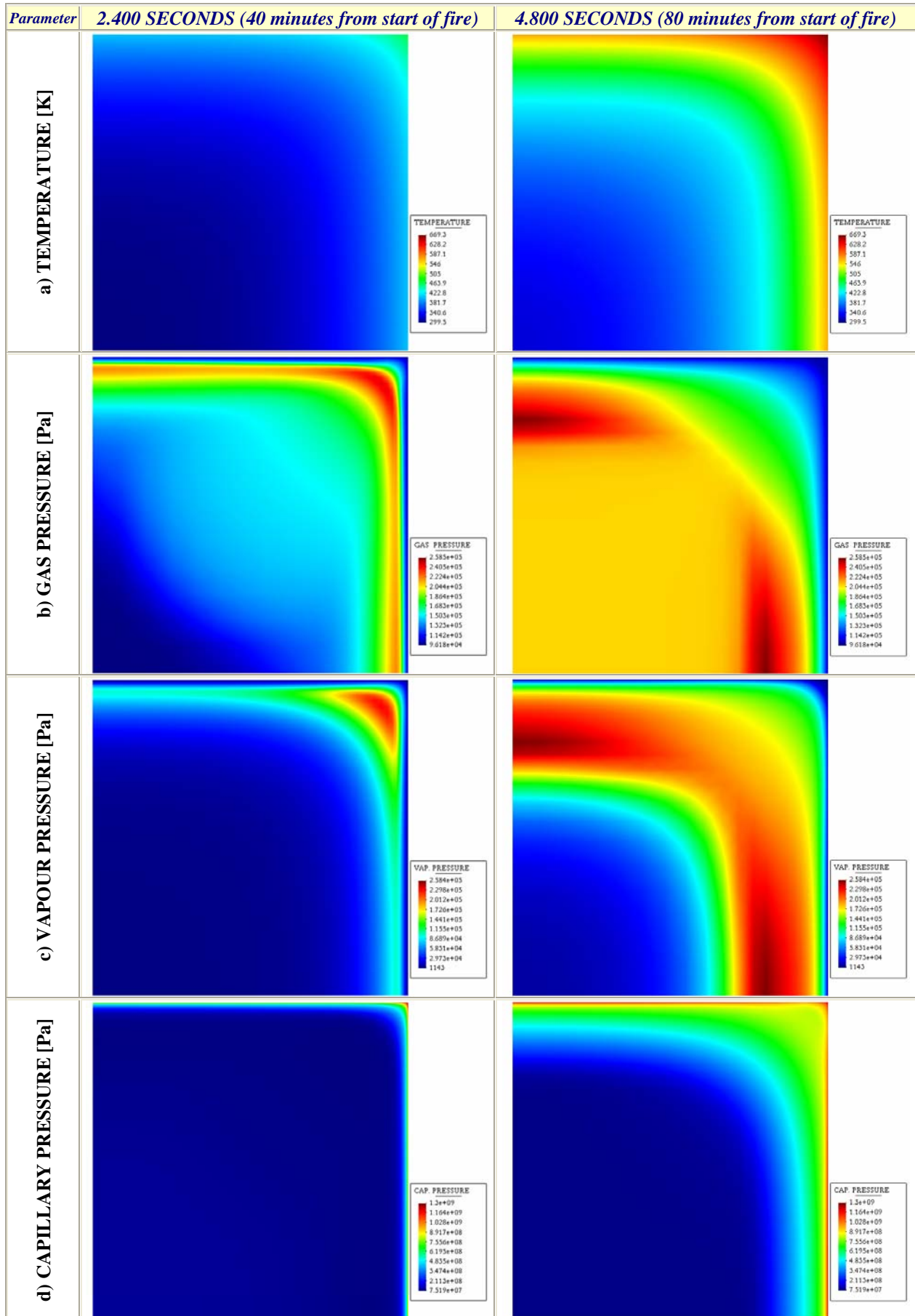


Figure 7-5. Evolution of several parameters: 40 minutes and 80 minutes from the start of fire.

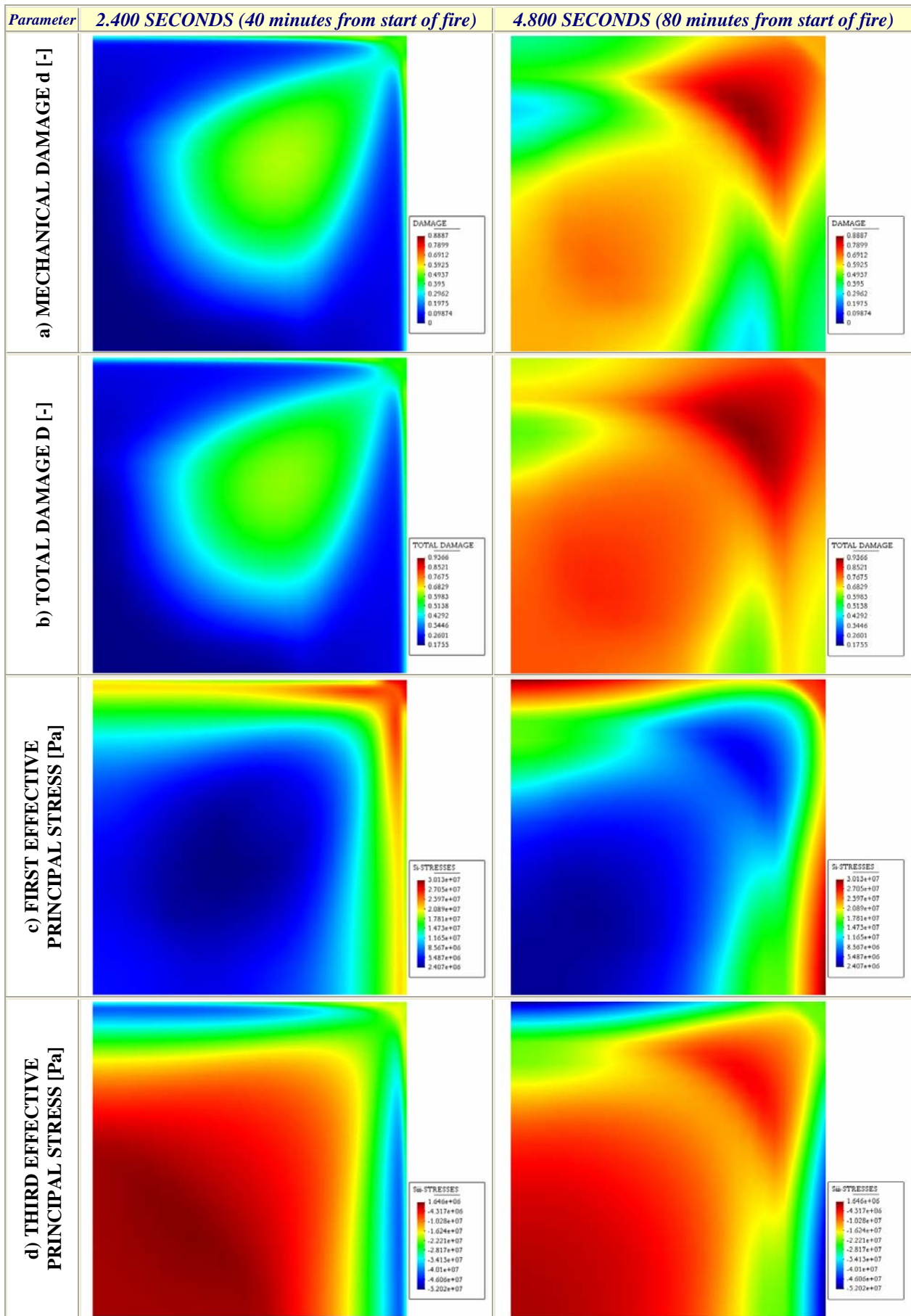


Figure 7-6. Evolution of several parameters: 40 minutes and 80 minutes from the start of fire.

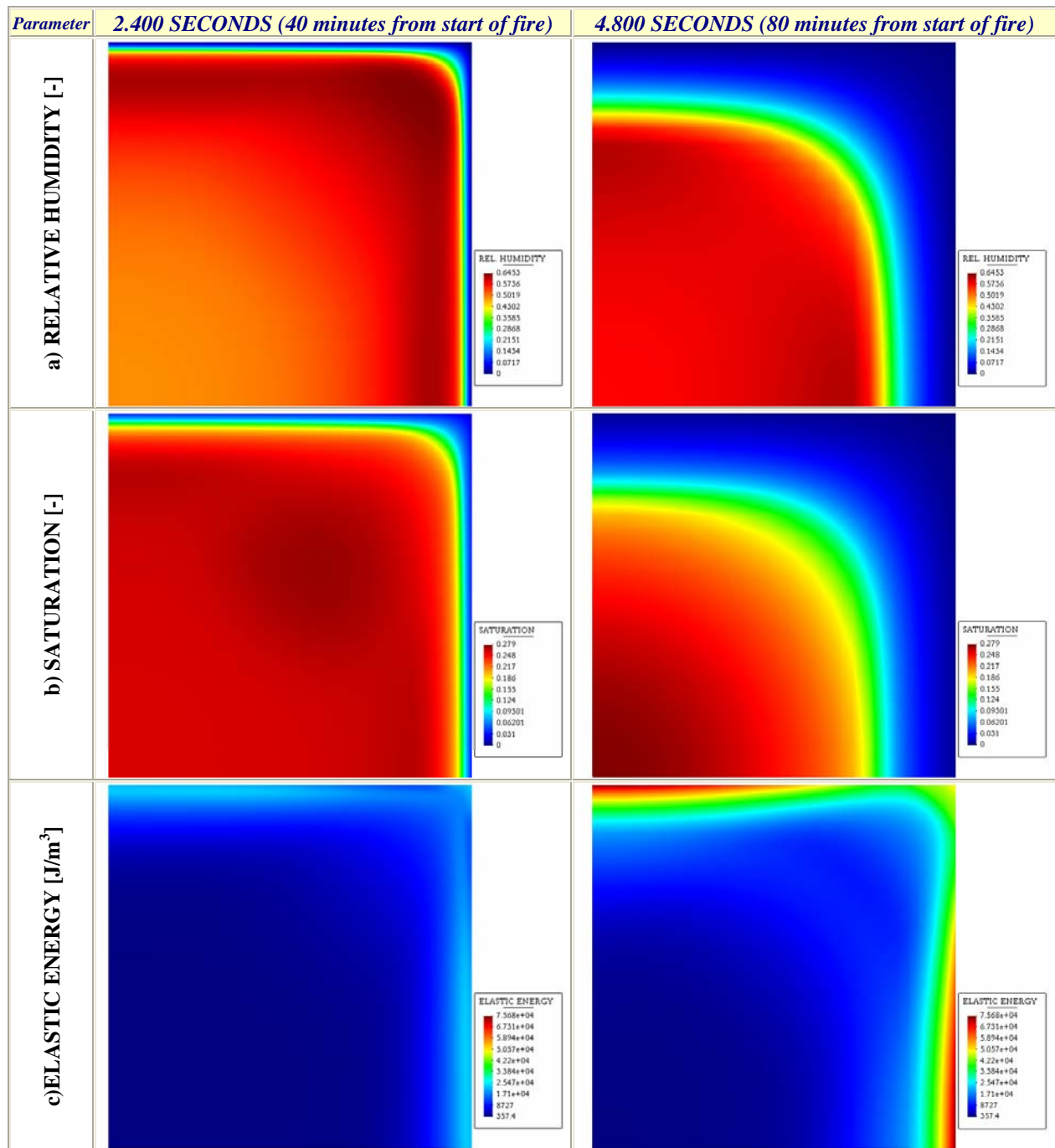


Figure 7-7. Evolution of several parameters: 40 minutes and 80 minutes from the start of fire.

This phenomenon, together with thermal dilatation of the outer part of the sample, while the internal remains at a much lower temperature, causes high tensile stresses and resulting material damaging – see figures 7-6 c) and d) and 7-6 a) and b) respectively –. This effect is particularly important in the corner zone of the sample, what is typical for concrete structural elements of a similar shape. At the same time, the temperature increase causes significant thermo-chemical degradation of concrete in the heated zone – see figure 7-6 b) – increasing additionally deterioration of the surface zone. High values of the vapour pressure and the total damage parameter in the corner zone, close to the surface, indicate a serious risk of explosive spalling (total damage in the corner reaches values of 0,9566 at 40 minutes from the start of the slow fire considered, suggesting an almost complete fracture of the concrete material in this zone).

Several experimental tests [1-3] showed that, in this kind of concrete element geometry, Thermal Spalling often occurs in the corner zone (see figures 7-1 and 7-2), what is qualitatively confirmed by the results of these numerical simulations. It is particularly graphic to observe that both the mechanical and total damage distributions present the shape of the head of an arrow, shape observed within all the simulations described in the available literature [6].

In the inner zones of the column, higher values of the relative humidity are observed – see figure 7-7 a) – as a result of advective flow of vapour caused by vapour pressure gradients – see figure 7-5 c) – and consequent vapour condensation in the colder, internal part of the structural element. From the enclosed figures, once more it is observed that hygral and thermal phenomena, as well as concrete deterioration, have a very complex and strongly coupled character, so they cannot be analyzed with enough accuracy by means of uncoupled and simplified models.

7.4.2 Heuristic Analysis of the Cooling Stage

7.4.2.1 SLOW ENVIRONMENTAL COOLING

At the start instant of the cooling process (4.920 seconds from the beginning of heating), the maximum temperature is reached at the heated surface – and, more precisely, at the corner (see figure 7-14 a) –, being the zones close to the surface almost completely dry (see figure 7-22 a)).

The ‘moisture clog’ is situated 4 centimetres away from the surface and 9 centimetres away from the corner (figure 7-22 a)) matching this position with that corresponding to the maximum value of the vapour pressure (see figure 7-16 a)) caused by intensive water evaporation in the temperature range 100-200 °C (see figure 7-14 a)). It is remarkable that the maximum values of the vapour pressure do not appear close to the corner but at the symmetry axes of the square column (190.000 Pa against 238.000 Pa).

The stated increase of the vapour pressure, together with thermal dilatation of the outer part of the sample, while the internal remains at a much lower temperature, causes high tensile stresses and resulting material damaging – see figures 7-18 a) and 7-19 a) respectively –, especially at the zone of the corner where the highest values of mechanical damage arise (0,8868 at 4,9 centimetres from surface, as shown on figure 7-18 a), while it is only half this value (0,4415) at the surface at the symmetry axes of the column).

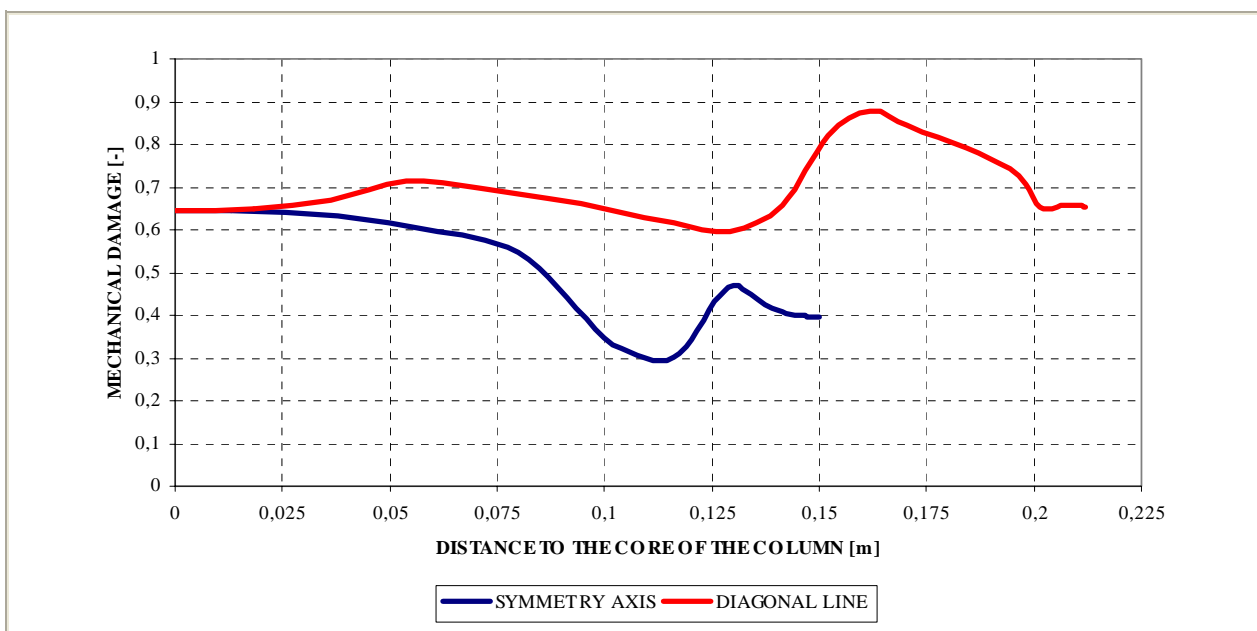


Figure 7-8. Distribution of the mechanical damage d values 4.920 sec from the start of fire (start of the cooling process).

From figure 7-8 it is remarkable that the level of mechanical damage at the core of the square column is at this instant higher than those corresponding to any depth along its symmetry axes. At this instant, the elastic energy is mostly accumulated close to the surface (figure 7-24 a)), precisely in the abovementioned layer – what leads to an energetic viability of Thermal Spalling occurrence of the layers close to the surface –. Besides this, at this start instant the heat flux moves inwards from the surface, while water vapour fluxes are addressed, from the moisture clog, both towards the heated surfaces and inwards due to the gradients of vapour pressure. The latter flux means vapour condensation when it reaches colder layers.

As the cooling process starts (beyond 4.920 seconds), the temperature gradients in the square column become progressively lower since the surface temperature decreases while the inner temperatures increase (figure 7-14 a)). Besides this, it is observed that the value corresponding to the peak of vapour pressure is progressively reduced during the environment cooling; this sharp decrease of the vapour pressure values – see figures 7-16 b) and c) – (together with a decrease in the elastic strain energy – see figures 7-24 b) and c) –) may lead to a progressive decrease of the Thermal Spalling risk despite mechanical damage values increase during cooling until the end of the environmental slow cooling process.

As the cooling process continues, the zones with the maximum mechanical damage grow (see figure 7-9 where it is shown the evolution of the extension of the zones where the Total damage D value is above 0,75). Indeed, during the environmental cooling process the cooled surfaces increase considerably their Total Damage values (more than a 20 per cent, see figure 7-10), especially those surfaces far from the corner. It is remarkable that the inner locations that showed the maximum values of the Total Damage parameter at the end of the heating stage, do not increase significantly these values during the cooling stage.

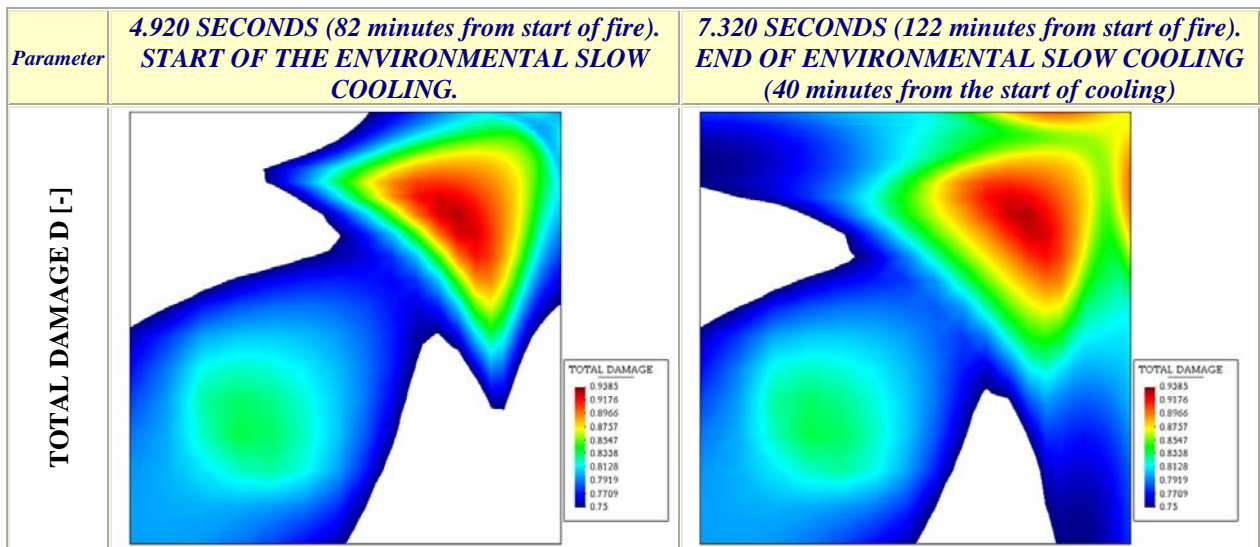


Figure 7-9. Zones of the square column with Total Damage higher than 0,75 at the start and end of environmental slow cooling.

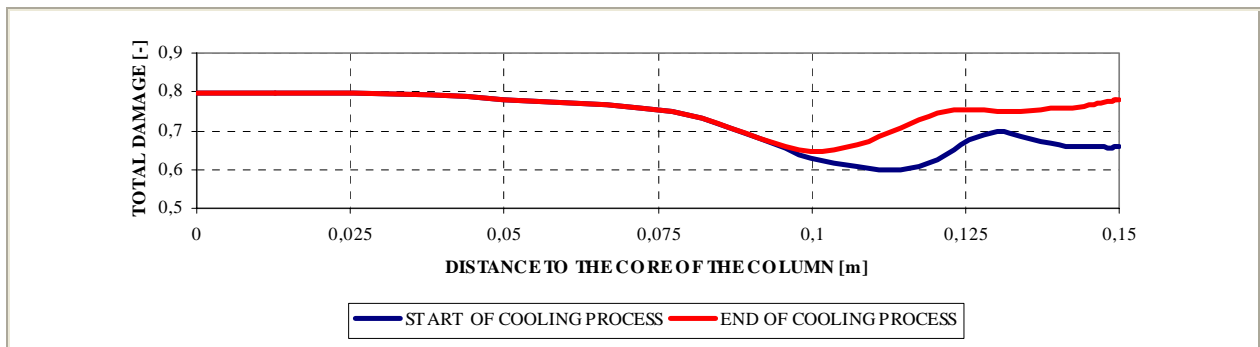


Figure 7-10. Distribution of the Total damage d values at the start and end of the cooling process, at the symmetry axis.

The maximum value of the elastic strain energy (figures 7-24 b) and c)), considerably lower than at the beginning of the cooling process, does not appear any more at the surface but at 5 centimetres inwards. It is also remarkable that forty minutes after the start of the environmental cooling process (7.320 seconds from the start of the fire) all of the stresses components have decreased their values at the zones next to the cooled surfaces and increased them at the core of the square column, as it can be observed both in figures 7-11 to 7-13 (first, second and third effective principal stresses respectively) and in figures 7-20 and 7-21, being tensile in the direction perpendicular to the main diagonal of the square column – first effective principal stress – and of compressive nature in the direction of the diagonal – third effective principal stress –. The effective stress in the longitudinal direction of the square column is mainly tensile except at the end of the cooling process, when close to the corner arise compressive values:

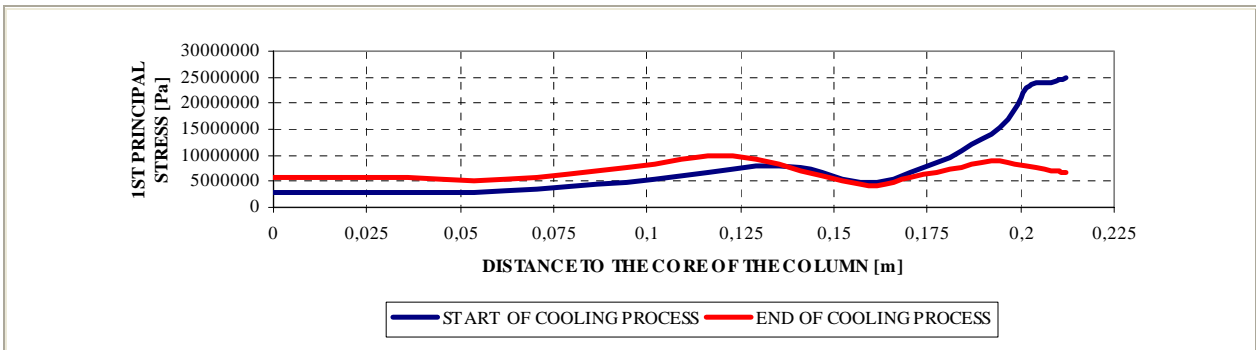


Figure 7-11. Distribution of the first effective principal stress at the start and end of the cooling process, along the diagonal of the square column (remark: the first principal stress is oriented orthogonal to the diagonal of the column).

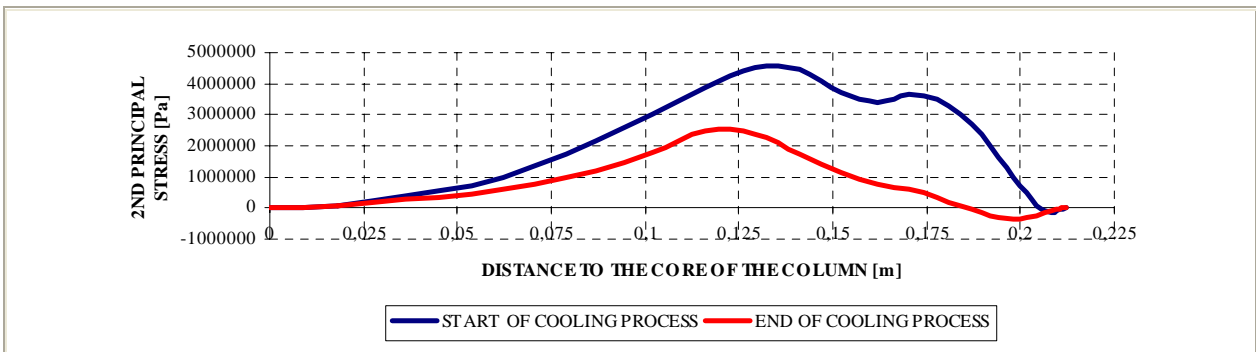


Figure 7-12. Distribution of the second effective principal stress at the start and end of the cooling process, along the diagonal of the square column (remark: the second principal stress is oriented in the longitudinal direction of the column).

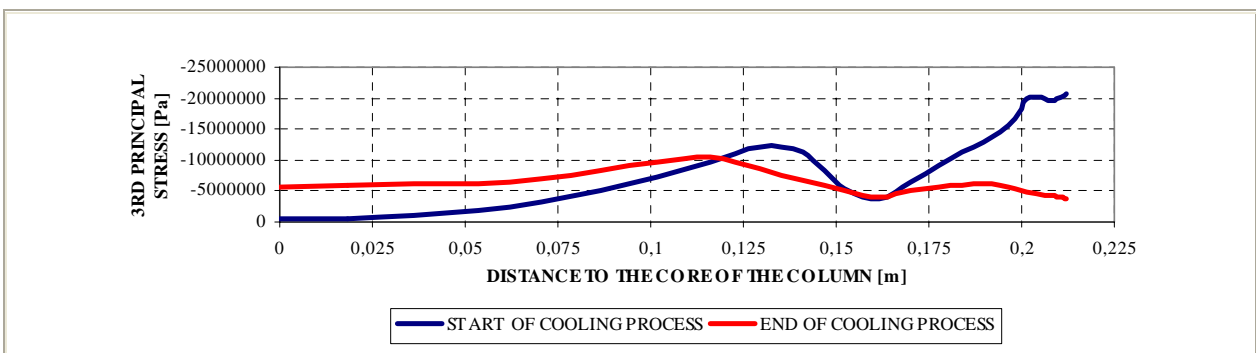


Figure 7-13. Distribution of the third effective principal stress at the start and end of the cooling process, along the diagonal of the square column (remark: the third principal stress is oriented in the direction of the diagonal of the column).

Related to the evolution of the variables impeding Thermal Spalling, the average values of traction strength, \bar{f}_t , tend to increase during cooling in the layers within the first five centimetres from the corner (due to their temperature decrease) but they tend to decrease in the most inner layers (due to their temperature increase) – see figure 7-14 a) to c) –.

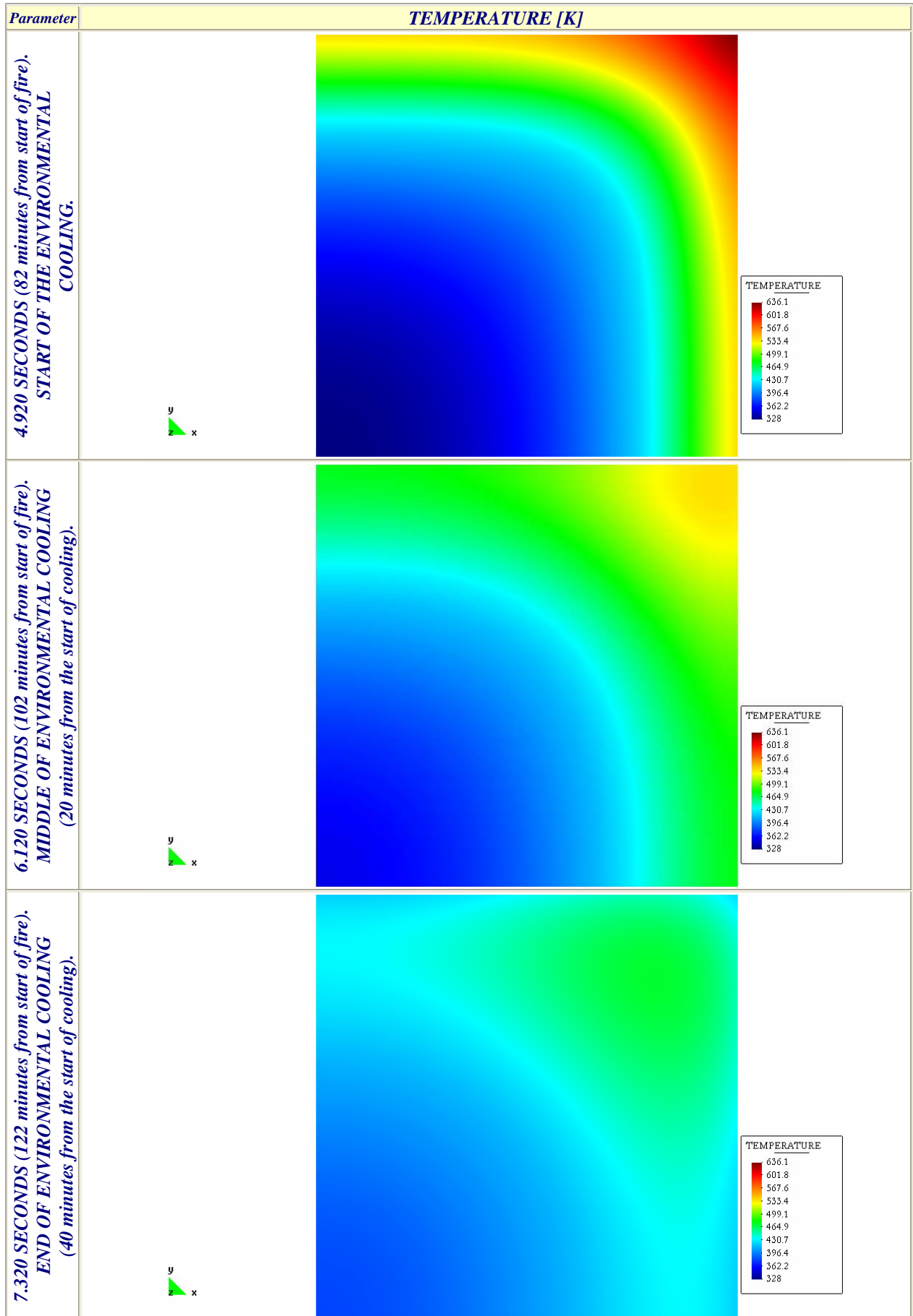


Figure 7-14. Evolution of Temperature during the Slow Environmental Cooling stage.

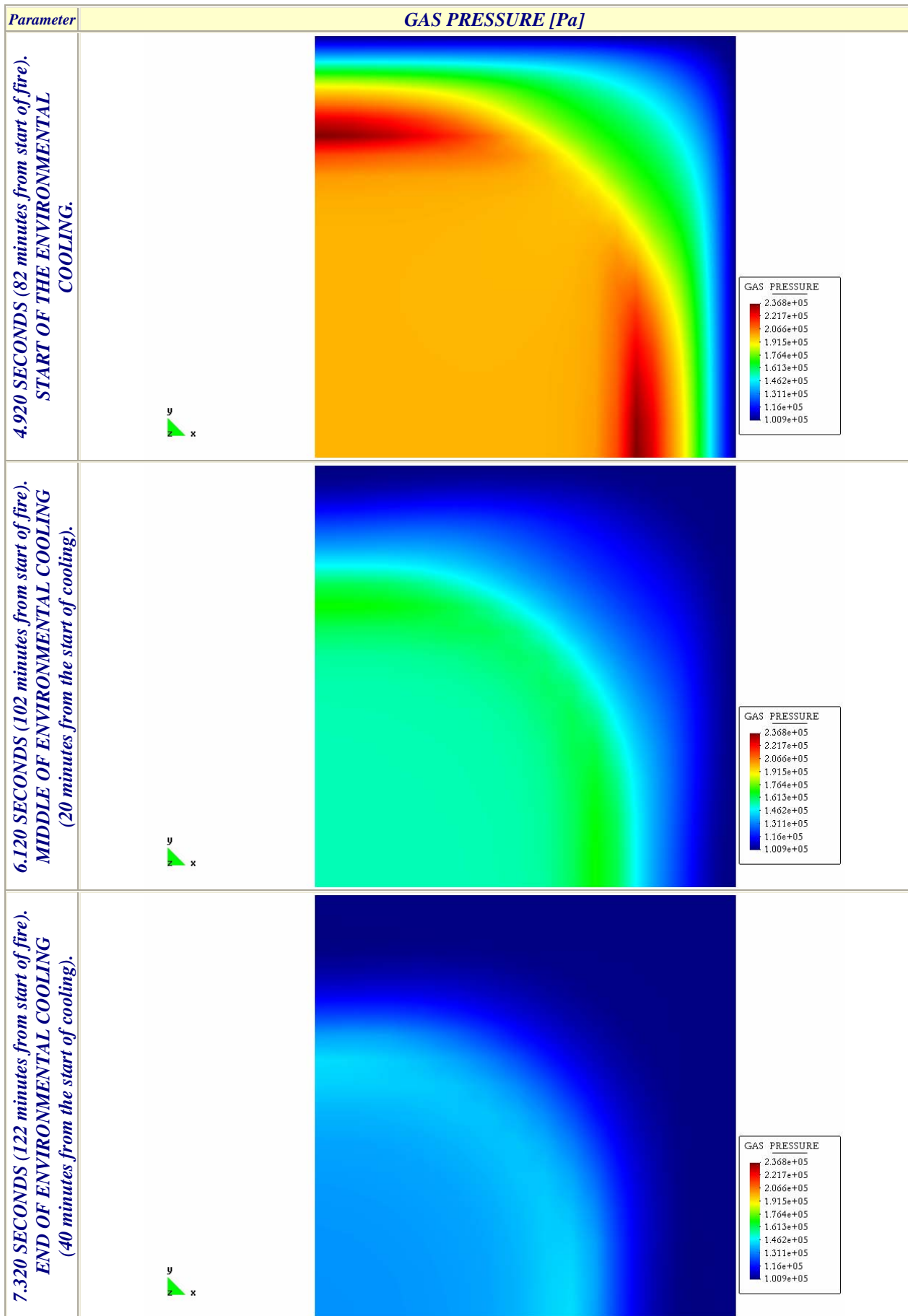


Figure 7-15. Evolution of Gas Pressure during the Slow Environmental Cooling stage.

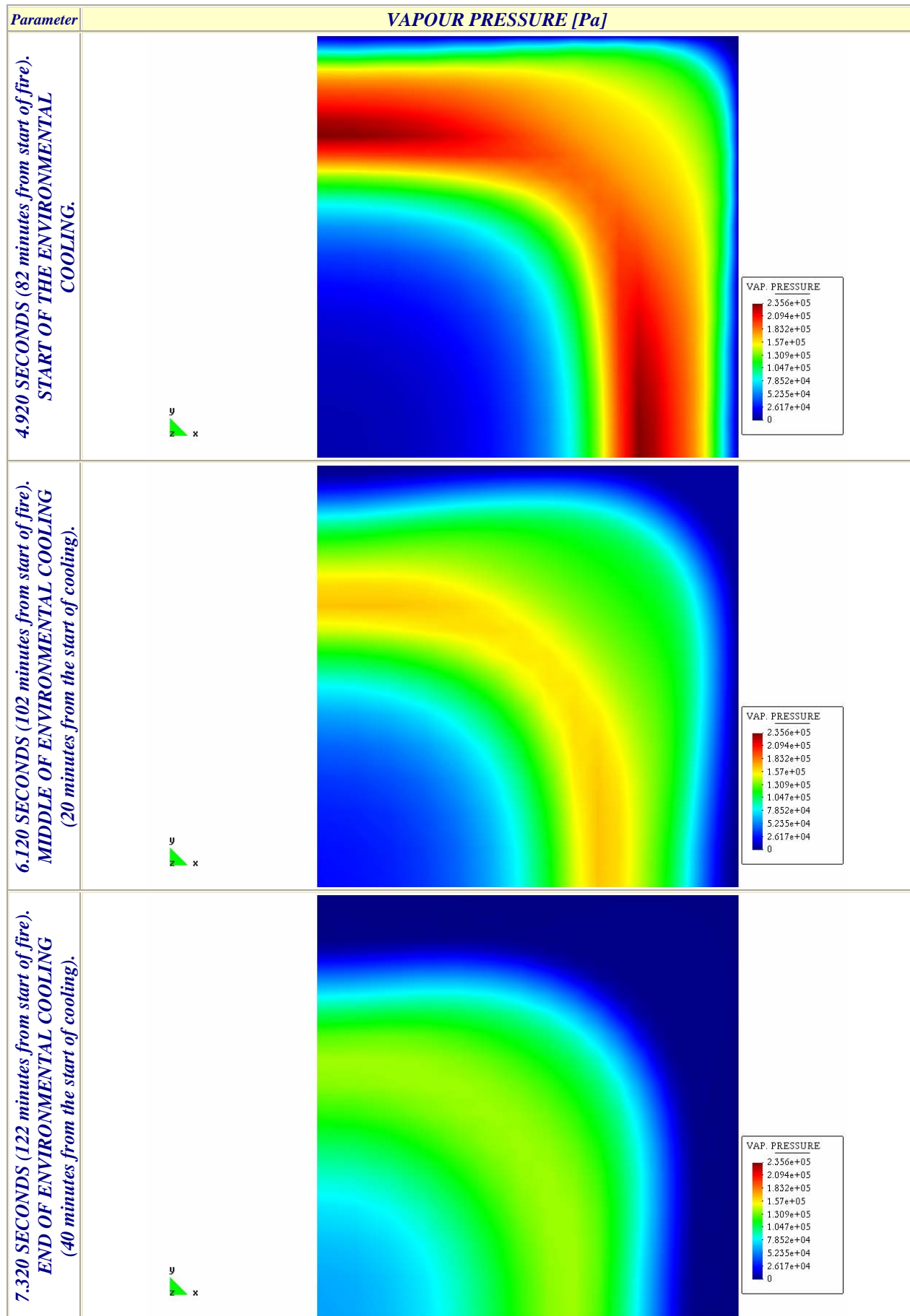


Figure 7-16. Evolution of Vapour Pressure during the Slow Environmental Cooling stage.

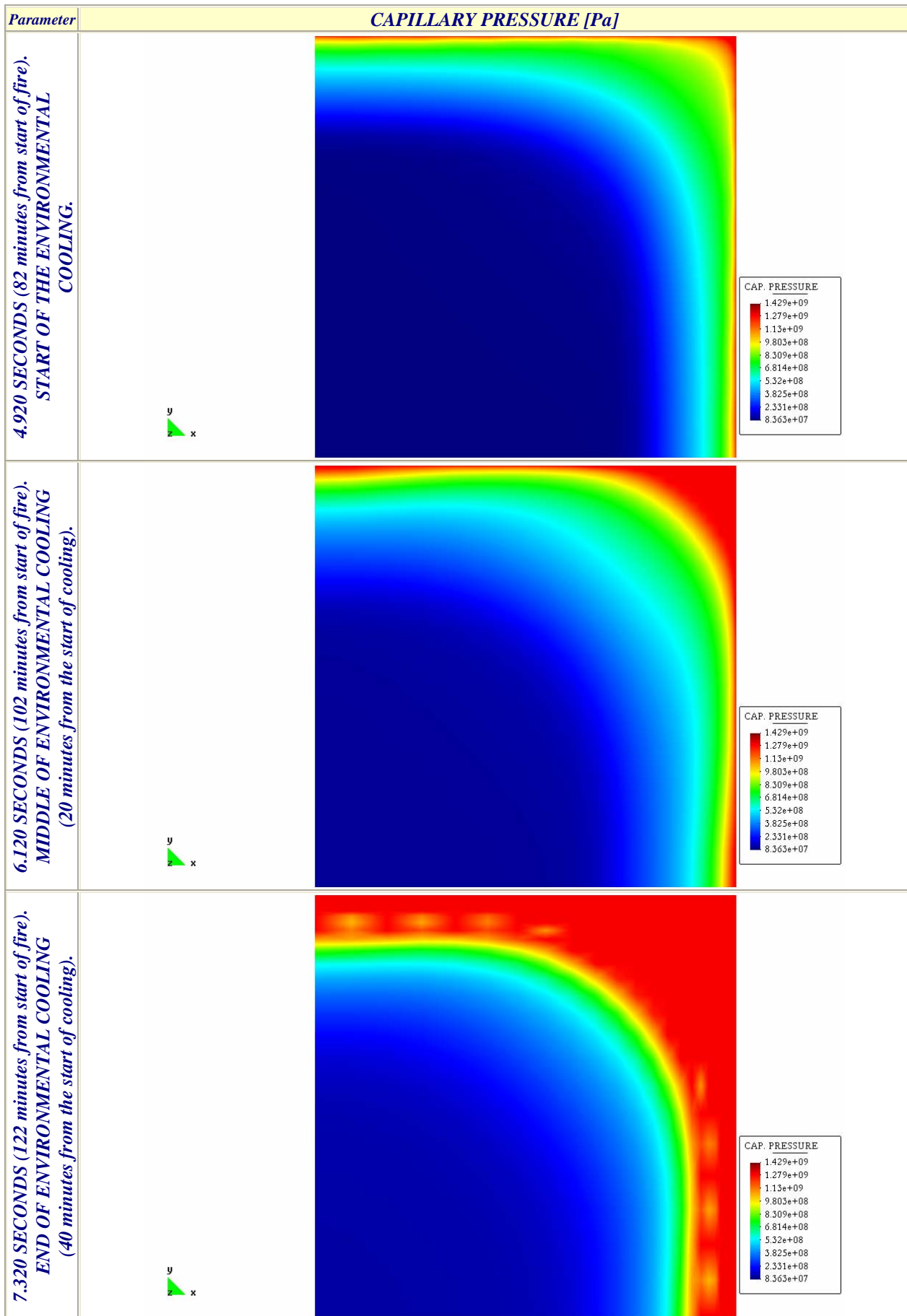


Figure 7-17. Evolution of Capillary Pressure during the Slow Environmental Cooling stage.

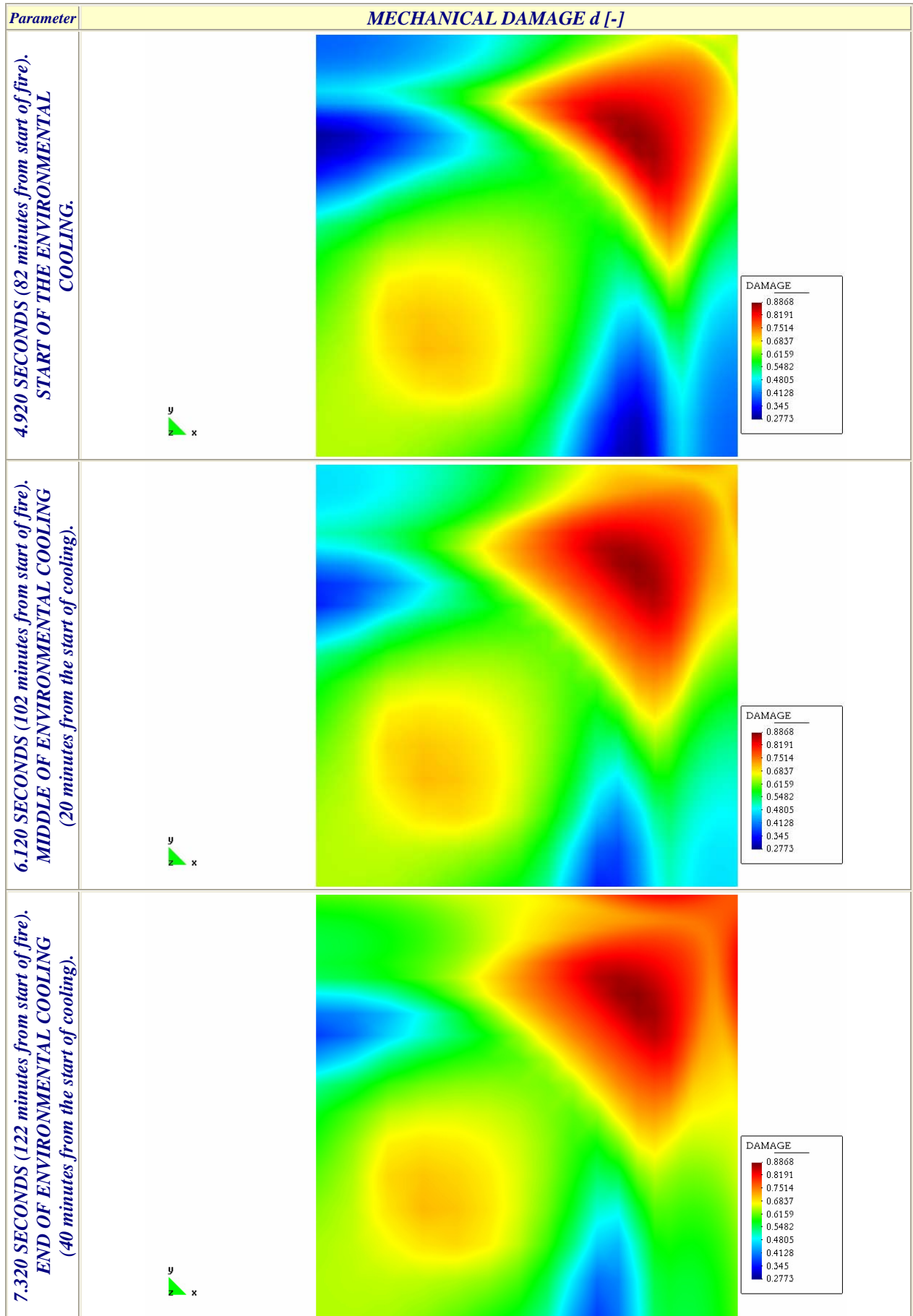


Figure 7-18. Evolution of Mechanical Damage during the Slow Environmental Cooling stage.

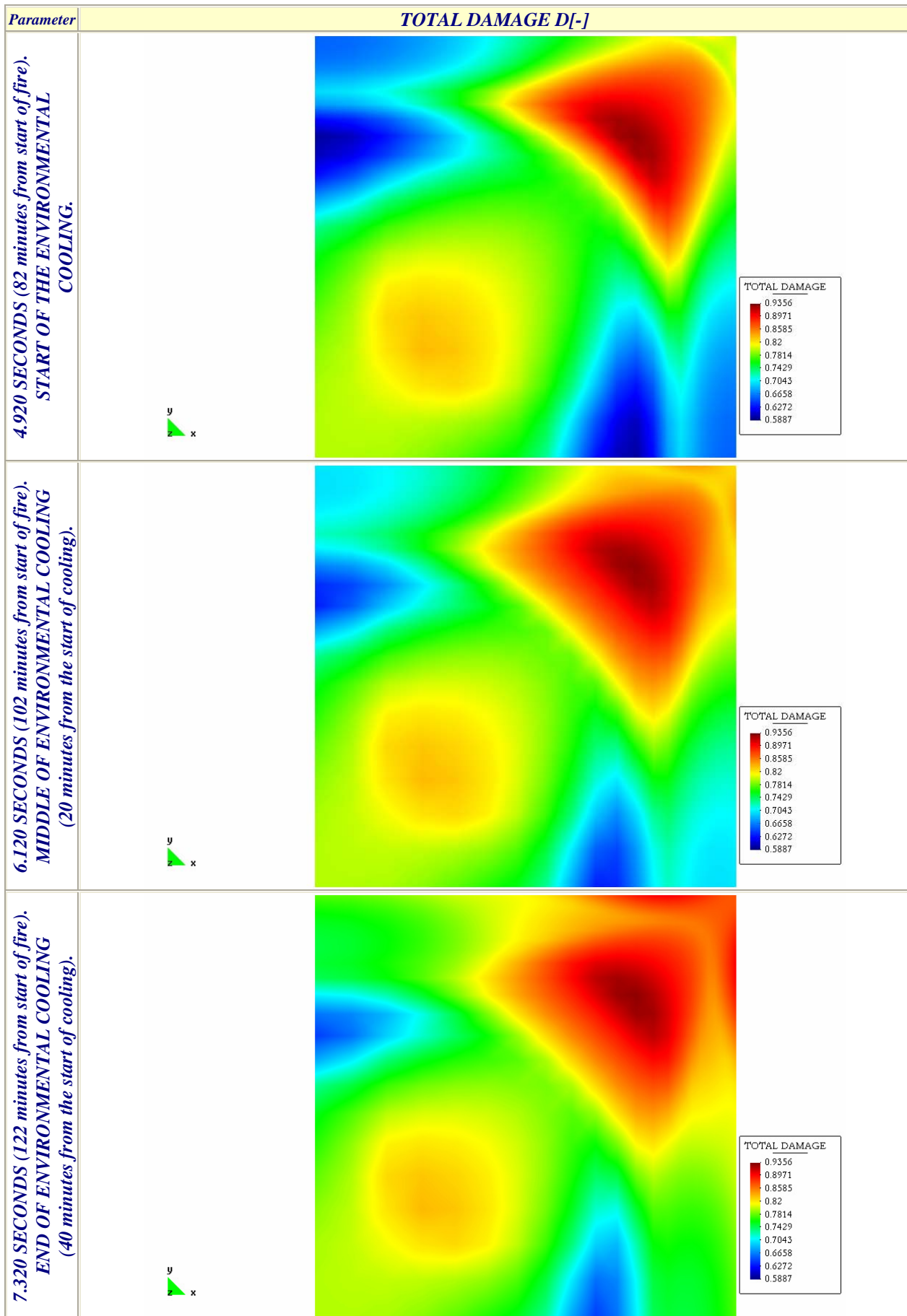


Figure 7-19. Evolution of Total Damage during the Slow Environmental Cooling stage.

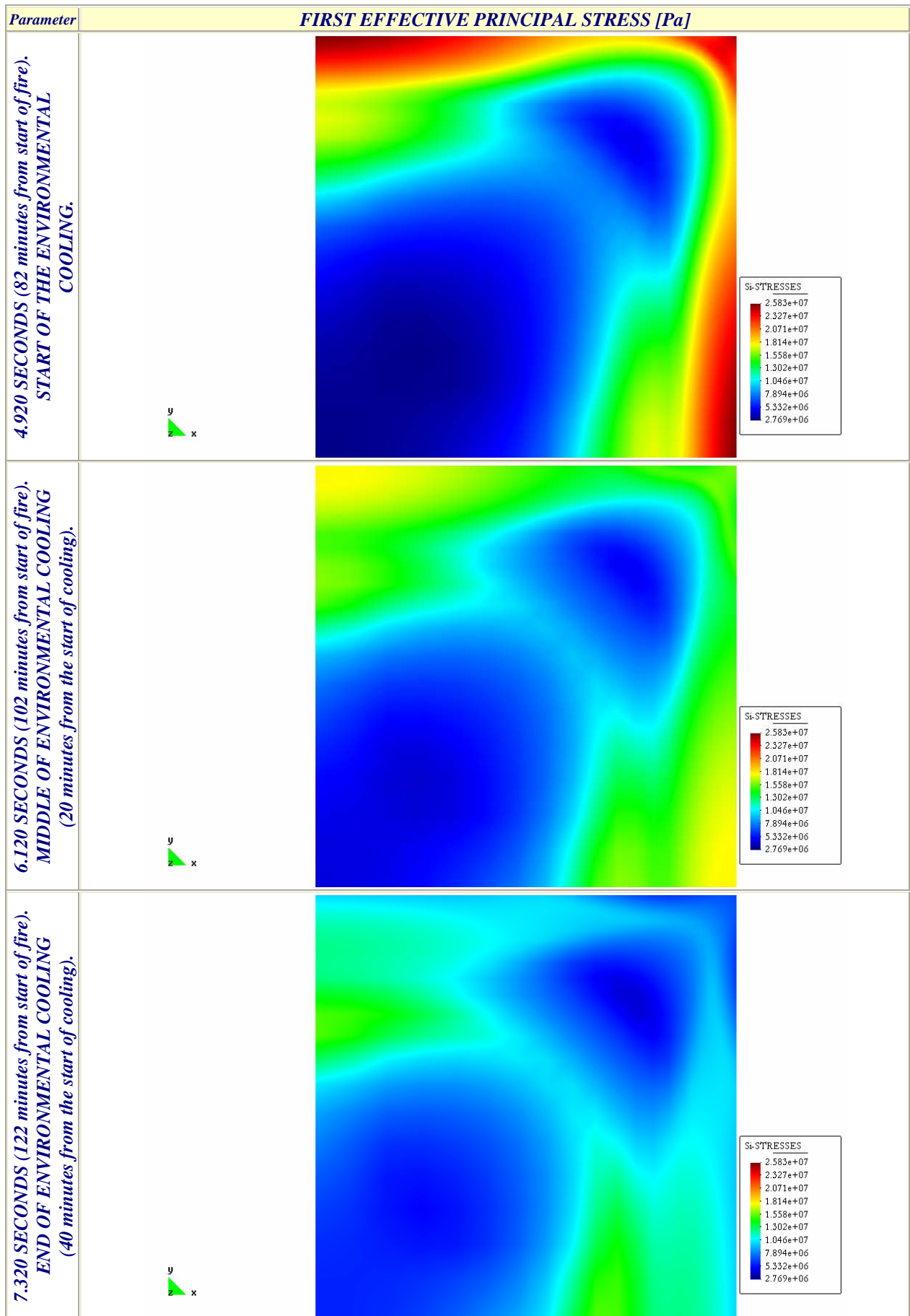


Figure 7-20. Evolution of First Effective Principal Stress during the Slow Environmental Cooling stage.

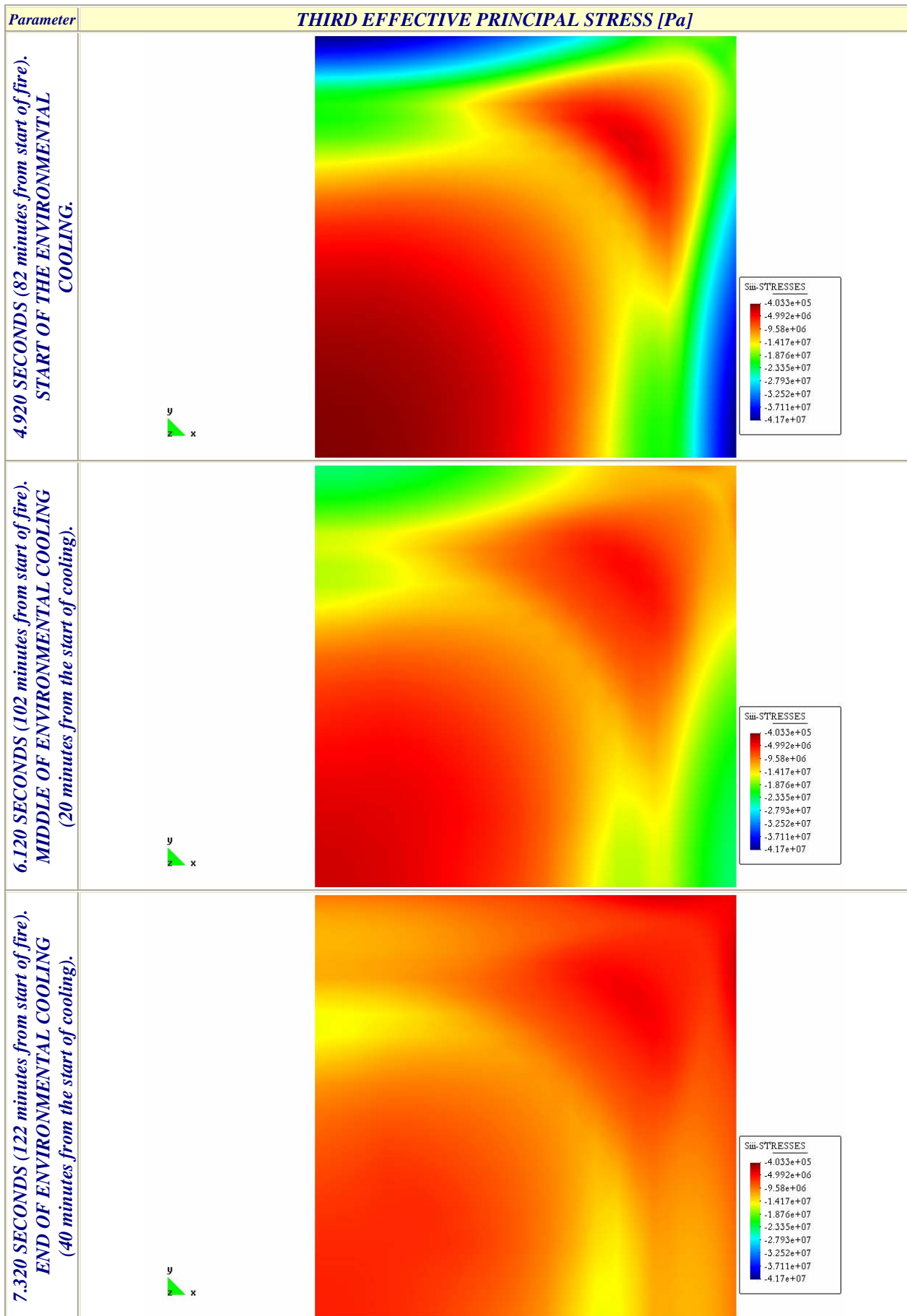


Figure 7-21. Evolution of Third Effective Principal Stress during the Slow Environmental Cooling stage.

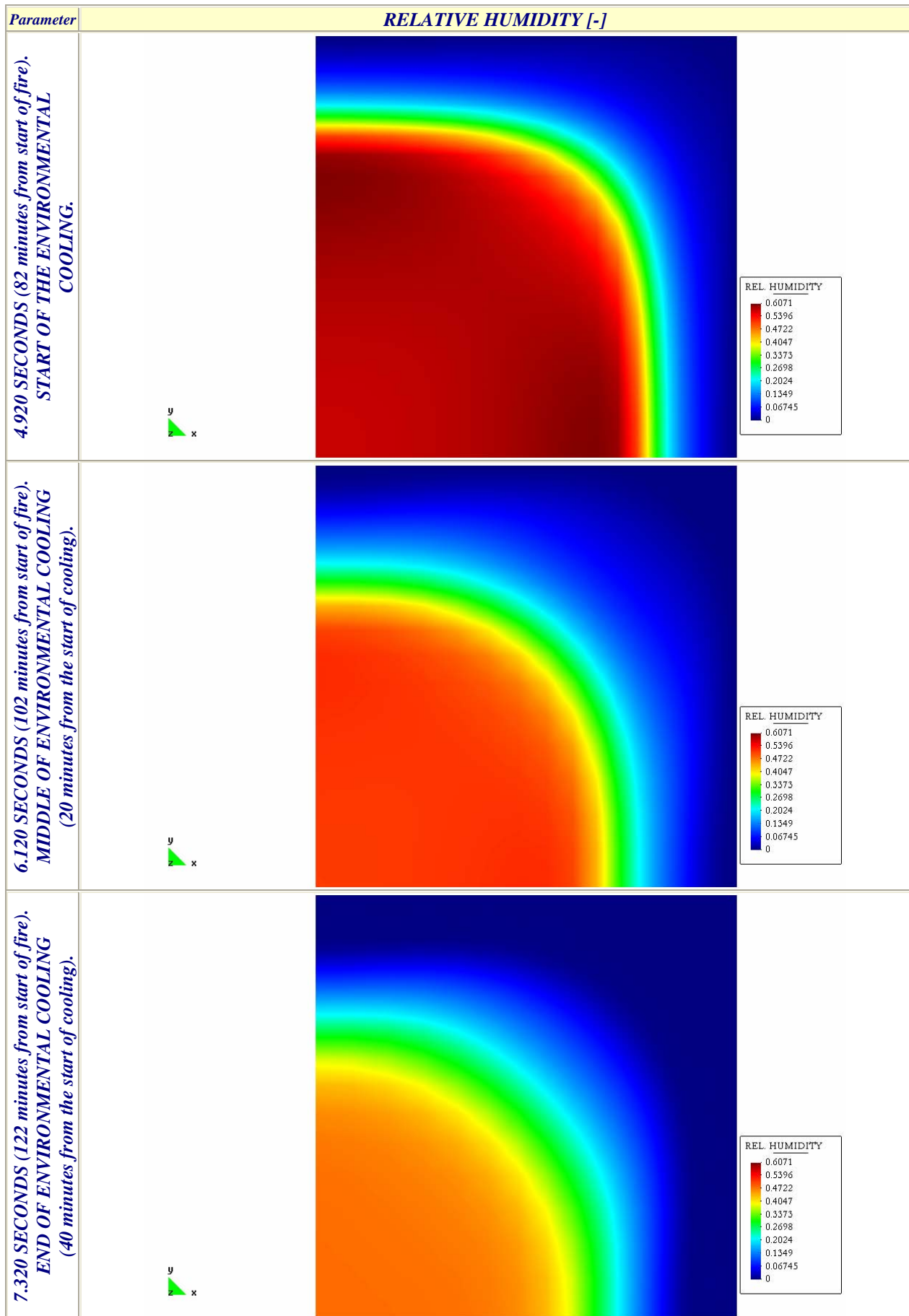


Figure 7-22. Evolution of Relative Humidity during the Slow Environmental Cooling stage.

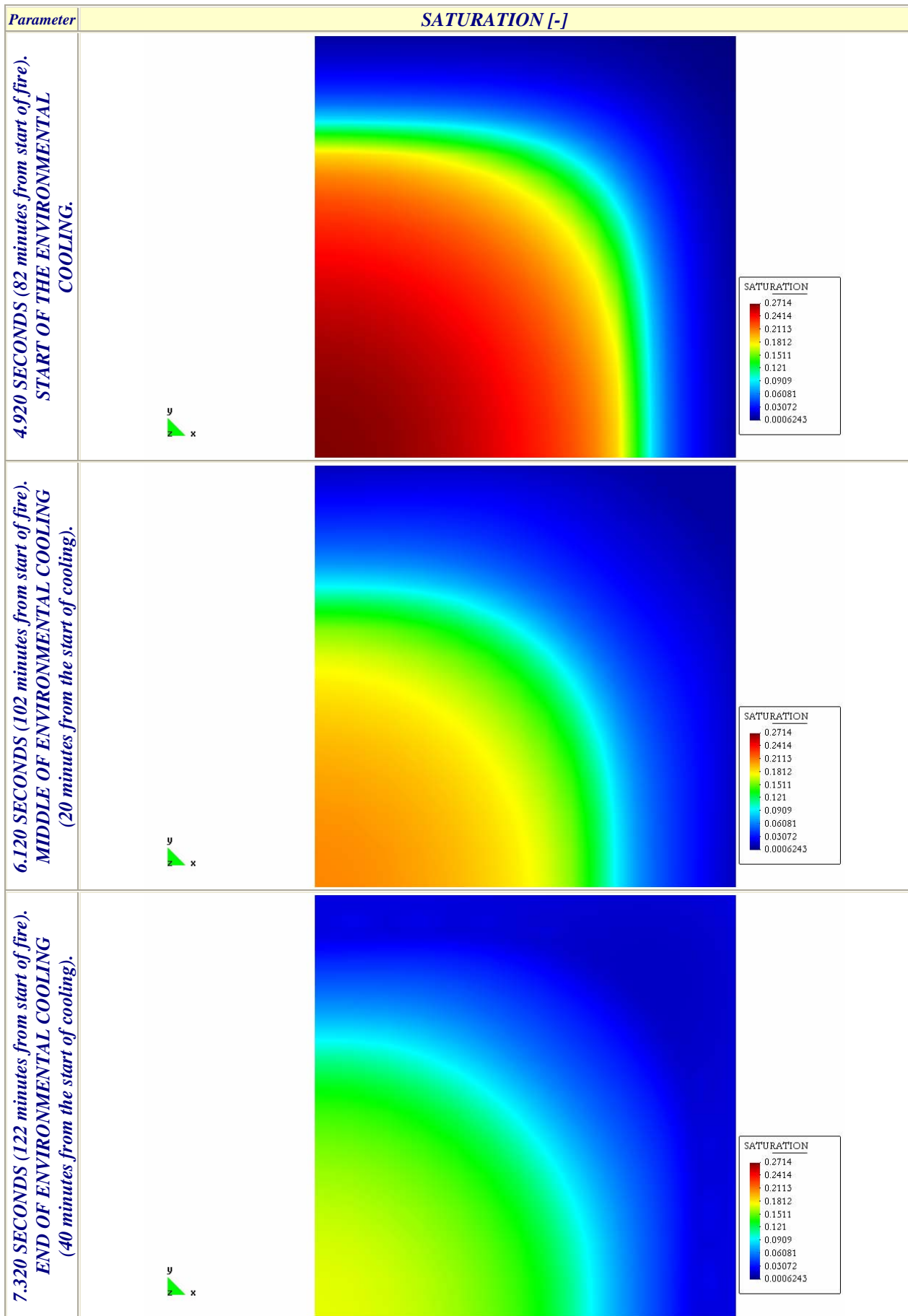


Figure 7-23. Evolution of Saturation during the Slow Environmental Cooling stage.

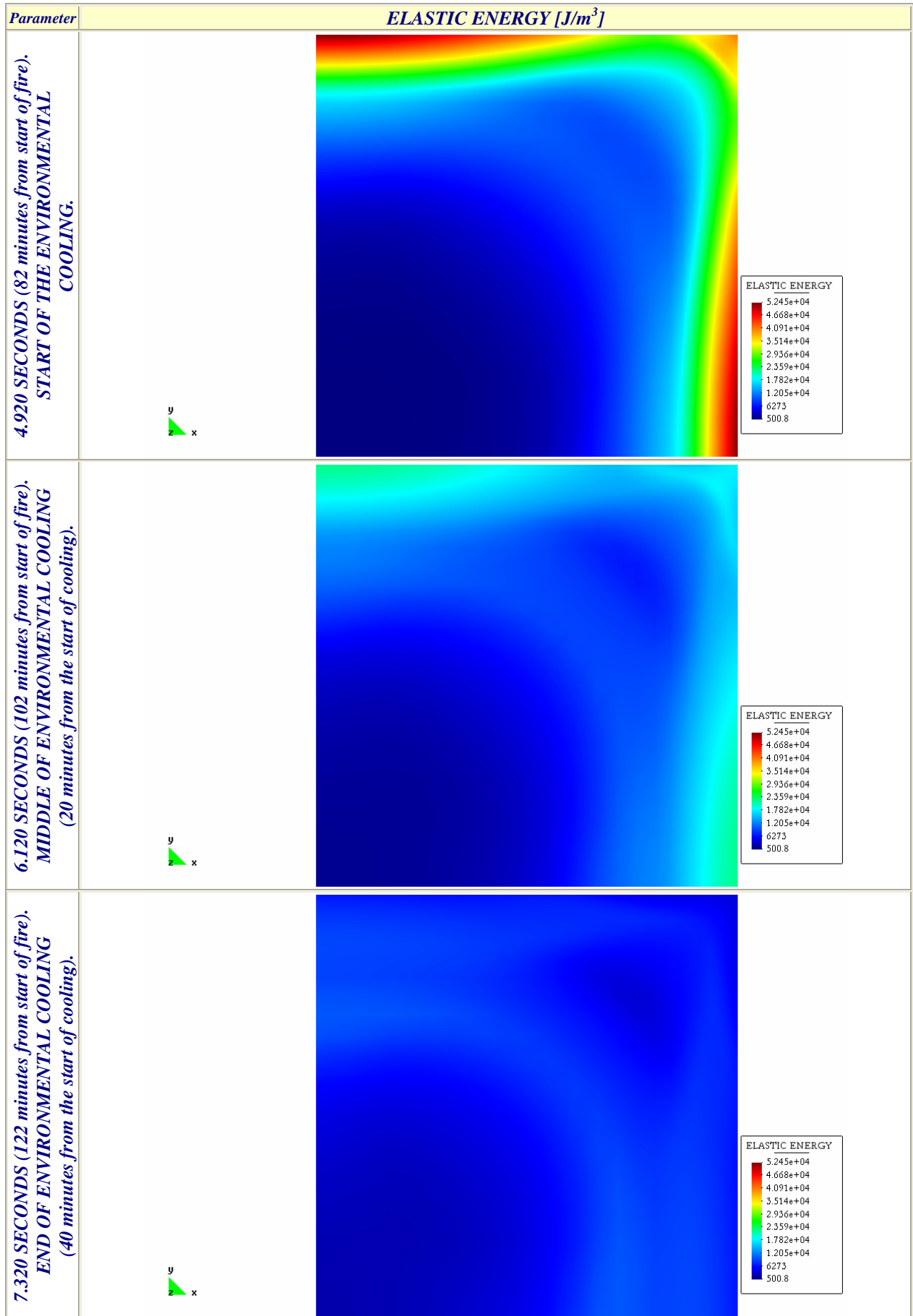


Figure 7-24. Evolution of Elastic Energy during the Slow Environmental Cooling stage.

7.4.2.2 FAST ENVIRONMENTAL COOLING

Analogously to what occurred in the slow environmental cooling case, as the fast environmental cooling process starts (beyond 4.920 seconds), the temperature gradients in the square column become progressively lower since the surface temperature decreases while the inner temperatures increase (figure 7-31 a). Besides this, it is observed that the value corresponding to the peak of vapour pressure is progressively reduced during the environment cooling; this sharp decrease of the vapour pressure values – see figures 7-33 b) and c) – (together with a decrease in the elastic strain energy – see figures 7-41 b) and c) –) may lead to a progressive decrease of the Thermal Spalling risk despite mechanical damage values increase during cooling until the end of the environmental slow cooling process. These decreasing trends occur especially during the constant ambient temperature stage due to the shortness of the fast environmental cooling process (only 20 seconds). As the cooling process continues, there appear new zones with high values of mechanical damage – i.e. cracking – (see figure 7-25 where it is shown the evolution of the extension of the zones where the Total damage D value is above 0,75). Indeed, during the whole environmental cooling and constant ambient temperature processes, and more precisely during the decreasing temperature stage, the cooled surfaces (and neighbouring zones) increase considerably their Total Damage values: the Total Damage increases at the surface control points detailed on figure 7-26 are, from the symmetry axis and right to the corner, a 20%, 17%, 10%, 12% and 10% respectively, so the increase of cracking during the cooling process is observed especially at those parts of the surfaces far from the corner (although the cracking levels of these zones are still lower than at the corner).

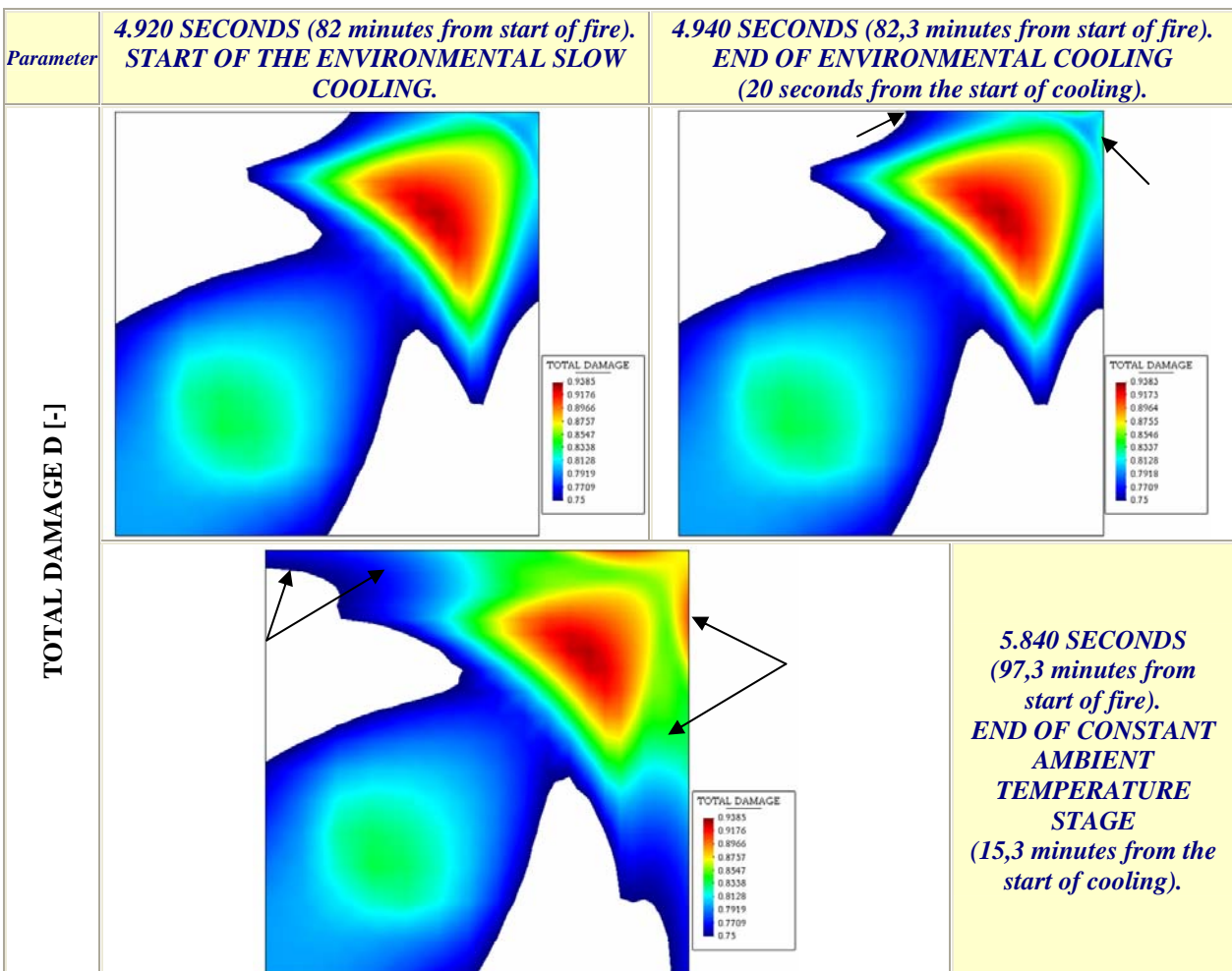


Figure 7-25. Zones of the square column with Total Damage higher than 0,75 at the start and end of environmental fast cooling, and at the end of the constant ambient temperature stage.

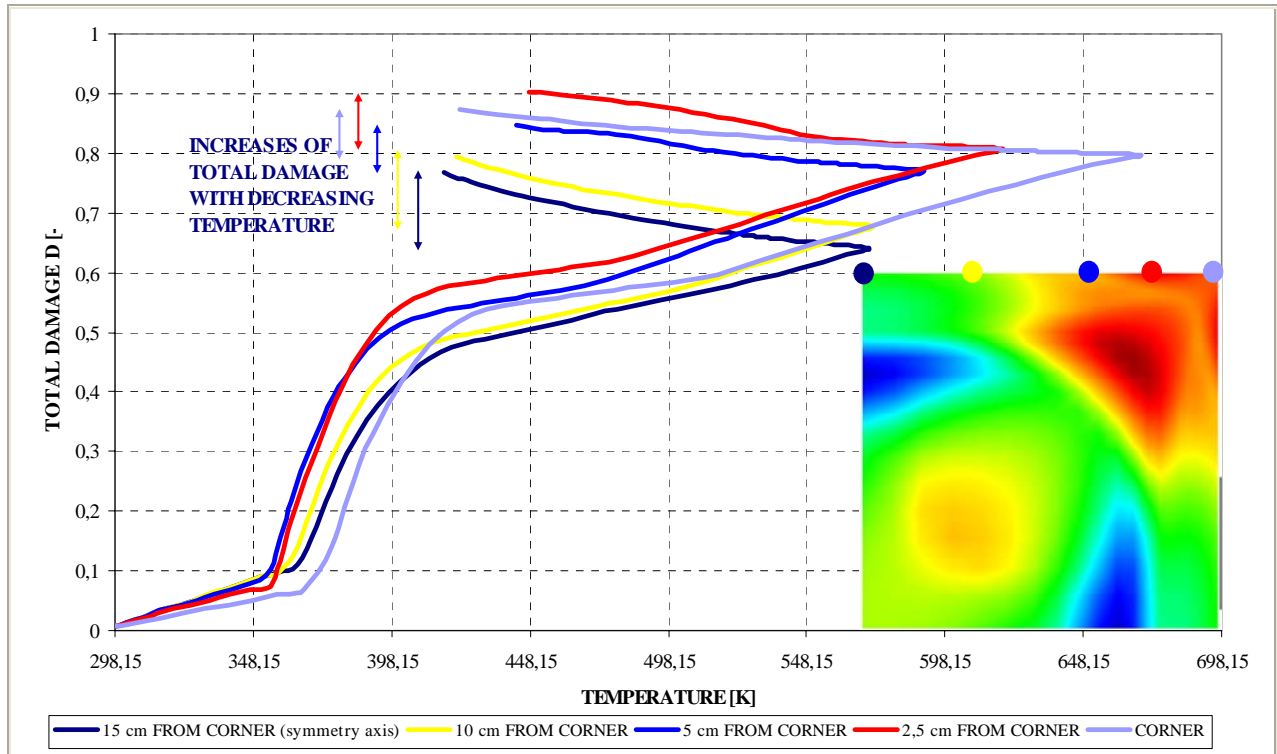


Figure 7-26 Evolution of the Total Damage with the Temperature on the cooled surface of the square column, at several distances from the corner, at the end of the fast environmental cooling process.

It is remarkable that the inner locations that showed the maximum values of the Total Damage parameter at the end of the heating stage, do not increase significantly these values during the cooling stage (see figure 7-27):

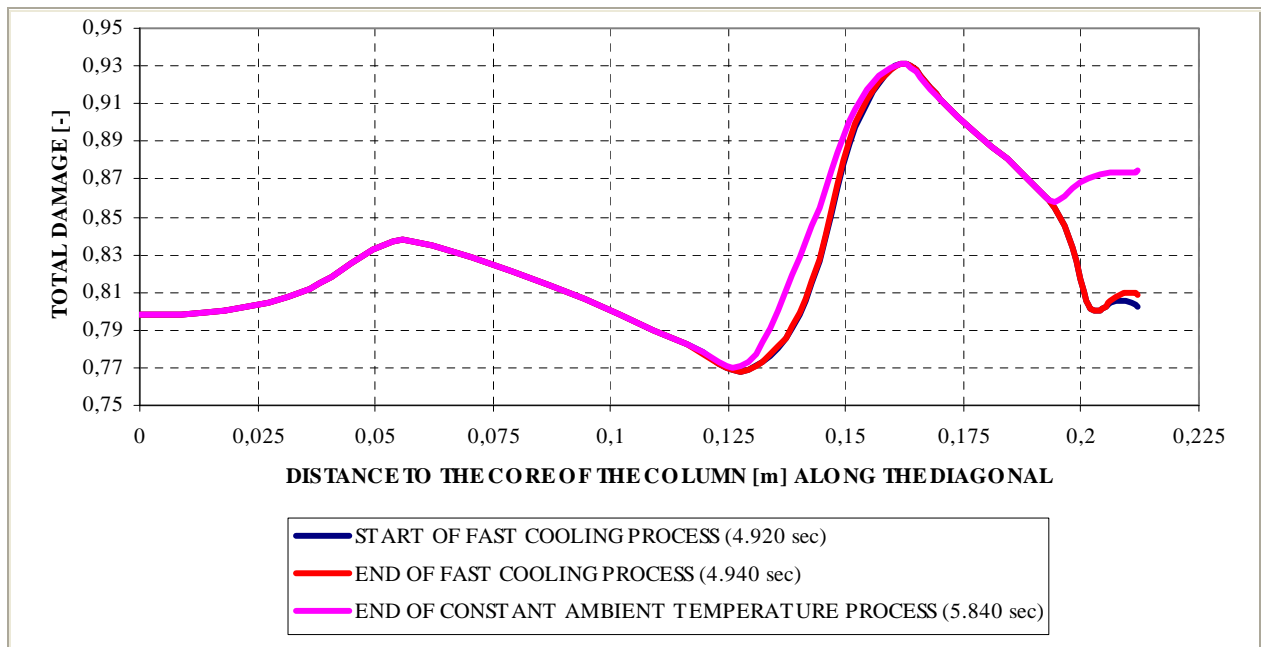


Figure 7-27. Distribution of the Total damage d values at the start and end of the cooling process, and after the constant ambient temperature process, along the diagonal line of the column.

The maximum value of the elastic strain energy (figures 7-41 b) and c)), considerably lower than at the beginning of the cooling process, does not appear any more at the surface but at 3,5 centimetres inwards. It is also remarkable that 20 seconds after the start of the cooling process only at the zones close to the surface all of the effective stresses components have varied, i.e. decreased. After 15,3 minutes after the start of the environmental cooling process (97,3 minutes

or 5.840 seconds from the start of the fire) all of the effective stresses components have decreased their values significantly at the zones next to the cooled surfaces and increased them (in the cases of the first and third effective principal stresses) at the core of the square column, as it can be observed both in figures 7-28 to 7-30 (first, second and third effective principal stresses respectively) and in figures 7-37 and 7-38, being tensile in the direction perpendicular to the main diagonal of the square column – first effective principal stress – and of compressive nature in the direction of the diagonal – third effective principal stress –. The effective stress in the longitudinal direction of the square column is mainly tensile except at the end of the cooling process, when close to the corner arise compressive values:

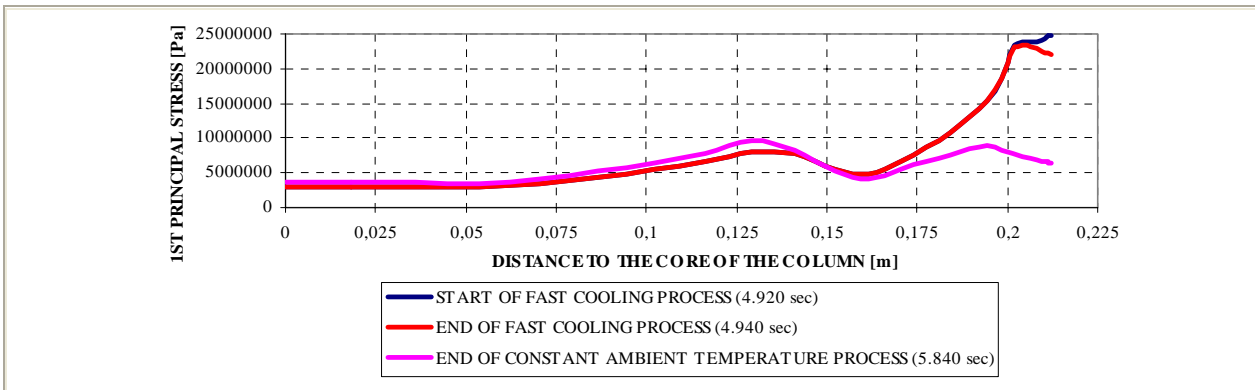


Figure 7-28. Distribution of the 1st effective principal stress at the start and end of the cooling process, and after the constant ambient temperature process, along the diagonal of the square column (remark: the 1st principal stress is oriented orthogonal to the diagonal of the column).

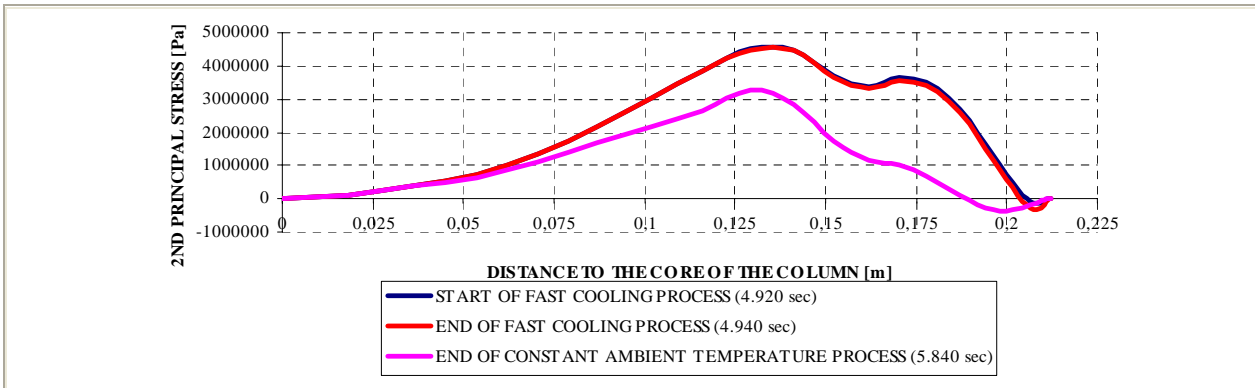


Figure 7-29. Distribution of the 2nd effective principal stress at the start and end of the cooling process, and after the constant ambient temperature process, along the diagonal of the square column (remark: the 2nd principal stress is oriented in the longitudinal direction of the column).

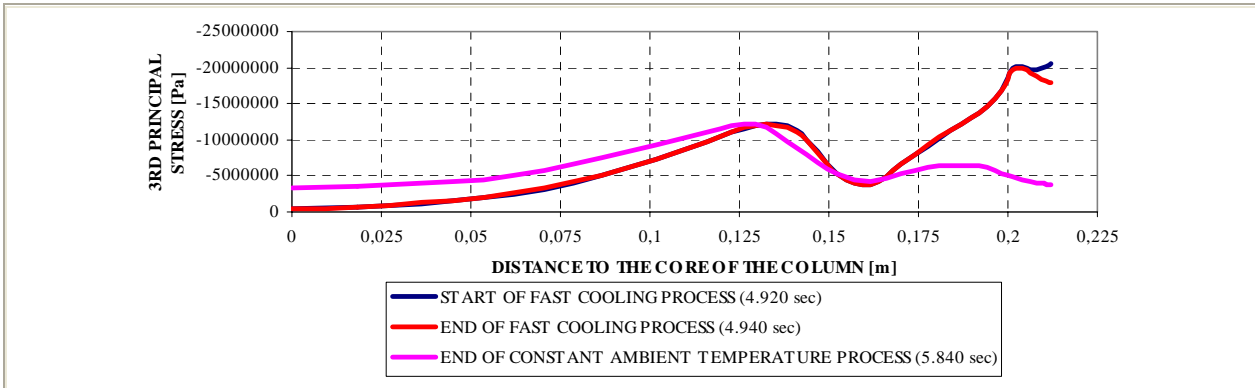


Figure 7-30. Distribution of the 3rd effective principal stress at the start and end of the cooling process, and after the constant ambient temperature process, along the diagonal of the square column (remark: the 3rd principal stress is oriented in the direction of the diagonal of the column).

Related to the evolution of the variables impeding Thermal Spalling, again the average values of traction strength, \bar{f}_t , tend to increase during cooling in the layers within the first five centimetres from the corner (due to their temperature decrease) but they tend to decrease in the most inner layers (due to their temperature increase) – see figure 7-31 a) to c) –.

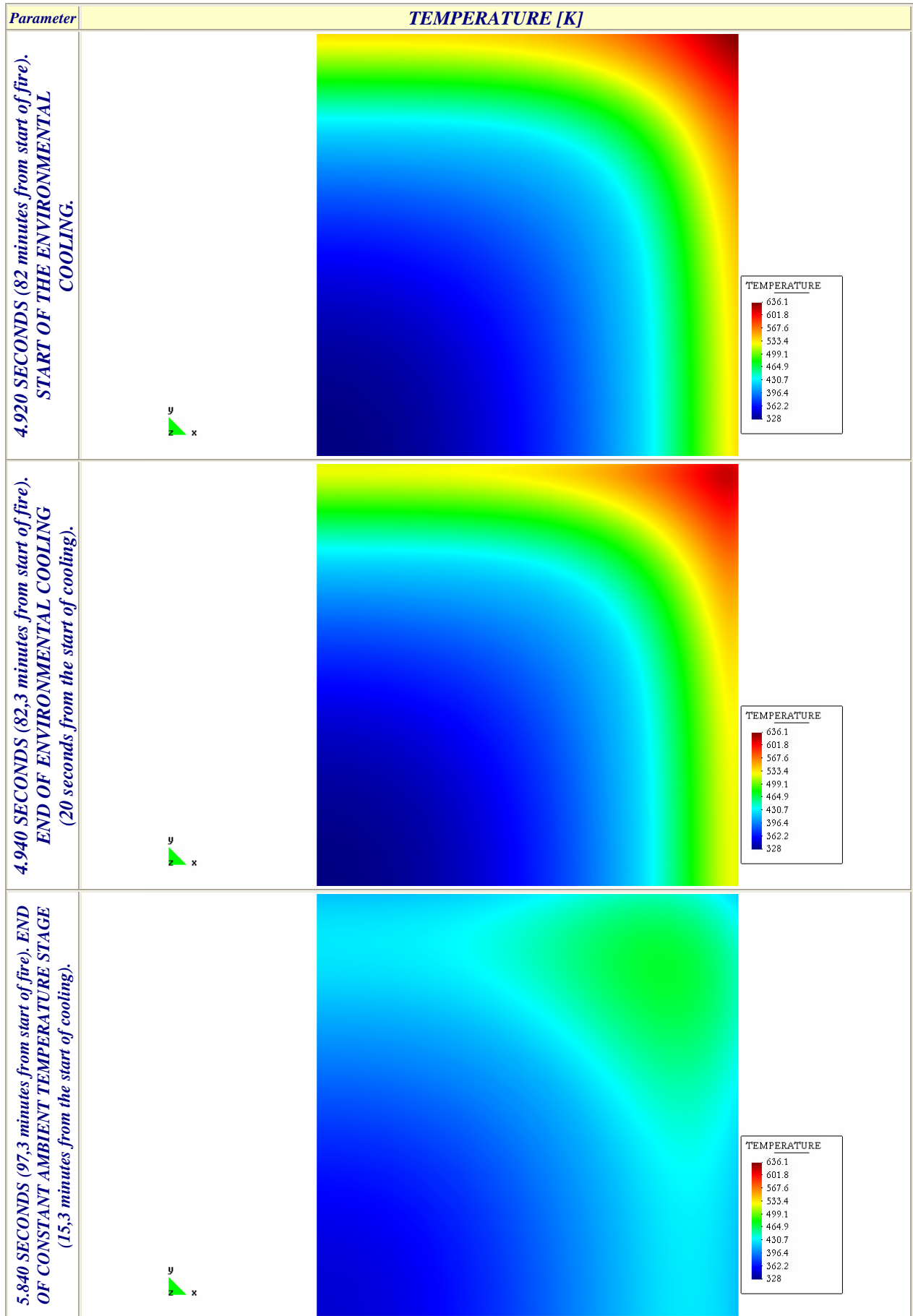


Figure 7-31. Evolution of Temperature during the Fast Environmental Cooling stage.

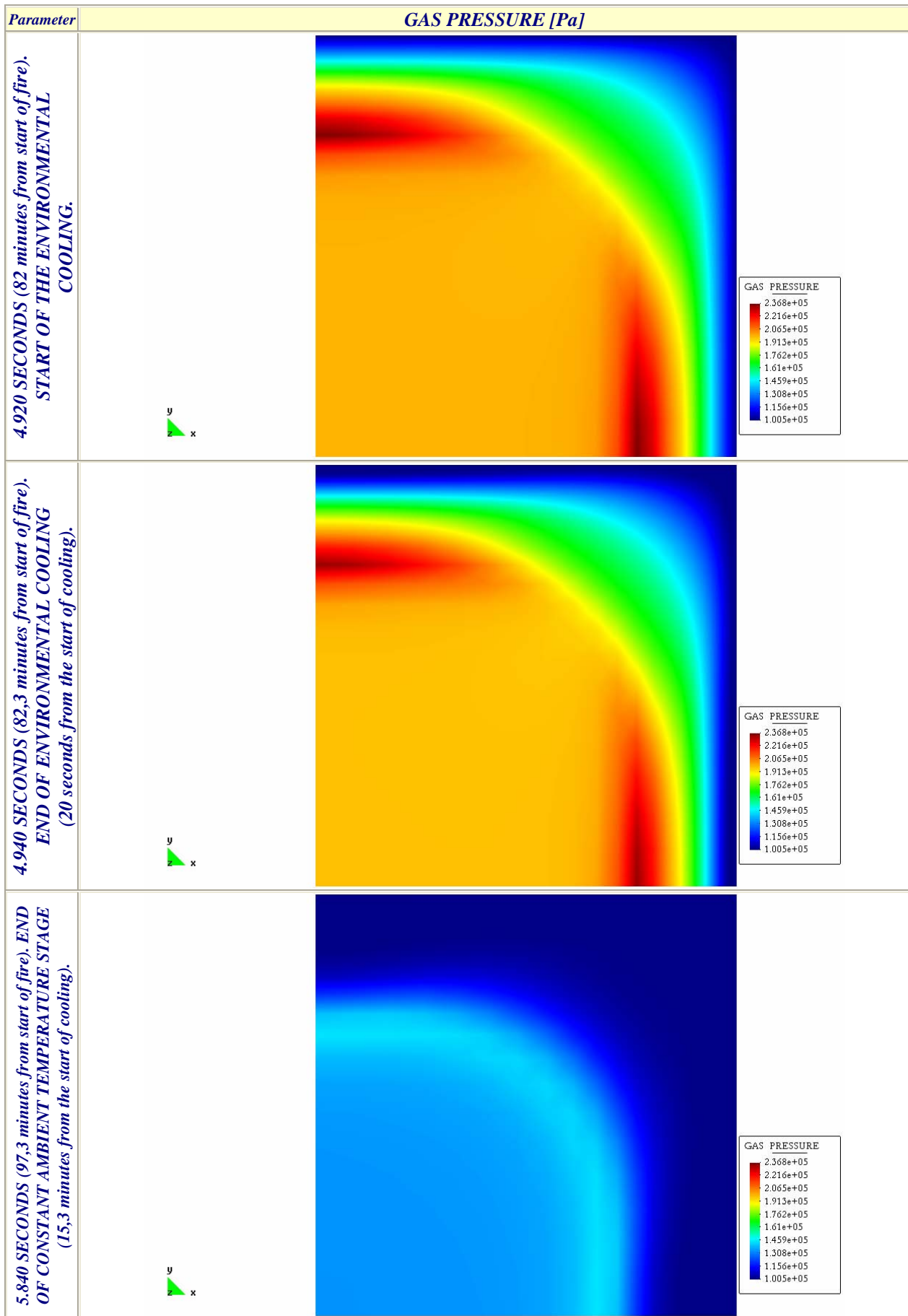


Figure 7-32. Evolution of Gas Pressure during the Fast Environmental Cooling stage.

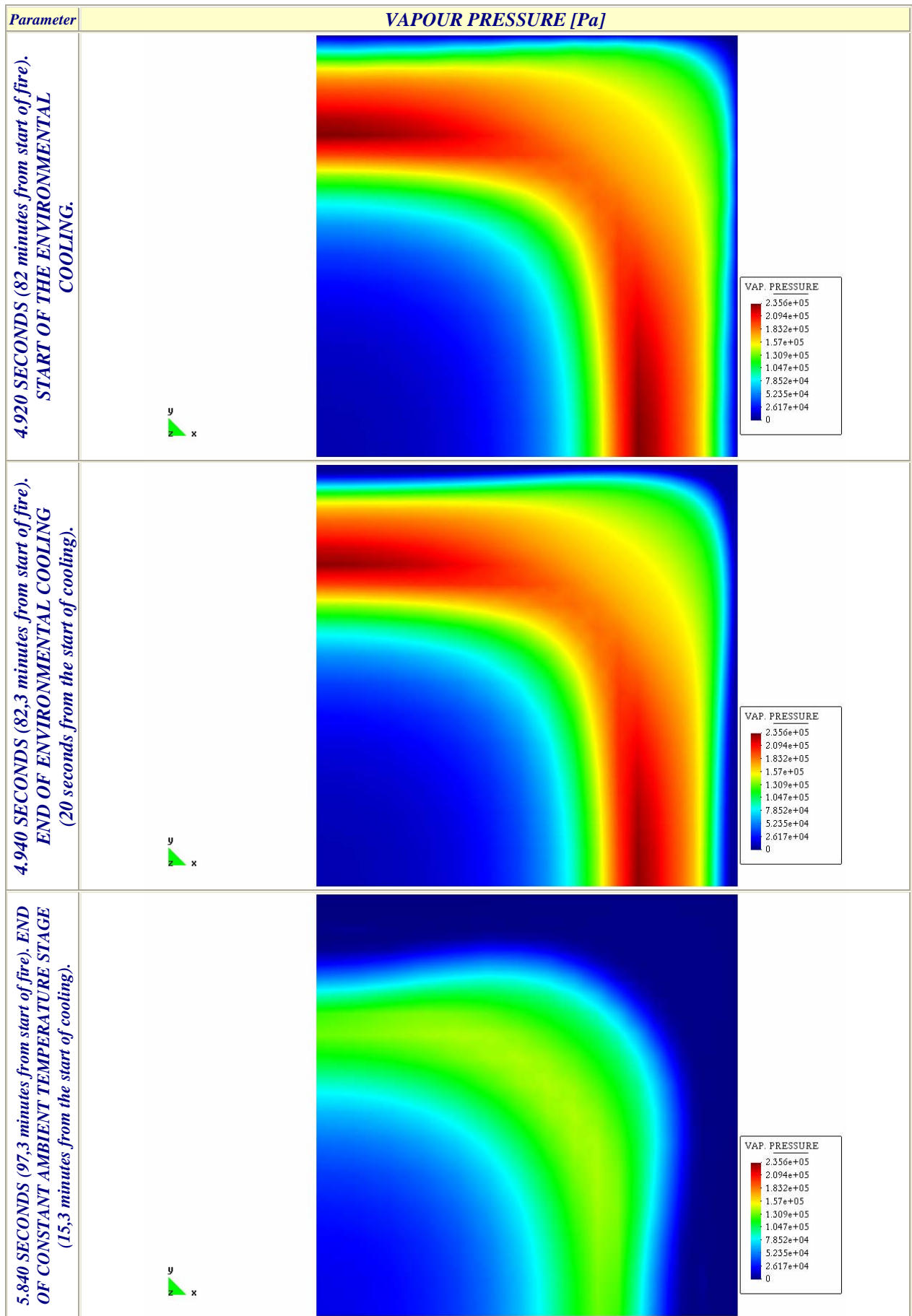


Figure 7-33. Evolution of Vapour Pressure during the Fast Environmental Cooling stage.

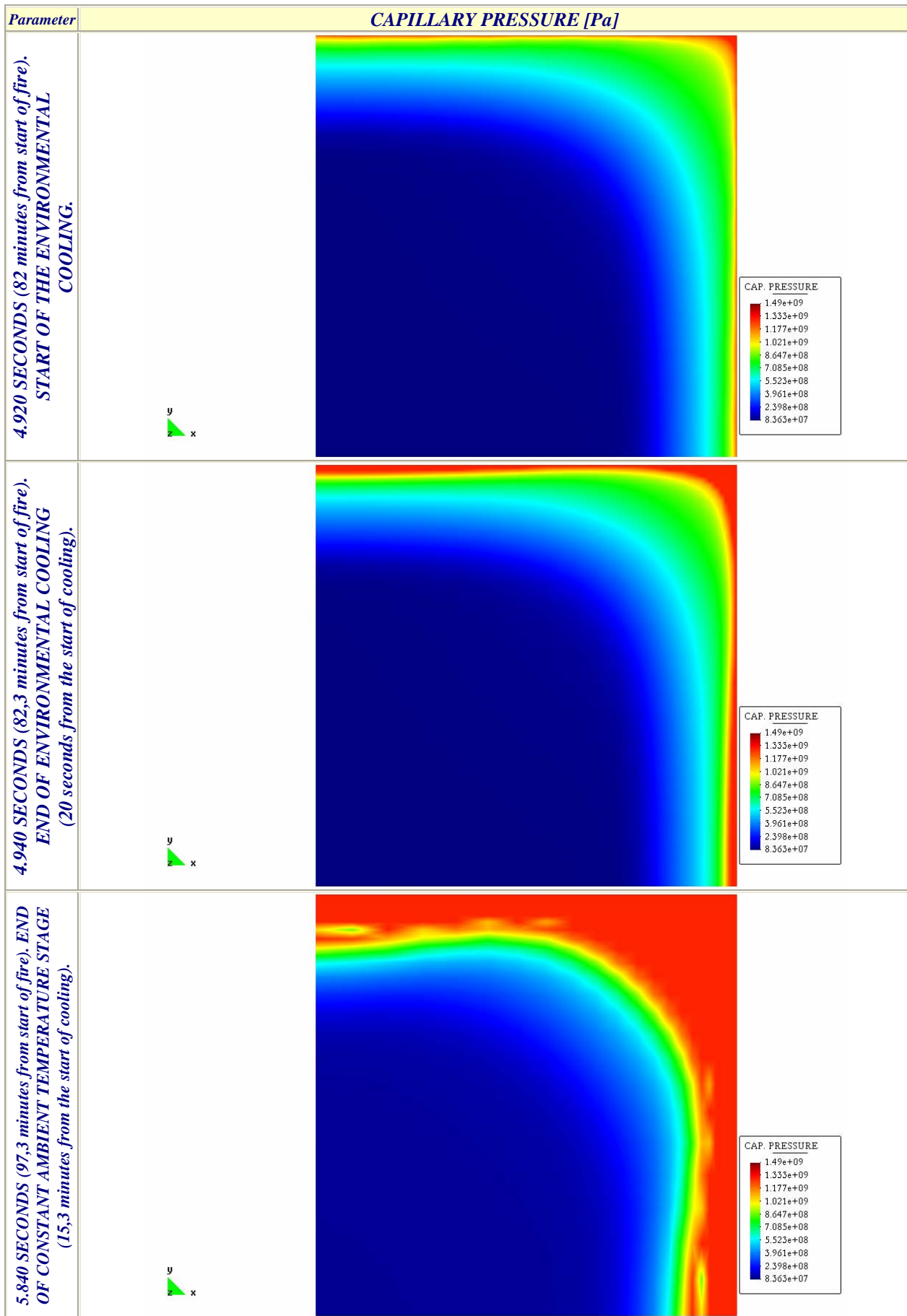


Figure 7-34. Evolution of Capillary Pressure during the Fast Environmental Cooling stage.

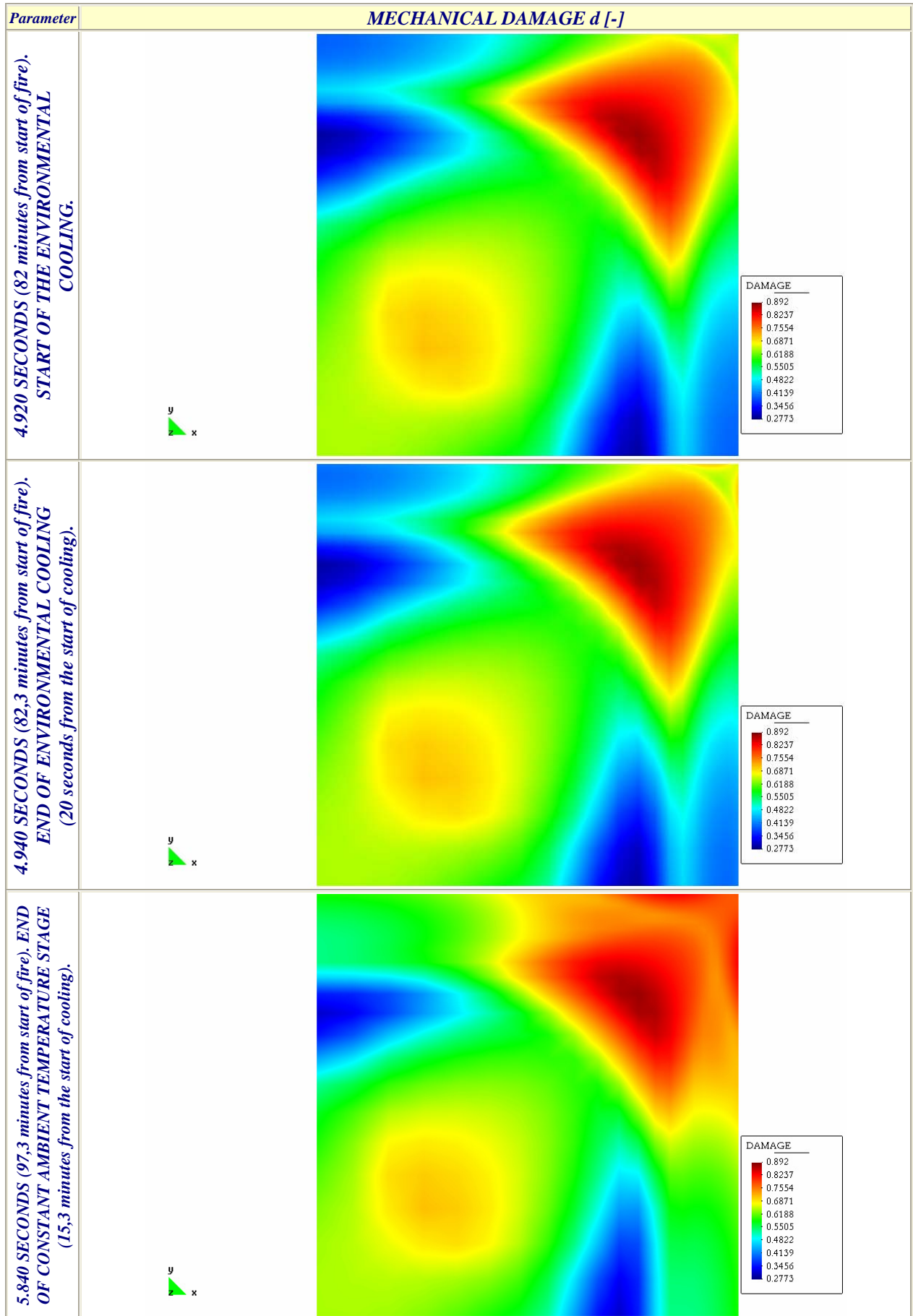


Figure 7-35. Evolution of Mechanical Damage during the Fast Environmental Cooling stage.

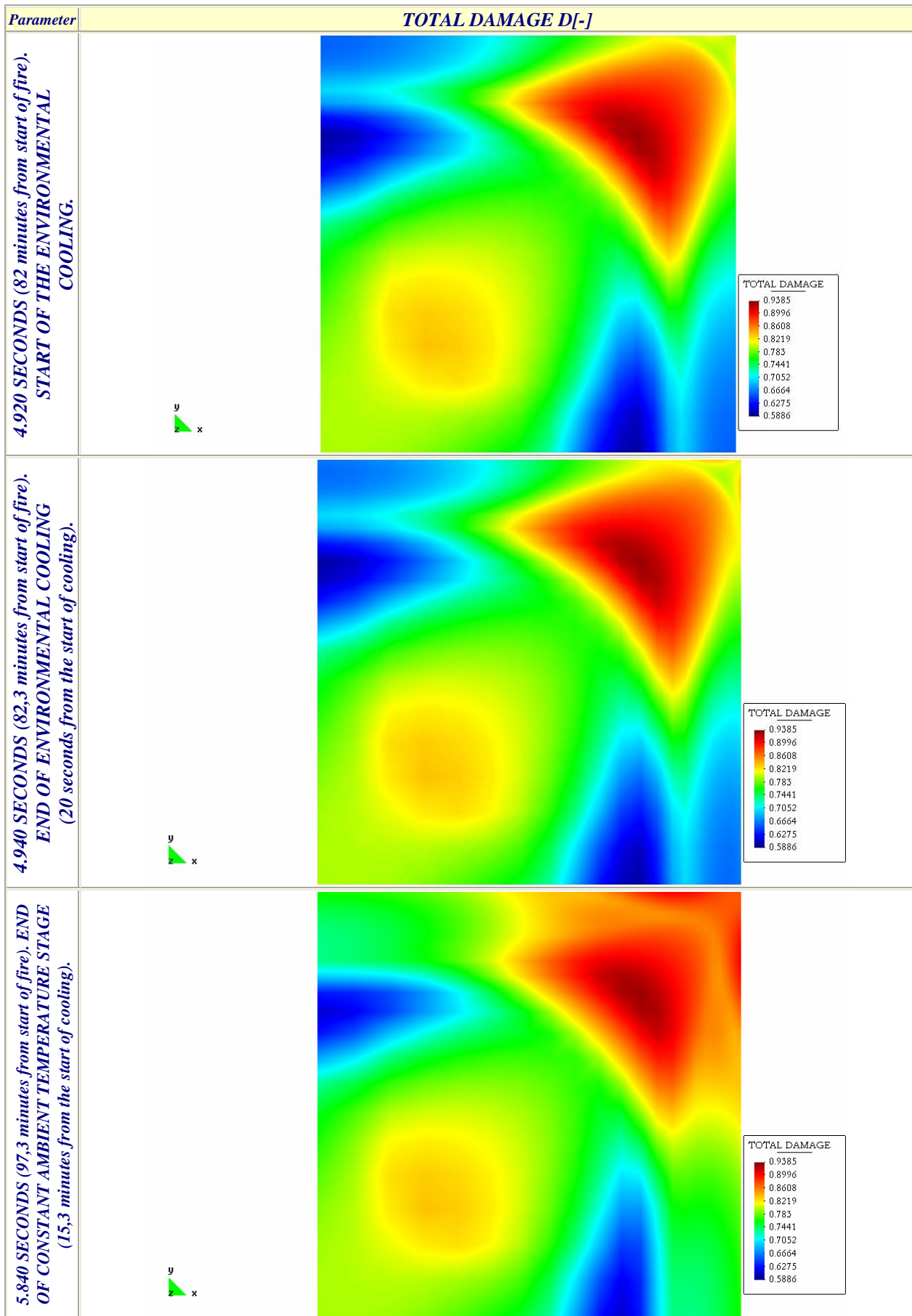


Figure 7-36. Evolution of Total Damage during the Fast Environmental Cooling stage.

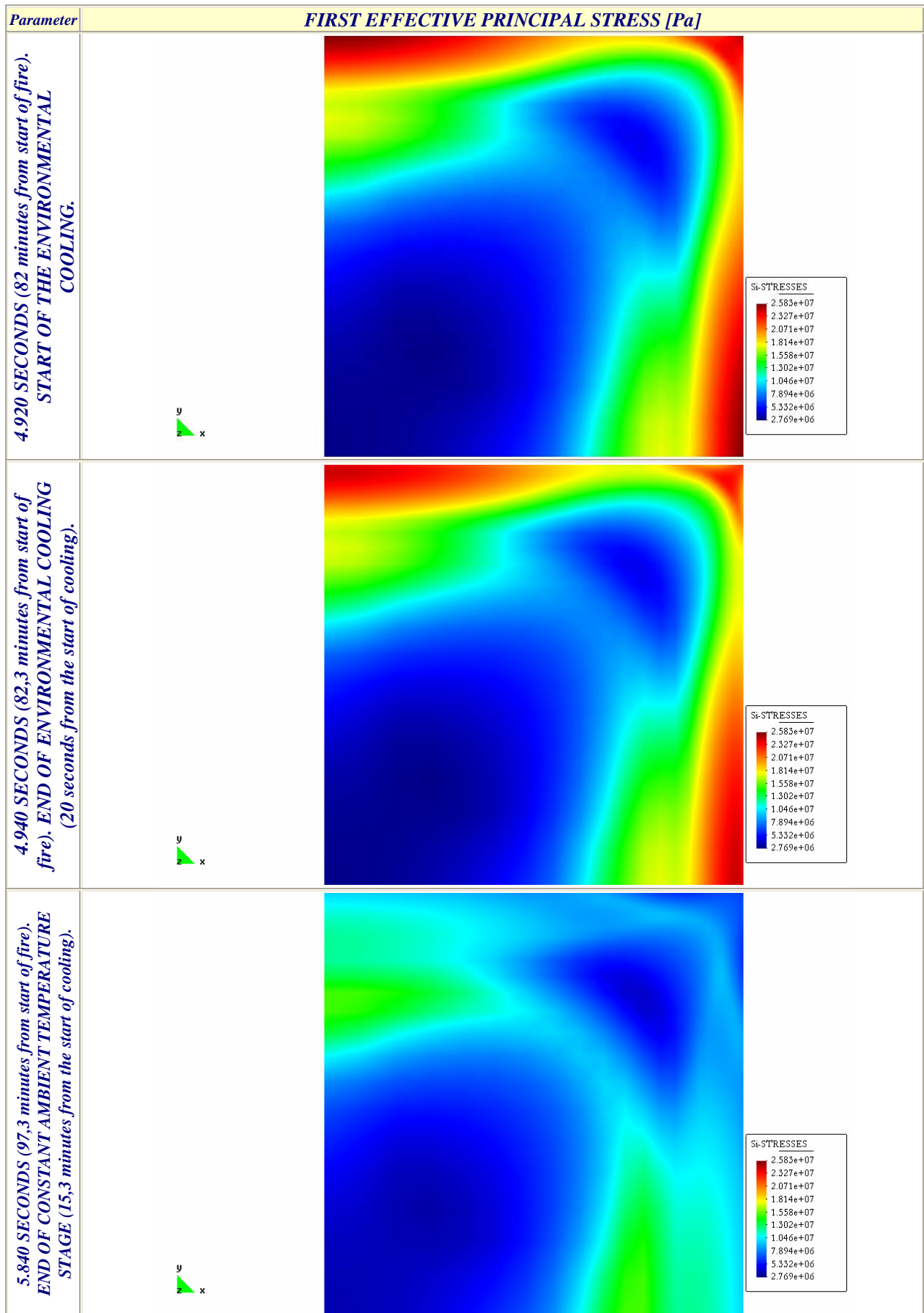


Figure 7-37. Evolution of First Effective Principal Stress during the Fast Environmental Cooling stage.

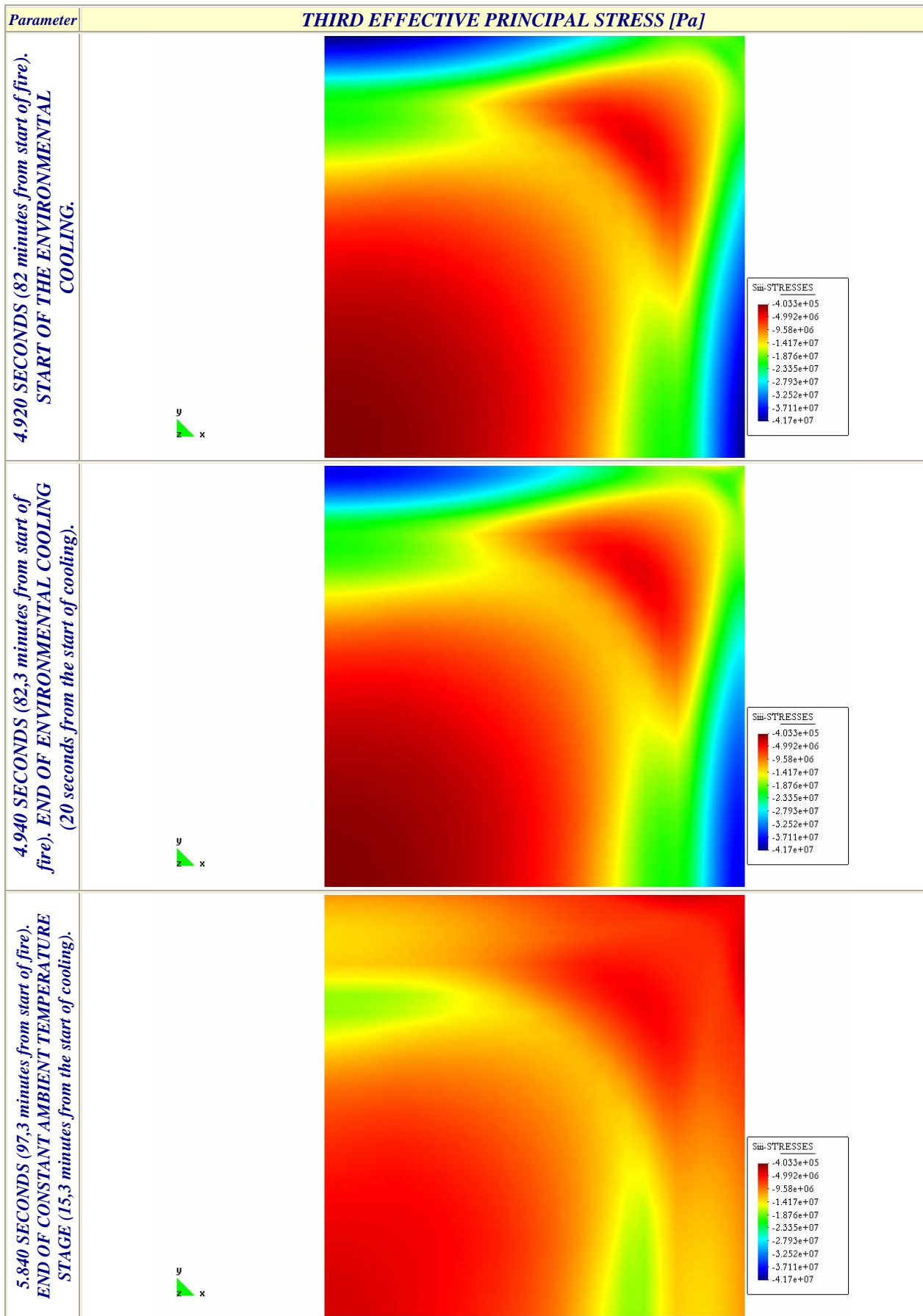


Figure 7-38. Evolution of Third Effective Principal Stress during the Fast Environmental Cooling stage.

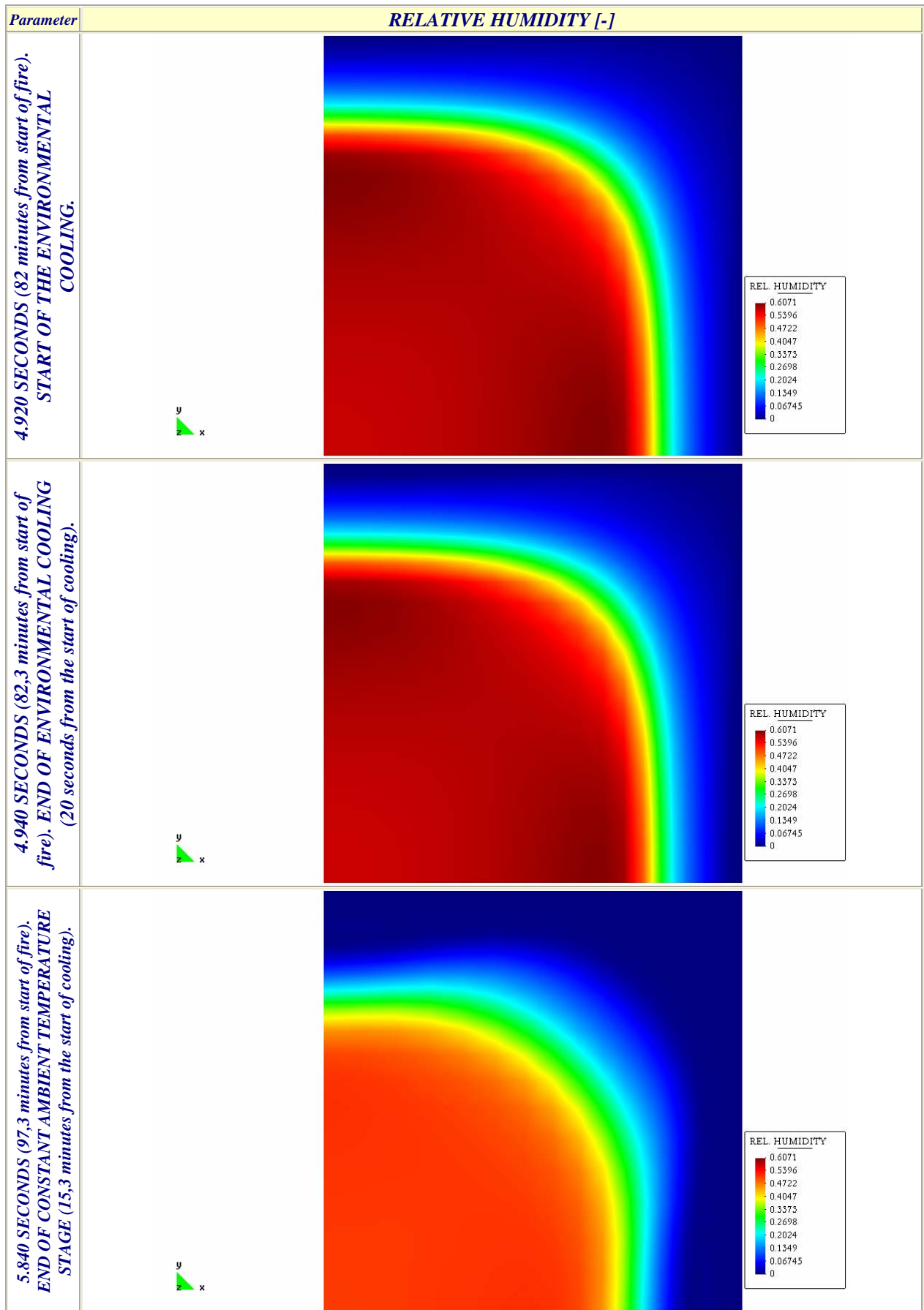


Figure 7-39. Evolution of Relative Humidity during the Fast Environmental Cooling stage.

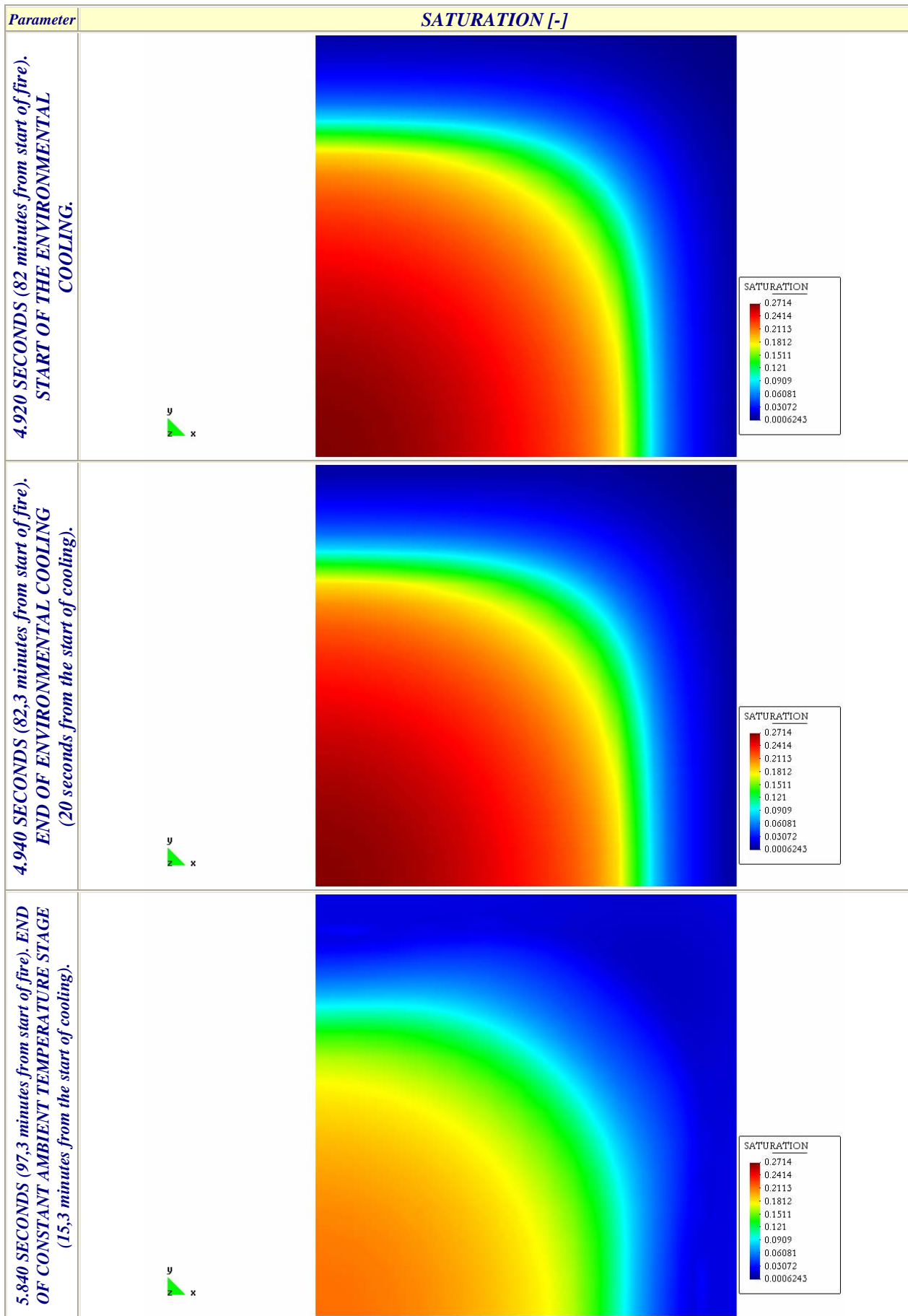


Figure 7-40. Evolution of Saturation during the Fast Environmental Cooling stage.

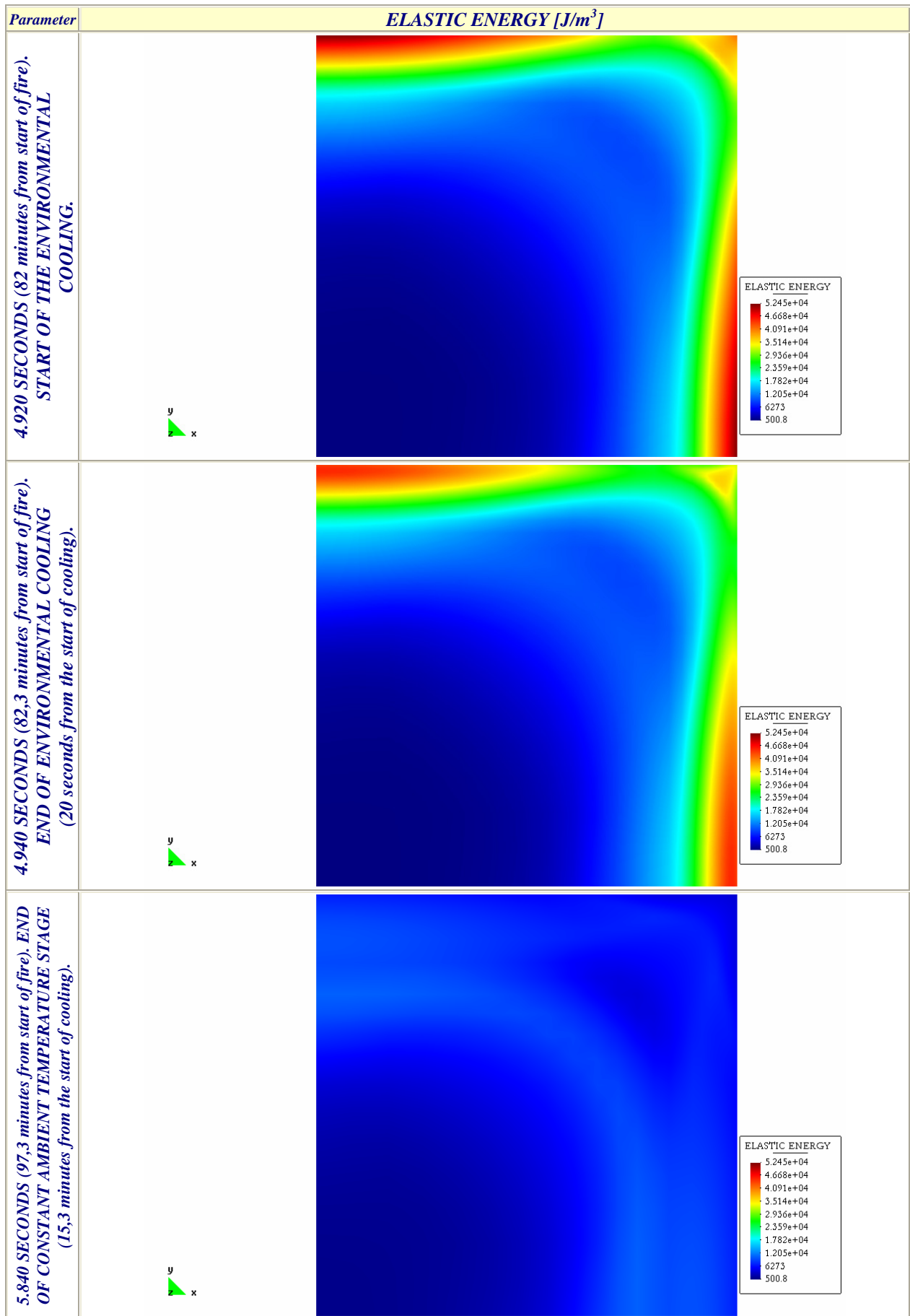


Figure 7-41. Evolution of Elastic Energy during the Fast Environmental Cooling stage.

Finally figure 7-42 shows, as a complement of figure 7-25, the Total Damage distribution at the end of the fast environmental cooling stage (at 5.840 seconds, more precisely) where the zones with Total Damage values higher than the 82,5 per cent (i.e. zones almost completely destroyed) have been removed. From this clear it can be easily observed the thermal spalling (and later, when the vapour pressure has decreased, the simple cracking due to the restrained elastic energy) of the corner of the square column, being that the most dangerous Thermal Spalling Type (observe that the concrete destroyed zones would include the position of the corner reinforcing bars).

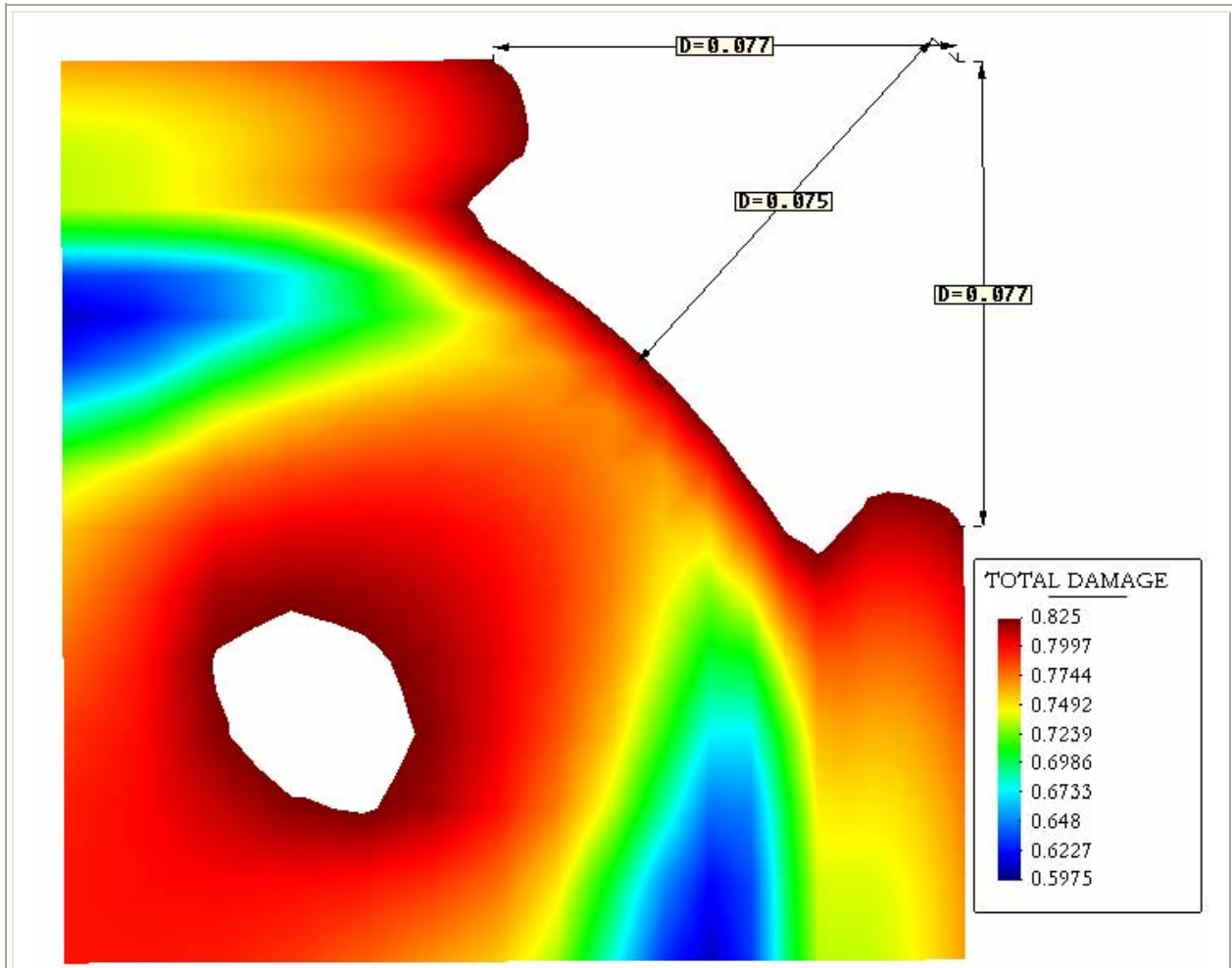


Figure 7-42. Total Damage evolution at the end of the Fast Environmental Cooling stage, having removed the zones where $D > 0,825$ (i.e. zones almost completely destroyed), being representative for the Corner Thermal Spalling first (probably at 3.840 seconds from the beginning of the heating process since at this instant appear the maximum values of vapour pressure), and later by the additional cracking due to restrained elastic energy during the cooling process (see figure 7-25 to observe this increase).

7.5 RESUME OF THE CONCLUSIONS OF THE CHAPTER

7.5.1 About the Heuristic Analysis of Cooling Processes in HSC Square Columns

An introductory heuristic analysis of the effect of cooling processes on the hygro-thermo-chemo-mechanical state of a square column, manufactured with High-Strength concrete, during the development of a natural fire in a High-Rise Building has been developed and presented, by means of the advanced Hitecosp Software [5], as an introductory extension of the analyses already presented in *Chapter 6: Analysis of cooling processes in High Strength Concretes* to cases with bidimensional fluxes – of both heat and mass – such as square columns.

A set of state variables and other related parameters mainly concerning the level of damage in the square column have been selected and evaluated to accomplish the stated heuristic analysis. This set of variables and parameters has already been defined and explained in depth in paragraph 6.2.2 of *Chapter 6*. Hence, comparing the evolution of the values of the variables favouring Thermal Spalling – such as high local values of gas overpressure, $p^g - p_{atm}$, and mechanical damage parameter, d , high values of averaged transversal traction stresses, $\bar{\sigma}_{th}$, and constrained elastic energy \bar{U} – against those corresponding to the factors impeding Thermal Spalling – such as high average values of traction strength, \bar{f}_t , and specific fracture energy, $\bar{G}f$, for the material layer between a current position and the heated surface – it has been observed that the risk of Thermal Spalling is, taking into account the heuristic validity of this conclusion, lower as the environment cools either under slow or fast cooling rates (0,2 and 20 °C/second respectively). This trend is mainly due to sharp decreases of the vapour pressure values, the elastic strain energy and the stress components.

However, during the environmental cooling processes simulated both the Mechanical Damage, i.e. cracking, and the Total Damage parameters values have shown increasing values (over a 20 per cent increase) at positions where temperature was actually decreasing, especially at the zones close to the heated and later cooled surfaces and, more precisely, far from the corner (although the cracking levels of these zones are still lower than at the corner).

7.5.2 About extended tasks to go more deeply into Thermal Spalling Research in Square Columns

1. The degree of saturation with liquid water S (considering together hygroscopic and capillary water, if the latter is contained in the pores) is an experimentally determined function of capillary pressure (matrix potential) p^c , and temperature T (since hysteresis phenomena are not considered here, it is assumed to be a unique function of capillary pressure). Usually presented graphically in the form of the sorption isotherms, this function is needed for realistic modelling of hygro-thermic behaviour of concrete and it must be determined during sorption tests at several temperatures. Within all of the calculations included in this Chapter the sorption isotherms corresponding to the heating stages have also been considered during the cooling ones, being therefore still a need to work out sorption isotherms specific for cooling stages.
2. Since the concrete cover of the steel reinforcing bars is reduced due to the spalled-off pieces, there is a need of studying what will happen after the first superficial pieces have spalled-off, being possible – but not corroborated – that Thermal Spalling phenomena accelerates as successive layers are progressively spalled-off until the reinforcement bars are reached and exposed directly to fire.
3. On the other hand, there is still a need for a mathematical model allowing analysing the hygro-thermal, chemical and deterioration processes in concrete structures at high temperature more precisely, and which will allow us to predict the thermal spalling phenomenon using purely ‘mechanical’ criteria, and not ‘heuristic’ ones, as the presented here. This should possibly take into account a stochastic nature of the phenomenon and its both local and global character. In some authors’ opinion [7], the latter could be considered, for example, by using a multi-scale type model, involving a micro-level for predicting physical properties of the concrete components (i.e. cement paste, Inter-phase Transition Zone and aggregate), a meso-level for analysis of their interactions (e.g. by means of fracture mechanics), and finally, a macro-scale for evaluation of the whole structure performance at given ambient conditions. The model used in this chapter, after appropriate modifications, could be used for the macro-scale analysis.

4. Finally, the development of Spalling Indexes correlated against experimental data suitable for cases with bidimensional fluxes of heat and mass are necessary to excerpt mechanistic and not heuristic conclusions for square columns.

7.6 BIBLIOGRAPHY OF THE CHAPTER

Bibliography of the chapter

- [1] V.R. Kodur, M.A. Sultan, *Structural behaviour of high strength concrete columns exposed to fire*, Proceedings: International Symposium on High Performance and Reactive Powder Concrete, Vol. 4, 217-232, Sherbrooke, Quebec, 1998.
- [2] V.K.R. Kodur, R. McGrath, *Performance of High Strength Concrete Columns Under Severe Fire Conditions*, Proceedings Third International Conference on Concrete Under Severe Conditions, Vancouver, BC, Canada, pp. 254-268, 2001.
- [3] V.K.R. Kodur, R. McGrath, P. Leroux, J.C. Latour, *Experimental Studies for evaluating the Fire Endurance of High Strength Concrete Columns*, Research Report No. 197 of the Fire Research Program, Institute for Research in Construction - National Research Council Canada, May 2005.
- [4] UNE-EN 1991-1-2, *Eurocódigo 1: Acciones en estructuras. Parte 1-2: Acciones generales. Acciones en estructuras expuestas al fuego*, Mayo 2004.
- [5] Brite Euram III BRPR-CT95-0065 HITECO, *Understanding and industrial application of High Performance Concrete in High Temperature Environment – Final report*, 1999.
- [6] D. Gawin, F. Pesavento, B.A. Schrefler, *Modelling of hygro-thermal behaviour of concrete at high temperature with thermo-chemical and mechanical material degradation*, Comput. Methods Appl. Mech. Engrg . 192 (2003) 1731-1771.
- [7] D. Gawin, F. Pesavento, B.A. Schrefler, *Towards prediction of the thermal spalling risk through a multi-phase porous media model of concrete*, Comput. Methods Appl. Mech. Engrg . 195 (2006) 5707-5729.

Bibliography of the annexes

- [A.1] Brite Euram III BRPR-CT95-0065 HITECO, *Understanding and industrial application of High Performance Concrete in High Temperature Environment – Theoretical Manual*, April 2006.
- [A.2] Brite Euram III BRPR-CT95-0065 HITECO, *Understanding and industrial application of High Performance Concrete in High Temperature Environment – User Guide*, May 2006.

Appendix 7A. INPUT FILES FOR THE HYGRO-THERMO-CHEMO-MECHANICAL CALCULATIONS OF A SQUARE COLUMN

(See next pages)

Appendix 7A

Appendix 7A.1 INPUT FILES FOR THE HYGRO-THERMO-CHEMO-MECHANICAL CALCULATIONS OF A SQUARE COLUMN

In this Appendix are shown the Input files developed for the calculations of the square column done by means of the software Hitecosp [A.1]. These Input files are composed by four sections [A.2]:

- Block 1: Contains the name of used files and the title of the problem,
- Block 2: Contains the general data of the problem,
- Block 3: Contains the data for the mesh generation and the numbering of the nodes,
- Block 4: Contains the data for the initial and the boundary conditions.

In order to understand the Input files included herein, a general description of the contents of each block – excerpted from the User Guide [A.2] – is attached next:

FIRST BLOCK. NAME OF THE USED FILES AND TITLE OF THE PROBLEM.

The first block is that of the general data or control data of the execution. Its structure is described in the following:

- Title (c72)*
- Restart_code (i), Problem_type (i)*
- File_name_BIN_preceding (c20) [only if Restart_code = 2]*
- File_name_BIN_succeeding (c20)*
- File_name_PRN (c20)*
- Time_step (r), Steps_number (i), Print_steps_number (i)*
- Convergence_criterion (r), Max_number_iterations (i)*
- Grav_acc (r), Grav_angle (r)*
- Code_pre (i), x_scale_factor (r), y_scale_factor (r)*
- Nodes_number (i), Elements_number (i), Element_nodes_num (i), Gauss_points_num(i)*
- Conditioned_nodes_num (i)*

The meaning of the above shown data is summarised in *table 7A-1*:

DATA	MEANING	VALUE
Title	Title of the job in execution	
Restart_code	Code which indicates if it is a first execution or a restart	= -1 if first execution with constant initial conditions; = 1 if first execution with initial conditions varying for each node; = 2 if restart
Problem type	Problem type Indicates the type of the problem	= 0 if 2D Plain; = 1 if 2D Axial-symmetric
File_name_BIN_preceding	Name of the binary file produced in the previous execution	It has to be indicated only if it is a restart
File_name_BIN_succeeding	Name of the binary file to be produced at the end of the execution	---
File_name_PRN	Name of the output file	---
Time step	Advised time step	---
Steps_number	Number of time steps	---
Print_steps_number	Number of time steps after which the results are saved	---
Convergence_criterion	Value of the convergence criterion	Of the order of magnitude of 1.E-5

Max_number_iterations	Maximum number of iterations inside a time step	E.g. 30
Grav_acc	Value of the gravity acceleration	---
Grav_angle	Angle between the gravity and the mesh	---
Code_pre	Code for the mesh generation	= 0 if Castem2000 or GID are used; = 1 if with auto-generation
x_scale_factor	Scale factor of the mesh for the x axis	---
y_scale_factor	Scale factor of the mesh for the y axis	---
Nodes_number	Number of nodes of the mesh	---
Elements_number	Number of elements of the mesh	---
Element_nodes_num	Number of nodes for an element	= 8 if quad with 8 nodes
Gauss_points_num	Number of integration points	= 3 if 3x3
Conditioned_node_num	Number of nodes on which one or more boundary conditions are imposed	---

Table 7A-1. Meaning of the parameters of Block 1.

Important: At the beginning of a transitory (first run), with the absolute time equal to zero, it is necessary to proceed with an execution of 10 time steps equal to 1.-06 seconds. In fact at the initial instant the system is not in a state of equilibrium because the initial conditions for the thermo hygral D.O.F. (e.g. gas pressure, capillary pressure and temperature), do not correspond to the initial conditions for the mechanical D.O.F. (e.g. X and Y displacements).

BLOCK 2: GENERAL DATA FOR THE MESH GENERATION

The second block includes the data which describe the mesh.

When the input file has been produced with the codes Castem2000 or GID (Code_pre =0) it is necessary to give:

Node_num (i) , X_coor (r) , Y_coor (r) for every node

Element_num (i) , (num_node_k (i) , per k=1,Element_nodes_num), Material_id for every element

When the auto-generation of a simple mesh (rectangular and subdivided in rows and columns) is desired (Code_pre = 1):

Num_rows (i) , Num_columns (i) , Nodes_numeration_code (i)
(Column_k_coor_x (r) , k=1,Num_columns + 1)
(Row_k_coor_y (r) , k=1,Num_rows + 1)
Num_mat
Element_from, Element_to, Element_step, Material_id for Num_mat rows

The meaning of the mentioned data is summarised in table 7A-2:

DATA	MEANING	VALUE
Node_num	Identifier number of the node	---
X_coor	X co-ordinate of the node	---
Y_coor	Y co-ordinate of the node	---
Element_num	Identifier number of the element	---
Num_node_k	Id. number of the k-th node	---
Material_id	Identifier of the material	---
Num_rows	Number of rows of elements	---
Num_columns	Number of columns of elements	---
Nodes_numeration_code	Code for the automatic numeration of the nodes	= 0 if it numbers according to the rows; = 1 if it numbers according to the

		columns
Column_k_coor_x	X co-ordinate of the k-th column of nodes	---
Row_k_coor_y	Y co-ordinate of the k-th row of nodes	---
Num_mat	Total number of materials to assign to elements	---
Element_from	First element to assign this material	---
Element_to	Last element to assign this material	---
Element_step	Number of elements after which to assign this material	---
Material_id	Identifier of the material	---

Table 7A-2. Meaning of the parameters of Block 2.

BLOCK 3: DATA FOR THE INITIAL CONDITIONS

The third block is that of the data which define the initial conditions of the system. These are the following:

In case of first run with constant conditions on all the mesh (Restart_code = -1) :

$$P_g(r), P_c(r), T(r), U_x(r), U_y(r)$$

In case of first run where the initial conditions vary for each node (Restart_code = 1):

$$ID(i), P_g(r), P_c(r), T(r), U_x(r), U_y(r) \text{ for every node}$$

In the following table the meaning of the data is shown:

DATA	MEANING	VALUE
ID	Identifier of the node useful for the user	integer
P _g	Initial gas pressure	E.g.: 0.0 Pa
P _c	Initial capillary pressure	E.g.: 0.0 Pa
T	Initial temperature	E.g.: 298.15 K
U _x	Initial x displacement	E.g.: 0.0
U _y	Initial y displacement	E.g.: 0.0

Table 7A-3. Meaning of the parameters of Block 3.

BLOCK 4: DATA FOR THE BOUNDARY CONDITIONS

The last but also the larger block is the one which contains the data of the boundary conditions (constraints and loads) of the system. For every conditioned node the following data must be given:

$$Conditions_num(i), Conditioned_node_num(i)$$

$$Dof_id(i), Condition_id(i), Value(r), Coefficient(i) \text{ /for every condition}$$

The meaning of the data to give is summarised in tables 7A-4 and 7A-5:

DATA	MEANING	VALUE
Conditions_num	Number of the imposed conditions	Not greater than 5
Conditioned_node_num	Number of the conditioned node	---
Dof_id	Identifier of the conditioned d.o.f	See next table
Condition_id	Identifier of the imposed condition	See next table
Value	Assigned value	See next table
Coefficient	Assigned coefficient	See next table

Table 7A-4. Meaning of the parameters of Block 4.

Dof_id	DOF	Cond_id	Condition	Value	Coefficient
1	PG	1	Imposed value	Fixed PG Pa	0.0 =
		2	Imposed flux of dry air	Fixed air flux Kg m ² s ⁻¹	0.0 =
2	PC	1	Imposed value	Fixed PC Pa	0.0 =
		2	Imposed flux of dry air	Fixed vapour flux Kg m ² s ⁻¹	0.0 =
		3	Imposed value of water vapour	Fixed room RH =	e.g. 0.05 m/s
		4	Imposed value of vapour pressure	Fixed vapour pressure Pa	e.g. 0.05
3	T	1	Imposed value	Fixed T K	0.0 =
		2	Imposed heat flux	Fixed heat flux W m ²	298.15 K
		3	Var. heat flux (convection)	Fixed room T K (convect.)	e.g. 20Wm ⁻² K ⁻¹
		4	Var. heat flux (radiation+convection)	Fixed room T K (radiation)	e.g. 20
4	UX	1	Imposed value	Fixed Ux m	0.0 =
		2	Distributed load	Fixed stress Pa	0.0 =
5	UY	1	Imposed value	Fixed Uy m	0.0 =
		2	Distributed load	Fixed stress Pa	0.0 =

Table 7A-5. Types of values of the parameters of Block 4.

Since it is not worthy to include herein the Input files corresponding to each of the cases calculated, only that corresponding to the Slow Environmental Cooling case will follow (it corresponds to the first stage of the calculations among the series of five calculations stages developed for each case, being identical for the Fast Environmental Cooling case except for the number of time steps and their size).

SLOW ENVIRONMENTAL COOLING CASE – FIRST STAGE

```

$ Description of the simulation
Show environmental cooling of a Square Column*
$ Restart code , Problem type code
-1,0
$ Names of the output file and the binary file to be produced
'column_01.BIN'
'column_01.PRN'
$ Time and number step, number of time steps after which the results are saved
1e-6,10,10
$ Value of the convergence criterion, maximum number of iterations
1e-5,30
$ Gravity acceleration, angle between the gravity acceleration and the mesh
0,0
$ Code for the mesh generation, scale factors of the mesh for the x and y axis
0,0.01,0.01
$ Nodes, elements, nodes for an element, number of integration points
1976, 625, 8,3
$ Number of nodes on which one or more boundary conditions are imposed
200
$ x and y coordinates of the nodes
1 0.000000 0.000000 23 3.174443 1.284870
2 0.642435 0.000000 24 1.284870 3.174443
3 0.000000 0.642435 25 2.554504 2.554504
4 1.284870 0.000000 26 3.794381 0.000000
5 0.000000 1.284870 27 0.000000 3.794381
6 0.642435 1.284870 28 3.794381 0.642435
7 1.284870 0.642435 29 0.642435 3.794381
8 1.284870 1.284870 30 3.794381 1.284870
9 1.919687 0.000000 31 1.284870 3.794381
10 0.000000 1.919687 32 3.174443 2.554504
11 1.284870 1.919687 33 2.554504 3.174443
12 1.919687 1.284870 34 3.794381 1.919687
13 0.000000 2.554504 35 1.919687 3.794381
14 2.554504 0.000000 36 4.392778 0.000000
15 0.642435 2.554504 37 0.000000 4.392778
16 2.554504 0.642435 38 3.794381 2.554504
17 2.554504 1.284870 39 2.554504 3.794381
18 1.284870 2.554504 40 1.284870 4.392778
19 3.174443 0.000000 41 4.392778 1.284870
20 0.000000 3.174443 42 3.174443 3.794381
21 2.554504 1.919687 43 3.794381 3.174443
22 1.919687 2.554504 44 4.991174 0.000000
    
```

45	0.000000	4.991174	122	0.000000	8.215468
46	4.991174	0.642435	123	8.215468	0.000000
47	0.642435	4.991174	124	0.642435	8.215468
48	2.554504	4.392778	125	8.215468	0.642435
49	4.392778	2.554504	126	6.133152	5.562163
50	4.991174	1.284870	127	5.562163	6.133152
51	1.284870	4.991174	128	1.284870	8.215468
52	4.991174	1.919687	129	8.215468	1.284870
53	1.919687	4.991174	130	6.671821	4.991174
54	3.794381	3.794381	131	4.991174	6.671821
55	5.562163	0.000000	132	8.215468	1.919687
56	0.000000	5.562163	133	1.919687	8.215468
57	2.554504	4.991174	134	4.392778	7.210489
58	4.991174	2.554504	135	7.210489	4.392778
59	5.562163	1.284870	136	3.794381	7.712979
60	1.284870	5.562163	137	7.712979	3.794381
61	4.392778	3.794381	138	2.554504	8.215468
62	3.794381	4.392778	139	8.215468	2.554504
63	4.991174	3.174443	140	6.133152	6.133152
64	3.174443	4.991174	141	8.679020	0.000000
65	5.562163	2.554504	142	0.000000	8.679020
66	2.554504	5.562163	143	7.210489	4.991174
67	6.133152	0.000000	144	4.991174	7.210489
68	0.000000	6.133152	145	1.284870	8.679020
69	6.133152	0.642435	146	8.679020	1.284870
70	0.642435	6.133152	147	3.174443	8.215468
71	6.133152	1.284870	148	8.215468	3.174443
72	1.284870	6.133152	149	2.554504	8.679020
73	4.991174	3.794381	150	8.679020	2.554504
74	3.794381	4.991174	151	8.215468	3.794381
75	6.133152	1.919687	152	3.794381	8.215468
76	1.919687	6.133152	153	6.671821	6.133152
77	6.133152	2.554504	154	6.133152	6.671821
78	2.554504	6.133152	155	5.562163	7.210489
79	4.392778	4.991174	156	7.210489	5.562163
80	4.991174	4.392778	157	9.142571	0.000000
81	6.671821	0.000000	158	0.000000	9.142571
82	0.000000	6.671821	159	0.642435	9.142571
83	5.562163	3.794381	160	9.142571	0.642435
84	3.794381	5.562163	161	7.712979	4.991174
85	1.284870	6.671821	162	4.991174	7.712979
86	6.671821	1.284870	163	9.142571	1.284870
87	6.133152	3.174443	164	1.284870	9.142571
88	3.174443	6.133152	165	4.392778	8.215468
89	4.991174	4.991174	166	8.215468	4.392778
90	2.554504	6.671821	167	9.142571	1.919687
91	6.671821	2.554504	168	1.919687	9.142571
92	7.210489	0.000000	169	6.133152	7.210489
93	0.000000	7.210489	170	7.210489	6.133152
94	6.133152	3.794381	171	3.794381	8.679020
95	3.794381	6.133152	172	8.679020	3.794381
96	0.642435	7.210489	173	9.142571	2.554504
97	7.210489	0.642435	174	2.554504	9.142571
98	7.210489	1.284870	175	0.000000	9.565519
99	1.284870	7.210489	176	9.565519	0.000000
100	1.919687	7.210489	177	8.215468	4.991174
101	7.210489	1.919687	178	4.991174	8.215468
102	4.991174	5.562163	179	1.284870	9.565519
103	5.562163	4.991174	180	9.565519	1.284870
104	6.133152	4.392778	181	3.174443	9.142571
105	4.392778	6.133152	182	9.142571	3.174443
106	2.554504	7.210489	183	7.210489	6.671821
107	7.210489	2.554504	184	6.671821	7.210489
108	6.671821	3.794381	185	7.712979	6.133152
109	3.794381	6.671821	186	6.133152	7.712979
110	7.712979	0.000000	187	9.142571	3.794381
111	0.000000	7.712979	188	3.794381	9.142571
112	1.284870	7.712979	189	2.554504	9.565519
113	7.712979	1.284870	190	9.565519	2.554504
114	7.210489	3.174443	191	5.562163	8.215468
115	3.174443	7.210489	192	8.215468	5.562163
116	6.133152	4.991174	193	9.988467	0.000000
117	4.991174	6.133152	194	0.000000	9.988467
118	7.712979	2.554504	195	0.642435	9.988467
119	2.554504	7.712979	196	9.988467	0.642435
120	7.210489	3.794381	197	8.679020	4.991174
121	3.794381	7.210489	198	4.991174	8.679020

199	1.284870	9.988467	276	0.642435	11.433558
200	9.988467	1.284870	277	11.433558	0.642435
201	4.392778	9.142571	278	11.433558	1.284870
202	9.142571	4.392778	279	1.284870	11.433558
203	1.919687	9.988467	280	10.370189	4.991174
204	9.988467	1.919687	281	4.991174	10.370189
205	7.210489	7.210489	282	11.433558	1.919687
206	6.133152	8.215468	283	1.919687	11.433558
207	8.215468	6.133152	284	10.751912	4.392778
208	3.794381	9.565519	285	4.392778	10.751912
209	9.565519	3.794381	286	8.215468	8.215468
210	2.554504	9.988467	287	7.210489	9.142571
211	9.988467	2.554504	288	9.142571	7.210489
212	10.370189	0.000000	289	2.554504	11.433558
213	0.000000	10.370189	290	11.433558	2.554504
214	9.142571	4.991174	291	6.133152	9.988467
215	4.991174	9.142571	292	9.988467	6.133152
216	10.370189	1.284870	293	11.092735	3.794381
217	1.284870	10.370189	294	3.794381	11.092735
218	3.174443	9.988467	295	11.734639	0.000000
219	9.988467	3.174443	296	0.000000	11.734639
220	7.712979	7.210489	297	11.734639	1.284870
221	7.210489	7.712979	298	1.284870	11.734639
222	8.215468	6.671821	299	4.991174	10.751912
223	6.671821	8.215468	300	10.751912	4.991174
224	8.679020	6.133152	301	11.433558	3.174443
225	6.133152	8.679020	302	3.174443	11.433558
226	2.554504	10.370189	303	8.679020	8.215468
227	10.370189	2.554504	304	8.215468	8.679020
228	3.794381	9.988467	305	7.712979	9.142571
229	9.988467	3.794381	306	9.142571	7.712979
230	9.142571	5.562163	307	9.565519	7.210489
231	5.562163	9.142571	308	7.210489	9.565519
232	0.000000	10.751912	309	11.734639	2.554504
233	10.751912	0.000000	310	2.554504	11.734639
234	0.642435	10.751912	311	9.988467	6.671821
235	10.751912	0.642435	312	6.671821	9.988467
236	4.991174	9.565519	313	12.035720	0.000000
237	9.565519	4.991174	314	0.000000	12.035720
238	10.751912	1.284870	315	11.433558	3.794381
239	1.284870	10.751912	316	3.794381	11.433558
240	9.988467	4.392778	317	10.370189	6.133152
241	4.392778	9.988467	318	6.133152	10.370189
242	10.751912	1.919687	319	0.642435	12.035720
243	1.919687	10.751912	320	12.035720	0.642435
244	7.210489	8.215468	321	12.035720	1.284870
245	8.215468	7.210489	322	1.284870	12.035720
246	9.142571	6.133152	323	10.751912	5.562163
247	6.133152	9.142571	324	5.562163	10.751912
248	3.794381	10.370189	325	11.092735	4.991174
249	10.370189	3.794381	326	4.991174	11.092735
250	2.554504	10.751912	327	1.919687	12.035720
251	10.751912	2.554504	328	12.035720	1.919687
252	11.092735	0.000000	329	11.433558	4.392778
253	0.000000	11.092735	330	4.392778	11.433558
254	9.988467	4.991174	331	8.215468	9.142571
255	4.991174	9.988467	332	9.142571	8.215468
256	1.284870	11.092735	333	12.298902	0.000000
257	11.092735	1.284870	334	0.000000	12.298902
258	10.751912	3.174443	335	2.554504	12.035720
259	3.174443	10.751912	336	12.035720	2.554504
260	7.712979	8.215468	337	7.210489	9.988467
261	8.215468	7.712979	338	9.988467	7.210489
262	7.210489	8.679020	339	3.794381	11.734639
263	8.679020	7.210489	340	11.734639	3.794381
264	6.671821	9.142571	341	1.284870	12.298902
265	9.142571	6.671821	342	12.298902	1.284870
266	9.565519	6.133152	343	10.751912	6.133152
267	6.133152	9.565519	344	6.133152	10.751912
268	2.554504	11.092735	345	12.035720	3.174443
269	11.092735	2.554504	346	3.174443	12.035720
270	10.751912	3.794381	347	11.433558	4.991174
271	3.794381	10.751912	348	4.991174	11.433558
272	5.562163	9.988467	349	2.554504	12.298902
273	9.988467	5.562163	350	12.298902	2.554504
274	11.433558	0.000000	351	0.000000	12.562085
275	0.000000	11.433558	352	12.562085	0.000000

353	0.642435	12.562085	430	12.298902	4.991174
354	12.562085	0.642435	431	4.991174	12.298902
355	8.679020	9.142571	432	13.212338	1.284870
356	9.142571	8.679020	433	1.284870	13.212338
357	9.565519	8.215468	434	12.562085	4.392778
358	8.215468	9.565519	435	4.392778	12.562085
359	12.035720	3.794381	436	12.789751	3.794381
360	3.794381	12.035720	437	3.794381	12.789751
361	9.988467	7.712979	438	13.017418	3.174443
362	7.712979	9.988467	439	3.174443	13.017418
363	12.562085	1.284870	440	0.000000	13.407257
364	1.284870	12.562085	441	13.407257	0.000000
365	7.210489	10.370189	442	0.642435	13.407257
366	10.370189	7.210489	443	13.407257	0.642435
367	6.671821	10.751912	444	2.554504	13.212338
368	10.751912	6.671821	445	13.212338	2.554504
369	11.092735	6.133152	446	1.284870	13.407257
370	6.133152	11.092735	447	13.407257	1.284870
371	1.919687	12.562085	448	12.035720	6.133152
372	12.562085	1.919687	449	6.133152	12.035720
373	5.562163	11.433558	450	7.210489	11.433558
374	11.433558	5.562163	451	11.433558	7.210489
375	11.734639	4.991174	452	4.991174	12.562085
376	4.991174	11.734639	453	12.562085	4.991174
377	0.000000	12.789751	454	10.751912	8.215468
378	12.789751	0.000000	455	8.215468	10.751912
379	12.035720	4.392778	456	9.142571	9.988467
380	4.392778	12.035720	457	9.988467	9.142571
381	2.554504	12.562085	458	1.919687	13.407257
382	12.562085	2.554504	459	13.407257	1.919687
383	12.789751	1.284870	460	3.794381	13.017418
384	1.284870	12.789751	461	13.017418	3.794381
385	12.298902	3.794381	462	0.000000	13.572444
386	3.794381	12.298902	463	13.572444	0.000000
387	9.142571	9.142571	464	13.572444	1.284870
388	8.215468	9.988467	465	1.284870	13.572444
389	9.988467	8.215468	466	2.554504	13.407257
390	7.210489	10.751912	467	13.407257	2.554504
391	10.751912	7.210489	468	12.789751	4.991174
392	3.174443	12.562085	469	4.991174	12.789751
393	12.562085	3.174443	470	13.737630	0.000000
394	11.433558	6.133152	471	0.000000	13.737630
395	6.133152	11.433558	472	12.562085	5.562163
396	0.000000	13.017418	473	5.562163	12.562085
397	13.017418	0.000000	474	13.017418	4.392778
398	12.035720	4.991174	475	4.392778	13.017418
399	4.991174	12.035720	476	6.133152	12.298902
400	13.017418	0.642435	477	12.298902	6.133152
401	0.642435	13.017418	478	13.212338	3.794381
402	12.789751	2.554504	479	3.794381	13.212338
403	2.554504	12.789751	480	0.642435	13.737630
404	13.017418	1.284870	481	13.737630	0.642435
405	1.284870	13.017418	482	6.671821	12.035720
406	12.562085	3.794381	483	12.035720	6.671821
407	3.794381	12.562085	484	11.734639	7.210489
408	13.017418	1.919687	485	7.210489	11.734639
409	1.919687	13.017418	486	3.174443	13.407257
410	0.000000	13.212338	487	13.407257	3.174443
411	13.212338	0.000000	488	7.712979	11.433558
412	10.370189	8.215468	489	11.433558	7.712979
413	8.215468	10.370189	490	1.284870	13.737630
414	11.092735	7.210489	491	13.737630	1.284870
415	7.210489	11.092735	492	8.215468	11.092735
416	9.142571	9.565519	493	11.092735	8.215468
417	9.565519	9.142571	494	13.572444	2.554504
418	7.712979	10.751912	495	2.554504	13.572444
419	10.751912	7.712979	496	10.751912	8.679020
420	9.988467	8.679020	497	8.679020	10.751912
421	8.679020	9.988467	498	10.370189	9.142571
422	6.671821	11.433558	499	9.142571	10.370189
423	11.433558	6.671821	500	9.988467	9.565519
424	11.734639	6.133152	501	9.565519	9.988467
425	6.133152	11.734639	502	1.919687	13.737630
426	12.035720	5.562163	503	13.737630	1.919687
427	5.562163	12.035720	504	13.876209	0.000000
428	2.554504	13.017418	505	0.000000	13.876209
429	13.017418	2.554504	506	3.794381	13.407257

507	13.407257	3.794381	584	6.133152	13.017418
508	13.876209	1.284870	585	10.751912	9.565519
509	1.284870	13.876209	586	9.565519	10.751912
510	4.991174	13.017418	587	14.339640	1.284870
511	13.017418	4.991174	588	1.284870	14.339640
512	13.737630	2.554504	589	9.988467	10.370189
513	2.554504	13.737630	590	10.370189	9.988467
514	6.133152	12.562085	591	13.737630	4.392778
515	12.562085	6.133152	592	4.392778	13.737630
516	0.000000	14.014789	593	0.000000	14.434294
517	14.014789	0.000000	594	14.434294	0.000000
518	14.014789	0.642435	595	14.434294	0.642435
519	0.642435	14.014789	596	0.642435	14.434294
520	12.035720	7.210489	597	13.572444	4.991174
521	7.210489	12.035720	598	4.991174	13.572444
522	1.284870	14.014789	599	14.244987	2.554504
523	14.014789	1.284870	600	2.554504	14.244987
524	11.433558	8.215468	601	7.210489	12.562085
525	8.215468	11.433558	602	12.562085	7.210489
526	3.794381	13.572444	603	1.284870	14.434294
527	13.572444	3.794381	604	14.434294	1.284870
528	3.174443	13.737630	605	0.000000	14.511374
529	13.737630	3.174443	606	14.511374	0.000000
530	4.392778	13.407257	607	5.562163	13.407257
531	13.407257	4.392778	608	13.407257	5.562163
532	13.876209	2.554504	609	14.014789	3.794381
533	2.554504	13.876209	610	3.794381	14.014789
534	9.142571	10.751912	611	14.434294	1.919687
535	10.751912	9.142571	612	1.919687	14.434294
536	13.212338	4.991174	613	14.339640	2.554504
537	4.991174	13.212338	614	2.554504	14.339640
538	9.988467	9.988467	615	6.133152	13.212338
539	14.129888	0.000000	616	13.212338	6.133152
540	0.000000	14.129888	617	1.284870	14.511374
541	14.014789	1.919687	618	14.511374	1.284870
542	1.919687	14.014789	619	12.035720	8.215468
543	13.017418	5.562163	620	8.215468	12.035720
544	5.562163	13.017418	621	0.000000	14.588453
545	6.133152	12.789751	622	14.588453	0.000000
546	12.789751	6.133152	623	3.174443	14.244987
547	1.284870	14.129888	624	14.244987	3.174443
548	14.129888	1.284870	625	0.642435	14.588453
549	6.671821	12.562085	626	14.588453	0.642435
550	12.562085	6.671821	627	4.991174	13.737630
551	0.000000	14.244987	628	13.737630	4.991174
552	14.244987	0.000000	629	13.017418	6.671821
553	2.554504	14.014789	630	6.671821	13.017418
554	14.014789	2.554504	631	14.129888	3.794381
555	3.794381	13.737630	632	3.794381	14.129888
556	13.737630	3.794381	633	9.142571	11.433558
557	7.210489	12.298902	634	11.433558	9.142571
558	12.298902	7.210489	635	1.284870	14.588453
559	0.642435	14.244987	636	14.588453	1.284870
560	14.244987	0.642435	637	0.000000	14.650614
561	7.712979	12.035720	638	14.650614	0.000000
562	12.035720	7.712979	639	2.554504	14.434294
563	1.284870	14.244987	640	14.434294	2.554504
564	14.244987	1.284870	641	9.988467	10.751912
565	13.407257	4.991174	642	10.751912	9.988467
566	4.991174	13.407257	643	7.210489	12.789751
567	8.215468	11.734639	644	12.789751	7.210489
568	11.734639	8.215468	645	14.014789	4.392778
569	14.339640	0.000000	646	4.392778	14.014789
570	0.000000	14.339640	647	14.650614	1.284870
571	8.679020	11.433558	648	1.284870	14.650614
572	11.433558	8.679020	649	0.000000	14.712775
573	14.129888	2.554504	650	14.712775	0.000000
574	2.554504	14.129888	651	1.919687	14.588453
575	14.014789	3.174443	652	14.588453	1.919687
576	3.174443	14.014789	653	0.642435	14.712775
577	1.919687	14.244987	654	14.712775	0.642435
578	14.244987	1.919687	655	2.554504	14.511374
579	9.142571	11.092735	656	14.511374	2.554504
580	11.092735	9.142571	657	7.712979	12.562085
581	3.794381	13.876209	658	12.562085	7.712979
582	13.876209	3.794381	659	14.244987	3.794381
583	13.017418	6.133152	660	3.794381	14.244987

661	13.407257	6.133152	738	1.284870	14.921416
662	6.133152	13.407257	739	14.762425	2.554504
663	13.876209	4.991174	740	2.554504	14.762425
664	4.991174	13.876209	741	14.129888	4.991174
665	14.762425	0.000000	742	4.991174	14.129888
666	0.000000	14.762425	743	14.511374	3.794381
667	1.284870	14.712775	744	3.794381	14.511374
668	14.712775	1.284870	745	0.000000	15.000000
669	14.434294	3.174443	746	15.000000	0.000000
670	3.174443	14.434294	747	1.284870	14.952200
671	12.298902	8.215468	748	14.952200	1.284870
672	8.215468	12.298902	749	12.562085	8.215468
673	2.554504	14.588453	750	8.215468	12.562085
674	14.588453	2.554504	751	0.642435	15.000000
675	14.812074	0.000000	752	15.000000	0.642435
676	0.000000	14.812074	753	1.919687	14.890633
677	14.762425	1.284870	754	14.890633	1.919687
678	1.284870	14.762425	755	2.554504	14.812074
679	5.562163	13.737630	756	14.812074	2.554504
680	13.737630	5.562163	757	14.976100	1.284870
681	0.642435	14.812074	758	1.284870	14.976100
682	14.812074	0.642435	759	13.737630	6.133152
683	3.794381	14.339640	760	6.133152	13.737630
684	14.339640	3.794381	761	14.712775	3.174443
685	1.919687	14.712775	762	3.174443	14.712775
686	14.712775	1.919687	763	13.212338	7.210489
687	8.679020	12.035720	764	7.210489	13.212338
688	12.035720	8.679020	765	15.000000	1.284870
689	14.851354	0.000000	766	1.284870	15.000000
690	0.000000	14.851354	767	14.851354	2.554504
691	1.284870	14.812074	768	2.554504	14.851354
692	14.812074	1.284870	769	3.794381	14.588453
693	2.554504	14.650614	770	14.588453	3.794381
694	14.650614	2.554504	771	14.952200	1.919687
695	11.734639	9.142571	772	1.919687	14.952200
696	9.142571	11.734639	773	14.014789	5.562163
697	14.014789	4.991174	774	5.562163	14.014789
698	4.991174	14.014789	775	14.434294	4.392778
699	13.017418	7.210489	776	4.392778	14.434294
700	7.210489	13.017418	777	4.991174	14.244987
701	0.000000	14.890633	778	14.244987	4.991174
702	14.890633	0.000000	779	14.890633	2.554504
703	6.133152	13.572444	780	2.554504	14.890633
704	13.572444	6.133152	781	9.142571	12.035720
705	0.642435	14.890633	782	12.035720	9.142571
706	14.890633	0.642435	783	15.000000	1.919687
707	14.851354	1.284870	784	1.919687	15.000000
708	1.284870	14.851354	785	7.712979	13.017418
709	4.392778	14.244987	786	13.017418	7.712979
710	14.244987	4.392778	787	3.794381	14.650614
711	11.433558	9.565519	788	14.650614	3.794381
712	9.565519	11.433558	789	14.921416	2.554504
713	0.000000	14.921416	790	2.554504	14.921416
714	14.921416	0.000000	791	14.812074	3.174443
715	3.794381	14.434294	792	3.174443	14.812074
716	14.434294	3.794381	793	2.554504	14.952200
717	9.988467	11.092735	794	14.952200	2.554504
718	11.092735	9.988467	795	6.133152	13.876209
719	3.174443	14.588453	796	13.876209	6.133152
720	14.588453	3.174443	797	9.988467	11.433558
721	2.554504	14.712775	798	11.433558	9.988467
722	14.712775	2.554504	799	4.991174	14.339640
723	1.919687	14.812074	800	14.339640	4.991174
724	14.812074	1.919687	801	2.554504	14.976100
725	10.751912	10.370189	802	14.976100	2.554504
726	10.370189	10.751912	803	3.794381	14.712775
727	1.284870	14.890633	804	14.712775	3.794381
728	14.890633	1.284870	805	8.215468	12.789751
729	14.952200	0.000000	806	12.789751	8.215468
730	0.000000	14.952200	807	10.751912	10.751912
731	0.642435	14.952200	808	15.000000	2.554504
732	14.952200	0.642435	809	2.554504	15.000000
733	13.407257	6.671821	810	7.210489	13.407257
734	6.671821	13.407257	811	13.407257	7.210489
735	0.000000	14.976100	812	14.890633	3.174443
736	14.976100	0.000000	813	3.174443	14.890633
737	14.921416	1.284870	814	4.392778	14.588453

815	14.588453	4.392778	892	14.952200	4.392778
816	14.762425	3.794381	893	4.392778	14.952200
817	3.794381	14.762425	894	14.339640	6.133152
818	12.562085	8.679020	895	6.133152	14.339640
819	8.679020	12.562085	896	5.562163	14.588453
820	13.737630	6.671821	897	14.588453	5.562163
821	6.671821	13.737630	898	15.000000	4.392778
822	14.434294	4.991174	899	4.392778	15.000000
823	4.991174	14.434294	900	4.991174	14.812074
824	14.952200	3.174443	901	14.812074	4.991174
825	3.174443	14.952200	902	7.210489	13.876209
826	3.794381	14.812074	903	13.876209	7.210489
827	14.812074	3.794381	904	9.988467	12.035720
828	14.244987	5.562163	905	12.035720	9.988467
829	5.562163	14.244987	906	13.017418	8.679020
830	14.014789	6.133152	907	8.679020	13.017418
831	6.133152	14.014789	908	14.851354	4.991174
832	12.298902	9.142571	909	4.991174	14.851354
833	9.142571	12.298902	910	14.434294	6.133152
834	14.851354	3.794381	911	6.133152	14.434294
835	3.794381	14.851354	912	11.433558	10.751912
836	3.174443	15.000000	913	10.751912	11.433558
837	15.000000	3.174443	914	14.890633	4.991174
838	14.511374	4.991174	915	4.991174	14.890633
839	4.991174	14.511374	916	12.789751	9.142571
840	14.712775	4.392778	917	9.142571	12.789751
841	4.392778	14.712775	918	8.215468	13.407257
842	14.890633	3.794381	919	13.407257	8.215468
843	3.794381	14.890633	920	14.712775	5.562163
844	13.572444	7.210489	921	5.562163	14.712775
845	7.210489	13.572444	922	6.671821	14.244987
846	12.035720	9.565519	923	14.244987	6.671821
847	9.565519	12.035720	924	4.991174	14.921416
848	8.215468	13.017418	925	14.921416	4.991174
849	13.017418	8.215468	926	14.511374	6.133152
850	14.921416	3.794381	927	6.133152	14.511374
851	3.794381	14.921416	928	7.712979	13.737630
852	6.133152	14.129888	929	13.737630	7.712979
853	14.129888	6.133152	930	14.014789	7.210489
854	11.734639	9.988467	931	7.210489	14.014789
855	9.988467	11.734639	932	14.952200	4.991174
856	14.588453	4.991174	933	4.991174	14.952200
857	4.991174	14.588453	934	14.976100	4.991174
858	3.794381	14.952200	935	4.991174	14.976100
859	14.952200	3.794381	936	9.565519	12.562085
860	10.370189	11.433558	937	12.562085	9.565519
861	11.433558	10.370189	938	15.000000	4.991174
862	10.751912	11.092735	939	4.991174	15.000000
863	11.092735	10.751912	940	5.562163	14.812074
864	14.976100	3.794381	941	14.812074	5.562163
865	3.794381	14.976100	942	14.588453	6.133152
866	14.812074	4.392778	943	6.133152	14.588453
867	4.392778	14.812074	944	9.988467	12.298902
868	13.407257	7.712979	945	12.298902	9.988467
869	7.712979	13.407257	946	14.129888	7.210489
870	5.562163	14.434294	947	7.210489	14.129888
871	14.434294	5.562163	948	13.572444	8.215468
872	3.794381	15.000000	949	8.215468	13.572444
873	15.000000	3.794381	950	14.650614	6.133152
874	4.991174	14.650614	951	6.133152	14.650614
875	14.650614	4.991174	952	12.035720	10.370189
876	6.133152	14.244987	953	10.370189	12.035720
877	14.244987	6.133152	954	5.562163	14.890633
878	13.737630	7.210489	955	14.890633	5.562163
879	7.210489	13.737630	956	14.434294	6.671821
880	14.014789	6.671821	957	6.671821	14.434294
881	6.671821	14.014789	958	13.017418	9.142571
882	14.890633	4.392778	959	9.142571	13.017418
883	4.392778	14.890633	960	10.751912	11.734639
884	14.712775	4.991174	961	11.734639	10.751912
885	4.991174	14.712775	962	11.433558	11.092735
886	9.142571	12.562085	963	11.092735	11.433558
887	12.562085	9.142571	964	14.712775	6.133152
888	8.215468	13.212338	965	6.133152	14.712775
889	13.212338	8.215468	966	5.562163	14.952200
890	4.991174	14.762425	967	14.952200	5.562163
891	14.762425	4.991174	968	7.210489	14.244987

969	14.244987	7.210489	1046	14.952200	6.671821
970	8.679020	13.407257	1047	11.433558	11.734639
971	13.407257	8.679020	1048	11.734639	11.433558
972	14.762425	6.133152	1049	14.712775	7.210489
973	6.133152	14.762425	1050	7.210489	14.712775
974	7.712979	14.014789	1051	13.017418	9.988467
975	14.014789	7.712979	1052	9.988467	13.017418
976	15.000000	5.562163	1053	15.000000	6.671821
977	5.562163	15.000000	1054	6.671821	15.000000
978	13.737630	8.215468	1055	7.210489	14.762425
979	8.215468	13.737630	1056	14.762425	7.210489
980	14.812074	6.133152	1057	8.215468	14.244987
981	6.133152	14.812074	1058	14.244987	8.215468
982	14.588453	6.671821	1059	9.565519	13.407257
983	6.671821	14.588453	1060	13.407257	9.565519
984	12.562085	9.988467	1061	14.812074	7.210489
985	9.988467	12.562085	1062	7.210489	14.812074
986	14.339640	7.210489	1063	8.679020	14.014789
987	7.210489	14.339640	1064	14.014789	8.679020
988	9.142571	13.212338	1065	13.737630	9.142571
989	13.212338	9.142571	1066	9.142571	13.737630
990	14.851354	6.133152	1067	14.588453	7.712979
991	6.133152	14.851354	1068	7.712979	14.588453
992	14.890633	6.133152	1069	14.851354	7.210489
993	6.133152	14.890633	1070	7.210489	14.851354
994	8.215468	13.876209	1071	14.339640	8.215468
995	13.876209	8.215468	1072	8.215468	14.339640
996	6.133152	14.921416	1073	12.562085	10.751912
997	14.921416	6.133152	1074	10.751912	12.562085
998	7.210489	14.434294	1075	7.210489	14.890633
999	14.434294	7.210489	1076	14.890633	7.210489
1000	12.035720	10.751912	1077	13.212338	9.988467
1001	10.751912	12.035720	1078	9.988467	13.212338
1002	9.565519	13.017418	1079	14.921416	7.210489
1003	13.017418	9.565519	1080	7.210489	14.921416
1004	14.712775	6.671821	1081	7.210489	14.952200
1005	6.671821	14.712775	1082	14.952200	7.210489
1006	6.133152	14.952200	1083	12.035720	11.433558
1007	14.952200	6.133152	1084	11.433558	12.035720
1008	11.433558	11.433558	1085	8.215468	14.434294
1009	6.133152	14.976100	1086	14.434294	8.215468
1010	14.976100	6.133152	1087	14.712775	7.712979
1011	7.712979	14.244987	1088	7.712979	14.712775
1012	14.244987	7.712979	1089	9.142571	13.876209
1013	7.210489	14.511374	1090	13.876209	9.142571
1014	14.511374	7.210489	1091	7.210489	14.976100
1015	6.133152	15.000000	1092	14.976100	7.210489
1016	15.000000	6.133152	1093	15.000000	7.210489
1017	9.142571	13.407257	1094	7.210489	15.000000
1018	13.407257	9.142571	1095	13.017418	10.370189
1019	12.789751	9.988467	1096	10.370189	13.017418
1020	9.988467	12.789751	1097	8.215468	14.511374
1021	8.215468	14.014789	1098	14.511374	8.215468
1022	14.014789	8.215468	1099	14.244987	8.679020
1023	6.671821	14.812074	1100	8.679020	14.244987
1024	14.812074	6.671821	1101	14.812074	7.712979
1025	13.737630	8.679020	1102	7.712979	14.812074
1026	8.679020	13.737630	1103	12.789751	10.751912
1027	7.210489	14.588453	1104	10.751912	12.789751
1028	14.588453	7.210489	1105	9.988467	13.407257
1029	10.370189	12.562085	1106	13.407257	9.988467
1030	12.562085	10.370189	1107	14.014789	9.142571
1031	14.890633	6.671821	1108	9.142571	14.014789
1032	6.671821	14.890633	1109	9.565519	13.737630
1033	14.650614	7.210489	1110	13.737630	9.565519
1034	7.210489	14.650614	1111	14.588453	8.215468
1035	12.298902	10.751912	1112	8.215468	14.588453
1036	10.751912	12.298902	1113	11.092735	12.562085
1037	8.215468	14.129888	1114	12.562085	11.092735
1038	14.129888	8.215468	1115	7.712979	14.890633
1039	13.572444	9.142571	1116	14.890633	7.712979
1040	9.142571	13.572444	1117	12.298902	11.433558
1041	14.434294	7.712979	1118	11.433558	12.298902
1042	7.712979	14.434294	1119	14.650614	8.215468
1043	12.035720	11.092735	1120	8.215468	14.650614
1044	11.092735	12.035720	1121	11.734639	12.035720
1045	6.671821	14.952200	1122	12.035720	11.734639

1123	7.712979	14.952200	1200	14.650614	9.142571
1124	14.952200	7.712979	1201	9.142571	14.650614
1125	9.142571	14.129888	1202	14.952200	8.679020
1126	14.129888	9.142571	1203	8.679020	14.952200
1127	14.434294	8.679020	1204	9.988467	14.129888
1128	8.679020	14.434294	1205	14.129888	9.988467
1129	14.712775	8.215468	1206	13.572444	10.751912
1130	8.215468	14.712775	1207	10.751912	13.572444
1131	13.572444	9.988467	1208	14.434294	9.565519
1132	9.988467	13.572444	1209	9.565519	14.434294
1133	15.000000	7.712979	1210	14.712775	9.142571
1134	7.712979	15.000000	1211	9.142571	14.712775
1135	10.751912	13.017418	1212	11.433558	13.017418
1136	13.017418	10.751912	1213	13.017418	11.433558
1137	8.215468	14.762425	1214	15.000000	8.679020
1138	14.762425	8.215468	1215	8.679020	15.000000
1139	14.244987	9.142571	1216	9.142571	14.762425
1140	9.142571	14.244987	1217	14.762425	9.142571
1141	14.812074	8.215468	1218	12.562085	12.035720
1142	8.215468	14.812074	1219	12.035720	12.562085
1143	13.407257	10.370189	1220	14.244987	9.988467
1144	10.370189	13.407257	1221	9.988467	14.244987
1145	14.014789	9.565519	1222	13.407257	11.092735
1146	9.565519	14.014789	1223	11.092735	13.407257
1147	8.215468	14.851354	1224	14.812074	9.142571
1148	14.851354	8.215468	1225	9.142571	14.812074
1149	8.679020	14.588453	1226	14.014789	10.370189
1150	14.588453	8.679020	1227	10.370189	14.014789
1151	9.988467	13.737630	1228	9.142571	14.851354
1152	13.737630	9.988467	1229	14.851354	9.142571
1153	12.562085	11.433558	1230	9.565519	14.588453
1154	11.433558	12.562085	1231	14.588453	9.565519
1155	9.142571	14.339640	1232	13.737630	10.751912
1156	14.339640	9.142571	1233	10.751912	13.737630
1157	14.890633	8.215468	1234	11.433558	13.212338
1158	8.215468	14.890633	1235	13.212338	11.433558
1159	12.035720	12.035720	1236	14.890633	9.142571
1160	8.215468	14.921416	1237	9.142571	14.890633
1161	14.921416	8.215468	1238	9.988467	14.339640
1162	10.751912	13.212338	1239	14.339640	9.988467
1163	13.212338	10.751912	1240	14.921416	9.142571
1164	14.952200	8.215468	1241	9.142571	14.921416
1165	8.215468	14.952200	1242	9.142571	14.952200
1166	14.976100	8.215468	1243	14.952200	9.142571
1167	8.215468	14.976100	1244	13.017418	11.734639
1168	14.712775	8.679020	1245	11.734639	13.017418
1169	8.679020	14.712775	1246	14.976100	9.142571
1170	14.434294	9.142571	1247	9.142571	14.976100
1171	9.142571	14.434294	1248	14.712775	9.565519
1172	9.988467	13.876209	1249	9.565519	14.712775
1173	13.876209	9.988467	1250	14.434294	9.988467
1174	8.215468	15.000000	1251	9.988467	14.434294
1175	15.000000	8.215468	1252	10.751912	13.876209
1176	13.017418	11.092735	1253	13.876209	10.751912
1177	11.092735	13.017418	1254	12.789751	12.035720
1178	9.142571	14.511374	1255	12.035720	12.789751
1179	14.511374	9.142571	1256	9.142571	15.000000
1180	12.789751	11.433558	1257	15.000000	9.142571
1181	11.433558	12.789751	1258	12.562085	12.298902
1182	14.244987	9.565519	1259	12.298902	12.562085
1183	9.565519	14.244987	1260	14.511374	9.988467
1184	8.679020	14.812074	1261	9.988467	14.511374
1185	14.812074	8.679020	1262	10.370189	14.244987
1186	10.751912	13.407257	1263	14.244987	10.370189
1187	13.407257	10.751912	1264	13.407257	11.433558
1188	12.562085	11.734639	1265	11.433558	13.407257
1189	11.734639	12.562085	1266	9.565519	14.812074
1190	12.298902	12.035720	1267	14.812074	9.565519
1191	12.035720	12.298902	1268	13.737630	11.092735
1192	14.014789	9.988467	1269	11.092735	13.737630
1193	9.988467	14.014789	1270	14.014789	10.751912
1194	13.737630	10.370189	1271	10.751912	14.014789
1195	10.370189	13.737630	1272	14.588453	9.988467
1196	14.588453	9.142571	1273	9.988467	14.588453
1197	9.142571	14.588453	1274	14.890633	9.565519
1198	14.890633	8.679020	1275	9.565519	14.890633
1199	8.679020	14.890633	1276	12.035720	13.017418

1277	13.017418	12.035720	1354	10.751912	14.650614
1278	14.650614	9.988467	1355	11.433558	14.129888
1279	9.988467	14.650614	1356	14.129888	11.433558
1280	13.572444	11.433558	1357	13.407257	12.298902
1281	11.433558	13.572444	1358	12.298902	13.407257
1282	9.565519	14.952200	1359	14.952200	10.370189
1283	14.952200	9.565519	1360	10.370189	14.952200
1284	10.751912	14.129888	1361	14.434294	11.092735
1285	14.129888	10.751912	1362	11.092735	14.434294
1286	12.562085	12.562085	1363	14.712775	10.751912
1287	14.434294	10.370189	1364	10.751912	14.712775
1288	10.370189	14.434294	1365	13.212338	12.562085
1289	9.988467	14.712775	1366	12.562085	13.212338
1290	14.712775	9.988467	1367	10.370189	15.000000
1291	9.565519	15.000000	1368	15.000000	10.370189
1292	15.000000	9.565519	1369	12.789751	13.017418
1293	13.407257	11.734639	1370	13.017418	12.789751
1294	11.734639	13.407257	1371	14.762425	10.751912
1295	9.988467	14.762425	1372	10.751912	14.762425
1296	14.762425	9.988467	1373	13.737630	12.035720
1297	14.244987	10.751912	1374	12.035720	13.737630
1298	10.751912	14.244987	1375	11.433558	14.244987
1299	9.988467	14.812074	1376	14.244987	11.433558
1300	14.812074	9.988467	1377	11.734639	14.014789
1301	12.035720	13.212338	1378	14.014789	11.734639
1302	13.212338	12.035720	1379	14.812074	10.751912
1303	11.433558	13.737630	1380	10.751912	14.812074
1304	13.737630	11.433558	1381	14.588453	11.092735
1305	11.092735	14.014789	1382	11.092735	14.588453
1306	14.014789	11.092735	1383	14.851354	10.751912
1307	14.851354	9.988467	1384	10.751912	14.851354
1308	9.988467	14.851354	1385	14.339640	11.433558
1309	10.370189	14.588453	1386	11.433558	14.339640
1310	14.588453	10.370189	1387	14.890633	10.751912
1311	13.017418	12.298902	1388	10.751912	14.890633
1312	12.298902	13.017418	1389	13.876209	12.035720
1313	14.339640	10.751912	1390	12.035720	13.876209
1314	10.751912	14.339640	1391	13.407257	12.562085
1315	12.789751	12.562085	1392	12.562085	13.407257
1316	12.562085	12.789751	1393	10.751912	14.921416
1317	14.890633	9.988467	1394	14.921416	10.751912
1318	9.988467	14.890633	1395	13.017418	13.017418
1319	14.921416	9.988467	1396	14.434294	11.433558
1320	9.988467	14.921416	1397	11.433558	14.434294
1321	13.876209	11.433558	1398	14.952200	10.751912
1322	11.433558	13.876209	1399	10.751912	14.952200
1323	9.988467	14.952200	1400	14.712775	11.092735
1324	14.952200	9.988467	1401	11.092735	14.712775
1325	10.751912	14.434294	1402	14.976100	10.751912
1326	14.434294	10.751912	1403	10.751912	14.976100
1327	10.370189	14.712775	1404	12.298902	13.737630
1328	14.712775	10.370189	1405	13.737630	12.298902
1329	14.976100	9.988467	1406	15.000000	10.751912
1330	9.988467	14.976100	1407	10.751912	15.000000
1331	12.035720	13.407257	1408	14.244987	11.734639
1332	13.407257	12.035720	1409	11.734639	14.244987
1333	15.000000	9.988467	1410	12.035720	14.014789
1334	9.988467	15.000000	1411	14.014789	12.035720
1335	11.092735	14.244987	1412	11.433558	14.511374
1336	14.244987	11.092735	1413	14.511374	11.433558
1337	10.751912	14.511374	1414	13.572444	12.562085
1338	14.511374	10.751912	1415	12.562085	13.572444
1339	13.737630	11.734639	1416	14.812074	11.092735
1340	11.734639	13.737630	1417	11.092735	14.812074
1341	10.370189	14.812074	1418	13.407257	12.789751
1342	14.812074	10.370189	1419	12.789751	13.407257
1343	14.014789	11.433558	1420	14.588453	11.433558
1344	11.433558	14.014789	1421	11.433558	14.588453
1345	13.017418	12.562085	1422	13.212338	13.017418
1346	12.562085	13.017418	1423	13.017418	13.212338
1347	10.751912	14.588453	1424	12.035720	14.129888
1348	14.588453	10.751912	1425	14.129888	12.035720
1349	13.572444	12.035720	1426	14.890633	11.092735
1350	12.035720	13.572444	1427	11.092735	14.890633
1351	10.370189	14.890633	1428	11.433558	14.650614
1352	14.890633	10.370189	1429	14.650614	11.433558
1353	14.650614	10.751912	1430	14.434294	11.734639

1431	11.734639	14.434294	1508	13.876209	13.017418
1432	12.562085	13.737630	1509	15.000000	11.734639
1433	13.737630	12.562085	1510	11.734639	15.000000
1434	14.952200	11.092735	1511	12.035720	14.762425
1435	11.092735	14.952200	1512	14.762425	12.035720
1436	14.712775	11.433558	1513	13.212338	13.737630
1437	11.433558	14.712775	1514	13.737630	13.812338
1438	14.014789	12.298902	1515	12.562085	14.339640
1439	12.298902	14.014789	1516	14.339640	12.562085
1440	14.244987	12.035720	1517	13.407257	13.572444
1441	12.035720	14.244987	1518	13.572444	13.407257
1442	11.092735	15.000000	1519	14.588453	12.298902
1443	15.000000	11.092735	1520	12.298902	14.588453
1444	11.433558	14.762425	1521	14.812074	12.035720
1445	14.762425	11.433558	1522	12.035720	14.812074
1446	13.407257	13.017418	1523	12.035720	14.851354
1447	13.017418	13.407257	1524	14.851354	12.035720
1448	14.812074	11.433558	1525	14.014789	13.017418
1449	11.433558	14.812074	1526	13.017418	14.014789
1450	13.876209	12.562085	1527	14.434294	12.562085
1451	12.562085	13.876209	1528	12.562085	14.434294
1452	12.035720	14.339640	1529	12.789751	14.244987
1453	14.339640	12.035720	1530	14.244987	12.789751
1454	14.588453	11.734639	1531	14.890633	12.035720
1455	11.734639	14.588453	1532	12.035720	14.890633
1456	14.851354	11.433558	1533	12.035720	14.921416
1457	11.433558	14.851354	1534	14.921416	12.035720
1458	13.737630	12.789751	1535	12.298902	14.712775
1459	12.789751	13.737630	1536	14.712775	12.298902
1460	14.890633	11.433558	1537	14.511374	12.562085
1461	11.433558	14.890633	1538	12.562085	14.511374
1462	14.434294	12.035720	1539	12.035720	14.952200
1463	12.035720	14.434294	1540	14.952200	12.035720
1464	11.433558	14.921416	1541	13.737630	13.407257
1465	14.921416	11.433558	1542	13.407257	13.737630
1466	13.017418	13.572444	1543	14.129888	13.017418
1467	13.572444	13.017418	1544	13.017418	14.129888
1468	14.712775	11.734639	1545	12.035720	14.976100
1469	11.734639	14.712775	1546	14.976100	12.035720
1470	14.244987	12.298902	1547	12.035720	15.000000
1471	12.298902	14.244987	1548	15.000000	12.035720
1472	12.562085	14.014789	1549	14.588453	12.562085
1473	14.014789	12.562085	1550	12.562085	14.588453
1474	14.952200	11.433558	1551	14.812074	12.298902
1475	11.433558	14.952200	1552	12.298902	14.812074
1476	13.212338	13.407257	1553	14.014789	13.212338
1477	13.407257	13.212338	1554	13.212338	14.014789
1478	11.433558	14.976100	1555	14.434294	12.789751
1479	14.976100	11.433558	1556	12.789751	14.434294
1480	14.511374	12.035720	1557	13.407257	13.876209
1481	12.035720	14.511374	1558	13.876209	13.407257
1482	15.000000	11.433558	1559	14.244987	13.017418
1483	11.433558	15.000000	1560	13.017418	14.244987
1484	14.812074	11.734639	1561	12.562085	14.650614
1485	11.734639	14.812074	1562	14.650614	12.562085
1486	14.129888	12.562085	1563	13.737630	13.572444
1487	12.562085	14.129888	1564	13.572444	13.737630
1488	12.035720	14.588453	1565	14.890633	12.298902
1489	14.588453	12.035720	1566	12.298902	14.890633
1490	13.737630	13.017418	1567	14.712775	12.562085
1491	13.017418	13.737630	1568	12.562085	14.712775
1492	14.890633	11.734639	1569	14.952200	12.298902
1493	11.734639	14.890633	1570	12.298902	14.952200
1494	14.650614	12.035720	1571	13.017418	14.339640
1495	12.035720	14.650614	1572	14.339640	13.017418
1496	13.407257	13.407257	1573	14.762425	12.562085
1497	14.434294	12.298902	1574	12.562085	14.762425
1498	12.298902	14.434294	1575	14.014789	13.407257
1499	14.014789	12.789751	1576	13.407257	14.014789
1500	12.789751	14.014789	1577	12.298902	15.000000
1501	14.244987	12.562085	1578	15.000000	12.298902
1502	12.562085	14.244987	1579	14.588453	12.789751
1503	14.952200	11.734639	1580	12.789751	14.588453
1504	11.734639	14.952200	1581	14.812074	12.562085
1505	12.035720	14.712775	1582	12.562085	14.812074
1506	14.712775	12.035720	1583	13.737630	13.737630
1507	13.017418	13.876209	1584	13.212338	14.244987

1585	14.244987	13.212338	1662	14.014789	14.014789
1586	14.434294	13.017418	1663	14.952200	13.017418
1587	13.017418	14.434294	1664	13.017418	14.952200
1588	14.851354	12.562085	1665	14.976100	13.017418
1589	12.562085	14.851354	1666	13.017418	14.976100
1590	13.407257	14.129888	1667	14.812074	13.212338
1591	14.129888	13.407257	1668	13.212338	14.812074
1592	14.890633	12.562085	1669	13.737630	14.339640
1593	12.562085	14.890633	1670	14.339640	13.737630
1594	14.511374	13.017418	1671	14.650614	13.407257
1595	13.017418	14.511374	1672	13.407257	14.650614
1596	12.789751	14.712775	1673	15.000000	13.017418
1597	14.712775	12.789751	1674	13.017418	15.000000
1598	12.562085	14.921416	1675	13.876209	14.244987
1599	14.921416	12.562085	1676	14.244987	13.876209
1600	14.014789	13.572444	1677	14.014789	14.129888
1601	13.572444	14.014789	1678	14.129888	14.014789
1602	13.876209	13.737630	1679	14.712775	13.407257
1603	13.737630	13.876209	1680	13.407257	14.712775
1604	12.562085	14.952200	1681	14.890633	13.212338
1605	14.952200	12.562085	1682	13.212338	14.890633
1606	12.562085	14.976100	1683	13.572444	14.588453
1607	14.976100	12.562085	1684	14.588453	13.572444
1608	13.017418	14.588453	1685	13.737630	14.434294
1609	14.588453	13.017418	1686	14.434294	13.737630
1610	14.244987	13.407257	1687	13.407257	14.762425
1611	13.407257	14.244987	1688	14.762425	13.407257
1612	12.562085	15.000000	1689	13.212338	14.952200
1613	15.000000	12.562085	1690	14.952200	13.212338
1614	14.434294	13.212338	1691	13.407257	14.812074
1615	13.212338	14.434294	1692	14.812074	13.407257
1616	12.789751	14.812074	1693	13.737630	14.511374
1617	14.812074	12.789751	1694	14.511374	13.737630
1618	13.017418	14.650614	1695	14.014789	14.244987
1619	14.650614	13.017418	1696	14.244987	14.014789
1620	13.737630	14.014789	1697	13.212338	15.000000
1621	14.014789	13.737630	1698	15.000000	13.212338
1622	14.890633	12.789751	1699	14.851354	13.407257
1623	12.789751	14.890633	1700	13.407257	14.851354
1624	13.407257	14.339640	1701	14.712775	13.572444
1625	14.339640	13.407257	1702	13.572444	14.712775
1626	14.712775	13.017418	1703	14.434294	13.876209
1627	13.017418	14.712775	1704	13.876209	14.434294
1628	13.572444	14.244987	1705	13.407257	14.890633
1629	14.244987	13.572444	1706	14.890633	13.407257
1630	14.952200	12.789751	1707	14.588453	13.737630
1631	12.789751	14.952200	1708	13.737630	14.588453
1632	13.017418	14.762425	1709	14.014789	14.339640
1633	14.762425	13.017418	1710	14.339640	14.014789
1634	14.588453	13.212338	1711	13.407257	14.921416
1635	13.212338	14.588453	1712	14.921416	13.407257
1636	13.407257	14.434294	1713	14.129888	14.244987
1637	14.434294	13.407257	1714	14.244987	14.129888
1638	13.737630	14.129888	1715	13.407257	14.952200
1639	14.129888	13.737630	1716	14.952200	13.407257
1640	12.789751	15.000000	1717	13.737630	14.650614
1641	15.000000	12.789751	1718	14.650614	13.737630
1642	13.017418	14.812074	1719	13.572444	14.812074
1643	14.812074	13.017418	1720	14.812074	13.572444
1644	14.014789	13.876209	1721	13.407257	14.976100
1645	13.876209	14.014789	1722	14.976100	13.407257
1646	14.851354	13.017418	1723	15.000000	13.407257
1647	13.017418	14.851354	1724	13.407257	15.000000
1648	14.511374	13.407257	1725	14.434294	14.014789
1649	13.407257	14.511374	1726	14.014789	14.434294
1650	13.212338	14.712775	1727	14.712775	13.737630
1651	14.712775	13.212338	1728	13.737630	14.712775
1652	14.890633	13.017418	1729	14.588453	13.876209
1653	13.017418	14.890633	1730	13.876209	14.588453
1654	14.244987	13.737630	1731	14.244987	14.244987
1655	13.737630	14.244987	1732	14.890633	13.572444
1656	14.921416	13.017418	1733	13.572444	14.890633
1657	13.017418	14.921416	1734	13.737630	14.762425
1658	13.572444	14.434294	1735	14.762425	13.737630
1659	14.434294	13.572444	1736	14.014789	14.511374
1660	13.407257	14.588453	1737	14.511374	14.014789
1661	14.588453	13.407257	1738	13.572444	14.952200

1739	14.952200	13.572444	1816	14.588453	14.434294
1740	14.434294	14.129888	1817	14.890633	14.129888
1741	14.129888	14.434294	1818	14.129888	14.890633
1742	14.812074	13.737630	1819	14.014789	15.000000
1743	13.737630	14.812074	1820	15.000000	14.014789
1744	14.244987	14.339640	1821	14.712775	14.339640
1745	14.339640	14.244987	1822	14.339640	14.712775
1746	14.712775	13.876209	1823	14.244987	14.812074
1747	13.876209	14.712775	1824	14.812074	14.244987
1748	13.572444	15.000000	1825	14.650614	14.434294
1749	15.000000	13.572444	1826	14.434294	14.650614
1750	14.014789	14.588453	1827	14.129888	14.952200
1751	14.588453	14.014789	1828	14.952200	14.129888
1752	14.851354	13.737630	1829	14.511374	14.588453
1753	13.737630	14.851354	1830	14.588453	14.511374
1754	14.890633	13.737630	1831	14.851354	14.244987
1755	13.737630	14.890633	1832	14.244987	14.851354
1756	14.014789	14.650614	1833	14.244987	14.890633
1757	14.650614	14.014789	1834	14.890633	14.244987
1758	14.434294	14.244987	1835	14.129888	15.000000
1759	14.244987	14.434294	1836	15.000000	14.129888
1760	14.921416	13.737630	1837	14.712775	14.434294
1761	13.737630	14.921416	1838	14.434294	14.712775
1762	13.876209	14.812074	1839	14.812074	14.339640
1763	14.812074	13.876209	1840	14.339640	14.812074
1764	14.952200	13.737630	1841	14.921416	14.244987
1765	13.737630	14.952200	1842	14.244987	14.921416
1766	14.588453	14.129888	1843	14.588453	14.588453
1767	14.129888	14.588453	1844	14.434294	14.762425
1768	14.014789	14.712775	1845	14.762425	14.434294
1769	14.712775	14.014789	1846	14.244987	14.952200
1770	13.737630	14.976100	1847	14.952200	14.244987
1771	14.976100	13.737630	1848	14.712775	14.511374
1772	14.511374	14.244987	1849	14.511374	14.712775
1773	14.244987	14.511374	1850	14.244987	14.976100
1774	13.737630	15.000000	1851	14.976100	14.244987
1775	15.000000	13.737630	1852	14.890633	14.339640
1776	14.434294	14.339640	1853	14.339640	14.890633
1777	14.339640	14.434294	1854	14.588453	14.650614
1778	14.890633	13.876209	1855	14.650614	14.588453
1779	13.876209	14.890633	1856	14.434294	14.812074
1780	14.014789	14.762425	1857	14.812074	14.434294
1781	14.762425	14.014789	1858	15.000000	14.244987
1782	14.588453	14.244987	1859	14.244987	15.000000
1783	14.244987	14.588453	1860	14.434294	14.851354
1784	14.812074	14.014789	1861	14.851354	14.434294
1785	14.014789	14.812074	1862	14.339640	14.952200
1786	14.952200	13.876209	1863	14.952200	14.339640
1787	13.876209	14.952200	1864	14.712775	14.588453
1788	14.712775	14.129888	1865	14.588453	14.712775
1789	14.129888	14.712775	1866	14.812074	14.511374
1790	14.434294	14.434294	1867	14.511374	14.812074
1791	14.851354	14.014789	1868	14.890633	14.434294
1792	14.014789	14.851354	1869	14.434294	14.890633
1793	15.000000	13.876209	1870	15.000000	14.339640
1794	13.876209	15.000000	1871	14.339640	15.000000
1795	14.244987	14.650614	1872	14.762425	14.588453
1796	14.650614	14.244987	1873	14.588453	14.762425
1797	14.014789	14.890633	1874	14.921416	14.434294
1798	14.890633	14.014789	1875	14.434294	14.921416
1799	14.588453	14.339640	1876	14.650614	14.712775
1800	14.339640	14.588453	1877	14.712775	14.650614
1801	14.434294	14.511374	1878	14.434294	14.952200
1802	14.511374	14.434294	1879	14.952200	14.434294
1803	14.812074	14.129888	1880	14.588453	14.812074
1804	14.129888	14.812074	1881	14.812074	14.588453
1805	14.014789	14.921416	1882	14.890633	14.511374
1806	14.921416	14.014789	1883	14.511374	14.890633
1807	14.712775	14.244987	1884	14.976100	14.434294
1808	14.244987	14.712775	1885	14.434294	14.976100
1809	14.014789	14.952200	1886	14.712775	14.712775
1810	14.952200	14.014789	1887	15.000000	14.434294
1811	14.014789	14.976100	1888	14.434294	15.000000
1812	14.976100	14.014789	1889	14.588453	14.851354
1813	14.244987	14.762425	1890	14.851354	14.588453
1814	14.762425	14.244987	1891	14.812074	14.650614
1815	14.434294	14.588453	1892	14.650614	14.812074

1893	14.511374	14.952200	1935	14.812074	14.890633
1894	14.952200	14.511374	1936	14.712775	15.000000
1895	14.762425	14.712775	1937	15.000000	14.712775
1896	14.712775	14.762425	1938	14.762425	14.952200
1897	14.890633	14.588453	1939	14.952200	14.762425
1898	14.588453	14.890633	1940	14.812074	14.921416
1899	14.921416	14.588453	1941	14.921416	14.812074
1900	14.588453	14.921416	1942	14.851354	14.890633
1901	15.000000	14.511374	1943	14.890633	14.851354
1902	14.511374	15.000000	1944	15.000000	14.762425
1903	14.712775	14.812074	1945	14.762425	15.000000
1904	14.812074	14.712775	1946	14.812074	14.952200
1905	14.890633	14.650614	1947	14.952200	14.812074
1906	14.650614	14.890633	1948	14.890633	14.890633
1907	14.952200	14.588453	1949	14.976100	14.812074
1908	14.588453	14.952200	1950	14.812074	14.976100
1909	14.712775	14.851354	1951	14.851354	14.952200
1910	14.851354	14.712775	1952	14.952200	14.851354
1911	14.976100	14.588453	1953	14.890633	14.921416
1912	14.588453	14.976100	1954	14.921416	14.890633
1913	14.762425	14.812074	1955	14.812074	15.000000
1914	14.812074	14.762425	1956	15.000000	14.812074
1915	14.588453	15.000000	1957	14.890633	14.952200
1916	15.000000	14.588453	1958	14.952200	14.890633
1917	14.890633	14.712775	1959	14.851354	15.000000
1918	14.712775	14.890633	1960	15.000000	14.851354
1919	14.650614	14.952200	1961	14.890633	14.976100
1920	14.952200	14.650614	1962	14.976100	14.890633
1921	14.812074	14.812074	1963	14.921416	14.952200
1922	14.712775	14.921416	1964	14.952200	14.921416
1923	14.921416	14.712775	1965	14.890633	15.000000
1924	14.650614	15.000000	1966	15.000000	14.890633
1925	15.000000	14.650614	1967	14.952200	14.952200
1926	14.890633	14.762425	1968	14.921416	15.000000
1927	14.762425	14.890633	1969	15.000000	14.921416
1928	14.851354	14.812074	1970	14.976100	14.952200
1929	14.812074	14.851354	1971	14.952200	14.976100
1930	14.712775	14.952200	1972	15.000000	14.952200
1931	14.952200	14.712775	1973	14.952200	15.000000
1932	14.712775	14.976100	1974	15.000000	14.976100
1933	14.976100	14.712775	1975	14.976100	15.000000
1934	14.890633	14.812074	1976	15.000000	15.000000

§ Connectivities and identifier of the element material

1	730	731	747	758	766	751	745	735	4
2	701	705	727	738	747	731	730	713	4
3	676	681	691	708	727	705	701	690	4
4	649	653	667	678	691	681	676	666	4
5	621	625	635	648	667	653	649	637	4
6	593	596	603	617	635	625	621	605	4
7	551	559	563	588	603	596	593	570	4
8	516	519	522	547	563	559	551	540	4
9	471	480	490	509	522	519	516	505	4
10	440	442	446	465	490	480	471	462	4
11	396	401	405	433	446	442	440	410	4
12	351	353	364	384	405	401	396	377	4
13	314	319	322	341	364	353	351	334	4
14	275	276	279	298	322	319	314	296	4
15	232	234	239	256	279	276	275	253	4
16	194	195	199	217	239	234	232	213	4
17	158	159	164	179	199	195	194	175	4
18	122	124	128	145	164	159	158	142	4
19	93	96	99	112	128	124	122	111	4
20	68	70	72	85	99	96	93	82	4
21	45	47	51	60	72	70	68	56	4
22	27	29	31	40	51	47	45	37	4
23	13	15	18	24	31	29	27	20	4
24	5	6	8	11	18	15	13	10	4
25	1	2	4	7	8	6	5	3	4
26	747	772	793	801	809	784	766	758	4
27	727	753	780	790	793	772	747	738	4
28	691	723	755	768	780	753	727	708	4
29	667	685	721	740	755	723	691	678	4
30	635	651	673	693	721	685	667	648	4
31	603	612	639	655	673	651	635	617	4
32	563	577	600	614	639	612	603	588	4
33	522	542	553	574	600	577	563	547	4
34	490	502	513	533	553	542	522	509	4

35	446	458	466	495	513	502	490	465	4
36	405	409	428	444	466	458	446	433	4
37	364	371	381	403	428	409	405	384	4
38	322	327	335	349	381	371	364	341	4
39	279	283	289	310	335	327	322	298	4
40	239	243	250	268	289	283	279	256	4
41	199	203	210	226	250	243	239	217	4
42	164	168	174	189	210	203	199	179	4
43	128	133	138	149	174	168	164	145	4
44	99	100	106	119	138	133	128	112	4
45	72	76	78	90	106	100	99	85	4
46	51	53	57	66	78	76	72	60	4
47	31	35	39	48	57	53	51	40	4
48	18	22	25	33	39	35	31	24	4
49	8	12	17	21	25	22	18	11	4
50	4	9	14	16	17	12	8	7	4
51	793	825	858	865	872	836	809	801	4
52	780	813	843	851	858	825	793	790	4
53	755	792	826	835	843	813	780	768	4
54	721	762	803	817	826	792	755	740	4
55	673	719	769	787	803	762	721	693	4
56	639	670	715	744	769	719	673	655	4
57	600	623	660	683	715	670	639	614	4
58	553	576	610	632	660	623	600	574	4
59	513	528	555	581	610	576	553	533	4
60	466	486	506	526	555	528	513	495	4
61	428	439	460	479	506	486	466	444	4
62	381	392	407	437	460	439	428	403	4
63	335	346	360	386	407	392	381	349	4
64	289	302	316	339	360	346	335	310	4
65	250	259	271	294	316	302	289	268	4
66	210	218	228	248	271	259	250	226	4
67	174	181	188	208	228	218	210	189	4
68	138	147	152	171	188	181	174	149	4
69	106	115	121	136	152	147	138	119	4
70	78	88	95	109	121	115	106	90	4
71	57	64	74	84	95	88	78	66	4
72	39	42	54	62	74	64	57	48	4
73	25	32	38	43	54	42	39	33	4
74	17	23	30	34	38	32	25	21	4
75	14	19	26	28	30	23	17	16	4
76	858	893	933	935	939	899	872	865	4
77	843	883	915	924	933	893	858	851	4
78	826	867	900	909	915	883	843	835	4
79	803	841	885	890	900	867	826	817	4
80	769	814	857	874	885	841	803	787	4
81	715	776	823	839	857	814	769	744	4
82	660	709	777	799	823	776	715	683	4
83	610	646	698	742	777	709	660	632	4
84	555	592	627	664	698	646	610	581	4
85	506	530	566	598	627	592	555	526	4
86	460	475	510	537	566	530	506	479	4
87	407	435	452	469	510	475	460	437	4
88	360	380	399	431	452	435	407	386	4
89	316	330	348	376	399	380	360	339	4
90	271	285	299	326	348	330	316	294	4
91	228	241	255	281	299	285	271	248	4
92	188	201	215	236	255	241	228	208	4
93	152	165	178	198	215	201	188	171	4
94	121	134	144	162	178	165	152	136	4
95	95	105	117	131	144	134	121	109	4
96	74	79	89	102	117	105	95	84	4
97	54	61	73	80	89	79	74	62	4
98	38	49	58	63	73	61	54	43	4
99	30	41	50	52	58	49	38	34	4
100	26	36	44	46	50	41	30	28	4
101	933	966	1006	1009	1015	977	939	935	4
102	915	954	993	996	1006	966	933	924	4
103	900	940	981	991	993	954	915	909	4
104	885	921	965	973	981	940	900	890	4
105	857	896	943	951	965	921	885	874	4
106	823	870	911	927	943	896	857	839	4
107	777	829	876	895	911	870	823	799	4
108	698	774	831	852	876	829	777	742	4
109	627	679	760	795	831	774	698	664	4
110	566	607	662	703	760	679	627	598	4
111	510	544	584	615	662	607	566	537	4

112	452	473	514	545	584	544	510	469	4
113	399	427	449	476	514	473	452	431	4
114	348	373	395	425	449	427	399	376	4
115	299	324	344	370	395	373	348	326	4
116	255	272	291	318	344	324	299	281	4
117	215	231	247	267	291	272	255	236	4
118	178	191	206	225	247	231	215	198	4
119	144	155	169	186	206	191	178	162	4
120	117	127	140	154	169	155	144	131	4
121	89	103	116	126	140	127	117	102	4
122	73	83	94	104	116	103	89	80	4
123	58	65	77	87	94	83	73	63	4
124	50	59	71	75	77	65	58	52	4
125	44	55	67	69	71	59	50	46	4
126	1006	1045	1081	1091	1094	1054	1015	1009	4
127	993	1032	1075	1080	1081	1045	1006	996	4
128	981	1023	1062	1070	1075	1032	993	991	4
129	965	1005	1050	1055	1062	1023	981	973	4
130	943	983	1027	1034	1050	1005	965	951	4
131	911	957	998	1013	1027	983	943	927	4
132	876	922	968	987	998	957	911	895	4
133	831	881	931	947	968	922	876	852	4
134	760	821	879	902	931	881	831	795	4
135	662	734	810	845	879	821	760	703	4
136	584	630	700	764	810	734	662	615	4
137	514	549	601	643	700	630	584	545	4
138	449	482	521	557	601	549	514	476	4
139	395	422	450	485	521	482	449	425	4
140	344	367	390	415	450	422	395	370	4
141	291	312	337	365	390	367	344	318	4
142	247	264	287	308	337	312	291	267	4
143	206	223	244	262	287	264	247	225	4
144	169	184	205	221	244	223	206	186	4
145	140	153	170	183	205	184	169	154	4
146	116	130	143	156	170	153	140	126	4
147	94	108	120	135	143	130	116	104	4
148	77	91	107	114	120	108	94	87	4
149	71	86	98	101	107	91	77	75	4
150	67	81	92	97	98	86	71	69	4
151	1081	1123	1165	1167	1174	1134	1094	1091	4
152	1075	1115	1158	1160	1165	1123	1081	1080	4
153	1062	1102	1142	1147	1158	1115	1075	1070	4
154	1050	1088	1130	1137	1142	1102	1062	1055	4
155	1027	1068	1112	1120	1130	1088	1050	1034	4
156	998	1042	1085	1097	1112	1068	1027	1013	4
157	968	1011	1057	1072	1085	1042	998	987	4
158	931	974	1021	1037	1057	1011	968	947	4
159	879	928	979	994	1021	974	931	902	4
160	810	869	918	949	979	928	879	845	4
161	700	785	848	888	918	869	810	764	4
162	601	657	750	805	848	785	700	643	4
163	521	561	620	672	750	657	601	557	4
164	450	488	525	567	620	561	521	485	4
165	390	418	455	492	525	488	450	415	4
166	337	362	388	413	455	418	390	365	4
167	287	305	331	358	388	362	337	308	4
168	244	260	286	304	331	305	287	262	4
169	205	220	245	261	286	260	244	221	4
170	170	185	207	222	245	220	205	183	4
171	143	161	177	192	207	185	170	156	4
172	120	137	151	166	177	161	143	135	4
173	107	118	139	148	151	137	120	114	4
174	98	113	129	132	139	118	107	101	4
175	92	110	123	125	129	113	98	97	4
176	1165	1203	1242	1247	1256	1215	1174	1167	4
177	1158	1199	1237	1241	1242	1203	1165	1160	4
178	1142	1184	1225	1228	1237	1199	1158	1147	4
179	1130	1169	1211	1216	1225	1184	1142	1137	4
180	1112	1149	1197	1201	1211	1169	1130	1120	4
181	1085	1128	1171	1178	1197	1149	1112	1097	4
182	1057	1100	1140	1155	1171	1128	1085	1072	4
183	1021	1063	1108	1125	1140	1100	1057	1037	4
184	979	1026	1066	1089	1108	1063	1021	994	4
185	918	970	1017	1040	1066	1026	979	949	4
186	848	907	959	988	1017	970	918	888	4
187	750	819	886	917	959	907	848	805	4
188	620	687	781	833	886	819	750	672	4

189	525	571	633	696	781	687	620	567	4
190	455	497	534	579	633	571	525	492	4
191	388	421	456	499	534	497	455	413	4
192	331	355	387	416	456	421	388	358	4
193	286	303	332	356	387	355	331	304	4
194	245	263	288	306	332	303	286	261	4
195	207	224	246	265	288	263	245	222	4
196	177	197	214	230	246	224	207	192	4
197	151	172	187	202	214	197	177	166	4
198	139	150	173	182	187	172	151	148	4
199	129	146	163	167	173	150	139	132	4
200	123	141	157	160	163	146	129	125	4
201	1242	1282	1323	1330	1334	1291	1256	1247	4
202	1237	1275	1318	1320	1323	1282	1242	1241	4
203	1225	1266	1299	1308	1318	1275	1237	1228	4
204	1211	1249	1289	1295	1299	1266	1225	1216	4
205	1197	1230	1273	1279	1289	1249	1211	1201	4
206	1171	1209	1251	1261	1273	1230	1197	1178	4
207	1140	1183	1221	1238	1251	1209	1171	1155	4
208	1108	1146	1193	1204	1221	1183	1140	1125	4
209	1066	1109	1151	1172	1193	1146	1108	1089	4
210	1017	1059	1105	1132	1151	1109	1066	1040	4
211	959	1002	1052	1078	1105	1059	1017	988	4
212	886	936	985	1020	1052	1002	959	917	4
213	781	847	904	944	985	936	886	833	4
214	633	712	797	855	904	847	781	696	4
215	534	586	641	717	797	712	633	579	4
216	456	501	538	589	641	586	534	499	4
217	387	417	457	500	538	501	456	416	4
218	332	357	389	420	457	417	387	356	4
219	288	307	338	361	389	357	332	306	4
220	246	266	292	311	338	307	288	265	4
221	214	237	254	273	292	266	246	230	4
222	187	209	229	240	254	237	214	202	4
223	173	190	211	219	229	209	187	182	4
224	163	180	200	204	211	190	173	167	4
225	157	176	193	196	200	180	163	160	4
226	1323	1360	1399	1403	1407	1367	1334	1330	4
227	1318	1351	1388	1393	1399	1360	1323	1320	4
228	1299	1341	1380	1384	1388	1351	1318	1308	4
229	1289	1327	1364	1372	1380	1341	1299	1295	4
230	1273	1309	1347	1354	1364	1327	1289	1279	4
231	1251	1288	1325	1337	1347	1309	1273	1261	4
232	1221	1262	1298	1314	1325	1288	1251	1238	4
233	1193	1227	1271	1284	1298	1262	1221	1204	4
234	1151	1195	1233	1252	1271	1227	1193	1172	4
235	1105	1144	1186	1207	1233	1195	1151	1132	4
236	1052	1096	1135	1162	1186	1144	1105	1078	4
237	985	1029	1074	1104	1135	1096	1052	1020	4
238	904	953	1001	1036	1074	1029	985	944	4
239	797	860	913	960	1001	953	904	855	4
240	641	726	807	862	913	860	797	717	4
241	538	590	642	725	807	726	641	589	4
242	457	498	535	585	642	590	538	500	4
243	389	412	454	496	535	498	457	420	4
244	338	366	391	419	454	412	389	361	4
245	292	317	343	368	391	366	338	311	4
246	254	280	300	323	343	317	292	273	4
247	229	249	270	284	300	280	254	240	4
248	211	227	251	258	270	249	229	219	4
249	200	216	238	242	251	227	211	204	4
250	193	212	233	235	238	216	200	196	4
251	1399	1435	1475	1478	1483	1442	1407	1403	4
252	1388	1427	1461	1464	1475	1435	1399	1393	4
253	1380	1417	1449	1457	1461	1427	1388	1384	4
254	1364	1401	1437	1444	1449	1417	1380	1372	4
255	1347	1382	1421	1428	1437	1401	1364	1354	4
256	1325	1362	1397	1412	1421	1382	1347	1337	4
257	1298	1335	1375	1386	1397	1362	1325	1314	4
258	1271	1305	1344	1355	1375	1335	1298	1284	4
259	1233	1269	1303	1322	1344	1305	1271	1252	4
260	1186	1223	1265	1281	1303	1269	1233	1207	4
261	1135	1177	1212	1234	1265	1223	1186	1162	4
262	1074	1113	1154	1181	1212	1177	1135	1104	4
263	1001	1044	1084	1118	1154	1113	1074	1036	4
264	913	963	1008	1047	1084	1044	1001	960	4
265	807	863	912	962	1008	963	913	862	4

266	642	718	798	861	912	863	807	725	4
267	535	580	634	711	798	718	642	585	4
268	454	493	524	572	634	580	535	496	4
269	391	414	451	489	524	493	454	419	4
270	343	369	394	423	451	414	391	368	4
271	300	325	347	374	394	369	343	323	4
272	270	293	315	329	347	325	300	284	4
273	251	269	290	301	315	293	270	258	4
274	238	257	278	282	290	269	251	242	4
275	233	252	274	277	278	257	238	235	4
276	1475	1504	1539	1545	1547	1510	1483	1478	4
277	1461	1493	1532	1533	1539	1504	1475	1464	4
278	1449	1485	1522	1523	1532	1493	1461	1457	4
279	1437	1469	1505	1511	1522	1485	1449	1444	4
280	1421	1455	1488	1495	1505	1469	1437	1428	4
281	1397	1431	1463	1481	1488	1455	1421	1412	4
282	1375	1409	1441	1452	1463	1431	1397	1386	4
283	1344	1377	1410	1424	1441	1409	1375	1355	4
284	1303	1340	1374	1390	1410	1377	1344	1322	4
285	1265	1294	1331	1350	1374	1340	1303	1281	4
286	1212	1245	1276	1301	1331	1294	1265	1234	4
287	1154	1189	1219	1255	1276	1245	1212	1181	4
288	1084	1121	1159	1191	1219	1189	1154	1118	4
289	1008	1048	1083	1122	1159	1121	1084	1047	4
290	912	961	1000	1043	1083	1048	1008	962	4
291	798	854	905	952	1000	961	912	861	4
292	634	695	782	846	905	854	798	711	4
293	524	568	619	688	782	695	634	572	4
294	451	484	520	562	619	568	524	489	4
295	394	424	448	483	520	484	451	423	4
296	347	375	398	426	448	424	394	374	4
297	315	340	359	379	398	375	347	329	4
298	290	309	336	345	359	340	315	301	4
299	278	297	321	328	336	309	290	282	4
300	274	295	313	320	321	297	278	277	4
301	1539	1570	1604	1606	1612	1577	1547	1545	4
302	1532	1566	1593	1598	1604	1570	1539	1533	4
303	1522	1552	1582	1589	1593	1566	1532	1523	4
304	1505	1535	1568	1574	1582	1552	1522	1511	4
305	1488	1520	1550	1561	1568	1535	1505	1495	4
306	1463	1498	1528	1538	1550	1520	1488	1481	4
307	1441	1471	1502	1515	1528	1498	1463	1452	4
308	1410	1439	1472	1487	1502	1471	1441	1424	4
309	1374	1404	1432	1451	1472	1439	1410	1390	4
310	1331	1358	1392	1415	1432	1404	1374	1350	4
311	1276	1312	1346	1366	1392	1358	1331	1301	4
312	1219	1259	1286	1316	1346	1312	1276	1255	4
313	1159	1190	1218	1258	1286	1259	1219	1191	4
314	1083	1117	1153	1188	1218	1190	1159	1122	4
315	1000	1035	1073	1114	1153	1117	1083	1043	4
316	905	945	984	1030	1073	1035	1000	952	4
317	782	832	887	937	984	945	905	846	4
318	619	671	749	818	887	832	782	688	4
319	520	558	602	658	749	671	619	562	4
320	448	477	515	550	602	558	520	483	4
321	398	430	453	472	515	477	448	426	4
322	359	385	406	434	453	430	398	379	4
323	336	350	382	393	406	385	359	345	4
324	321	342	363	372	382	350	336	328	4
325	313	333	352	354	363	342	321	320	4
326	1604	1631	1664	1666	1674	1640	1612	1606	4
327	1593	1623	1653	1657	1664	1631	1604	1598	4
328	1582	1616	1642	1647	1653	1623	1593	1589	4
329	1568	1596	1627	1632	1642	1616	1582	1574	4
330	1550	1580	1608	1618	1627	1596	1568	1561	4
331	1528	1556	1587	1595	1608	1580	1550	1538	4
332	1502	1529	1560	1571	1587	1556	1528	1515	4
333	1472	1500	1526	1544	1560	1529	1502	1487	4
334	1432	1459	1491	1507	1526	1500	1472	1451	4
335	1392	1419	1447	1466	1491	1459	1432	1415	4
336	1346	1369	1395	1423	1447	1419	1392	1366	4
337	1286	1315	1345	1370	1395	1369	1346	1316	4
338	1218	1254	1277	1311	1345	1315	1286	1258	4
339	1153	1180	1213	1244	1277	1254	1218	1188	4
340	1073	1103	1136	1176	1213	1180	1153	1114	4
341	984	1019	1051	1095	1136	1103	1073	1030	4
342	887	916	958	1003	1051	1019	984	937	4

343	749	806	849	906	958	916	887	818	4
344	602	644	699	786	849	806	749	658	4
345	515	546	583	629	699	644	602	550	4
346	453	468	511	543	583	546	515	472	4
347	406	436	461	474	511	468	453	434	4
348	382	402	429	438	461	436	406	393	4
349	363	383	404	408	429	402	382	372	4
350	352	378	397	400	404	383	363	354	4
351	1664	1689	1715	1721	1724	1697	1674	1666	4
352	1653	1682	1705	1711	1715	1689	1664	1657	4
353	1642	1668	1691	1700	1705	1682	1653	1647	4
354	1627	1650	1680	1687	1691	1668	1642	1632	4
355	1608	1635	1660	1672	1680	1650	1627	1618	4
356	1587	1615	1636	1649	1660	1635	1608	1595	4
357	1560	1584	1611	1624	1636	1615	1587	1571	4
358	1526	1554	1576	1590	1611	1584	1560	1544	4
359	1491	1513	1542	1557	1576	1554	1526	1507	4
360	1447	1476	1496	1517	1542	1513	1491	1466	4
361	1395	1422	1446	1477	1496	1476	1447	1423	4
362	1345	1365	1391	1418	1446	1422	1395	1370	4
363	1277	1302	1332	1357	1391	1365	1345	1311	4
364	1213	1235	1264	1293	1332	1302	1277	1244	4
365	1136	1163	1187	1222	1264	1235	1213	1176	4
366	1051	1077	1106	1143	1187	1163	1136	1095	4
367	958	989	1018	1060	1106	1077	1051	1003	4
368	849	889	919	971	1018	989	958	906	4
369	699	763	811	868	919	889	849	786	4
370	583	616	661	733	811	763	699	629	4
371	511	536	565	608	661	616	583	543	4
372	461	478	507	531	565	536	511	474	4
373	429	445	467	487	507	478	461	438	4
374	404	432	447	459	467	445	429	408	4
375	397	411	441	443	447	432	404	400	4
376	1715	1738	1765	1770	1774	1748	1724	1721	4
377	1705	1733	1755	1761	1765	1738	1715	1711	4
378	1691	1719	1743	1753	1755	1733	1705	1700	4
379	1680	1702	1728	1734	1743	1719	1691	1687	4
380	1660	1683	1708	1717	1728	1702	1680	1672	4
381	1636	1658	1685	1693	1708	1683	1660	1649	4
382	1611	1628	1655	1669	1685	1658	1636	1624	4
383	1576	1601	1620	1638	1655	1628	1611	1590	4
384	1542	1564	1583	1603	1620	1601	1576	1557	4
385	1496	1518	1541	1563	1583	1564	1542	1517	4
386	1446	1467	1490	1514	1541	1518	1496	1477	4
387	1391	1414	1433	1458	1490	1467	1446	1418	4
388	1332	1349	1373	1405	1433	1414	1391	1357	4
389	1264	1280	1304	1339	1373	1349	1332	1293	4
390	1187	1206	1232	1268	1304	1280	1264	1222	4
391	1106	1131	1152	1194	1232	1206	1187	1143	4
392	1018	1039	1065	1110	1152	1131	1106	1060	4
393	919	948	978	1025	1065	1039	1018	971	4
394	811	844	878	929	978	948	919	868	4
395	661	704	759	820	878	844	811	733	4
396	565	597	628	680	759	704	661	608	4
397	507	527	556	591	628	597	565	531	4
398	467	494	512	529	556	527	507	487	4
399	447	464	491	503	512	494	467	459	4
400	441	463	470	481	491	464	447	443	4
401	1765	1787	1809	1811	1819	1794	1774	1770	4
402	1755	1779	1797	1805	1809	1787	1765	1761	4
403	1743	1762	1785	1792	1797	1779	1755	1753	4
404	1728	1747	1768	1780	1785	1762	1743	1734	4
405	1708	1730	1750	1756	1768	1747	1728	1717	4
406	1685	1704	1726	1736	1750	1730	1708	1693	4
407	1655	1675	1695	1709	1726	1704	1685	1669	4
408	1620	1645	1662	1677	1695	1675	1655	1638	4
409	1583	1602	1621	1644	1662	1645	1620	1603	4
410	1541	1558	1575	1600	1621	1602	1583	1563	4
411	1490	1508	1525	1553	1575	1558	1541	1514	4
412	1433	1450	1473	1499	1525	1508	1490	1458	4
413	1373	1389	1411	1438	1473	1450	1433	1405	4
414	1304	1321	1343	1378	1411	1389	1373	1339	4
415	1232	1253	1270	1306	1343	1321	1304	1268	4
416	1152	1173	1192	1226	1270	1253	1232	1194	4
417	1065	1090	1107	1145	1192	1173	1152	1110	4
418	978	995	1022	1064	1107	1090	1065	1025	4
419	878	903	930	975	1022	995	978	929	4

420	759	796	830	880	930	903	878	820	4
421	628	663	697	773	830	796	759	680	4
422	556	582	609	645	697	663	628	591	4
423	512	532	554	575	609	582	556	529	4
424	491	508	523	541	554	532	512	503	4
425	470	504	517	518	523	508	491	481	4
426	1809	1827	1846	1850	1859	1835	1819	1811	4
427	1797	1818	1833	1842	1846	1827	1809	1805	4
428	1785	1804	1823	1832	1833	1818	1797	1792	4
429	1768	1789	1808	1813	1823	1804	1785	1780	4
430	1750	1767	1783	1795	1808	1789	1768	1756	4
431	1726	1741	1759	1773	1783	1767	1750	1736	4
432	1695	1713	1731	1744	1759	1741	1726	1709	4
433	1662	1678	1696	1714	1731	1713	1695	1677	4
434	1621	1639	1654	1676	1696	1678	1662	1644	4
435	1575	1591	1610	1629	1654	1639	1621	1600	4
436	1525	1543	1559	1585	1610	1591	1575	1553	4
437	1473	1486	1501	1530	1559	1543	1525	1499	4
438	1411	1425	1440	1470	1501	1486	1473	1438	4
439	1343	1356	1376	1408	1440	1425	1411	1378	4
440	1270	1285	1297	1336	1376	1356	1343	1306	4
441	1192	1205	1220	1263	1297	1285	1270	1226	4
442	1107	1126	1139	1182	1220	1205	1192	1145	4
443	1022	1038	1058	1099	1139	1126	1107	1064	4
444	930	946	969	1012	1058	1038	1022	975	4
445	830	853	877	923	969	946	930	880	4
446	697	741	778	828	877	853	830	773	4
447	609	631	659	710	778	741	697	645	4
448	554	573	599	624	659	631	609	575	4
449	523	548	564	578	599	573	554	541	4
450	517	539	552	560	564	548	523	518	4
451	1846	1862	1878	1885	1888	1871	1859	1850	4
452	1833	1853	1869	1875	1878	1862	1846	1842	4
453	1823	1840	1856	1860	1869	1853	1833	1832	4
454	1808	1822	1838	1844	1856	1840	1823	1813	4
455	1783	1800	1815	1826	1838	1822	1808	1795	4
456	1759	1777	1790	1801	1815	1800	1783	1773	4
457	1731	1745	1758	1776	1790	1777	1759	1744	4
458	1696	1710	1725	1740	1758	1745	1731	1714	4
459	1654	1670	1686	1703	1725	1710	1696	1676	4
460	1610	1625	1637	1659	1686	1670	1654	1629	4
461	1559	1572	1586	1614	1637	1625	1610	1585	4
462	1501	1516	1527	1555	1586	1572	1559	1530	4
463	1440	1453	1462	1497	1527	1516	1501	1470	4
464	1376	1385	1396	1430	1462	1453	1440	1408	4
465	1297	1313	1326	1361	1396	1385	1376	1336	4
466	1220	1239	1250	1287	1326	1313	1297	1263	4
467	1139	1156	1170	1208	1250	1239	1220	1182	4
468	1058	1071	1086	1127	1170	1156	1139	1099	4
469	969	986	999	1041	1086	1071	1058	1012	4
470	877	894	910	956	999	986	969	923	4
471	778	800	822	871	910	894	877	828	4
472	659	684	716	775	822	800	778	710	4
473	599	613	640	669	716	684	659	624	4
474	564	587	604	611	640	613	599	578	4
475	552	569	594	595	604	587	564	560	4
476	1878	1893	1908	1912	1915	1902	1888	1885	4
477	1869	1883	1898	1900	1908	1893	1878	1875	4
478	1856	1867	1880	1889	1898	1883	1869	1860	4
479	1838	1849	1865	1873	1880	1867	1856	1844	4
480	1815	1829	1843	1854	1865	1849	1838	1826	4
481	1790	1802	1816	1830	1843	1829	1815	1801	4
482	1758	1772	1782	1799	1816	1802	1790	1776	4
483	1725	1737	1751	1766	1782	1772	1758	1740	4
484	1686	1694	1707	1729	1751	1737	1725	1703	4
485	1637	1648	1661	1684	1707	1694	1686	1659	4
486	1586	1594	1609	1634	1661	1648	1637	1614	4
487	1527	1537	1549	1579	1609	1594	1586	1555	4
488	1462	1480	1489	1519	1549	1537	1527	1497	4
489	1396	1413	1420	1454	1489	1480	1462	1430	4
490	1326	1338	1348	1381	1420	1413	1396	1361	4
491	1250	1260	1272	1310	1348	1338	1326	1287	4
492	1170	1179	1196	1231	1272	1260	1250	1208	4
493	1086	1098	1111	1150	1196	1179	1170	1127	4
494	999	1014	1028	1067	1111	1098	1086	1041	4
495	910	926	942	982	1028	1014	999	956	4
496	822	838	856	897	942	926	910	871	4

497	716	743	770	815	856	838	822	775	4
498	640	656	674	720	770	743	716	669	4
499	604	618	636	652	674	656	640	611	4
500	594	606	622	626	636	618	604	595	4
501	1908	1919	1930	1932	1936	1924	1915	1912	4
502	1898	1906	1918	1922	1930	1919	1908	1900	4
503	1880	1892	1903	1909	1918	1906	1898	1889	4
504	1865	1876	1886	1896	1903	1892	1880	1873	4
505	1843	1855	1864	1877	1886	1876	1865	1854	4
506	1816	1825	1837	1848	1864	1855	1843	1830	4
507	1782	1796	1807	1821	1837	1825	1816	1799	4
508	1751	1757	1769	1788	1807	1796	1782	1766	4
509	1707	1718	1727	1746	1769	1757	1751	1729	4
510	1661	1671	1679	1701	1727	1718	1707	1684	4
511	1609	1619	1626	1651	1679	1671	1661	1634	4
512	1549	1562	1567	1597	1626	1619	1609	1579	4
513	1489	1494	1506	1536	1567	1562	1549	1519	4
514	1420	1429	1436	1468	1506	1494	1489	1454	4
515	1348	1353	1363	1400	1436	1429	1420	1381	4
516	1272	1278	1290	1328	1363	1353	1348	1310	4
517	1196	1200	1210	1248	1290	1278	1272	1231	4
518	1111	1119	1129	1168	1210	1200	1196	1150	4
519	1028	1033	1049	1087	1129	1119	1111	1067	4
520	942	950	964	1004	1049	1033	1028	982	4
521	856	875	884	920	964	950	942	897	4
522	770	788	804	840	884	875	856	815	4
523	674	694	722	761	804	788	770	720	4
524	636	647	668	686	722	694	674	652	4
525	622	638	650	654	668	647	636	626	4
526	1930	1938	1946	1950	1955	1945	1936	1932	4
527	1918	1927	1935	1940	1946	1938	1930	1922	4
528	1903	1913	1921	1929	1935	1927	1918	1909	4
529	1886	1895	1904	1914	1921	1913	1903	1896	4
530	1864	1872	1881	1891	1904	1895	1886	1877	4
531	1837	1845	1857	1866	1881	1872	1864	1848	4
532	1807	1814	1824	1839	1857	1845	1837	1821	4
533	1769	1781	1784	1803	1824	1814	1807	1788	4
534	1727	1735	1742	1763	1784	1781	1769	1746	4
535	1679	1688	1692	1720	1742	1735	1727	1701	4
536	1626	1633	1643	1667	1692	1688	1679	1651	4
537	1567	1573	1581	1617	1643	1633	1626	1597	4
538	1506	1512	1521	1551	1581	1573	1567	1536	4
539	1436	1445	1448	1484	1521	1512	1506	1468	4
540	1363	1371	1379	1416	1448	1445	1436	1400	4
541	1290	1296	1300	1342	1379	1371	1363	1328	4
542	1210	1217	1224	1267	1300	1296	1290	1248	4
543	1129	1138	1141	1185	1224	1217	1210	1168	4
544	1049	1056	1061	1101	1141	1138	1129	1087	4
545	964	972	980	1024	1061	1056	1049	1004	4
546	884	891	901	941	980	972	964	920	4
547	804	816	827	866	901	891	884	840	4
548	722	739	756	791	827	816	804	761	4
549	668	677	692	724	756	739	722	686	4
550	650	665	675	682	692	677	668	654	4
551	1946	1951	1957	1961	1965	1959	1955	1950	4
552	1935	1942	1948	1953	1957	1951	1946	1940	4
553	1921	1928	1934	1943	1948	1942	1935	1929	4
554	1904	1910	1917	1926	1934	1928	1921	1914	4
555	1881	1890	1897	1905	1917	1910	1904	1891	4
556	1857	1861	1868	1882	1897	1890	1881	1866	4
557	1824	1831	1834	1852	1868	1861	1857	1839	4
558	1784	1791	1798	1817	1834	1831	1824	1803	4
559	1742	1752	1754	1778	1798	1791	1784	1763	4
560	1692	1699	1706	1732	1754	1752	1742	1720	4
561	1643	1646	1652	1681	1706	1699	1692	1667	4
562	1581	1588	1592	1622	1652	1646	1643	1617	4
563	1521	1524	1531	1565	1592	1588	1581	1551	4
564	1448	1456	1460	1492	1531	1524	1521	1484	4
565	1379	1383	1387	1426	1460	1456	1448	1416	4
566	1300	1307	1317	1352	1387	1383	1379	1342	4
567	1224	1229	1236	1274	1317	1307	1300	1267	4
568	1141	1148	1157	1198	1236	1229	1224	1185	4
569	1061	1069	1076	1116	1157	1148	1141	1101	4
570	980	990	992	1031	1076	1069	1061	1024	4
571	901	908	914	955	992	990	980	941	4
572	827	834	842	882	914	908	901	866	4
573	756	767	779	812	842	834	827	791	4

574	692	707	728	754	779	767	756	724	4
575	675	689	702	706	728	707	692	682	4
576	1957	1963	1967	1971	1973	1968	1965	1961	4
577	1948	1954	1958	1964	1967	1963	1957	1953	4
578	1934	1941	1947	1952	1958	1954	1948	1943	4
579	1917	1923	1931	1939	1947	1941	1934	1926	4
580	1897	1899	1907	1920	1931	1923	1917	1905	4
581	1868	1874	1879	1894	1907	1899	1897	1882	4
582	1834	1841	1847	1863	1879	1874	1868	1852	4
583	1798	1806	1810	1828	1847	1841	1834	1817	4
584	1754	1760	1764	1786	1810	1806	1798	1778	4
585	1706	1712	1716	1739	1764	1760	1754	1732	4
586	1652	1656	1663	1690	1716	1712	1706	1681	4
587	1592	1599	1605	1630	1663	1656	1652	1622	4
588	1531	1534	1540	1569	1605	1599	1592	1565	4
589	1460	1465	1474	1503	1540	1534	1531	1492	4
590	1387	1394	1398	1434	1474	1465	1460	1426	4
591	1317	1319	1324	1359	1398	1394	1387	1352	4
592	1236	1240	1243	1283	1324	1319	1317	1274	4
593	1157	1161	1164	1202	1243	1240	1236	1198	4
594	1076	1079	1082	1124	1164	1161	1157	1116	4
595	992	997	1007	1046	1082	1079	1076	1031	4
596	914	925	932	967	1007	997	992	955	4
597	842	850	859	892	932	925	914	882	4
598	779	789	794	824	859	850	842	812	4
599	728	737	748	771	794	789	779	754	4
600	702	714	729	732	748	737	728	706	4
601	1967	1970	1972	1974	1976	1975	1973	1971	4
602	1958	1962	1966	1969	1972	1970	1967	1964	4
603	1947	1949	1956	1960	1966	1962	1958	1952	4
604	1931	1933	1937	1944	1956	1949	1947	1939	4
605	1907	1911	1916	1925	1937	1933	1931	1920	4
606	1879	1884	1887	1901	1916	1911	1907	1894	4
607	1847	1851	1858	1870	1887	1884	1879	1863	4
608	1810	1812	1820	1836	1858	1851	1847	1828	4
609	1764	1771	1775	1793	1820	1812	1810	1786	4
610	1716	1722	1723	1749	1775	1771	1764	1739	4
611	1663	1665	1673	1698	1723	1722	1716	1690	4
612	1605	1607	1613	1641	1673	1665	1663	1630	4
613	1540	1546	1548	1578	1613	1607	1605	1569	4
614	1474	1479	1482	1509	1548	1546	1540	1503	4
615	1398	1402	1406	1443	1482	1479	1474	1434	4
616	1324	1329	1333	1368	1406	1402	1398	1359	4
617	1243	1246	1257	1292	1333	1329	1324	1283	4
618	1164	1166	1175	1214	1257	1246	1243	1202	4
619	1082	1092	1093	1133	1175	1166	1164	1124	4
620	1007	1010	1016	1053	1093	1092	1082	1046	4
621	932	934	938	976	1016	1010	1007	967	4
622	859	864	873	898	938	934	932	892	4
623	794	802	808	837	873	864	859	824	4
624	748	757	765	783	808	802	794	771	4
625	729	736	746	752	765	757	748	732	4

\$ Initial conditions

101325,9.3779e7, 298.15, 0, 0

\$ Boundary conditions

	2	1			4	1		0.000000	0.000000
4	1		0.000000	0.000000	5	1	26	0.000000	0.000000
5	1		0.000000	0.000000	4	1	27	0.000000	0.000000
5	1	2	0.000000	0.000000	5	1	36	0.000000	0.000000
4	1	3	0.000000	0.000000	4	1	37	0.000000	0.000000
5	1	4	0.000000	0.000000	5	1	44	0.000000	0.000000
4	1	5	0.000000	0.000000	4	1	45	0.000000	0.000000
5	1	9	0.000000	0.000000	5	1	45	0.000000	0.000000
4	1	10	0.000000	0.000000	4	1	55	0.000000	0.000000
4	1	13	0.000000	0.000000	5	1	56	0.000000	0.000000
4	1	14	0.000000	0.000000	4	1	67	0.000000	0.000000
5	1	19	0.000000	0.000000	5	1	68	0.000000	0.000000
5	1	20	0.000000	0.000000	4	1	81	0.000000	0.000000

5	1		0.000000	0.000000	5	1	441	0.000000	0.000000
4	1	82	0.000000	0.000000	5	1	462	0.000000	0.000000
	1	92	0.000000	0.000000	4	1	463	0.000000	0.000000
5	1	93	0.000000	0.000000	5	1	470	0.000000	0.000000
4	1	110	0.000000	0.000000	5	1	471	0.000000	0.000000
5	1	111	0.000000	0.000000	4	1	504	0.000000	0.000000
4	1	122	0.000000	0.000000	5	1	505	0.000000	0.000000
4	1	123	0.000000	0.000000	4	1	516	0.000000	0.000000
5	1	141	0.000000	0.000000	4	1	517	0.000000	0.000000
5	1	142	0.000000	0.000000	5	1	539	0.000000	0.000000
4	1	157	0.000000	0.000000	5	1	540	0.000000	0.000000
5	1	158	0.000000	0.000000	4	1	551	0.000000	0.000000
4	1	175	0.000000	0.000000	4	1	552	0.000000	0.000000
4	1	176	0.000000	0.000000	5	1	569	0.000000	0.000000
5	1	193	0.000000	0.000000	5	1	570	0.000000	0.000000
5	1	194	0.000000	0.000000	4	1	593	0.000000	0.000000
4	1	212	0.000000	0.000000	4	1	594	0.000000	0.000000
5	1	213	0.000000	0.000000	5	1	605	0.000000	0.000000
4	1	232	0.000000	0.000000	4	1	606	0.000000	0.000000
4	1	233	0.000000	0.000000	5	1	621	0.000000	0.000000
5	1	252	0.000000	0.000000	4	1	622	0.000000	0.000000
5	1	253	0.000000	0.000000	5	1	637	0.000000	0.000000
4	1	274	0.000000	0.000000	4	1	638	0.000000	0.000000
5	1	275	0.000000	0.000000	5	1	649	0.000000	0.000000
4	1	295	0.000000	0.000000	4	1	650	0.000000	0.000000
5	1	296	0.000000	0.000000	5	1	665	0.000000	0.000000
4	1	313	0.000000	0.000000	5	1	666	0.000000	0.000000
5	1	314	0.000000	0.000000	4	1	675	0.000000	0.000000
4	1	333	0.000000	0.000000	5	1	676	0.000000	0.000000
5	1	334	0.000000	0.000000	4	1	689	0.000000	0.000000
4	1	351	0.000000	0.000000	5	1	690	0.000000	0.000000
4	1	352	0.000000	0.000000	4	1	701	0.000000	0.000000
5	1	377	0.000000	0.000000	4	1	702	0.000000	0.000000
4	1	378	0.000000	0.000000	5	1	713	0.000000	0.000000
5	1	396	0.000000	0.000000	4	1	714	0.000000	0.000000
4	1	397	0.000000	0.000000	5	1	729	0.000000	0.000000
5	1	410	0.000000	0.000000	5	1	730	0.000000	0.000000
4	1	411	0.000000	0.000000	4	1	735	0.000000	0.000000
5	1	440	0.000000	0.000000	4	1	736	0.000000	0.000000
4	1		0.000000	0.000000					

2	3	0.000000	0.025000				
3	4	298.150000	20.000000	1	3	1956	
				2	1	101325.000000	0.000000
	3	1888		3	3	0.000000	0.025000
1	1	101325.000000	0.000000	3	4	298.150000	20.000000
2	3	0.000000	0.025000				
3	4	298.150000	20.000000	1	3	1959	
				2	1	101325.000000	0.000000
	3	1901		3	3	0.000000	0.025000
1	1	101325.000000	0.000000	3	4	298.150000	20.000000
2	3	0.000000	0.025000				
3	4	298.150000	20.000000	1	3	1960	
				2	1	101325.000000	0.000000
	3	1902		3	3	0.000000	0.025000
1	1	101325.000000	0.000000	3	4	298.150000	20.000000
2	3	0.000000	0.025000				
3	4	298.150000	20.000000	1	3	1965	
				2	1	101325.000000	0.000000
	3	1915		3	3	0.000000	0.025000
1	1	101325.000000	0.000000	3	4	298.150000	20.000000
2	3	0.000000	0.025000				
3	4	298.150000	20.000000	1	3	1966	
				2	1	101325.000000	0.000000
	3	1916		3	3	0.000000	0.025000
1	1	101325.000000	0.000000	3	4	298.150000	20.000000
2	3	0.000000	0.025000				
3	4	298.150000	20.000000	1	3	1968	
				2	1	101325.000000	0.000000
	3	1924		3	3	0.000000	0.025000
1	1	101325.000000	0.000000	3	4	298.150000	20.000000
2	3	0.000000	0.025000				
3	4	298.150000	20.000000	1	3	1969	
				2	1	101325.000000	0.000000
	3	1925		3	3	0.000000	0.025000
1	1	101325.000000	0.000000	3	4	298.150000	20.000000
2	3	0.000000	0.025000				
3	4	298.150000	20.000000	1	3	1972	
				2	1	101325.000000	0.000000
	3	1936		3	3	0.000000	0.025000
1	1	101325.000000	0.000000	3	4	298.150000	20.000000
2	3	0.000000	0.025000				
3	4	298.150000	20.000000	1	3	1973	
				2	1	101325.000000	0.000000
	3	1937		3	3	0.000000	0.025000
1	1	101325.000000	0.000000	3	4	298.150000	20.000000
2	3	0.000000	0.025000				
3	4	298.150000	20.000000	1	3	1974	
				2	1	101325.000000	0.000000
	3	1944		3	3	0.000000	0.025000
1	1	101325.000000	0.000000	3	4	298.150000	20.000000
2	3	0.000000	0.025000				
3	4	298.150000	20.000000	1	3	1975	
				2	1	101325.000000	0.000000
	3	1945		3	3	0.000000	0.025000
1	1	101325.000000	0.000000	3	4	298.150000	20.000000
2	3	0.000000	0.025000				
3	4	298.150000	20.000000	1	3	1976	
				2	1	101325.000000	0.000000
	3	1955		3	3	0.000000	0.025000
1	1	101325.000000	0.000000	3	4	298.150000	20.000000
2	3	0.000000	0.025000				
3	4	298.150000	20.000000	\$ Stop input data file			

*THIS PAGE IS INTENTIONALLY
LEFT BLANK*

Chapter 8

CONCLUSIONS

8.1	GENERAL CONCLUSIONS	833
8.1.1	General Conclusions from <i>Chapter 3 – Modelling of Hygro-Thermal Behaviour of Concrete at High Temperature with Thermo-Chemical and Mechanical Material Degradation</i>	833
8.1.2	General Conclusions from <i>Chapter 4 – Spalling Nomograms</i>	833
8.1.2.1	ABOUT THE TIME AND POSITION OF MAIN FRACTURE AND THE SENSITIVITY ANALYSIS	834
8.1.2.2	ABOUT THE SPALLING NOMOGRAMS AND THE ENERGETIC ANALYSIS OF THERMAL SPALLING.....	836
8.1.2.3	ABOUT THE EVOLUTION OF EACH PARAMETER AFFECTING THE PHYSICS OF THERMAL SPALLING PHENOMENA.....	838
8.1.3	General Conclusions from <i>Chapter 5 – Preliminary and simplified analysis of cooling effect on HSCs spalling behaviour</i>.....	840
8.1.4	General Conclusions from <i>Chapter 6 – Analysis of cooling processes in High Strength Concretes</i>.....	841
8.1.4.1	ABOUT THE COOLING PHENOMENOLOGICAL AND MECHANISTIC ANALYSIS	842
8.1.4.2	ABOUT THE COMPARATIVE ANALYSIS	844
8.1.4.3	ABOUT THE ATLAS OF INFORMATION FOR THE ANALYSIS OF THE INFLUENCE OF PARAMETERS NOT RELATED TO COOLING PROCESSES.....	847
8.1.5	General Conclusions from <i>Chapter 7 – Heuristic analysis of cooling processes in high strength concrete square columns</i>.....	848
8.2	PROPOSED EXTENDED TASKS FOR FUTURE RESEARCH WORKS	849
8.2.1	Proposed Extended tasks related to <i>Chapter 3 – Modelling of Hygro-Thermal Behaviour of Concrete at High Temperature with Thermo-Chemical and Mechanical Material Degradation</i>	849
8.2.2	Proposed Extended tasks related to <i>Chapter 4 – Spalling Nomograms</i>	849
8.2.3	Proposed Extended tasks related to <i>Chapter 6 – Analysis of cooling processes in High Strength Concretes</i>	849
8.2.4	Proposed Extended tasks related to <i>Chapter 7 – Heuristic analysis of cooling processes in high strength concrete square columns</i>	850
8.3	BIBLIOGRAPHY OF THE CHAPTER	851

*THIS PAGE IS INTENTIONALLY
LEFT BLANK*

Chapter 8

CONCLUSIONS

The aim of this Chapter is to collect in a single document the general conclusions derived from each of the independent works developed in the previous Chapters. Although the general conclusions derived from each of these Chapters are exposed at their last paragraphs, the author has considered necessary, in sight of the final extent of this Thesis, to include this collection of all of the conclusions in order to ease a fast review of the contributions and conclusions achieved.

Finally, in this Chapter are also collected the extended tasks proposed by the Author to go further in the analysis fields dealt herein.

8.1 GENERAL CONCLUSIONS**8.1.1 General Conclusions from *Chapter 3 – Modelling of Hygro-Thermal Behaviour of Concrete at High Temperature with Thermo-Chemical and Mechanical Material Degradation***

A mathematical model for the analysis of hygro-thermal behaviour of concrete as a multi-phase porous material at high temperatures, including the range above the critical point of water and taking into account material deterioration, has been presented (*Model of Padova, [1]*). A full development of the model equations, starting from the macroscopic balances of mass, energy and linear momentum, obtained elsewhere by means of the Hybrid Mixture Theory, for all constituents of the medium, has been presented. Constitutive relations for concrete at high temperature, and in particular those concerning material damage, have been discussed. The classical isotropic non-local damage theory appropriate modification to take into account both the mechanical damage and the thermo-chemical material deterioration at high temperature has been described. The final form of the model governing equations, their discretization by means of the F.E.M., and a method of their numerical solution have been presented.

8.1.2 General Conclusions from *Chapter 4 – Spalling Nomograms*

The original contributions worked out from the developments included in *Chapter 4* have been the following:

- a. The development of a spectrum of spalling nomograms addressed, as an starting point, to evaluate the sensitivity of the hygro-thermo-chemo-mechanical processes involved on the High-Strength concretes behaviour under a natural fire to some relevant parameters whose values may be chosen from a very early stage of High-Rise Buildings design or already known in case of existing High-Rise Buildings, such as the initial moisture content of concrete, its intrinsic permeability, the rate of temperature increase (fire intensity), the porosity, compressive strength, type of aggregate and, in general, the whole set of hygro-thermo-chemical properties of concrete, and the dimensions of the structural element,
- b. The analysis of the energetic viability of spalling and, hence, of the spalling risk and expectable type (either violent and explosive or slow in nature) in every possible set of conditions so both Designers and Fire Fighting Services will have a valuable information in order to take decisions about design and about the expectable consequences of fire fighting actions from a really intuitive, graphical and immediate point of view,

- c. The discerning of what is the energetic contribution of compressed gas to spalling occurrence and what is that corresponding to the constrained elastic energy since, as it has been recognised by many relevant authors [1], the relative importance of the build-up of high pore pressure close to the heated concrete surface (as a result of rapid evaporation of the moisture) and the release of the stored energy (due to the thermal stresses resulting from high values of restrained strains caused by temperature gradients) has not been already established and needs further studies.

These original contributions and achievements have resulted in the following Conclusions (in order to understand them more deeply, the reader is addressed to each corresponding Chapter).

8.1.2.1 ABOUT THE TIME AND POSITION OF MAIN FRACTURE AND THE SENSITIVITY ANALYSIS

1. As an starting point, it has been evaluated the sensitivity of the hygro-thermo-chemo-mechanical processes involved on the High-Strength concretes behaviour under a natural fire to some relevant parameters whose values may be chosen from a very early stage of High-Rise Buildings design or already known in case of existing High-Rise Buildings, such as the initial moisture content of concrete, its intrinsic permeability, the rate of temperature increase (fire intensity), the porosity, compressive strength, type of aggregate – and, in general, the whole set of hygro-thermo-chemical properties of concrete –, and the dimensions of the structural element.

2. Considering the physics of the phenomena involved in thermal spalling in heated concrete presented in previous paragraphs, it has resulted quite obvious that a high initial moisture content, a high heating rate, a low concrete porosity (hence also permeability), an additional compressive load parallel to the heated surface, and the use of aggregates with high thermal expansion are in general factors favouring Thermal Spalling. The following main particular conclusions have been reached from the works presented in this chapter (it must be remembered that the conclusions presented hereon are valid for the ranges of study of each parameter detailed on paragraph 4.3.2.):

- 2.1. The time and position of the main fracture of concrete elements heated during a natural fire in a High-Rise building – and hence the Thermal Spalling risk – have been determined (*paragraph 4.5.2.*), by means of the analysis of the evolution of a carefully selected Spalling Index, for a total amount of ninety one possible situations with different values of the Initial Saturation Degree, Intrinsic Permeability, Thickness of the structural concrete element, Heating profile and general definition of the Material.

- 2.1.1. For the High Strength Concrete considered – C60 – the worst case from the spalling point of view has clearly been the #82–TH12K019RH60PAR3C60 case, combining the lowest value of the intrinsic permeability at ambient temperature, the highest value of the initial saturation degree and the fastest heating profile (the Hydrocarbon Heating Curve). The same combinations have resulted to be the worst when considering each of the slower heating curves (ISO and Slow), both for C60 and C90 (Ultra High Strength Concrete) materials (combinations #27–TH24K019RH60PAR1C60 and #45–TH12K019RH60PAR1C90 respectively).

- 2.1.2. The position of main fracture in C90 material (U.H.S.C.) has been determined closer to the heated surface than in the C60 (H.S.C.) case. Furthermore, the selected Spalling Index values have resulted lower in C90 (U.H.S.C.) cases, mainly due to higher cracking and mechanical damage levels in C90 – which leads to lower gas pressure values – and to the lower restrained

elastic energy in C90 (U.H.S.C.) cases derived from the already stated closeness of the main fracture to the heated surface in C90 (U.H.S.C.) cases.

2.1.3. About the influence of the heating profile: as the heating profile considered is faster and more severe (Slow → ISO → Hydrocarbon), independently of the material considered, the following trends arise for all the combinations of the Initial Saturation Degree and the Intrinsic Permeability:

2.1.3.1. The Is4 Spalling Index values increase.

2.1.3.2. The number of combinations of the Initial Saturation Degree and the Intrinsic Permeability where Thermal Spalling occurs increases.

2.1.3.3. The time at which it is found the maximum risk of spalling (maximum value of the Is4 spalling index) decreases.

2.1.3.4. The position of the main fracture is closer to the heated surface.

2.1.4. About the influence of the material is as follows: independently of the heating curve considered, the following trends arise for all the combinations of the Initial Saturation Degree and the Intrinsic Permeability:

2.1.4.1. The Is4 Spalling Index values are higher for C60 (H.S.C.) than for C90 (U.H.S.C.).

2.1.4.2. The number of combinations of the Initial Saturation Degree and the Intrinsic Permeability where Thermal Spalling occurs is higher for C60 (H.S.C.) material.

2.1.4.3. The time at which it is found the maximum risk of spalling (maximum value of the Is4 Spalling Index) is higher for C60 (H.S.C.) material (later in time), but as it is expectable from the situation detailed in last paragraphs – lower gas pressure and restrained elastic energy in the C90 (U.H.S.C.) cases – it will be less violent in type (see conclusions in paragraph 4.6.2) for C90 (U.H.S.C.) materials.

2.1.4.4. The position of the main fracture is closer to the heated surface for C90 (U.H.S.C.) material just in some cases (mainly for the Slow Heating curve). In the rest of cases, there are no significant differences between the position of the main fracture between C60 (H.S.C.) and C90 (U.H.S.C.).

2.1.4.5. There is a well-defined trend with the mechanical damage values, being significantly higher in the cases corresponding to C90 (U.H.S.C.) material.

2.1.5. The value of the intrinsic permeability and the heating profiles have shown a determinant role in the Thermal Spalling phenomena, independently of the initial saturation degree to which hygro-thermo-chemical-mechanical processes occurred during Thermal Spalling have presented much less sensitivity within the ranges considered. The sensitivity of results to the Intrinsic Permeability and the Heating Profile is higher on C60 material (H.S.C.) than in C90 material (U.H.S.C.).

2.2. The thickness of the structural element does not appear to be, in the range considered within this chapter, with any influence on Thermal Spalling processes since they arise close to the heated surface. However, it has an influence on the liquid and vapour water fluxes far from the heated surface, which could have a significant influence on the matters studied herein if an extremely slow or very long duration heating profile

was considered – only in cases that would not be representative of natural fires in High-Rise buildings –.

8.1.2.2 ABOUT THE SPALLING NOMOGRAMS AND THE ENERGETIC ANALYSIS OF THERMAL SPALLING

1. The data referred to in last paragraph, together with other relevant results concerning Thermal Spalling such as the available energy in each situation, have been represented on a set of eight charts in the initial saturation degree – intrinsic permeability domain, so it has been possible to define some dangerous regions with respect to the spalling occurrence (*paragraph 4.5.3*). These nomograms have shown, through a fast, graphical and intuitive methodology understandable for all of their expected users, the following conclusions common to all of them (other particular conclusions for some of the nomograms can be read in paragraphs 4.5.3.1 to 4.5.3.8 but are out of the scope of this resume):

- 1.1. Most of the analyzed cases experiment Thermal Spalling – energetically viable – (at only 2-4 minutes from the start of the fire when considering the Hydrocarbon heating curve, 10 minutes from the start of the fire when considering the ISO heating curve and later on, at about 1 hour, for the slowest heating curve admitted by Eurocode regulation [18]), especially when considering C60 material (H.S.C.).
- 1.2. The worst combination of the Initial Saturation Degree and the Intrinsic Permeability, from the point of view of Thermal Spalling risk, is always featured by $S = 60\%$ and $k_0 = 10^{-19} \text{ m}^2$.
- 1.3. The best combination of the Initial Saturation Degree and the Intrinsic Permeability, from the point of view of Thermal Spalling risk, is always featured by $S = 40\%$ and $k_0 = 10^{-17} \text{ m}^2$.
- 1.4. It is observed a little sensitivity of the I_{s4} Spalling Index values to the Initial Saturation Degree. On the contrary, it is observed a very pronounced sensitivity of the I_{s4} spalling index values to the Intrinsic Permeability level – the larger increase of the I_{s4} spalling index value is found when changing the Intrinsic Permeability from $k_0 = 10^{-18} \text{ m}^2$ to $k_0 = 10^{-19} \text{ m}^2$, so this last value seems to be an upper limit for Intrinsic Permeability from the point of view of Thermal Spalling –.

2. It has also been analyzed the energetic viability of Thermal Spalling and, hence, of the spalling risk and its expectable type (either violent and explosive or slow in nature) in every possible set of conditions so both Designers and Fire Fighting Services have a valuable information in order to take decisions about design and about the expectable consequences of fire fighting actions from a really intuitive, graphical and immediate point of view.

Beyond this result, it has also been estimated the energetic contributions to Thermal Spalling occurrence of both the compressed gas and the constrained elastic energy since the relative importance of the build-up of high pore pressure closed to the heated concrete surface (as a result of rapid evaporation of the moisture) and the release of the stored energy (due to the thermal stresses resulting from high values of restrained strains caused by temperature gradients), had not been already established. The expectable type of spalling, either violent and explosive or slow in nature, in every possible set of conditions has been determined through the calculation of the velocity of the spalled-off pieces and the following conclusions have arisen:

- 2.1. About the influence of the heating profile: as the heating profile considered is faster and more severe (Slow → ISO → Hydrocarbon), independently of the material considered, the following trends arise for all the combinations of the Initial Saturation Degree and the Intrinsic Permeability:

- 2.1.1. The average velocity of the spalled pieces increases.
- 2.1.2. About the energetic analysis comparison, the following conclusions are only referred to heating curves ISO and Slow, since the lack of convergence of Hydrocarbon cases may lead to deceptive conclusions about this particular matter:
 - The relative contribution of the constrained elastic energy decreases as the heating profile increases its speed and severity. On the other hand, the relative contribution of the work done by compressed gas increases. This might be due to higher gas pressures arising with faster heating profiles.
- 2.2. About the influence of the material is as follows: independently of the heating curve considered, the following trends arise for all the combinations of the Initial Saturation Degree and the Intrinsic Permeability:
 - 2.2.1. The average velocity of the spalled pieces is higher for C60 material (H.S.C.),
 - 2.2.2. About the energetic analysis comparison, the following conclusions are only referred to heating curves ISO and Slow, since the lack of convergence of Hydrocarbon cases may lead to deceptive conclusions about this particular matter:
 - The relative contribution of the constrained elastic energy is higher for the C90 material (U.H.S.C.) than for the C60 material (H.S.C.). This trend is more pronounced for high values of the Intrinsic Permeability (10^{-17} and 10^{-18} m²) than for 10^{-19} m².
- 2.3. About the relative energetic contribution of compressed gas and the constrained elastic energy to spalling occurrence, it is observed that:
 - 2.3.1. For the highest levels of the Intrinsic Permeability, the main contributor is the constrained elastic energy ΔU .
 - 2.3.2. For the lowest levels of the Intrinsic Permeability, the main contributor is the compressed gas W .
 - 2.3.3. The Initial Saturation Degree does not affect significantly, within the considered range of values, to the relative energetic contribution of both factors.
- 2.4. The highest average velocity of the spalled-off pieces, among all of the cases analyzed, is case #82-TH12K019RH60PAR3C60 corresponding to the Hydrocarbon heating curve and C60 material (H.S.C.).
- 2.5. Referring only to cases with Slow and ISO Heating curves, the case with the highest average velocity of the spalled-off pieces is case #27-TH24K019RH60PAR1C60, corresponding to an Initial Saturation Degree at 60%, an Intrinsic Permeability value of 10^{-19} m², an ISO heating curve and C60 material. The mean velocity of the spalled-off pieces considering only the spalling cases not related to Hydrocarbon heating curve is 7,1 m/s and its median value is 4,8 m/s (considering zero values for the cases where spalling is not occurring).
- 2.6. The distribution of average velocities of spalled pieces evaluated for each combination indicates the existence of two peaks, lying with the range of $4,5 < v \leq 6,0$ m/s and of $7,5 < v \leq 9,0$ m/s. As it can be observed on figure 4-38 these results show good accordance with the experimental results obtained by [32] recording

spalling events by means of a high-speed camera, giving insight into the size/shape and velocity of the spalled pieces.

8.1.2.3 ABOUT THE EVOLUTION OF EACH PARAMETER AFFECTING THE PHYSICS OF THERMAL SPALLING PHENOMENA

1. Related to the temperature-evolution of the Gas and Vapour Pressures and the Total Damage, the following general conclusions have arisen (other particular conclusions for some of the comparisons developed can be read in paragraphs 4.5.4.1 to 4.5.4.6 but are out of the scope of this resume):

- 1.1. The maximum absolute gas pressure reached during the three hours of simulations is always found, for all of the depths considered, within the temperature range of 473 ± 50 K, being this the temperature at which spalling is usually observed. This fact suggests that despite the I_{s4} maximum values are achieved at higher temperatures, Thermal Spalling may be occurring before the instants corresponding to these maxima, as it was explained on table 4-43.
- 1.2. Gas pressure values corresponding both to its absolute maxima and to the instant where the I_{s4} Spalling Index reaches its maximum value at each case, at the position of the main fracture, range from the values exposed on next table:

<i>Material</i>	<i>Heating Profile</i>	<i>Range of Gas Pressure Absolute maximum [MPa]</i>	<i>Range of Gas Pressure Value at the instant of maximum I_{s4} at the main fracture position [MPa]</i>
C60 (H.S.C.)	Hydrocarbon	$1,2 \leq p^g \leq 5,7$ *	$0,2 \leq p^g \leq 4,4$ *
	ISO 834	$0,6 \leq p^g \leq 2,7$	$0,4 \leq p^g \leq 2,0$
	Parametric-Slow	$0,3 \leq p^g \leq 1,8$	$0,2 \leq p^g \leq 1,3$
C90 (U.H.S.C.)	Hydrocarbon	$0,9 \leq p^g \leq 4,8$ *	$0,4 \leq p^g \leq 2,1$ *
	ISO 834	$0,5 \leq p^g \leq 2,6$	$0,2 \leq p^g \leq 1,2$
	Parametric-Slow	$0,3 \leq p^g \leq 1,3$	$0,1 \leq p^g \leq 0,8$

Table 4-60 and 8-1. Gas Pressure values ranges for different types of Heating Profiles and materials.

***Remark:** Results corresponding to 12 centimetres cases, taking into account that some of the cases featuring Hydrocarbon heating curve have not converged during the three hours of simulation, so their corresponding gas pressure values may be even higher.

- 1.3. It is observed a slight increase of the maximum absolute gas and vapour pressures as the Initial Saturation Degree increases, but the temperature at which these maxima appear is not affected. This increase is higher when considering the Slow heating curve. The maximum absolute vapour pressure values matches in time with the maximum of gas pressure. The difference between gas and vapour pressure is, for the Hydrocarbon heating curve cases, much lower than in the case featured by a Slow heating curve.
- 1.4. On the contrary, it is clearly observed a pronounced sensitivity of both the maximum absolute gas pressure and the pressure corresponding to the maximum I_{s4} Spalling Index with the values of the Intrinsic Permeability, increasing all of these pressures as the latter decreases. The temperature at which these maxima are found decreases when increasing Intrinsic Permeability, so it can be easily concluded that low values of Intrinsic Permeability may lead to spalling phenomena more violent but not necessarily occurring earlier.

- 1.5. Analogously, as Intrinsic Permeability increases the Total Damage level at the temperatures showing both the maximum absolute gas pressure and the pressure corresponding to the maximum I_{s4} Spalling Index decrease – being this decrease slight at the cases featured by C90 material (U.H.S.C.). At the inner layers, among 5 and 10 centimetres away from the heated surface, it is observed that the material is not completely cracked at the end of the simulation and that the final Total Damage level also decreases as Intrinsic Permeability increases.
 - 1.6. It is worthy to remark that the evolution curve of Total Damage at all of the depths considered present a singularity – in the form of a sudden reduction of its slope, reduction almost to zero in the cases featured by the Hydrocarbon heating curve – at the temperatures where gas and vapour pressure maxima are reached. This fact suggests that the compressed gas contribution to material damaging is significant.
2. Related to the time-evolution of the Vapour Pressure and the Mechanical Damage distributions, the following general conclusions have arisen (other particular conclusions for some of the comparisons developed can be read in paragraphs 4.5.6 but are out of the scope of this resume):
- 2.1. For the set of cases adopted as a reference, featured by a 12 centimetres thick structural element of C60 material (H.S.C.) and with an ISO heating curve applied (cases 1 to 9), beyond what explained on previous paragraphs it is observed that:
 - 2.1.1. The depth where the vapour pressure shows its maximum values increases with time up to an absolute heating time of 9.600 seconds, instant at which the maximum value (much lower than in the previous stages) moves towards the heated surface. The maximum absolute vapour pressure reached at each instant matches the gas pressure maximum (in depth and absolute time) and is always found within the temperature range of 473 ± 50 K, being this the temperature at which spalling is usually observed. This fact suggests that despite the I_{s4} maximum values are achieved at higher temperatures, within the range of 573 ± 25 K, spalling may be occurring before the instants corresponding to these maxima, as it was explained on table 4-43.
 - 2.1.2. The regions where mechanical damage values are maxima at any certain instant are those most exposed to temperature rising (close to the heated surface). However, one must remember that a lower depth does not necessarily mean higher Total/Mechanical Damage levels at the same temperature.
 - 2.1.3. It is observed a slight increase of the maximum value of the vapour pressure and a decrease of its corresponding depth as the Initial Saturation Degree increases. On the other hand, it is clearly observed a pronounced sensitivity of the maximum absolute vapour pressure with the values of the Intrinsic Permeability, increasing this pressure as the latter decreases. The depth at which these maxima are found increases with Intrinsic Permeability.
 - 2.1.4. As Intrinsic Permeability increases the Mechanical Damage level at a certain depth decreases.
 - 2.2. From the comparison of the set of cases adopted as a reference, against the rest of possible situations, it is observed that:
 - 2.2.1. A slower heating curve leads to a maximum vapour pressure value much closer to the heated surface and with a higher value at any certain instant.

- 2.2.2. In reference to the material influence, the change from C60 (H.S.C.) to C90 (U.H.S.C.) makes the maximum vapour pressure value arise closer to the heated surface while being lower, independently of the heating profile. At any instant, cases with C90 material (U.H.S.C.) show larger differences of vapour pressure values with respect to the saturation vapour pressure corresponding to the temperature at each depth than in case with C60 material (H.S.C.). These differences increase with time due to the progressive drying of material.
- 2.2.3. If one compares the vapour pressure spatial distributions corresponding to the instant at which the heated surface temperature is 473 K, temperature above which thermal spalling is usually observed, it is again observed than in these conditions C90 material (U.H.S.C.) shows lower vapour pressure values (being its maximum closer to the surface). On the other hand, a slower heating profile leads to a much wider but lower distribution of vapour pressure values, mainly due to a characteristic higher absolute time that enables larger diffusion and capillary processes.
- 2.2.4. The mechanical damage levels are lower when considering a Slow heating profile, being in these cases the depths at which the maximum value of the vapour pressure appears also lower (if the same absolute instant is compared).
- 2.2.5. In the cases featured by a thickness of 24 centimetres and an ISO heating profile the spatial distribution of the vapour pressure and the mechanical damage are the same as for 12 centimetres during the initial heating stages. However, for higher absolute times – 7.200 and 10.800 seconds – these distributions are qualitatively different since there exist diffusion and capillary processes towards the non-heated surface which are not present in the cases of 12 centimetres, where certain vapour and liquid water fluxes are exchanged with the non-heated atmosphere, leading to a wider distribution of the vapour pressure distribution and varying the mechanical damage distribution beyond the first 12 centimetres (this fact does not affect significantly to the Thermal Spalling phenomena since, as it has been explained in the paragraph related to the spalling nomograms, they take place in layers located much closer to the heated surface).

8.1.3 General Conclusions from *Chapter 5 – Preliminary and simplified analysis of cooling effect on HSCs spalling behaviour*

The first achievement of *Chapter 5* has been to establish a methodology for a preliminary and simplified analysis of the effect of a forced cooling on the spalling behaviour of High Strength (and Very High Strength) Concretes in order to evaluate if it was significant enough to justify a relevant, greater and deeper work concerning this matter.

A secondary contribution of this Chapter has been to formulate some preliminary conclusions that later on helped to orientate better the analysis done on models of a much higher complexity and requiring huge computational and postprocessing efforts, while testing the methodology to be used in the advanced analyses developed in *Chapter 6 – Analysis of Cooling Processes in High Strength Concretes* and *Chapter 7 – Heuristic analysis of Cooling Processes in High Strength Concrete Square Columns*.

These original contributions and achievements have resulted in the following Conclusions (in order to understand them more deeply, the reader is addressed to each corresponding Chapter):

1. It has been found that the methodology shown in *Chapter 5* for the preliminary and simplified analysis of the effect of a forced cooling on the spalling behaviour of High Strength (and Very High Strength) Concretes is reliable and that the results obtained show clearly that a fast “forced” cooling – at least – may have an unfavourable effect which is definitely significant enough to justify a relevant, greater and deeper work concerning this matter. However, this is only a preliminary and simplified conclusion that might change completely when introducing extremely relevant considerations such as the fact that some of the material properties whose definition is necessary to accomplish the hygro-thermo-chemo mechanical calculations developed herein do not show a ‘reversible’ trend when temperature cycles are applied to structural elements so must be taken into account through an ‘irreversible’ definition, considerations included within the advanced analyses developed in *Chapter 6*.
2. As a secondary conclusion of this Chapter, it has been worked out that the models developed for the cooling simulations will necessarily have to be defined with a high-order finite elements mesh and a design developed from the physical knowledge of the processes involved of the models developed for the simulations, since it has been observed that – specially with fast “forced” coolings – huge gradients of the variables may appear during calculations. This fact would later lead to higher computational times and resources needs.
3. A third and final conclusion of this Chapter, is that thermal creep has a significant effect on the results dealt to develop the conclusions exposed herein. For this reason, without considering thermal creep the values of the I_{s4} spalling index are important from a comparative point of view or for structural elements where thermal creep might not be significant (mainly cases where no strong constraints are applied). Since up to the date of this preliminary and simplified analysis there are not any software releases available capable to predict hygro-thermo-chemo-mechanical behaviour considering thermal creep during a cooling process a release including this phenomena is a need that will have to be met in other research works beyond the scope of this Thesis to enable the development of the same analyses described in *Chapter 6* for structural elements with strong restraints.

8.1.4 General Conclusions from *Chapter 6* – Analysis of cooling processes in High Strength Concretes

The original contributions worked out from the developments included in *Chapter 6* have been the following:

- a. The phenomenological and mechanistic analysis of the effect of a spectrum of cooling processes – representative of the most expectable actions to be developed by the Fire Fighting Services during the progress of a natural fire in a High-Rise Building – on the hygro-thermo-chemo-mechanical state of a structural element manufactured with High-Strength concrete.
- b. The development of a comparative analysis to compare the final hygro-thermo-chemo-mechanical state of a structural element after the development of different types – and subtypes – of cooling processes, including comparisons about the Environment vs. Structural element’s Surface cooling attacks, among different start instants and for several velocities of the cooling processes.
- c. The supply of the information needed for the analysis of the influence on the hygro-thermo-chemo-mechanical behaviour of the structural element during the cooling processes of several parameters non-related to the own cooling processes – such as the initial moisture content of concrete, its intrinsic permeability, the rate of temperature increase (fire intensity), the porosity, compressive strength, type of aggregate and, in general, the whole set of hygro-thermo-chemical properties of

concrete –, and for the generation of an extension of the Spalling Nomograms initially obtained just for heating processes and described previously on Chapter 4. Although the generation of the stated Spalling Nomograms for the cooling stage has not been an objective of this Thesis, and it is proposed as an extended task for future research works, in Appendix 6A has been analyzed if the variation of any of these parameters leads to an increase of the maximum value of the adopted Spalling Index I_{s4} (i.e. the risk of Thermal Spalling) during the cooling stage of the cases dealt in this Chapter.

These original contributions and achievements have resulted in the following Conclusions (in order to understand them more deeply, the reader is addressed to each corresponding Chapter).

8.1.4.1 ABOUT THE COOLING PHENOMENOLOGICAL AND MECHANISTIC ANALYSIS

The phenomenological and mechanistic analysis of the effect of a spectrum of cooling processes – representative of the most expectable actions to be developed by the Fire Fighting Services during the progress of a natural fire in a High-Rise Building – on the hygro-thermo-chemo-mechanical state of a structural element manufactured with High-Strength concrete has been developed by means of the advanced Hitecosp Software [2] (see paragraph 6.5.2).

The structural element selected for the analyses developed in this chapter is analogous to that considered in *Chapter 4 – Spalling Nomograms*, since it was as more versatile as possible in order to achieve results applicable to most of the High Strength Concrete structural elements usually found in High-Rise Buildings. Its complete typological description is included in paragraph 4.3 of Chapter 4.

The adopted Heating profiles have been obtained, analogously to what is done in *Chapter 4*, from the time-temperature parametric curves defined in the Eurocode 1, Part 1-2 [28], since this is an European regulation widely spread and prestigious document where parametric curves have been defined on an experimental bases, definition that is described on paragraph 4.3.2.4.1 of Chapter 4. The complete description of the adopted Heating profiles is included in paragraph 6.4.3.1.

The definition of the Cooling profiles has been developed in sight of their Physical Background and of Fire Fighting Experiences described in the available bibliography (see paragraph 6.4.3.2.3) and from the development of several Computational Fluid Dynamics simulations of natural fires in an office (see paragraph 6.4.3.2.4), being the basic aim of these simulations to arrange more information about the temperature evolution of the surface of structural elements where a water jet/spray is directly applied, since this was a basic information needed to discern the cooling effect on the hygro-thermo-chemo-mechanical state of a structural element manufactured with High-Strength concrete. The selected office is where this Thesis is being written, owned by the PhD Student and writer, as it constitutes a typical-plan office common to many High-Rise Buildings sited in a building exclusively containing offices and consisted of an actual typical-plan office of $A_f = 43,12 \text{ m}^2$, a total walls surface of $A_t = 152,70 \text{ m}^2$ and 2,50 m in height:

A total amount of 16 Computational Fluid Dynamics simulations (requiring each a computational effort longer than four days) have been developed by means of *Fire Dynamics Simulator* software [48,49] on a 135.000 uniformly distributed cells model for several flow rates of a hose-nozzle ranging from 96 up to 220 litres per minute, different droplets mean diameters ranging from 250 to 1.000 μm , several cone angles ranging from 3° - 6° to 3° - 60° and different initial velocities of the droplets ranging from 10 to 15 m/s. The evolution of the temperature at

the wall surface where the water jet has been applied has been deducted by means of a set of 36 thermocouples, resulting a general cooling rate of -10 °C/s and two particular extremely high cooling rates of $-136,6\text{ °C/s}$ and $-32,36\text{ °C/s}$ respectively, all of them introduced in the subsequent hygro-thermo-chemo-mechanical calculations.

Two types of cooling profiles have been chosen in sight of what has been exposed on previous paragraphs (see paragraph 6.4.3.2.5): Environmental Cooling Profiles, where the cooling action is applied to the air in contact with the surface of the structural element, and Surface Cooling Profiles, where the cooling effect is applied directly to the surface of the structural element. Among them, several subtypes of cooling profiles are defined starting from different instants and depending on the actions following the cooling processes: within the Environmental Cooling Profiles, the environmental temperature has been progressively decreased according to three cooling rates ($-0,2\text{ °C/s}$, $-2,0\text{ °C/s}$. and $-20,0\text{ °C/s}$.) until it has reached ambient temperature, which is considered 25 °C , following the calculations with a constant ambient temperature until the whole structural element show a temperature within the range *Ambient Temperature* $\pm 10\text{°C}$; on the other hand, within the Surface Cooling Profiles, as just explained all of them have been, in general, characterized by a cooling rate of the surface of the structural element of $-10,0\text{ °C/s}$ (by apart of some particular analyses introducing the most extreme values of the cooling rates), followed by three different actions after the end of the surface cooling process to ambient temperature: ‘*Followed by Heating*’, where after the surface cooling stage the environment heating profile keeps governing the evolution of the temperature in the structural element, ‘*Followed by an imposed constant Surface Temperature*’, where the surface temperature is also decreased at the cooling rate previously described until the ambient temperature is reached on the surface and then it is kept constant in order to simulate keeping the water jet applied on the surface for some time more, and finally ‘*Divided into Two/Three Periods*’, where the intention of this subtype of surface cooling has been to simulate the action of the water jet applied on the surface of the structural element in several sweeps, which might be a realistic situation when fire fighters move the nozzle around in cyclic sweeps.

Next, the cooling phenomenological and mechanistic analysis of a total amount of 29 reference cases have been developed by means of the advanced Hitecosp Software [2] (see Table 6-30 on paragraph 6.5.1 for an Atlas of the analyzed cases) (requiring each a computational effort longer than three days).

The phenomenological and mechanistic analysis of each reference case is deeply described in each corresponding subparagraph of paragraph 6.5.2, including the analysis of the evolution of several critical parameters such as the selected Spalling Index I_{s4} , the mechanical damage d , the velocity of spalled-off pieces v , the gas pressure p^g , the vapour pressure p^v , the saturation degree S , the relative humidity RH , the temperature T , the elastic energy U , the stress in the longitudinal direction σ_{xx} and the stress in the transversal direction σ_{yy} .

The only conclusion common to all of the reference cases consists on that from none of them have resulted increasing values of the selected Spalling Index I_{s4} during the cooling stages (neither during environmental cooling processes nor during surface cooling processes) not increasing, therefore, the Thermal Spalling risk during cooling stages. However, especially within the environmental cooling cases the mechanical damage – i.e. the cracking level – increases dramatically during the cooling stage both in value and in extent towards the inner layers increasing, hence, the depth of the structural element where Thermal Spalling is both energetically and mechanically viable and leading to more massive Thermal Spalling phenomena being expectable. On the other hand, surface cooling processes followed either by a heating stage or divided into two/three periods introduce a quite local effect on the overall hygro-thermo-chemo-mechanical behaviour of the structural element limited to the layers close to the

heated/cooled surface. For a deeper and particularized description of the conclusions arisen from each analysis the reader is addressed to the corresponding paragraph of this Chapter.

Additionally, some particular phenomena of interest and the development of certain analyses have also been included in order to enhance the usefulness of the results deduced in this Chapter as a necessary base to work out research tasks beyond the aims selected.

Hence, as a secondary contribution of the analyses of this Chapter the description and analysis of the infiltration of the environmental humidity inside the structural element during the cooling processes has been developed (see paragraph 6.5.2.8.2): during the cooling processes analyzed it has been observed that there is an infiltration – across both surfaces of the structural element – of the humidity of the environment towards the inner layers. This effect happens since a constant vapour pressure of the environment has been imposed at both sides of the structural element – see paragraph 6.4.1 explaining the boundary conditions used in the calculations – and, hence, as the temperature in the environment decreases its relative humidity increases (being approximately the 50% at the initial ambient temperature) and vice versa. These increases in the structural element relative humidity are significant since it rises from almost zero at the beginning of the cooling processes values up to a 30 per cent value at the end of the cooling. It has also been observed that the slower the environmental cooling process is the greater the environmental relative humidity infiltration occurs.

Introductory analyses of the effect of the maximum temperature and damage reached in the concrete of the structural element have also been included in paragraph 6.5.2.8.3 in order to enable the evaluation the final value of several basic mechanical (and thermal) properties needed to calculate the load-carrying capacity of any structural element during and after a fire situation, introducing several examples showing the usefulness of exploiting the results obtained in this Chapter to estimate, for instance, the minimum value of the compressive strength achieved during the heating/cooling process – needed to evaluate the structural state of a heated structural element – or the residual value of the Young's Modulus of concrete (a reasonable comprehension of which is obtained from the final distributions of the mechanical damage). This constitutes another secondary original contribution of this Thesis since, up to this date, the only existing works addressed to evaluate, for instance, the residual Young's Modulus of a structural element after a fire are experimentally based.

Further introductory analyses have been also included in paragraph 6.5.2.8.4 in order to show, by means of an example, the usefulness of knowing the maximum temperatures achieved at any position during the heating/cooling processes of each case to estimate the strength and several deformation properties of steel reinforcing bars at elevated temperatures such as the residual relation between the adherence breakage stress ($\tau_{u,inc}$) after the fire and that previous to it (τ_u).

8.1.4.2 ABOUT THE COMPARATIVE ANALYSIS

The development of a comparative analysis to compare the final hygro-thermo-chemo-mechanical state of a structural element after the development of different types – and subtypes – of cooling processes, including comparisons about the Environment vs. Structural element's Surface cooling attacks, among different start instants and for several velocities of the cooling processes has been developed (see paragraph 6.5.3). This comparison has been developed on two of the selected reference cases: reference case #05 – TH12K018RH50PAR1C60 and reference case #14 – TH12K018RH50PAR2C60.

Within the comparison of the cases where an environmental cooling process has been considered (see paragraph 6.5.3.1.1), the analyzed state has been that corresponding to the instant when the entire structural element has lowed down its temperature under the ambient

temperature plus ten degrees. The main conclusions of this comparative analysis have shown that, regarding the maximum value of the Spalling Index selected herein, I_{s4} , all of the cases dealt (the three subtypes of environmental cooling) lead to identical maximum values since these maxima have appeared prior to the start of the cooling process. Related to the final distribution of the mechanical damage values (and, hence, of the cracking level of the structural element) non-significant differences have been found between those corresponding to Medium and Fast environmental cooling processes. However, the final state of the structural element after a Slow environmental cooling have shown higher levels of cracking both in value and, what it is equally unfavourable due to the loss of resistant surface, in its extent towards inner layers. While in the reference case #05 – TH12K018RH50PAR1C60, in both the Medium and Fast environmental cooling cases the maximum values of the cracking level have appeared much sooner – what may lead to a longer and more severe exposition of the reinforcing bars to fire action –, in the reference case #14 – TH12K018RH50PAR2C60 all of the subtypes of environmental cooling have lead to the appearance of the highest levels of cracking almost simultaneously, with the only difference that the values of the mechanical damage corresponding to the Slow case have kept increasing slightly until the end of the process. Related to the final relative humidity corresponding to a Slow environmental cooling this has resulted lower at all the depths of the structural element than in the rest of cases, probably due both to a longer stay at high temperatures and to a higher level of cracking that has enabled water loss towards the environment. Finally, referred to the residual longitudinal stress (xx) although its distributions for all the cases are quite similar close to the heated/cooled surface – where high compressive stresses have arisen – in several inner layers the Slow environmental cooling case has resulted significantly more stressed in the reference case #05 – TH12K018RH50PAR1C60, while both Medium and Fast environmental cooling processes have lead to higher residual stresses in the reference case #14 – TH12K018RH50PAR2C60. In conclusion, from the comparison of these three subtypes of environmental cooling it has been deduced that a low environmental cooling rate (i.e. Slow) leads to structural elements more widely damaged (cracked) and with residual stresses higher in the reference case #05 – TH12K018RH50PAR1C60 but not in the reference case #14 – TH12K018RH50PAR2C60, being the latter a not so expected conclusion.

In the meantime, in those cases where a surface cooling process has been applied (see paragraph 6.5.3.1.2), the structural element state after three hours from the beginning of the natural fire in a High-Rise Building has been analyzed and compared. Again, regarding the maximum value of the Spalling Index selected herein, I_{s4} , all of the cases dealt (the three subtypes of surface cooling) have lead to identical maximum values since these maxima appear prior to the start of the cooling process. The cases ‘*Followed by heating*’ and ‘*Divided into 2/3 periods*’ have lead to qualitative and quantitatively analogous results at the end of the 3 hours from the beginning of the fire, being Thermal Spalling energetically viable from really early stages up to the end (in this cases, tensile longitudinal stresses keep present until the end of the 3 hours process). On the contrary, the case ‘*Followed by an imposed constant temperature*’ has shown that at early stages Thermal Spalling is not energetically viable any longer up to the end of the calculation. This fact obviously occurs due to the contribution of the second (and third) heating processes that take place in the cases ‘*Followed by heating*’ and ‘*Divided into 2/3 periods*’ (otherwise, an unfavourable effect of the surface cooling on the thermal spalling risk would have to be understood, conclusion that has not derived at all from any of the cases analyzed in this Chapter). Related to the final distribution of the mechanical damage values (and, hence, of the cracking level of the structural element) non-significant differences have been found between those corresponding to ‘*Followed by heating*’ and ‘*Divided into 2/3 periods*’ processes, what suggests a quite local and limited effect of the second and third surface cooling process developed in the ‘*Divided into 2/3 periods*’ case. In the meantime, in the ‘*Followed by an imposed constant temperature*’ case it is remarkable the faster increase rate of mechanical

damage close to the surface if compared to the others but only in a narrow layer close to the heated/cooled surface. Regarding the final distribution of temperature in the structural element, it is remarkable that no significant differences have arisen between the ‘*Followed by heating*’ and ‘*Divided into 2/3 periods*’ cases despite introducing in the latter additional surface cooling processes. Referred to the residual longitudinal stress (xx), its distributions for both the ‘*Followed by heating*’ and ‘*Divided into 2/3 periods*’ cases have resulted quite similar at all the depths – arising elsewhere tensile stresses in the longitudinal directions and compressive in the transversal one –. In conclusion, from the comparison of these three subtypes of surface cooling it is deduced that the number of temperature cycles of similar amplitude – i.e. the number of sweeps done by the Fire-Fighter applying the water jet on the surface of the structural element (among one and three cycles/sweeps) – does not appear to lead to significant differences after 3 hours from the start of the natural fire. With respect to the case where the water jet is kept applied to the surface of the wall over a longer period: in the reference case #05 – TH12K018RH50PAR1C60 it has been observed that higher cracking rates appear in a narrow layer close to the heated/cooled surface; on the other hand, in the reference case #14 – TH12K018RH50PAR2C60 it has been observed a considerably faster increase rate of mechanical damage close to the surface – if compared to the rest of the cases – arising hence the maximum of the mechanical damage value in this case, only in 2 minutes after the start of the cooling process, beyond the maximum cracking levels that are achieved in almost 2 hours in the ‘*Followed by heating*’ and ‘*Divided into 3 periods*’ cases, denoting this trend a quite unfavourable effect, from a mechanistic point of view, of a long application of a water jet on the heated surface of a structural element.

A comparative analysis has also been developed in order to discern the effect of the type of cooling – environmental cooling, surface cooling or not cooling at all – on the hygro-thermo-chemo-mechanical state of a structural element (especially after the extinguishment of a fire in a High-Rise Building) in the reference case #14 – TH12K018RH50PAR2C60 (see paragraph 6.5.3.1.3):

First (see paragraph 6.5.3.1.3.1), a comparison of the final state of a structural element existent in a room of a High-Rise Building where fire fighting actions (in the form of environmental slow cooling processes starting either at 1.800 or at 3.360 seconds) are / are not introduced during the natural fire evolution – for this purpose, the parametric cooling curves provided by Eurocode 1 Part 1-2 [3] have been adopted to simulate the natural cooling of the enclosure –. Hence, it is remarkable that the case where no ‘forced cooling’ actions are introduced, i.e. the case with natural cooling, has resulted the only case (among those compared) showing a very long period during the natural cooling process at which Thermal Spalling has been energetically and mechanically viable, i.e. up to nineteen hours after the fire has begun. Related to the final distribution of the mechanical damage values (and, hence, of the cracking level of the structural element) extremely significant differences have been found: the final state of the structural element after a Slow environmental cooling starting at 3.360 seconds have shown high levels of cracking in much wider and deeper extents towards inner layers than when the cooling process has been started earlier at 1.800 seconds. However, the more significant difference in the mechanical damage distribution and evolution have appeared at the natural cooling case, in which the mechanical damage values existent at 10.800 seconds, i.e. the start of the natural cooling process, have resulted kept almost constant during a very long cooling period, i.e. from three to sixteen hours from the start of the fire, showing moderately high values (higher than the 60 per cent) at all the depths of the structural element whereas, at sixteen hours from the start of the fire – i.e. thirteen hours after the start of the natural cooling process – mechanical damage values have begun to increase again at all the depths of the structural element without stopping this increase until the end of the calculation developed and reaching ‘completely

fractured' values at the layers close to the heated/cooled surface. The main conclusion of the comparison of these three types of cooling is that a natural cooling process has lead – in the reference case analyzed – to structural elements more widely (and more severely) damaged (cracked) but with residual stresses not necessarily higher than those introducing environmental cooling actions, being this a not so expected conclusion. However, it is important to observe that at the positions where reinforcing bars are expected to be located mechanical damage values arisen in the case with an environmental slow cooling starting at 3.360 seconds have resulted higher (about a ten per cent) than those corresponding to the case including a natural cooling process (at least up to the extent of the available calculated instants in the natural cooling case named).

Second (see paragraph 6.5.3.1.3.2), the calculation case where no cooling actions (neither environmental nor surface) have been introduced during the three first hours from the beginning of the fire has been compared against the case where one/three surface cooling processes have been introduced at 3.360 seconds from the beginning of the fire. The main conclusion arisen from this comparison has been to describe a rather local effect of the surface cooling processes considered in this chapter for the *Surface + Heating* and *Surface + Repeating* cases, with locally higher values of the cracking level when surface cooling actions have been introduced. It is remarkable, that this local effect trend has not been extendable to the case *Surface followed by an imposed constant ambient temperature* where the cooling effect is not local.

Finally, the influence of other parameters such as the cooling process start instant has also been analyzed for the reference case #14 – TH12K018RH50PAR2C60. Within the environmental cooling cases (see paragraph 6.5.3.2.1.1), the main conclusions arisen have shown that the later the slow environmental cooling starts the higher the Spalling Index maximum value becomes, the higher amount of energy is available for Thermal Spalling (although it is not mechanically viable due to longitudinal compressive stresses), the higher residual longitudinal compressive stresses arise, the higher the cracking level becomes at inner layers, and the lower the remaining relative humidity results in all the depths of the structural element. On the contrary, within the *Surface cooling + Heating* cases (see paragraph 6.5.3.2.1.2) has been observed that the effect of the cooling start on the surface cooling cases is only local and does not result significant at all after three hours of heating.

8.1.4.3 ABOUT THE ATLAS OF INFORMATION FOR THE ANALYSIS OF THE INFLUENCE OF PARAMETERS NOT RELATED TO COOLING PROCESSES

The information needed for the analysis of the influence on the hygro-thermo-chemo-mechanical behaviour of the structural element during the cooling processes of several parameters non-related to the own cooling processes – such as the initial moisture content of concrete, its intrinsic permeability, the rate of temperature increase (fire intensity), the porosity, compressive strength, type of aggregate and, in general, the whole set of hygro-thermo-chemical properties of concrete –, and for the generation of an extension of the Spalling Nomograms initially obtained just for heating processes and described previously on *Chapter 4* has been provided (see paragraph 6.5.4 and Appendix 6A) as an atlas of information constituted by four Cartesian continuum representations of those parameters more representative of the Thermal Spalling risk for each of the forty five cases analyzed (what has represented a total amount of 180 figures).

Although the generation of the stated Spalling Nomograms for the cooling stage has not been an aim of this Thesis and it is proposed as an extended task for future research works, in Appendix 6A it has been analyzed if the variation of any of these parameters leads to an increase of the maximum value of the adopted Spalling Index Is_4 (i.e. the risk of Thermal Spalling) during the cooling stage of the cases dealt in this Chapter.

From the analysis of the evolution of the Spalling Index I_{s4} resulting at each case it has been clearly observed that the values of the Spalling Index I_{s4} always decrease at all the depths as soon as the surface cooling process starts being reduced, hence, the risk of Thermal Spalling during this process (what does not mean that Thermal Spalling is no longer viable during the surface cooling process if, for instance, layers where Thermal Spalling would be energetically viable but mechanical damage showed too low values during heating increase their level of cracking during the cooling stage enabling mechanically the development of Thermal Spalling).

The latter situation has been clearly detected in several of the analyzed cases.

8.1.5 General Conclusions from *Chapter 7 – Heuristic analysis of cooling processes in high strength concrete square columns*

The main original contribution of the works presented in *Chapter 7* has been the heuristic analysis of the effect of cooling processes on the hygro-thermo-chemo-mechanical state of a square column manufactured with High-Strength concrete.

These original contributions and achievements have resulted in the following Conclusions (in order to understand them more deeply, the reader is addressed to each corresponding Chapter):

1. An introductory heuristic analysis of the effect of cooling processes on the hygro-thermo-chemo-mechanical state of a square column, manufactured with High-Strength concrete, during the development of a natural fire in a High-Rise Building has been developed and presented, by means of the advanced Hitecosp Software [2], as an introductory extension of the analyses already presented in *Chapter 6: Analysis of cooling processes in High Strength Concretes* to cases with bidimensional fluxes – of both heat and mass – such as square columns.
2. A set of state variables and other related parameters mainly concerning the level of damage in the square column have been selected and evaluated to accomplish the stated heuristic analysis. This set of variables and parameters has already been defined and explained in depth in paragraph 6.2.2 of *Chapter 6*. Hence, comparing the evolution of the values of the variables favouring Thermal Spalling – such as high local values of gas overpressure, $p^g - p_{atm}$, and mechanical damage parameter, d , high values of averaged transversal traction stresses, $\bar{\sigma}_{th}$, and constrained elastic energy \bar{U} – against those corresponding to the factors impeding Thermal Spalling – such as high average values of traction strength, \bar{f}_t , and specific fracture energy, \bar{G}_f , for the material layer between a current position and the heated surface – it has been observed that the risk of Thermal Spalling is, taking into account the heuristic validity of this conclusion, lower as the environment cools either under slow or fast cooling rates (0,2 and 20 °C/second respectively). This trend is mainly due to sharp decreases of the vapour pressure values, the elastic strain energy and the stress components.

However, during the environmental cooling processes simulated both the Mechanical Damage, i.e. cracking, and the Total Damage parameters values have shown increasing values (over a 20 per cent increase) at positions where temperature was actually decreasing, especially at the zones close to the heated and later cooled surfaces and, more precisely, far from the corner (although the cracking levels of these zones are still lower than at the corner).

8.2 PROPOSED EXTENDED TASKS FOR FUTURE RESEARCH WORKS

8.2.1 Proposed Extended tasks related to *Chapter 3 – Modelling of Hygro-Thermal Behaviour of Concrete at High Temperature with Thermo-Chemical and Mechanical Material Degradation*

1. There is still a need for a mathematical model allowing analysing the hygro-thermal, chemical and deterioration processes in concrete structures at high temperature more precisely, and which will allow us to predict the thermal spalling phenomenon using purely ‘mechanical’ criteria, and not ‘heuristic’ ones, as the presented here. This should possibly take into account a stochastic nature of the phenomenon and its both local and global character. In some authors’ opinion [4], the latter could be considered, for example, by using a multi-scale type model, involving a micro-level for predicting physical properties of the concrete components (i.e. cement paste, Inter-phase Transition Zone and aggregate), a meso-level for analysis of their interactions (e.g. by means of fracture mechanics), and finally, a macro-scale for evaluation of the whole structure performance at given ambient conditions. The model used in this Thesis, after appropriate modifications, could be used for the macro-scale analysis.

8.2.2 Proposed Extended tasks related to *Chapter 4 – Spalling Nomograms*

1. In *Chapter 4* it has been established as the time where Thermal Spalling will take place, that corresponding to the maximum value of the I_{s4} Spalling Index. However, as it has been explained during the work, there are instants before reaching this point at which Thermal Spalling would be energetically viable but with lower levels of damage – cracking –. Therefore, it is still needed to analyze what is the time-evolution of the energy available for Thermal Spalling combined with the determination of the lowest level of cracking needed for its occurrence – remember that a crack thickness of 0,5 millimetres is assumed in the energetic analyses included in this thesis –. The former analysis is worked out in Chapter 6 of this Thesis.

2. As it has been exposed, the Thermal Spalling phenomena derived from the calculations developed usually occur at quite superficial layers of the heated concrete element (less than 1 centimetre from the heated surface for ISO heating cases, less than 2 centimetres in Slow heating cases and less than 5 millimetres in Hydrocarbon heating cases). This fact means that, although the reinforcing concrete cover is reduced due to the spalled-off pieces, it is not directly exposed to fire. There is a need of studying what will happen after the first superficial pieces have spalled-off, being possible – but not corroborated – that Thermal Spalling phenomena accelerates as successive layers are progressively spalled-off until the reinforcement bars are reached and exposed directly to fire.

3. Finally, an extension of all of these works – basically the development of Spalling Indexes correlated against experimental data – to cases with bidimensional fluxes of heat and mass are necessary to excerpt conclusions for certain structural elements such as square columns, where Corner Thermal Spalling is often the most dangerous type.

8.2.3 Proposed Extended tasks related to *Chapter 6 – Analysis of cooling processes in High Strength Concretes*

1. In Chapter 5 it was already observed that thermal creep may have a significant effect on the results dealt in this Chapter. If the conclusions deducted herein are needed for structural elements where strong restraints are expected, there is a prior need to develop a software release capable to predict hygro-thermo-chemo-mechanical behaviour considering thermal creep during cooling processes.

2. The degree of saturation with liquid water S (considering together hygroscopic and capillary water, if the latter is contained in the pores) is an experimentally determined function of

capillary pressure (matrix potential) p^c , and temperature T (since hysteresis phenomena are not considered here, it is assumed to be a unique function of capillary pressure). Usually presented graphically in the form of the sorption isotherms, this function is needed for realistic modelling of hygro-thermic behaviour of concrete and it must be determined during sorption tests at several temperatures. Within all of the calculations included in this Chapter the sorption isotherms corresponding to the heating stages have also been considered during the cooling ones, being therefore still a need to work out sorption isotherms specific for cooling stages.

3. Analogously to the extended task proposed from *Chapter 4*, since the concrete cover of the steel reinforcing bars is reduced due to the spalled-off pieces, there is a need of studying what will happen after the first superficial pieces have spalled-off, being possible – but not corroborated – that Thermal Spalling phenomena accelerates as successive layers are progressively spalled-off until the reinforcement bars are reached and exposed directly to fire.

4. As it was exposed on the State-Of-The-Art Chapter, there is an almost absolute lack of experimental phenomenological and mechanistic information about cooling processes in High Strength concretes. This is an unavoidable prior work to accomplish if the software release described on the first proposed extended task is to be developed.

5. The analysis of the influence on the hygro-thermo-chemo-mechanical behaviour of the structural element during the cooling processes of several parameters non-related to the own cooling processes – such as the initial moisture content of concrete, its intrinsic permeability, the rate of temperature increase (fire intensity), the porosity, compressive strength, type of aggregate and, in general, the whole set of hygro-thermo-chemical properties of concrete –, and the generation of an extension of the Spalling Nomograms initially obtained just for heating processes and described previously on *Chapter 4* is still pending and may be fulfilled starting from the atlas of information provided in Appendix 6A.

6. Finally, and again analogously to the extended task proposed from *Chapter 4*, an extension of all of these works – basically the development of Spalling Indexes correlated against experimental data – to cases with bidimensional fluxes of heat and mass are necessary to excerpt conclusions for cooling processes on certain structural elements such as square columns, where Corner Thermal Spalling is often the most dangerous type. For this reason, the analyses of square columns included in Chapter 7 may only be developed from a ‘heuristic’ point of view.

8.2.4 Proposed Extended tasks related to Chapter 7 – Heuristic analysis of cooling processes in high strength concrete square columns

Extended tasks proposed in sight of the calculations developed in this Chapter are also:

1. The need to work out sorption isotherms specific for cooling stages (see paragraph 8.2.3, subparagraph 2),
2. The need of studying what will happen after the first superficial pieces have spalled-off (see paragraph 8.2.3, subparagraph 3), and
3. The need of development of Spalling Indexes correlated against experimental data suitable for cases with bidimensional fluxes of heat and mass are necessary to excerpt mechanistic and not heuristic conclusions for square columns (see paragraph 8.2.3, subparagraph 6).

8.3 BIBLIOGRAPHY OF THE CHAPTER

- [1] D. Gawin, F. Pesavento, B.A. Schrefler, *Modelling of hygro-thermal behaviour of concrete at high temperature with thermo-chemical and mechanical material degradation*, Comput. Methods Appl. Mech. Engrg . 192 (2003) 1731-1771.
- [2] Brite Euram III BRPR-CT95-0065 HITECO, *Understanding and industrial application of High Performance Concrete in High Temperature Environment – Final report*, 1999.
- [3] UNE-EN 1991-1-2, *Eurocódigo 1: Acciones en estructuras. Parte 1-2: Acciones generales. Acciones en estructuras expuestas al fuego*, Mayo 2004.
- [4] D. Gawin, F. Pesavento, B.A. Schrefler, *Towards prediction of the thermal spalling risk through a multi-phase porous media model of concrete*, Comput. Methods Appl. Mech. Engrg . 195 (2006) 5707-5729.

*THIS PAGE IS INTENTIONALLY
LEFT BLANK*